TESIS DE LA UNIVERSIDAD
DE ZARAGOZA

2022

82

Alba Sanmiguel Vallelado

Study of the interactions between snowpack and forest cover in the Aragonese Pyrenees and their eco-hydrological implications

Director/es
López Moreno, Juan Ignacio
Morán Tejeda, Enrique

ISSN 2254-7606

Prensas de la Universidad
Universidad Zaragoza

ISSN 2254-7606

Universidad Zaragoza
1542

Tesis Doctoral

STUDY OF THE INTERACTIONS BETWEEN SNOWPACK AND FOREST COVER IN THE ARAGONESE PYRENEES AND THEIR ECO-HYDROLOGICAL IMPLICATIONS

Autor

Alba Sanmiguel Vallelado

Director/es

López Moreno, Juan Ignacio
Morán Tejeda, Enrique

UNIVERSIDAD DE ZARAGOZA
Escuela de Doctorado

Programa de Doctorado en Ordenación del Territorio y Medio Ambiente

2022

PhD thesis 2022

Study of the interactions between snowpack and forest cover in the Aragonese Pyrenees

and their eco-hydrological implications

Alba Sanmiguel Vallelado

Universidad Zaragoza

IPE CSIC

The cover of this Thesis features a photography of one the studied forest stands located in the Baños de Panticosa valley with views of the Algas peak (3036 m a.s.l.), the Garmonegro peak (3064 m a.s.l.), the Pondiellos peak (2917 m a.s.l.) and the Arnales peak (3002 m a.s.l.), from left to right.

Estudio de las interacciones entre el manto de nieve y la cubierta forestal en el Pirineo Aragonés y sus implicaciones eco-hidrológicas

Alba Sanmiguel Vallelado

Facultad de Filosofía y Letras

Departamento de Geografía y Ordenación del Territorio

Universidad de Zaragoza

Presentada para optar al título de Doctora
en Ordenación del Territorio y Medio Ambiente

Director	Dr. Juan Ignacio López Moreno
Segundo Director	Dr. Enrique Morán Tejeda

Enero, 2022

Compendium of publications

This Thesis is presented as a compendium of four research papers previously published. Hereafter, the publications that constitute the main body of this Thesis are fully referenced:

1. Sanmiguel-Vallelado, A., López-Moreno, J. I., Morán-Tejeda, E., Alonso-González, E., Navarro-Serrano, F. M., Rico, I. & Camarero, J. J. (2020). Variable effects of forest canopies on snow processes in a valley of the central Spanish Pyrenees. *Hydrological Processes*, *34*, 2247–2262. https://doi.org/10.1002/hyp.13721

2. Sanmiguel-Vallelado, A., Camarero, J. J., Gazol, A., Morán-Tejeda, E., Sangüesa-Barreda, G., Alonso-González, E., Gutiérrez, E., Alla, A. Q., Galván, J. D. & López-Moreno, J. I. (2019). Detecting snow-related signals in radial growth of Pinus uncinata mountain forests. *Dendrochronologia*, *57*, 125622. https://doi.org/10.1016/j.dendro.2019.125622

3. Sanmiguel-Vallelado, A., Camarero, J. J., Morán-Tejeda, E., Gazol, A., Colangelo, M., Alonso-González, E. & López-Moreno, J. I. (2021). Snow dynamics influence tree growth by controlling soil temperature in mountain pine forests. *Agricultural and Forest Meteorology*, *296*, 108205. https://doi.org/10.1016/j.agrformet.2020.108205

4. Sanmiguel-Vallelado, A., McPhee, J., Esmeralda Ojeda Carreño, P., Morán-Tejeda, E., Julio Camarero, J. & López-Moreno, J. I. (2022). Sensitivity of forest–snow interactions to climate forcing: Local variability in a Pyrenean valley. *Journal of Hydrology*, *605*, 127311. https://doi.org/10.1016/j.jhydrol.2021.127311

Funding

The author of this Thesis, Alba Sanmiguel Vallelado, was supported by a University Professor Training grant [FPU16/00902], funded by the Spanish Ministry of Universities. This pre-doctoral contract was effective in the Pyrenean Institute of Ecology (Spanish National Research Council, IPE-CSIC).

The different studies that conformed this Thesis were supported by the projects: "Bosque, nieve y recursos hídricos en el Pirineo ante el cambio global" funded by Fundación Iberdrola; CGL2014-52599-P (IBERNIEVE) funded by the Spanish Ministry of Science and Innovation; CGL2017-82216-R (HIDROIBERNIEVE) funded by the Spanish Ministry of Science and Innovation; and RTI2018-096884-B-C31 funded by the Spanish Ministry of Science and Innovation.

“Las montañas, al igual que los océanos y los desiertos, son nuestros jardines salvajes, tan necesarios e indispensables como el agua o el pan; no solamente porque el aire resulte más puro que en las ciudades, sino porque ante todo constituyen lugares de plenitud, donde el hombre puede caminar, correr, detenerse, contemplar, trepar, navegar, tener hambre, tener sed, utilizar el vigor de su cuerpo, y hacer respirar su corazón y su alma”

Gaston Rébuffat

Acknowledgements

Gracias

A Nacho, por enseñarme a ver con otros ojos un entorno tan cautivador como hostil, como son los Pirineos en invierno. El hacer en uno de estos valles una tesis a caballo entre la hidrología y la ecología forestal, y que además implicase mucho trabajo de campo, resultó una propuesta demasiado sugerente como para dejarla pasar. Y no me equivoqué, llevar a cabo este proyecto ha satisfecho tanto mi curiosidad por el mundo de la ciencia como mis ganas de montaña. Nacho me acogió en su grupo del IPE hace ya 7 años, siendo estudiante de máster. Luego me contrató como técnico del grupo, lo que me permitió mantenerme económicamente a flote hasta que conseguí un contrato predoctoral. Valoro enormemente la autonomía que me ha dado todo este tiempo, acompañada siempre de su orientación y apoyo. Su buen humor y cercanía hacen que rápidamente se difuminen los límites entre lo profesional y personal. *Gracias* por tu flexibilidad de cara a haberme permitido trabajar y vivir todos estos años en los Pirineos, donde he podido disfrutar plenamente de esta etapa vital.

A Enrique, por asumir conmigo el reto de dirigir una tesis por primera vez. Cuando instalamos el primer sensor en Baños de Panticosa no sabía que sería mi tesis la que saldría de allí, ni que él sería mi director. Desde entonces, su acompañamiento ha sido constante. Son muchas las ocasiones en las que Enrique ha sido la brújula que me ha ayudado a volver a orientarme y encontrar el camino, pues no es poco común sentir que se camina en círculos durante el transcurso de una tesis. Agradezco su especial dedicación a la hora de revisar los trabajos de investigación que forman esta tesis y el propio manuscrito final, pues ha resultado clave para sacarlos adelante. *Gracias* por tu trato desenfadado, por tu rigurosidad, y por toda la ayuda recibida.

A Chechu, también DIRECTOR de esta tesis, con mayúsculas, pese a que la burocracia no ha permitido que sea reconocido como tal en los papeles. Su tutela ha sido constante, sus ideas fundamentales y su orientación imprescindible. Me abrió las puertas de su mundo, el de los árboles, en el que me ha introducido con paciencia, contagiándome de su pasión. Puso a toda su gente a disposición de este proyecto, a los que agradezco de corazón la gran acogida que me dieron en el IPE de Zaragoza, pues hicieron agradables las largas jornadas de laboratorio. Sus emails siempre han sido un soplo de aire fresco (y no sólo por los emoticonos). Pues, aunque se llegara a la conclusión de que había que rehacer todo de nuevo, Chechu siempre me hacía creer que el trabajo había avanzado. Esta tesis no hubiera sido posible, ni de lejos, sin su grandísima ayuda. *Gracias*, por tu implicación, tus ánimos, y por tu forma de hacer las cosas.

A James McPhee, por abrir la puerta a una estancia científica atípica "en Chile" en tiempos de pandemia, y además, hacerlo fácil.

A J. Carlos González, Maite Echeverría y Juan de la Riva por facilitarme la navegación en el programa de doctorado. A Asunción Julián, Alfredo Ollero y Daniel Ballarín por introducirme en el mundo de la docencia universitaria.

A todos los coautores de los trabajos de investigación publicados en el marco de esta tesis, por sus valiosas aportaciones. A los editores y revisores de dichos trabajos, por la oportunidad de sacarlos a la luz en su mejor versión.

A los profesores de la Universidad de León y de la Universidad de Cantabria que me dejaron huella. *Gracias*, por enseñarme a ver este mundo de una manera transversal y con la ecología como base, por transformar mi curiosidad y amor por la naturaleza en interés por la ciencia. Y a Saúl Blanco, por iniciarme en la investigación con paciencia y dedicación.

A mis compañeros de tesis, Paco y Esteban, por esa comprensión entre doctorandos en las charlas que surgen mientras se camina por el monte, ya sea cargando un laser escáner a la espalda o en mitad de una ventisca.

A todos los ayudantes que he tenido en el trabajo de campo: Héctor, Paula, Guillem, Trevor, Esteban, Paco, David, Guille, Vari, Gandalf, Ibai, Sergio, Jesús, Antonio, y muy especialmente a Pedro, que al igual que te ancla una estación meteorológica con un alambre y dos bridas, te aconseja sentimentalmente. *Gracias* por acompañarme tantos y tantos días de campo, donde no faltó una sonrisa a pesar de que estuviéramos bajo cero y empapados.

A mis compañeros del IPE de Jaca, por cada día. Me siendo afortunada por haber podido disfrutar todo este tiempo de vuestra calidad humana, donde el más veterano comparte porrón con el recién llegado de prácticas mientras celebran un jueves lardero cualquiera. *Gracias* familia IPErina, habéis sido mi refugio.

A mis compañeros de cordada: los navarricos, los jacetanos de acogida y los del otro lado del Pre-Pirineo. Ellos son los responsables de que cada lunes cogiera con ganas el sentarme en la silla para ponerme a trabajar, no hay nada como llegar exhausta del fin de semana. A Alberto Urtasun, por marcar decisivamente esta etapa haciendo que el alpinismo sea mucho más que la vía de escape perfecta. *Gracias* a todos por esas vías *a pechote* que me han alimentado el alma.

A los amigos que ya traía conmigo. A esos compañeros del IPE que se han convertido en amigos. Soy afortunada por haberme encontrado con todos vosotros en el camino. *Gracias* por las horas de terapia gratuita, por todos esos momentos imborrables, y por todos los que vendrán.

A Guille, *por acompañar-me mientres escribiba a mía tesi en ixe ortal an as borrainas se subiban a flor.*

A mi familia, por su amor y apoyo incondicional, por enseñarme a esforzarme. A mi madre, por estar ahí siempre y a la vez habernos criado con libertad, por sus *mira a ver niña donde te metes.* A mi padre, por llevarnos a experimentar esa felicidad que sólo encontramos en el monte. A mi hermano, por dejarse engañar para palear nieve a cambio de una pizzeta, por sus baños de realidad, y por su mano en mi hombro.

Dedico este trabajo a los Pirineos,

pues me tienen embrujada desde que era una niña

Abstract

In main mid–latitude mountain areas, both snow and forests, constitute priority resources that have major economic and environmental roles. The Pyrenees are not an exception, where both elements coexists and interact in the altitudinal band comprised between 1600 and 2300–2500 m a.s.l., mostly comprising the subalpine belt. However, interactions between mountain forests and snowpack had not yet been fully addressed in this region. Even less was known regarding forest–snow interactions response to the warm–up process that is happening in this mountain range and it is expected to be accelerated in the following decades. This PhD Thesis overall objective is to deepen the knowledge on the forest–snow interactions in the Pyrenees, from an eco–hydrological perspective. It is presented as a compilation of four research publications, in which different specific objectives are assessed.

The main part of this interdisciplinary study was performed in a mountain valley located in the central Spanish Pyrenees, where the experimental setting comprised four forest stands of *Pinus uncinata* located at different elevations (from 1674 to 2104 m a.s.l.), exposure, forest structure and microclimatology because of the complex topography in this mountainous area. Snow cover, climate and soil conditions, tree phenology, xylogenesis, intra–annual radial growth and the concentration of sapwood and needle non–structural carbohydrates were intensively monitored in these forests stands over a time span from 2015 to 2020. In this context, a first research publication provided additional information about the forest cover effects on snowpack dynamics in this region and highlighted the similarities and differences in these effects among nearby areas and during different snow seasons. A second research publication identified for the first time a snow signal in the inter–annual radial growth

of *P. uncinata.* The research was contextualized in a wider spatio–temporal context, analyzing dendrochronologically 36 *P. uncinata* forests located in the main mountain ranges of the NE Iberian Peninsula and considering the snow conditions occurred there in last decades. A third research publication tested how seasonal dynamics in snowpack characteristics modified certain micro-climatic conditions and demonstrated that these snow influences determined in a large way the intra–annual radial growth of *P. uncinata* forests in the central Spanish Pyrenees experimental site. A fourth research publication explored how future changes in the Pyrenean climate can affect those current forest–snow interactions, by performing a sensitivity analysis by simulating the shifts in snow conditions at sampled central Spanish Pyrenees forests under various degrees of climate forcing.

This Thesis' results have shown that snow cover and *P. uncinata* forests interacted both ways in the studied sites, although these interactions are subjected to important spatial and temporal sources of variability. On the one hand, forest cover, mostly through canopy interception and energy balance alteration, determined snowpack distribution, magnitude and timing. On the other hand, snow cover, mostly through soil temperature conditions, influenced *P. uncinata* inter–annual and intra–annual radial growth, independent of the widely reported effect of growing season air temperature on *P. uncinata* tree–ring development. Furthermore, this Thesis has reported that forest cover will affect the snowpack sensitivity to future changes in climate in the Pyrenees. The issues addressed by this Thesis, entitled "*Study of the interactions between snowpack and forest cover in the Aragonese Pyrenees and their eco–hydrological implications*", are of high scientific interest, but also involve results with potential present and future applicability in forest and water resources management in the Pyrenees.

Resumen

En las montañas de latitudes medias los bosques y la nieve constituyen recursos naturales prioritarios, tanto desde el punto de vista medioambiental como del económico. Los Pirineos no son una excepción, dado que en esta cordillera ambos elementos coexisten e interaccionan complejamente en el rango altitudinal comprendido entre los 1600 y los 2300–2500 m s.n.m., ocupado en su mayor parte por el piso bioclimático subalpino. Sin embargo, las interacciones que tienen lugar entre los bosques de montaña y el manto de nieve en esta región no habían sido estudiadas en profundidad hasta el momento. Y menos aún se sabía acerca de la respuesta de las interacciones bosque–nieve al proceso de calentamiento que está aconteciendo en esta cordillera y que se espera se vea acelerado en las próximas décadas. De manera que, el principal objetivo de la presente Tesis Doctoral es avanzar en el conocimiento existente sobre las interacciones que se producen entre los bosques de montaña y el manto de nieve en los Pirineos, desde una perspectiva eco–hidrológica. La misma, se presenta como un compendio de cuatro publicaciones científicas, en las que diferentes objetivos específicos son evaluados.

La mayor parte de este estudio interdisciplinar tuvo lugar en un valle de montaña (Baños de Panticosa) localizado en el Pirineo central. El diseño experimental incluyó cuatro bosques de *Pinus uncinata* de diversas características ambientales, entre las cuales cabe mencionar su diferente elevación (desde 1674 a 2104 m s.n.m.), exposición, estructura forestal y microclimatología debido a la compleja topografía de este enclave montañoso. En estos bosques se monitorizó intensivamente, entre 2015 y 2020, la evolución del manto de nieve, las condiciones climáticas y del suelo, la fenología de los pinos, su xylogénesis, la variación intra–anual del radio de su tronco y la concentración de carbohidratos no estructurales presentes en su albura

y acículas jóvenes. En este marco se contextualizó la primera publicación científica que compone esta Tesis, la cual informó con detalle sobre los efectos que la cubierta forestal produce en la dinámica del manto de nieve en esta región, destacando las similitudes y diferencias que existen entre áreas cercanas y entre distintas temporadas de invierno. La segunda publicación científica, identificó por primera vez una señal nival en el crecimiento radial inter–anual de *P. uncinata*. Esta investigación se contextualizó en un contexto espacio–temporal más amplio, analizando dendrocronológicamente 36 bosques de *P. uncinata* localizados en las principales cordilleras montañosas del NE Peninsular y las condiciones nivales acontecidas en los mismos en las últimas décadas. La tercera publicación científica, describió cómo la dinámica estacional del manto de nieve es capaz de modificar ciertas condiciones microclimáticas de los bosques estudiados en el valle de Baños de Panticosa, y demostró cómo esta influencia nival determina en buena parte el crecimiento radial intra–anual de *P. uncinata*. La cuarta publicación científica, exploró cómo los futuros cambios del clima pirenaico podrían afectar a las actuales interacciones bosque–nieve que tienen lugar en el valle de Baños de Panticosa. Para ello, se simularon los cambios que experimenta la dinámica nival en los bosques estudiados bajo varios grados de forzamiento climático.

Los resultados obtenidos en esta Tesis demuestran, por tanto, que el manto de nieve y los bosques de *P. uncinata* interactúan en ambos sentidos en las áreas de montaña analizadas, si bien, tales interacciones están sujetas a importantes fuentes de variabilidad espacial y temporal. Por una parte, la cubierta forestal, principalmente debido a la intercepción que producen las copas de los pinos y a la alteración que produce en el balance de energía, determina la distribución del manto de nieve, su magnitud y su temporalidad. Por otra parte, el manto de nieve, principalmente mediante las modificaciones que produce en el régimen de temperaturas del suelo, influye en el crecimiento radial intra e inter–anual de *P. uncinata*, independientemente del ampliamente conocido efecto que tiene la temperatura del aire durante la temporada de crecimiento en la formación de sus anillos. Además, esta Tesis sugiere que la cubierta forestal puede tener un importante rol en la sensibilidad del manto de nieve ante los futuros cambios que se esperan en el clima de los Pirineos.

Las cuestiones abordadas en esta Tesis, titulada "*Estudio de las interacciones entre el manto de nieve y la cubierta forestal en el Pirineo Aragonés y sus implicaciones eco–hidrológicas*", son de gran interés científico, pero también proporcionan una valiosa información de gran aplicabilidad en la presente y futura gestión de los recursos hídricos y forestales del Pirineo.

Table of Contents

Chapter 1

Introduction

This section contains background information to allow the reader to understand this Thesis statement and arguments. Firstly, some basic concepts about the science of snow are described. Secondly, the fundamentals of mountain forests ecology are presented. Thirdly, it is introduced how both elements, snow and forests, interact both ways. Ultimately, the objectives and justification of this Thesis are addressed.

1.1 Snow

The cryosphere is a term derived from the Greek word *kryos* meaning cold. The term is used to describe any place on Earth where water is in its solid form at least one month of the year (Barry & Gan, 2011). Seasonally, the cryosphere encompasses more than 50% of the land, while it covers ∼10% of the land permanently (Vaughan et al., 2013). The components of the cryosphere include ice caps and ice sheets, glaciers, permafrost (ground ice), freshwater ice, sea ice, and snow cover, which is the largest component in extension (Figure 1.1). Ice is the solid phase of water and it usually presents a crystalline structure. There are other ices (e.g. dry ice), but they do not concern us here. Snow is a porous medium consisting of air, ice crystals and small amounts of chemical impurities. Ice crystals are formed in the atmosphere from the water vapor at a temperature below 0ºC, comprising the solid fraction of precipitation when falling to the Earth's surface (i.e. snowfall). Snow that has fallen on the ground and accumulated, is called snowpack. The density of snow can vary considerably, ranging from about 100 $kg \cdot m^{-3}$ for new snow to 500 $kg \cdot m^{-3}$ for wet old snow (Seibert et al., 2015). The freeze-thaw cycles of snowpack produce rounded large-grained snow, that under increasing pressure is compressed, and may forms firn at glaciers head surface. Firn or névé is the intermediate stage between snow and glacial ice, and reaches higher density values than snow (500–830 $kg \cdot m^{-3}$). Further compactation of firn results in glacial ice (850–917 $kg \cdot m^{-3}$), becoming impermeable to air and water.

Almost all of the Earth's snow-covered land area is located in the Northern Hemisphere (∼98%), where seasonal snow cover reaches an annual maximum extent of ∼47 million km^2 in January and February and a minimum of ∼3 million km^2 in August (Robinson & Frei, 2000). Snow cover is a key driver of the Earth's climate system, affecting local, regional and global atmospheric circulation. The energy balance of the lower atmosphere and the surface is strongly controlled by the physical particularities of snow cover, especially its high albedo and low thermal conductivity (Cohen, 1994). The annual snowfall fraction and the snow cover persistence increase in high latitudes and altitudes (Figure 1.2). It is estimated that 1773 km^3 of snowfall accumulates over the world's mountains each year (Daloz et al., 2020). Mountain snow has a relevant hydroecological influence in those areas (Seibert et al., 2021), as well as on surrounding regions (Huggel et al., 2015), as I will explain in the next section (Subsection 1.1.1).

1.1.1 Hydrological and ecological role of snow

Snow cover, climate and streamflow are intimately connected. Water reserves and seasonal variability of streamflows of snow-fed basins largely depend on snowpack dynamics (Morán-Tejeda et al., 2017), although other factors (e.g. variability in seasonal precipitation) may also affect (Sanmiguel-Vallelado et al., 2017). The study of snow forms part of surface-water hydrology, but groundwater hydrology is also involved since a part of the snow runoff behaves like subsurface flow (Singh, 2001). Seasonal snow is a critical component of the hydrological cycle particularly at high elevations and high latitudes (Armstrong & Brun, 2008) (Figure 1.3). Snow, together with surface water, soil

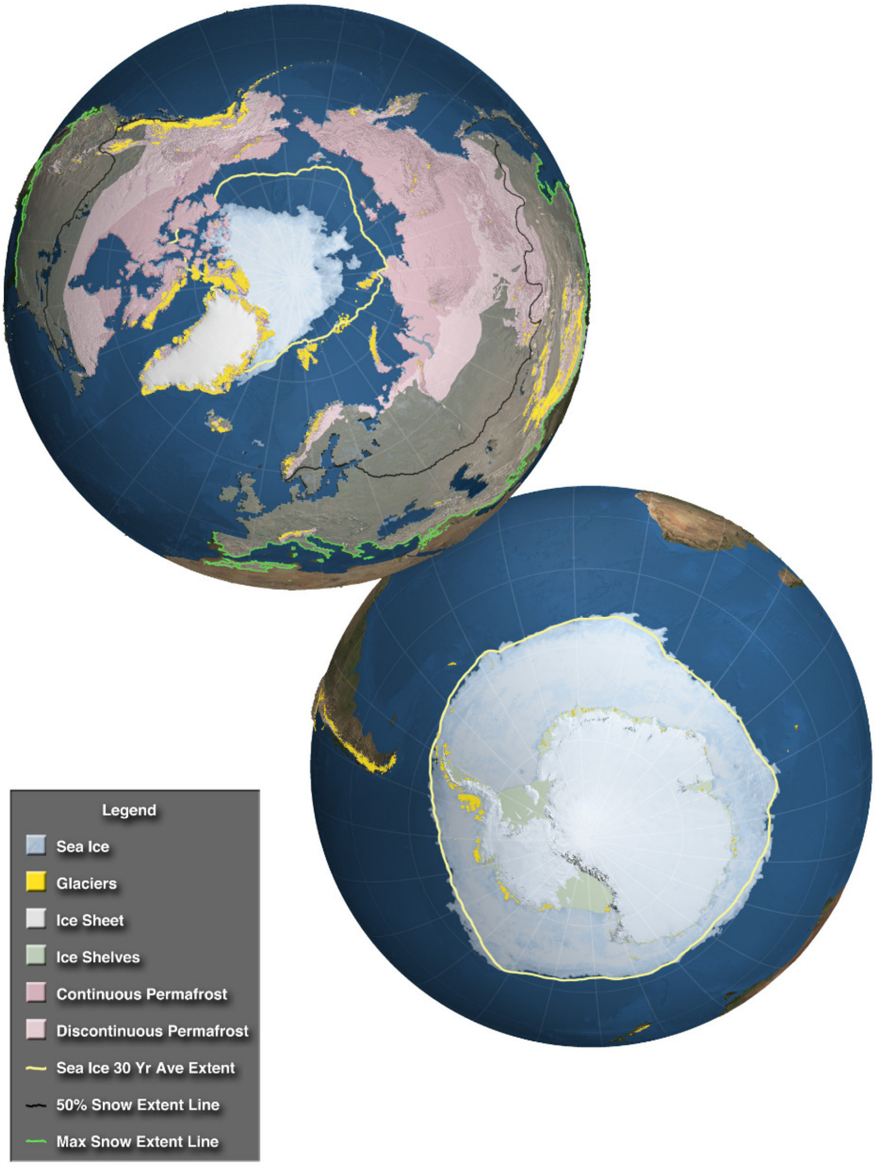

Figure 1.1: Geographical limits of the cryosphere in the Northern and Southern Hemispheres. Note that some elements located at low latitudes are not visible in this polar projection. Credit: Intergovernmental Panel on Climate Change (IPCC) in the Special Report on the Ocean and Cryosphere in a Changing Climate (2013).

and groundwater, is one major storage compartment of water which represents the 17% of the total terrestrial water storage in non-polar cold climate zones (Güntner et al., 2007). During the cold season, snowpack in mountains constitutes a natural reservoir of water, as it accumulates solid precipitation,

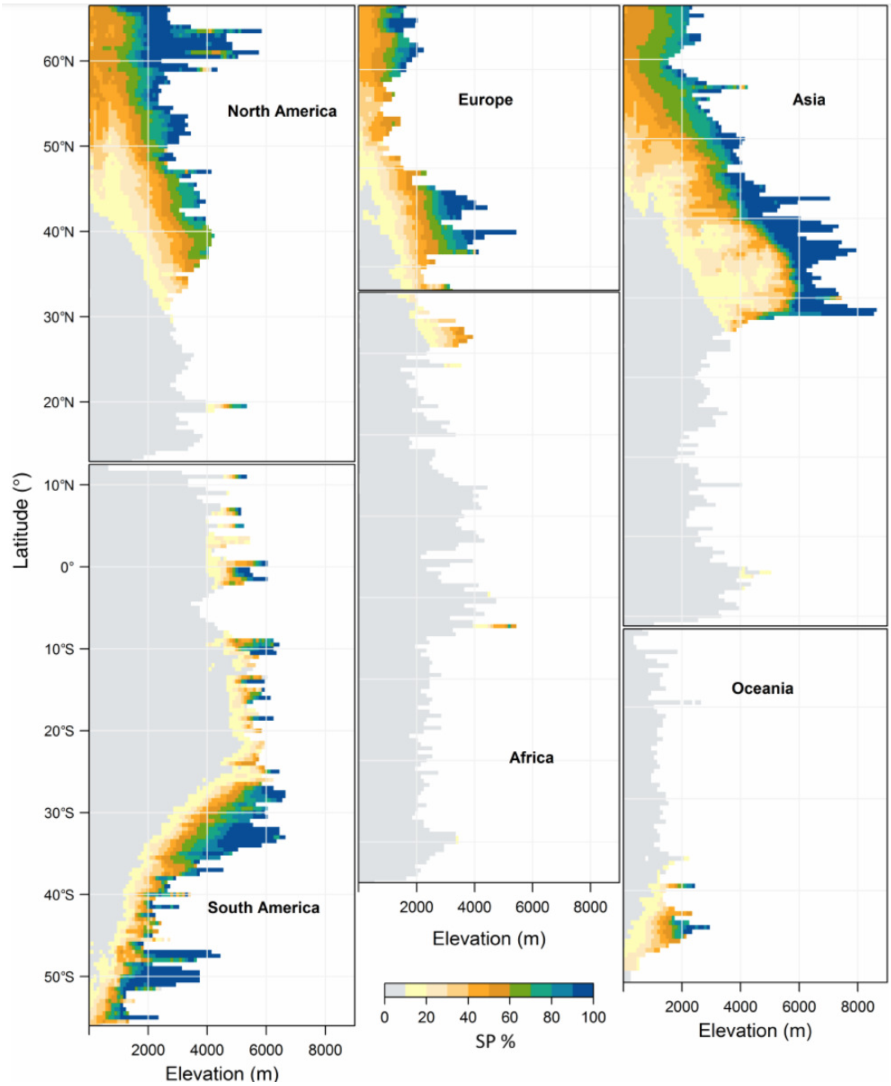

Figure 1.2: Average snow persistence (SP), i.e. the fraction of the year that snow is present on the ground, by latitude and elevation for North America, South America, Africa, Asia, Europe and Oceania (2001-2016). Credit: Hammond et al. (2018).

that contributes to the timing and magnitude of streamflow and affects water resource availability (Stewart, 2009). In spring and early summer, snowpack releases the stored water by melting and causes a peak in the annual runoff. Rain-on-snow events, i.e. rainfall onto the snow cover, also promote snowmelt and thus enhance the peak-shape of the hydrograph (Singh et al., 1997). A portion of snowmelt infiltrates the ground, feeding soil moisture and rechar-

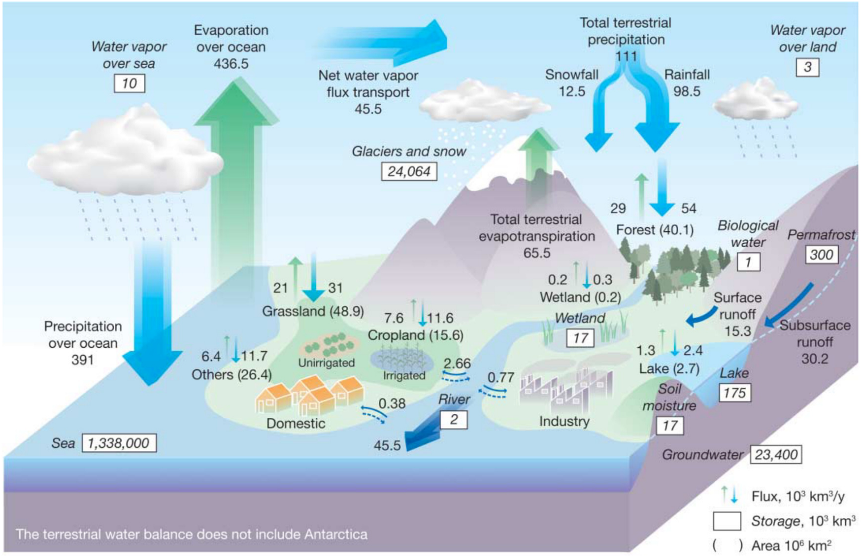

Figure 1.3: Diagram of the water cycle of Earth taking into account both natural and anthropogenic cycles. Water is always in movement on, above, and below the Earth's surface, and changing states between liquid, vapour and ice. These processes operate on different spatial and temporal scales. The direct groundwater discharge is included in river discharge. Credit: Oki and Kanae (2006).

ging groundwater (Singh, 2001). This water release from snowpack occurs when the water requirements of ecosystems and human activities are higher over the year (e.g. agriculture) and is key in the supply of water resources to nearby lowlands (Barnett et al., 2005; Biemans et al., 2019). In fact, it is considered that snow melt supply water for 20% of Earth's population and for 30% of global irrigation (Steppuhn, 1981). Thus, efficient water management requires knowledge of the snow storage and the expected melting rate (Dozier, 2011). It may appear that the technical understanding of snow hydrology is a relatively recent phenomenon, though the natural philosophy of the ancient Greek (Anaxagoras, 500–428 BCE) indicates an early understanding of the relationships between snowpack dynamics and streamflows: "*The Nile comes from the snow in Ethiopia which melts in summer and freezes in winter*" (Aet. Plac. iv 1; 385); "*And the Nile increases in summer because water flow down into it from snow at the north*" (Hipp. Phil. 8; Dox. 561) (Fairbanks, 1898). However, there is a general lack of appreciation by society of the importance of snow to everyday life (consumption, agriculture, hydropower, and domestic, industrial and municipal water), particularly in those arid regions whose headwaters are located in mountainous terrain. This is the case of Western USA, where snow melting is the source of more than 50% of total regional runoff (Li et al., 2017). Similarly, snowmelt runoff in the mountainous eastern part of Turkey constitutes 60–70% of the total yearly runoff (Acar et al., 2009). In Mediterranean regions, high-elevation areas (> 2000 m a.s.l.) are commonly dominated by snowmelt, whereas rainfall defines most of the hydrograph shape in the low-elevation areas (Fayad et al., 2017). Since the snow cover regime (i.e. timing, duration) is highly sensitive to changes in temperature and precipitation, the process of snow accumulation-melting are hotpots for climate change impacts (Beniston, 2003). That is an issue that I will address later at Subsection 1.1.3. Moreover, snow cover thickness influences the thermal regime of glaciers, whose melt contribution to runoff is of outmost interest in several glaciered basins (Kaser et al., 2010). This has related consequences for glacier response to climate change and outburst flood hazards. (Gilbert et al., 2012).

Snow cover is not only the environment, but also the mediator of snow-related ecosystems, modifying interactions between atmosphere, soil, nutrients, microorganisms, plants and animals (Jones et al., 2001). It is not unusual that seasonal snowpack covers the ground for more than half of the year in Artic and alpine regions. During this period, and afterwards, soil microclimate (temperature and moisture) is conditioned by snow cover dynamics (Hardy et al., 2001). Thus, soil organisms, vegetation and associated biogeochemical processes are also influenced by snow (Löffler, 2007). A well developed snowpack acts as a thermal insulator decoupling soil temperature from air temperature because snow has high shortwave albedo and low thermal conductivity (Zhang, 2005). This mechanism regulates the extent of soil freezing during winter; however, it also delays warming of soil in spring (Decker et al., 2003). Freezing soil temperatures during winter, induced by shallow snowpacks, inhibit soil microbial respiration, nitrogen mineralization and fine root growth in cold regions (Schimel et al., 2004; Wu, 2020). Moreover, a scarce snow cover during winter impacts negatively on the abundance of soil biota and changes in its community composition (Templer et al., 2012). Shallow and therefore ephemeral snowpacks, induce earlier soil warm up date in spring, which enhance soil microbial respiration by this time and may result in increased overall annual greenhouse gas emissions (Arndt et al., 2020; Wilson et al., 2020). On the other hand, snow melting provides water and nutrients to soil (Johannessen & Henriksen, 1978; Maurer & Bowling, 2014). Thereby, together with the above mentioned snow influences on microbial activity and decomposition rates, snow dynamics can alter the amount and timing of plant-available nutrients during the growing season (Rixen et al., 2008). The time of snowmelt significantly affects the life-cyle of plants by defining the start of the growing season and can influence plant growth (Kudo, 1991). Although I will introduce later on this chapter (Subsection 1.3.2) the particular snow influences on forest growth and functioning, it is worth mentioning that the date of snowmelt is one of the most important factors that define tree seasonal growth and tree-ring development in cold regions (Kirdyanov et al., 2003). Generally, increased snow cover, and therefore more lasting snowpack, negatively impact on plant productivity (Wipf & Rixen, 2010). Whereas, vascular plant, moss and lichen species in Arctic regions are highly dependent on the evolution of snow conditions, where a shorter snow cover duration accelerates their rates of extinction (Niittynen et al., 2018). Permanent and seasonally snow covered lands are considered a limiting factor for the distribution and ecology of terrestrial animals (Formozov, 1946). However, these areas also constitute important habitats for arthropods, birds and mammals that are adapted to snow-cover conditions (Rosvold, 2016). Some animal species are snow-dependent too, such as the wolverine (*Gulo gulo*), whose successful reproduction depends on spring snowpack for providing suitable denning sites (Magoun & Copeland, 1998). Both domestic and wild ungulate populations diet comprise higher quality forage promoted by delayed plant phenology induced by snowy winters (Mysterud & Austrheim, 2014). Predator-prey interactions can also be determined by snow conditions. For example, it has been observed how snow depth affects wolves kill rate, which increases in deep snowpacks (Huggard, 1993). Snowpack dynamics also affect freshwater ecosystems. Productivity of mountain lakes is influenced by annual snow conditions, because smaller spring snowpacks leads to warmer lake temperatures and higher nutrient concentrations (because they are not diluted by snowmelt) and, as a result, phytoplankton biomass is enhanced (Oleksy et al., 2020; Sadro et al., 2018). Similarly, snow dynamics influence water temperature and benthic organic matter of mountain streams, and thus, their macroinvertebrate community composition (Schütz et al., 2001). Maritime ecosystems are influenced by snow processes as well, especially those related to melt water (Vogt & Braun, 2004).

1.1.2 Influencing factors on snowpack

Snow formation

Earth Systems interact with the cryosphere, determining snow formation and snowpack development. The hydrosphere provides the water needed to form snow. The chemical and physical processes of forming snowfall involve three phases of water and occur in clouds, which form when supercooled water and suitable aerosols are present (Barrie, 1991). The temperature and moisture content of the atmosphere determine the type of snow crystal formed, which in turn confers particular characteristics to the snowpack (structure and density). The biosphere contributes to the snow crystal formation providing part of the particles that support this process in the form of bacteria, pollen and fungal spores (Christner et al., 2008). The external part of the geosphere, the lithosphere, provides the other part of the aerosols which constitute snow crystal condensation nuclei. The geosphere comprises the formation of mountains whose elevation establishes if precipitation falls as snow or rain, which determines the altitudinal limits of seasonal snowpack development (Theriault & Stewart, 2008). This is because elevation is important in determining temperature and precipitation gradients along mountainside. Air temperature gradients are characterised by a gradual reduction of air temperature upwards or polewards, determining where solid precipitations falls. But it is important to note that the ratio of air temperature change per elevation unit is variable in space and time due to their dependence on topography, seasonality and meteorological conditions (Barry, 1992; Navarro-Serrano et al., 2018). The relationship between precipitation and altitude is less consistent. Precipitation tends to increase with elevation through the orographic effect, since atmospheric uplift is caused by relief (Barry & Chorley, 2009). Nevertheless, this pattern can vary widely depending on the regions and synoptic situations (Sevruk & Mieglitz, 2002). For example, tropic mountain chains show precipitation regimes with near-sea maxima, with mid-elevation maxima, and those with approximately uniform precipitations rates across the altitudinal gradient (Barry, 1992).

Snow distribution and development

Snow variability differs from different spatial scales, and each has its own implications. At large spatial scales, snowfall distribution varies with latitude, elevation, geomorphological characteristics and the proximity to large bodies of water (Pomeroy & Brun, 2001). Nevertheless, snowfall distribution can vary largely among nearby areas due to changes in slope, aspect, vegetation and wind (Anderson et al., 2014). I will elaborate on the role of the forest on snow distribution and development in Subsection 1.3.1 below. Gravitational transport establishes a preferential snow deposition on moderate-angle slopes, while steep slopes suffer snow removal. Slope steepness and aspect also induce snow redistribution by avalanching (Kerr et al., 2013). Windy conditions redistribute the fallen snow over the landscape following these steps: (1) erosion of snow cover by the shear strength of wind, (2) transport of the blowing snow, and (3) snow deposition to favorable sites (high roughness or low exposure) (Pomeroy, 1988). The average snow accumulation on the downwind slopes is twice than on the windward slope, reaching a maximum in the downwind slope cornice. Thus, aspect determines the redistribution of snow by wind (Anderson et al., 2014).

Snowpack results from successive snowfalls, forming layers that are transformed before being buried by the following snowfall. Hence, snowpack development shares some similarities with geological stratification. Each layer presents unique properties that enable them to be differentiated over most of the snow season when we make a snow pit, for example. There is almost always present a vertical temperature gradient within the snowpack, where lower layers of the snowpack generally remains near to 0ºC while upper layers are affected by air temperature (Santeford & Smith, 1974). The direction of the temperature gradient can change in a short lapse of time, with the surface being sometimes warmer than the bottom, and vice versa. The temperature gradient within the snowpack generates sublimation and condensation of water vapour that change the shape and size of snow crystals. As a consequence, physical characteristics of snowpack change, including density, albedo, permeability, hardness and heat conductivity (Colbeck, 1982). These overall transformation processes are collectively referred to as metamorphism (LaChapelle & Armstrong, 1977). For example, small temperature gradients result in more bonding between structures and thus in higher snowpack density, while wide temperature gradients produce poorly bonded structures which results in lower snowpack density (Dominé et al., 2003). The mass of new snowfalls increases the pressure over the top layers of snowpack and also can promote snowpack metamorphism. Also, wind is an important driving force for snow metamorphism, since it changes snowpack mass and density and deposits aerosols inside (Aoki et al., 2000; Pomeroy & Li, 2000). In addition, windy conditions enhance sublimation, which has a relevant role in reducing the final snow accumulation in many cold regions (Strasser et al., 2008).

Temperature evolution within the snowpack is governed by conservation of energy, which is described by the first law of thermodynamics. It tells us that snowpack can exchange energy with its surroundings (i.e. atmosphere and ground) by the transmission of heat (Figure 1.4). The net energy exchanged is then equal to the change in the total heat content of snowpack (δQ). Accordingly, the snow energy balance comprises the following energy fluxes: net solar radiation (K), net thermal radiation (L), turbulent exchange compounded by sensible (Qh) and latent (Qe) heats, ground conduction (Qg) and advected heat (Qp); see equation (1.1). Positive signs indicate energy fluxes towards the snowpack (i.e. they are an energy source to the snowpack), while fluxes away from the snowpack are considered to be negative. This means that snowpack can gain or lose heat by means of one or more of these processes depending on specific weather and snow cover conditions (Van Mullem

& Garen, 2004). The sum of all energy fluxes is equal to the change in heat content of snowpack for a given period ($\delta Q/\delta t$). That is,

$$\delta Q/\delta t = K + L + Qe + Qh + Qg + Qp \tag{1.1}$$

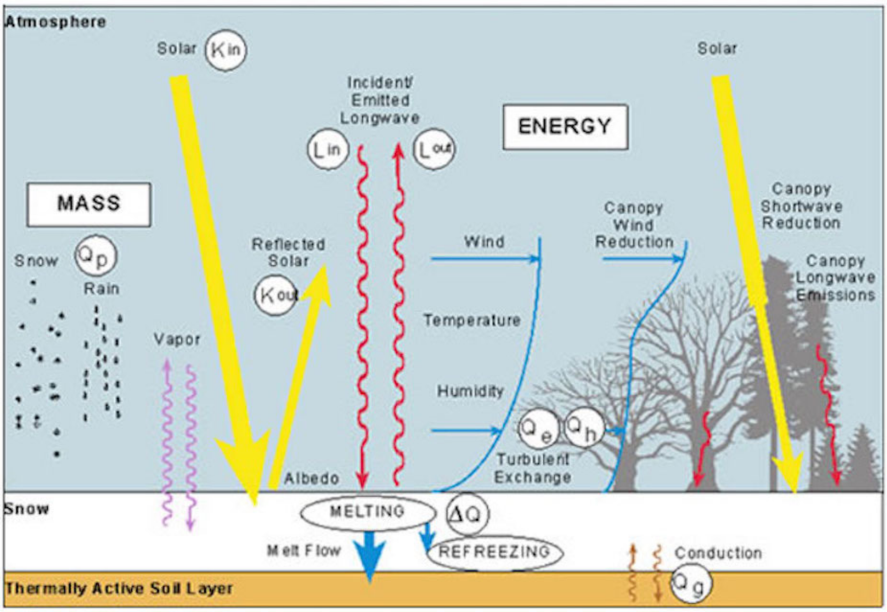

Figure 1.4: Diagram of the snowpack energy budget. K terms represent the solar inputs (incoming and outgoing). L terms represent longwave radiation (incoming and outgoing). Turbulent fluxes are represented as Qe term (latent heat) and Qh term (sensible heat). Qg term represents ground conduction. Qp term represents advected heat. Credit: Donald Cline, National Oceanic and Atmospheric Administration (NOAA), Washington DC, USA.

The net solar radiation is the difference between incoming minus reflected shortwave radiation. The incoming solar radiation depends on latitude, season, slope, aspect, atmospheric diffusion and landscape obstacles which produce a shadow effect on snowpack. A large fraction of the incoming solar radiation is reflected back into the atmosphere because the snow albedo is high: it ranges from 0.8–0.9 for fresh snow to 0.4–0.7 for old snow (Barry & Gan, 2011). Snow albedo usually decreases for a few days after a snowfall as a result of metamorphism or wind-blowing, because snow structures becomes more rounded and its ability to reflect incoming radiation decreases. Snow albedo also decreases due to particle accumulation on its surface (called *light absorbing particles*), as black carbon, dust or microbial growth (Skiles et al., 2018). The net thermal radiation is the difference between incoming longwave from the atmosphere, terrain, clouds and vegetation of the surroundings minus the outgoing longwave from the snowpack. Sensible heat transfer occurs at the snowpack surface if there is a temperature difference between snow and air, being positive if the air is warmer than the snow and negative if it is colder. Latent heat is exchanged with the surroundings in case of phase change of water, being positive in case of freezing or condensation and negative in case of evaporation, fusion or sublimation. Both turbulent fluxes, sensible and latent heats, are enhanced on windy days when the cooled air near the snowpack surface is mixed with warmer air above. Ground conduction occurs at the bottom of the snowpack if there is a temperature difference between snow and soil, being positive if the soil is warmer than the snow and negative if it is colder. Advected heat transfer occurs during rain-on-snow situations, being positive if rain temperature is warmer than the snow and negative if it is colder.

Snow melt

Seasonal snowpacks gains density during the season through metamorphism until the melt period, which is triggered by an increased input of solar radiation and temperature. Absorbed energy from the surroundings raises the snowpack temperature to a point at which the snowpack is isothermal (i.e. temperature remains constant along the snowpack) at 0ºC. The energy required to bring the snowpack to isothermal conditions is the *cold content* of the snowpack. When the entire snowpack is isothermal ($\delta Q = 0$), further absorption of energy (i.e. positive values of δQ) is used to melt snow. Then, the interstitial space around snow structures is embedded into melt water, which promotes a fast melting because heat is better transferred in liquid than in air (Colbeck, 1973). At the time when the snowpack cannot retain any more melt water in pore spaces, additional absorption of energy causes water output, producing runoff, soil infiltration or evaporation. However, it is necessary to consider that this is a simplified sequence of events. For example, it is not uncommon that melt water percolates into deeper snowpack layers (where temperature is < 0ºC) and refreezes, or melting may start on the snowpack surface before reaching the isothermal conditions within. Last but not least, snowpack generally experiences a daily freeze-thaw cycle.

1.1.3 Snow conditions in a changing climate and its implications

Studies dealing with historical snow trends stated that current climate change has already altered key variables which drive both snowpack development and ablation, resulting in annual anomalies in snow cover mass and extent (Figure 1.5). Warming temperatures have increased the liquid fraction of precipitation (rain) at the expense of its solid fraction (snowfall) during winter (Mote et al., 2005). On the other hand, earlier snowmelt and melt-out date are taking place (Klein et al., 2016). This all results in reduced snow cover extent (Figure 1.6), diminished snow mass and shortened snowpack duration (Choi et al., 2010; Notarnicola, 2020; Pulliainen et al., 2020). As a consequence, new snow drought hot spots have emerged, including eastern Russia, Europe and the western USA (Huning & AghaKouchak, 2020). Current warming have affected snow cover differently at different elevations due to the elevation-dependent warming (Pepin et al., 2015). Observations show a general decline in low-elevation snow cover due to climate change in recent decades, in terms of depth and extent, although its inter-annual variability is high. On average, the duration of snow cover has declined 5 days per decade, with a likely range from 0-10 days per decade (Hock et al., 2019). While, generalasing, at higher elevations snow cover trends are insignificant or unknown. In addition, contrasting findings arise from global to local scales, where in the latter case no historical trends or even increasing snow magnitude have been found in certain areas (associated to spatio-temporal variability of climate) (Pulliainen et al., 2020; Schöner et al., 2019).

Other studies have investigated the potential impacts of climate change on future snowpack conditions. Projections point to a continuous decline of snow cover in almost all regions throughout the 21st century (Beniston et al., 2018;

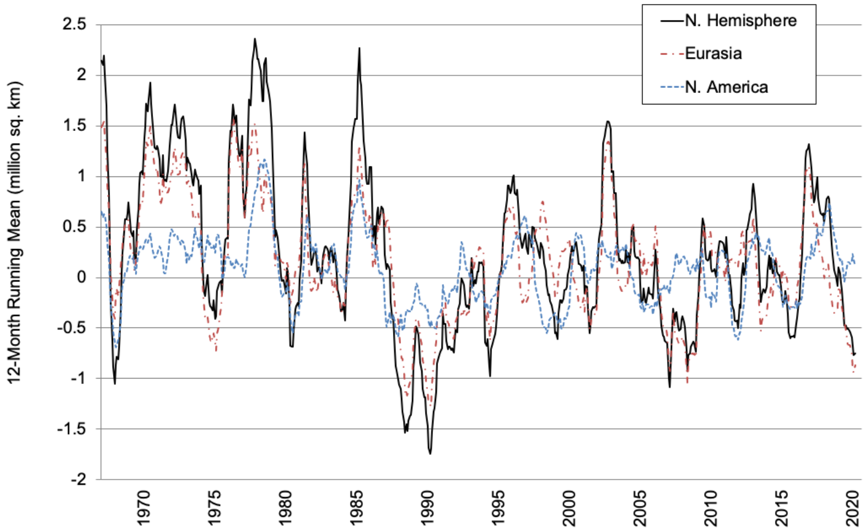

Figure 1.5: Twelve-month running anomalies of monthly snow cover extent (SCE) over Northern Hemisphere lands as a whole and Eurasia and North America separately plotted on the 7th month using values from November 1966 to December 2020. Anomalies were calculated from mean hemispheric SCE for the full period of record (25.1 million km^2). Credit: D.A. Robinson, Global Snow Lab of Rutgers University, New Jersey, USA.

Dedieu et al., 2014; Fyfe et al., 2017; Terzago et al., 2014; Vicuña et al., 2011). Hock et al. (2019) reported that a snow depth decrease by 10–40% is expected at low elevations for 2031–2050, regardless the future emission scenario considered, compared to 1986–2005. While for 2081–2100 these reductions are expected to increase by up to 50–90% considering the Representative Concentration Pathway 8.5[1]. The change in the date when snowpack disappears as the planet warms varies spatially, as evidenced by Evan and Eisenman (2021) who estimated that faster ablation rates will occur in coastal regions, the Arctic, the western USA, Central Europe and South America. All of the previously mentioned problems associated with water resources management in snow-fed basins may therefore increase as the climate continues warming (Simpkins, 2018; Whitaker et al., 2008).

Snow-dominated basins are especially sensitive to climate variability (Barnett

[1]The Representative Concentration Pathways (RCPs) comprise future scenarios that contain emission, concentration and land-use trajectories (Intergovernmental Panel on Climate Change, 2013). More specifically, RCP8.5 is a scenario in which the greenhouse gas concentrations, that closely correspond to the emissions trends, follows the upper range in the literature (i.e. high emission scenario) (van Vuuren et al., 2011).

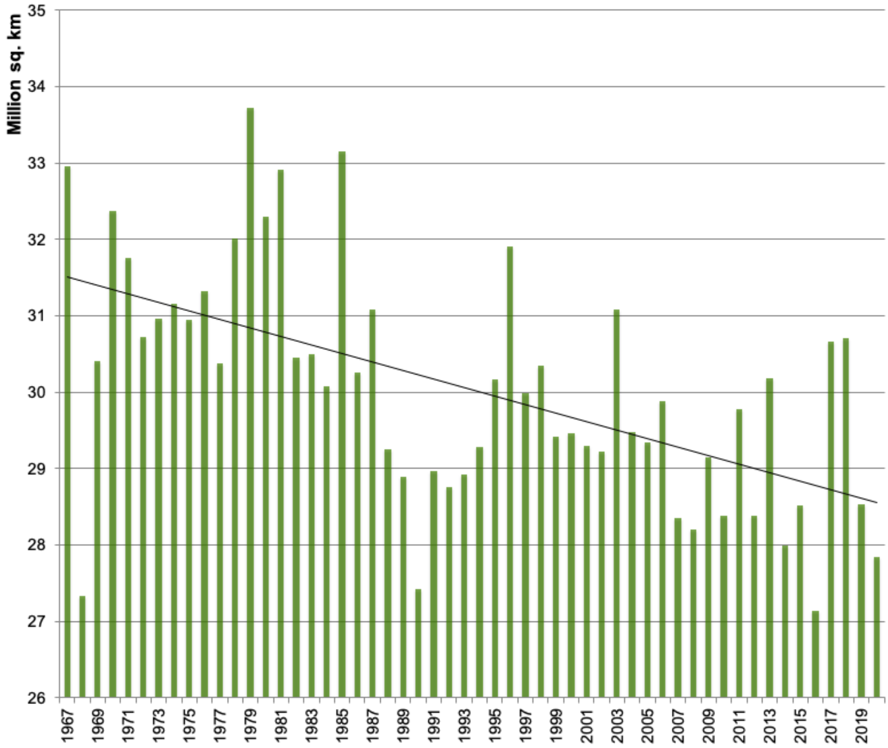

Figure 1.6: Spring Northern Hemisphere snow cover extent and linear least squares trends from 1967 to 2020. Spring season was calculated using 3-month means (March-April-May). Credit: D.A. Robinson, Global Snow Lab of Rutgers University, New Jersey, USA.

et al., 2005). In those areas, as well as surrounding lowlands, recent and projected changes in snowpack affect physical, biological and human systems, as I will describe below.

The most important effect is the influence on streamflow. The amount and seasonality of runoff in snow-fed basins have changed towards a generalised decoupling of mountain river regimes from headwater snowpack dynamics (López-Moreno et al., 2020). The previously mentioned changes in snow dynamics as a consequence of warming, have resulted in greater runoff in winter but lower runoff in spring and summer (Adam et al., 2009; Musselman et al., 2021). Earlier streamflow peaks are contributing to compromise reservoir storage (Barnett et al., 2005), even producing important shortages (AghaKouchak et al., 2014). That snow-related hydrological changes have produced local impacts on agriculture performance (Nüsser & Schmidt, 2017) and on hydropower generation (Einarsson & Jónsson, 2010; Kopytkovskiy et al., 2015; Weingartner et al., 2013). As a result of projected snow cover decline, streamflows in snow-dominated river basins will change further in amount and seasonality, producing enhanced negative impacts on agriculture, hydropower and water quality (Qin et al., 2020) (Figure 1.7).

Partly due to reduced snow cover, species composition and abundance in sea-

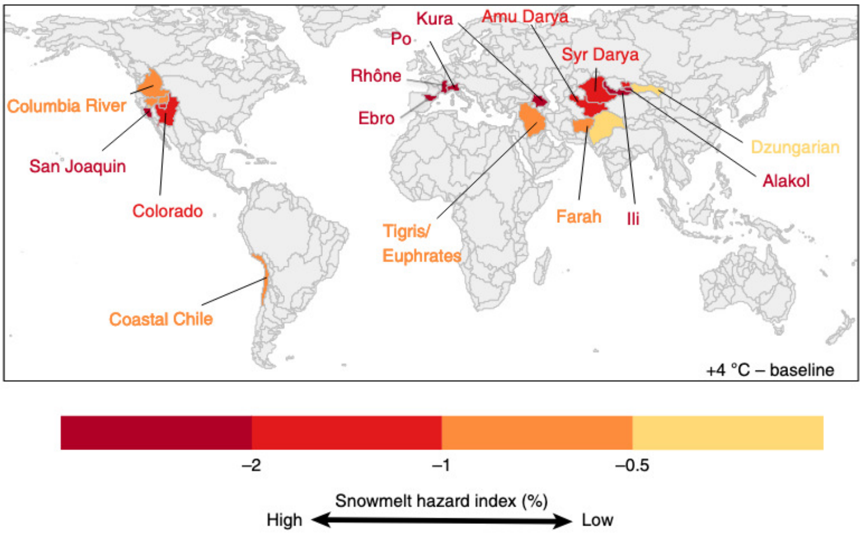

Figure 1.7: Basins at risk from changes in snowmelt under 4 °C warming, where irrigated agriculture is projected to be most vulnerable to snowmelt hazards. Snowmelt hazard index (SHI) is the product of projected decreases in the share of irrigation demand met by snowmelt runoff and expected increases in the share of demand met by alternative water sources. Credit: modified from Qin et al. (2020).

sonal snow-covered ecosystems have substantially changed, including plants, mammals, arthropods, birds, fish, lichen and fungi (Slatyer et al., 2021). Here, I provide some examples: the structure of several freshwater communities has been altered (Leach & Moore, 2014), new habitats have become available for absent plant species in the past (Bueno de Mesquita et al., 2018), the abundance of certain animals adapted to cold environments have declined (Pedersen et al., 2017), the plant productivity has increased in general (Wangchuk & Wangdi, 2018), local plant species richness has been increased through upslope migration (Winkler et al., 2016), some snow-dependent animal species ability to reproduce has been negatively impacted (Saalfeld et al., 2019), and foraging and predation relations have been altered (Atmeh et al., 2018). The current trends in snow-related changes in ecosystems are expected to continue, and the derived impacts are bound to intensify (Mustonen et al., 2018).

The frequency, magnitude and location of related natural hazards have been altered. In some regions, wet-snow avalanches have become more frequent (Pielmeier et al., 2013), rain-on-snow floods have increased at high elevations in winter (Freudiger et al., 2014) and, associated to early snowmelt, the quantity and magnitude of wildfires have increased (Westerling, 2016). On the other hand, people and infrastructure exposure to snow-related natural hazards has increased due to socioeconomic development, tourism and growing population (Haeberli & Whiteman, 2015). As snowpack continues to decline, most related natural hazards are projected to change in frequency, magnitude and areas affected (Agrawala, 2007; O'Gorman, 2014).

Snow-dependent economies have been negatively impacted in several regions. The functioning of low-elevation ski resorts has been threatened (Beaudin & Huang, 2014), some mountain routes have reduced their safety (Hoy et al., 2016), and the cultural aspects of mountain landscapes (aesthetic, spiritual, etc.) have been impacted causing a reduction of people well-being (Becken et al., 2013). Future snow cover changes are expected to continue negatively impacting recreational activities, tourism and cultural aspects of mountainous areas (Hendrikx et al., 2012). Some adaptation measures have been implemented to deal with the impacts of snow changes in tourism, agriculture or water supply, but nowadays there is still limited evidence on their effectiveness (Hock et al., 2019; Spandre et al., 2019; Sterle et al., 2020).

1.1.4 Snow in the Pyrenees

Mountainous regions that are under the influence of the Mediterranean climate receive most of the winter precipitation as snow, which is released as melt water in the spring and summer. The high inter- and intra-annual climate variability of Mediterranean regions results in significantly different hydrologic processes from those found in other snow-influenced regions. Fayad et al. (2017) reviewed the particularities of Mediterranean snowpacks, concluding that: (1) they show high inter- and intra-annual variability in terms of snow depth, snow density and snow water equivalent; (2) they experience higher densification rates; (3) radiation fluxes dominate their energy and mass balances, accounting for most of the energy available for melt, while the contribution of sensible and latent heat fluxes becomes notable towards the end of melting season; (4) snow sublimation predominates in the high-elevation areas while snowmelt dominates in the mid- to low-elevation terrain; and (5) the melting process is affected by heatwaves, dust deposition and rain-on-snow events. By the time snow melting happens, precipitation is scarce in these regions, since the climate of the Mediterranean is hot and dry during the summer and mild and wet during the winter (Lionello et al., 2006). Snowmelt smooths seasonal variability of Mediterranean streamflows, as a result of melting runoff contributions during the warm season, which in other case would diminish steeply. Therefore, snowmelt becomes an essential water resource for ecosystems and human activities settled in Mediterranean mountains and downstream areas (López-Moreno et al., 2008). For example, snowmelt provides essential runoff during the growing period of crops, being the agriculture a major activity in these regions. Besides, future scenarios for water resources in the Mediterranean region are expected to challenge its sustainability, quantity, quality and management (García-Ruiz et al., 2011).

The Mediterranean region is expected to be one of the most sensitive regions to climate change (Giorgi, 2006). Climate change over this region consists of a pronounced warming and a sharp decline in annual precipitation at the end of the 21st century, both especially marked in the warm season (Giorgi & Lionello, 2008). The Mediterranean mountains are no exception to it (Nogués Bravo et al., 2008). Currently the concern about their response to climate change is strengthened considering the rate of warming increases with elevation (Pepin et al., 2015). Snowpacks of Mediterranean mountains are highly sensitive to temperature increase, and among them, Pyrenean snowpacks are expected to be the most impacted by climate change (López-Moreno et al., 2017). The snow distribution in the Pyrenees shows large longitudinal, latitudinal and elevational gradients (Figure 1.8). Snow probabilities, which mean the average number of days covered by snow per year, increases from the southeast towards the northwest (Alonso-González et al., 2020a). This

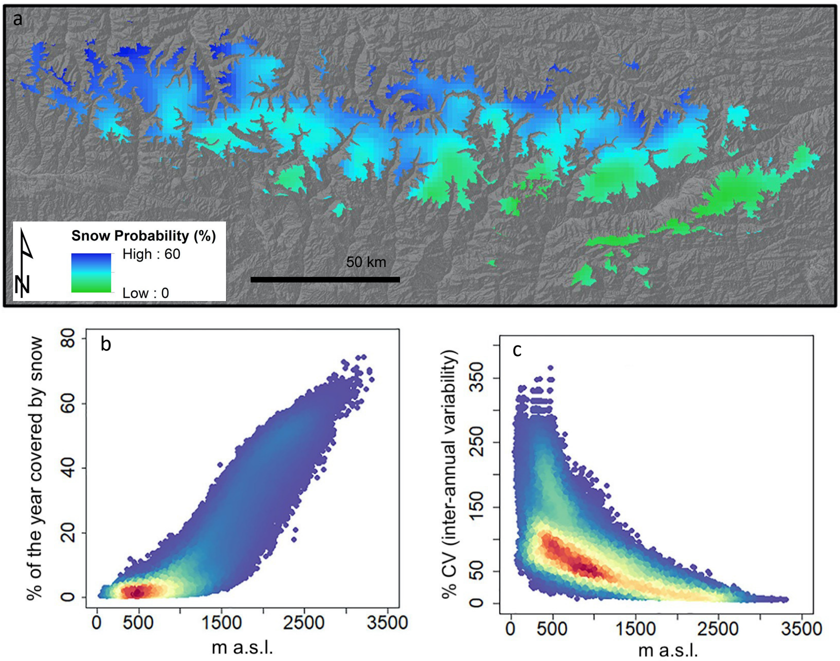

Figure 1.8: (a) Pyrenean spatial pattern of the average number of days covered by snow per year (temporal snow probability) during the 2000-2014 period. (b) Distribution of the temporal snow probability values along the elevation gradient in the Pyrenees. (c) Distribution of the inter-annual variability of the temporal snow probability (CV values) along the elevation gradient in the Pyrenees. Scatterplots (b, c) colours refer to the relative density of points, ranging from blue (lower values) to red (higher values). Credit: elaborated by compiling figures taken from Alonso-González et al. (2020a).

oblique gradient of Pyrenean snow distribution reflects, on the one hand, the north-south precipitation transition induced by the topographic barrier effect of this range to the winter weather types from the north and northwest (Serrano & Moreno, 2017), and on the other hand, the east-west Mediterranean-Atlantic gradient characterised by higher winter-spring precipitation westwards. The ground is snow-covered at least 50% of the time above 1600 m a.s.l. between December and April (Gascoin et al., 2015). Furthermore, as elevation increases, lower inter-annual variability of the temporal snow probability is observed (Alonso-González et al., 2020a). The winter North Atlantic Oscillation has a large influence on annual snowpack accumulation and duration on the southern slopes of the Pyrenees, controlling the direction of the wet air masses from the west and southwest related to this atmospheric pattern

(Alonso-González et al., 2020b). In addition, African dust episodes are not a rare event in these mountains, as a consequence, the deposition of these mineral dust particles produces significant spatial variability of snow albedo even at very small scales (Pey et al., 2020). Pyrenean snowmelt water contributes $\sim$40% of the spring runoff for the Ebro headwaters, being an essential resource for hydropower generation and lowland agriculture (López-Moreno & García-Ruiz, 2004). Besides, snow supports in the Pyrenees the major economic activity for several valleys throughout more than 30 ski resorts (Gilaberte-Búrdalo et al., 2017). To the date, climate change has impacted snow dynamics in the Pyrenees, where snowpack depth and duration has been reduced, and also, an earlier and faster snow melting is taking place (López-Moreno et al., 2020; Morán-Tejeda et al., 2017; Morán-Tejeda et al., 2014). It has been already observed a reduced water availability in the southern Pyrenees over the 20th century in response to the negative trend of snow accumulation, together with the occurred changes in precipitation, temperature and increased vegetation density in headwaters areas (López-Moreno et al., 2008). Fluvial regimes also reflect the mentioned changes in Pyrenean snow dynamics, with a reduced importance of spring discharge and the earlier occurrence of high waters peak (Morán-Tejeda et al., 2017; Sanmiguel-Vallelado et al., 2017). All of these changes occur as water demand increases, especially for agricultural activities. The evidence is clear: water managers have adapted long ago a reservoir management strategy based on a dramatic reduction in the water released downstream the dams, which corresponds to the minimum ecological flow for most of the year, to address with the progressive reduction of Pyrenean discharge (López-Moreno et al., 2004).

1.2 Mountain forests

Mountain[2] forests definitions usually include altitude, slope and local elevation range (Schönenberger & Brang, 2004). On a global scale, mountain forests can be defined as those forests growing in slopes located at 300–2500 m a.s.l. that show pronounced changes with elevation increment within a short distance or, as those forests growing at 2500 m a.s.l. or higher, regardless of the slope (Kapos et al., 2000). Thus, steep mountain forests can occur in the lowlands, especially on volcanic islands as the Caribbean where they occur at 300 m a.s.l. Whereas there are sites in certain tropical and subtropical mountain chains where mountain forests grow at elevations over 4000 m a.s.l. (Kappelle, 2004). Mountain forests cover 9 million km^2 on Earth's surface, comprising the 23% of total forest covering. In Europe, mountains cover more than 40% of the territory (Price et al., 2004), of which 41% is covered by forests (Price et al., 2011a). They are present on every continent, except Antarctica, and in every climatic zone. Both coniferous and broadleaved species can compound mountain forests. Forest growth is generally slower in mountains than in the surrounding territories, due to the thoughest environmental conditions; including more extreme climates, shallower soils and shorter growing seasons (Körner, 2003). They are hotspots of biodiversity and provide essential ecosystem services to human communities settled in mountains and surrounding areas such as regulation of water cycles, carbon uptake and soil formation, among others (Millennium Ecosystem Assessment, 2005). Furthermore, such areas are considered as *natural laboratories*, since mountain ecosystems are highly sensitive to global change (Loeffler et al., 2011). From a hydrological point of view, mountain forests strongly influence the quantity and quality of water supplies in those areas and lowlands (Hewlett, 1982). Mountain forest cover has experimented two different trends in recent decades: steady loss in developing countries due to deforestation, principally in tropical areas,

[2] Two well-stablished definitions of mountains are below indicated. In Blyth (2002), the world's mountainous terrain is defined by elevation alone if $>$ 2500 m a.s.l. or by a combination of elevation, slope and local elevation range at lower elevation (i.e. 1500–2500 m a.s.l. and slope $> 2^{\circ}$, 1000–1500 m a.s.l. and slope $> 5^{\circ}$ or local elevation range (7 km radius) $>$ 300 m, 300–1000 m a.s.l. and local elevation range (7 km radius) $>$ 300m). On the other hand, Körner et al. (2011) made no distinction by elevation, but apply a minimum 200 m elevational amplitude among $3x3 = 9$ grid points of $30''$ in $2.5'$ pixels.

and progressive expansion in industrialised countries by means of plantations and forest encroachment into grassland and scrubland after agricultural land abandonment (Price et al., 2011b).

1.2.1 Mountain forests ecosystem services

Ecosystem services refer to the benefits that people directly or indirectly obtain from the nature (Millennium Ecosystem Assessment, 2005). They can be categorised as provisioning, regulating, supporting, or cultural services (Haines-Young & Potschin, 2012). Based on Glushkova et al. (2020), the ecosystem services provided by mountain forests include the following:

Provisioning services: Mountain forests can provide wood (for use as fuel or as building material), food (e.g. berries, mushrooms, wild-game meat, honey, insects and fruits), medicines, and pasture for livestock (Butt & Price, 2000).

Regulating and supporting services: Mountain forest have a key role in preventing soil erosion and they actively reduce snow and rock avalanches since forest trees act as physical barriers that impede downslope mass movements, and passively mitigate their impacts below (Dorren et al., 2004). Mountain forests condition the hydrological cycle: they have a complex role in affecting evapotranspiration, soil moisture, surface roughness, water interception from precipitation or mist, and snow processes (Band et al., 1993; Juez et al., 2021). I will explain the latter below, in Subsection 1.3.1. Mountain forests exerts an active but slow mitigation of climate change through CO_2 absorption in biomass and soils (carbon sequestration), explained by the slow tree growth and biochemical processes that take place at high altitudes (Price et al., 2011c). Many of them are also global hotspots for biodiversity providing several habitats for different species and functioning as corridors and refuge areas (Estreguil et al., 2013).

Cultural services: Mountain forests also provide non-material benefits, including recreational and tourism potential (Peña et al., 2015). Moreover, several human communities settled in mountainous areas link their traditions and beliefs to these environments. Hence, in mountain regions around the world, forested areas are considered as sacred and are protected, often associated with strong aesthetic, mythological, cultural and spiritual values (Hong et al., 2002).

1.2.2 Influencing factors on tree growth in mountains

It is known that montane vegetation shows a strong elevational zonation since von Humboldt and Bonpland (1807) studies, at least. Environmental conditions (temperature, humidity, soil properties, wind and solar radiation) are linked with elevation, defining bioclimatic levels. In the course of evolution, plants developed adaptations to the particular conditions obtaining at each bioclimatic level and, as a result, vegetation changes at distinct elevations forming vegetation belts (Figure 1.9). These changes in climatic parameters are exacerbated in mountains, where steep elevation gradients take place. Four major vegetation belts can be defined from foothills to summits, with varying vegetation among them: colline (on the foothills, if its vegetation differs from that of the lowland zone), montane (at mid-mountain), subalpine (just below the forest limit) and alpine (above the forest limit) (Pedrotti, 2013). Along the mountainside, species richness decreases with increasing altitude, though endemism increases due to topographic isolation (Pedrotti, 2012).

Tree's crown, stem and roots are able to react to environmental conditions and determine the timing, rate and dynamics of tree growth. Stem radius changes are driven by two main processes: the growth of tree tissues and their hydration (i.e. shrinking and swelling) (Tatarinov & Čermák, 1999). Therefore, stem radius partly reflects the changes in stem water content, which are widely correlated with daily precipitation among others (Mäkinen et al., 2003). Here it is noteworthy to mention that tree growth occurs in two ways, including primary and secondary growth. Primary growth refers to root and shoot development which results in increases in height and length. While secondary growth refers to root, stem and branch increases of thickness. When we peel the bark off a branch, a white layer appears below the bark and above the wood: this is the cambium or cambial zone. Every year, the cambium creates new wood (i.e. xylem), on the inside and new bark on the outside (i.e. phloem or living bark) (Prislan et al., 2013). Therefore, xylogenesis is

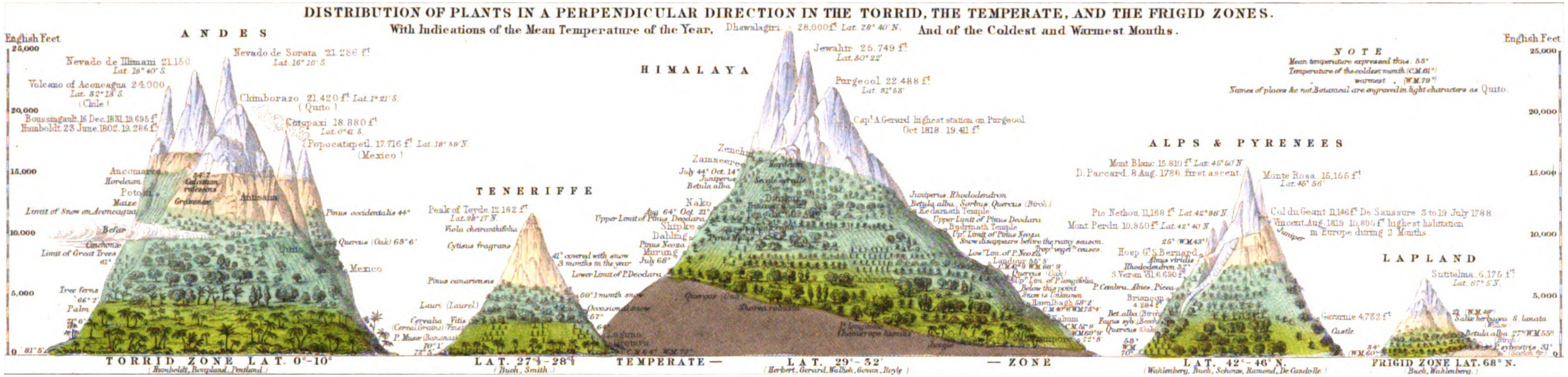

Figure 1.9: Altitudinal transitions between different types of forests within different latitude mountain systems, including the Andes, Tenerife island, the Himalaya, the Alps, the Pyrenees and Lapland. Credit: Johnston (1850).

the process of wood formation, which in conifers is made of two types of cells: tracheids (they constitute > 90% of the tissue and perform both the water conduction and the mechanical support) and parenchyma cells (they store and transport compounds). In temperate and cold seasonal regions, trees develop annually concentric structures called *tree-rings* or growth rings (Rathgeber et al., 2016). Dendrochronology is the study of tree-ring variables through the dating and measurement of annual rings. If growing conditions are favorable, the developed annual rings are wider than those created during poor growth conditions (Fritts, 1976). Nevertheless, tree-ring width also reflects internal tree factors, as age. As a tree gets older, its growth decreases (Serre, 1979). Xylem radial growth rate generally peak around the summer solstice, when the photoperiod is maximal, if we do not take into account environmental stress. This period usually marks the transition between the wood produced at the beginning of the growing season (i.e. earlywood) and the wood produced at the end of the growing season (i.e. latewood) (Cuny et al., 2014). Both woods anatomically and functionally differs, and that differentiation is driven by tracheid morphology (Rathgeber et al., 2006), since earlywood is formed by wide and thin-walled cells while latewood is formed by narrow and thick-walled cells (this pattern is generally observed in conifers) (Figure 1.10). It is important to note that the timing of actual xylem development differed from the timing of changes in stem radius (Mäkinen et al., 2003). The xylem carries water and nutrients from the root upward, while the phloem carries sugars from the leaves downward (Kozlowski & Pallardy, 1996). Through photosynthesis, trees produce sugar using sunlight, water and carbon dioxide. Sugar can be stored in the stem and roots as starch. Both sugar and starch (i.e. carbohydrates) are used to provide energy for tree maintenance (e.g. respiration, chemicals production, cell repair) and growth. Tree growth fixes more carbon from the atmosphere than respiration released back into it, thus world's forests constitute a large and persistent net sink of carbon (Pan et al., 2011).

Tree growth and forest productivity[3] are largely controlled by climate condi-

[3]Forest productivity refers to woody biomass accumulation (tons per hectare), which is also expressed as wood volume increment (cubic meters per hectare).

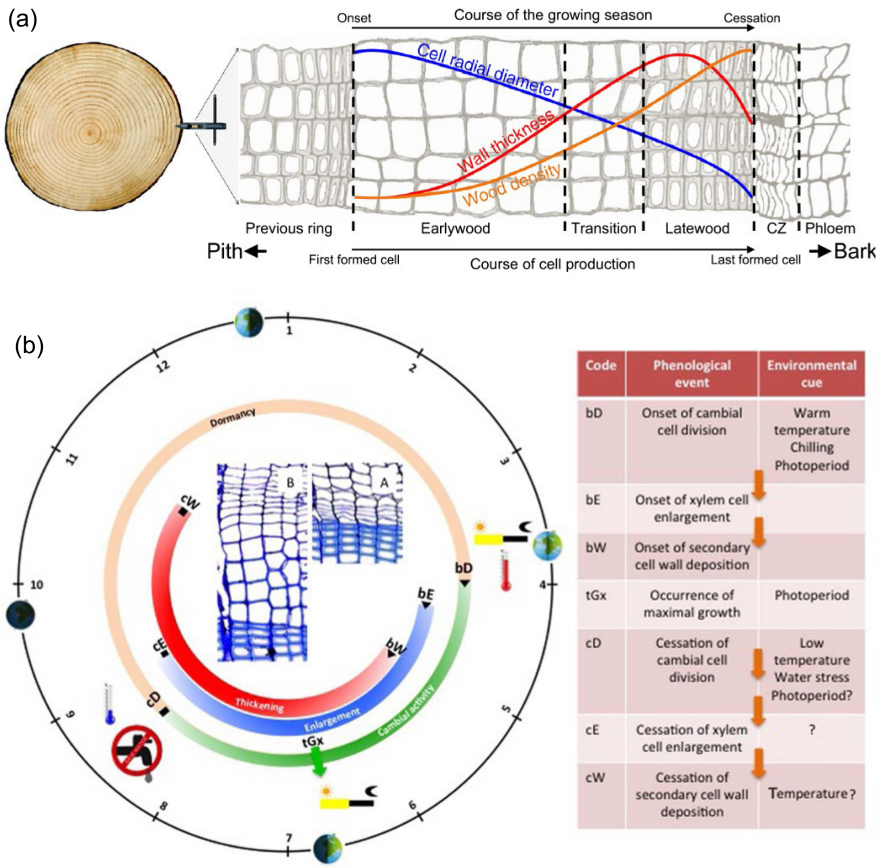

Figure 1.10: (a) Typical tree-ring structure in conifers. Between the latewood and the phloem is the cambial zone (CZ). Credit: Cuny et al. (2014). (b) Seasonal cycle of cambial activity and tree ring formation in temperate coniferous trees. The black circle represents the solar calendar; the orange/green circle illustrates the seasonal evolution of cambial activity, while the blue and red circles illustrate the seasonal evolution of wood formation (enlargement and thickening period respectively). Wood formation critical dates are listed in the adjacent table along with their corresponding environmental cues (question marks indicate uncertain roles or missing evidence). Arrows indicate causal relationships between phenological phases. In the center, two cross sections show the cambium and the xylem of a Scot pine tree during winter (A), and spring (B). Credit: Rathgeber et al. (2016).

tions during the year of ring formation and the previous year, as well as by past climate conditions and historical management (Marqués et al., 2021). A major limiting factor for forest growth and development in mountainous areas, including treeline formation, is cold air temperature (Harsch & Bader, 2011; Körner, 2012). With elevation increment, air temperature decreases reaching a point where tree growth is no longer possible due to a very short growing season. Moreover, mountain soils are usually shallower at higher altitudes, poorer in nutrients, experiment rapid erosion and usually show low water-holding capacities, which neither help to forest development (Müller et al., 2016). Thus, elevation determine forest stand structure and composition in mountain forests, as well as tree growth and form. Tree growth requires a minimum length of the growing season of 94 days and a mean of 6.0–6.4ºC of air temperature across all these days (Paulsen & Körner, 2014). Where these conditions are hardly fulfilled because of altitude, mountain forests experienced a strong decline in tree height and density, delimiting an ecotone called *treeline* or forest limit (Holtmeier, 2009). These areas are characterised with marked low air temperature, short growing seasons, strong winds and heavy snowfalls, hence, beyond this altitude forests have big difficulties for survival and regeneration. Although air temperature during the growing season is the primary factor causing the treeline position at global scale, other second-order factors significantly affect treeline formation at landscape scale, as nutrient limitation, insufficient carbon supply, limited regeneration, forest management, climatic stress (wind, snow abrasion) or natural disturbances (Camarero et al., 2015; Speed et al., 2010; Treml & Chuman, 2015; Wieser & Tausz, 2007). The altitude of the treeline varies greatly around the world, depending on latitude and climate, ranging from 700 m a.s.l. in the far North (e.g. northernmost white spruce in Alaska reach a latitude of ~68.7°N (Wilmking & Juday, 2005)) to 4800–4900 m a.s.l. in certain areas of the sub-tropical Andes and in the southeast Tibet (He et al., 2016; Miehe et al., 2007).

Growth-climate relationships in mountain forests vary from species to species, from site to site, and from year to year. Low air temperature during the cold season can damage the living tissues of trees (Jobbágy & Jackson, 2000). To avoid this fact, trees go through a period of dormancy to survive the harsh environmental conditions during winter in temperate and cold regions, while in tropical regions trees may grow all year round (Breitsprecher & Bethel, 1990; Delpierre et al., 2016). Together with increased temperature in spring and summer, photoperiod acts as the main environmental driver of the end of dormancy to the active period (i.e. growing season) (Körner, 2006). Warm spring and summer air temperatures lengthen the growing season by accelerating snowmelt, which increases soil temperatures, and all together can promote faster leaf, shoot and stem growth (Körner, 1998). Soil temperature influences nutrient uptake and root growth which may be reflected in aboveground tree growth rate (Weih & Karlsson, 2001). In xeric sites of subtropical and Mediterranean mountains, tree establishment and later growth can be strongly controlled by soil moisture availability, which depends on rainfall regime and/or snowmelt timing (Andrus et al., 2018; Villalba et al., 1994). Particular snow influences on forest dynamics will be introduced further in this chapter (Subsection 1.3.2). Slope aspect and steepness influence air temperature, soil moisture and incoming solar radiation, being major factors influencing tree growth. Thus, topographic position can determine the distribution and composition of mountain forests (Villalba et al., 1994). For example, in the Northern Hemisphere, earlier snow depletion and warmer summers may benefit tree growth on north-aspect (shaded) hillsides, while could also promote drought conditions on south-aspect (sunny) hillsides (Peterson & Peterson, 2011). Furthermore, it has been hypothesised for a long time that CO_2 may exert a fertilisation effect of tree growth, but is still unclear if current rising CO_2 concentrations promote photosynthetic rates (Hararuk et al., 2019; Nicolussi et al., 1995).

Natural and anthropogenic disturbances are critical drivers of composition, structure and functioning of mountain forests. Both types of disturbance regimes vary over time (Bebi et al., 2017; Senf & Seidl, 2021). Moreover, natural disturbances are highly climate-sensitive (Dale et al., 2001). One example of the strong influence exerted by human activities on forest dynamics is the fact that forest cover has significantly increased since 19th century due to the abandonment of agricultural activity in several mountain ranges of industrialised countries (Kozak, 2003; Rudel et al., 2005). In European mountains forests, the most frequent natural disturbances are produced by windstorms, insect outbreaks, snow avalanches and fires (Kulakowski et al., 2017). Dominant types of disturbances vary among regions, forest type, climate, topography, and the degree of cultural landscape modification. Wind disturbances have been a relevant natural driver of mountain forest dynamics in Europe over the last several centuries (Janda et al., 2017). Outbreaks of bark beetles and defoliators affect European forests dominated by pine, fir and spruce, among others, where low temperatures or poor forest connectivity are not a limitation (Stadelmann et al., 2013). In the ancient times, fires were spread in association to various land-use practices, as agriculture, pasture clearance and charcoal production (Vannière et al., 2008). The later cessation of transhumance during the late 19th century in Europe could also promote wildfire incidence and subsequent deforestation (Camarero et al., 2021). In recent centuries, the size and frequency of fires has declined in general, because of the implementation of fire management and increased forest fragmentation (Conedera et al., 2017). Lastly, favourable conditions for avalanche releases below treeline have decreased during the last decades (Teich et al., 2012), as a result, tree growth has been enhanced in the affected areas and the fragmentation of those forested landscapes has been reduced (Kulakowski et al., 2006).

1.2.3 Mountain forests responses to climate change

Mountain forests are particularly exposed to warming as a consequence of their location in high elevation areas (Pepin et al., 2015). However, the high topographic complexity of mountainous areas modulates the impacts of climate change on mountain forests, in other words, spatial heterogeneity contributes to ecological resilience (Albrich et al., 2020). The combined effects of recent increases in temperature and decreases in water availability in mountain forests have been already reported, including: changes in community composition and distribution (Lenoir et al., 2010), the establishment of new forest species (Walther et al., 2007), declining resilience to wildfires (Stevens-Rumann et al., 2018) and changes at the treeline (Vittoz et al., 2008) (Figure 1.11). Vegetation shift is an adaptation mechanism that allows populations to find climatically suitable sites. However, non-climatic factors can limit such shifts, including soil properties, nutrient availability, grazing, landscape fragmentation or species particularities (e.g. mycorrhizal symbiosis, dispersal capacity, etc.) (Camarero et al., 2015). Similarly, the colonization of new forest habitats, rather than previously forested habitats, may not be successful (Ibanez et al., 2009). Furthermore, recent warming has increased the size and frequency of natural disturbances across Europe mountains forests (Janda et al., 2017; Panayotov et al., 2017).

Future climate conditions are expected to produce changes in dominance of some tree species (Périé & de Blois, 2016). For example, simulations show that current dominance of conifers and abundant large trees in Central Alps mountain forests will experience a transition towards a broadleaved-dominate system with smaller trees (Albrich et al., 2020). Under warmer conditions, an upslope migration of the treeline is expected, as well as a tree encroachment and densification within the treeline ecotone (Harsch et al., 2009). However, forest expansion into alpine areas because climate warming can be strongly limited by geomorphic and geologic factors (Macias-Fauria & Johnson, 2013). In moisture-limited mountain forests, tree recruitment and tree growth is likely to decline due to drought-induced dieback, which may constrict certain species distributions (Allen et al., 2010; Andrus et al., 2018; Pompa-García et al., 2021). Warmer temperatures during growing season are expected to enhance growth rates, and thus, wood formation (Millar et al., 2004). But increasing temperatures will also drive phenology toward the species photoperiod threshold (Basler & Körner, 2012). Besides, warmer winters may enhance the survival possibilities of young trees (Klimeš, 2006). Therefore, winter warming is considered one of the most relevant drivers of treeline advance (Harsch et al., 2009). The expected forest expansion will improve the protection against natural hazards (Price et al., 2011c). While rising temperatures benefit tree growth, they also may enhance the expansion of forest pests to higher altitudes, affecting forest that are currently too cold to support beetle populations (Logan et al., 2003). In addition, regions that are becoming warmer but also drier, are likely to have higher risk of fire (Rocca et al., 2014). All in all, it is likely that the frequency and extent of forests disturbances will be promoted with future climate conditions, increased forest closure and expansion (Millar & Stephenson, 2015; Seidl et al., 2014). Climate change impacts on mountain forest may be irreversible, since cool-adapted specialists are expected to not being able to recover their dominance because warm-adapted

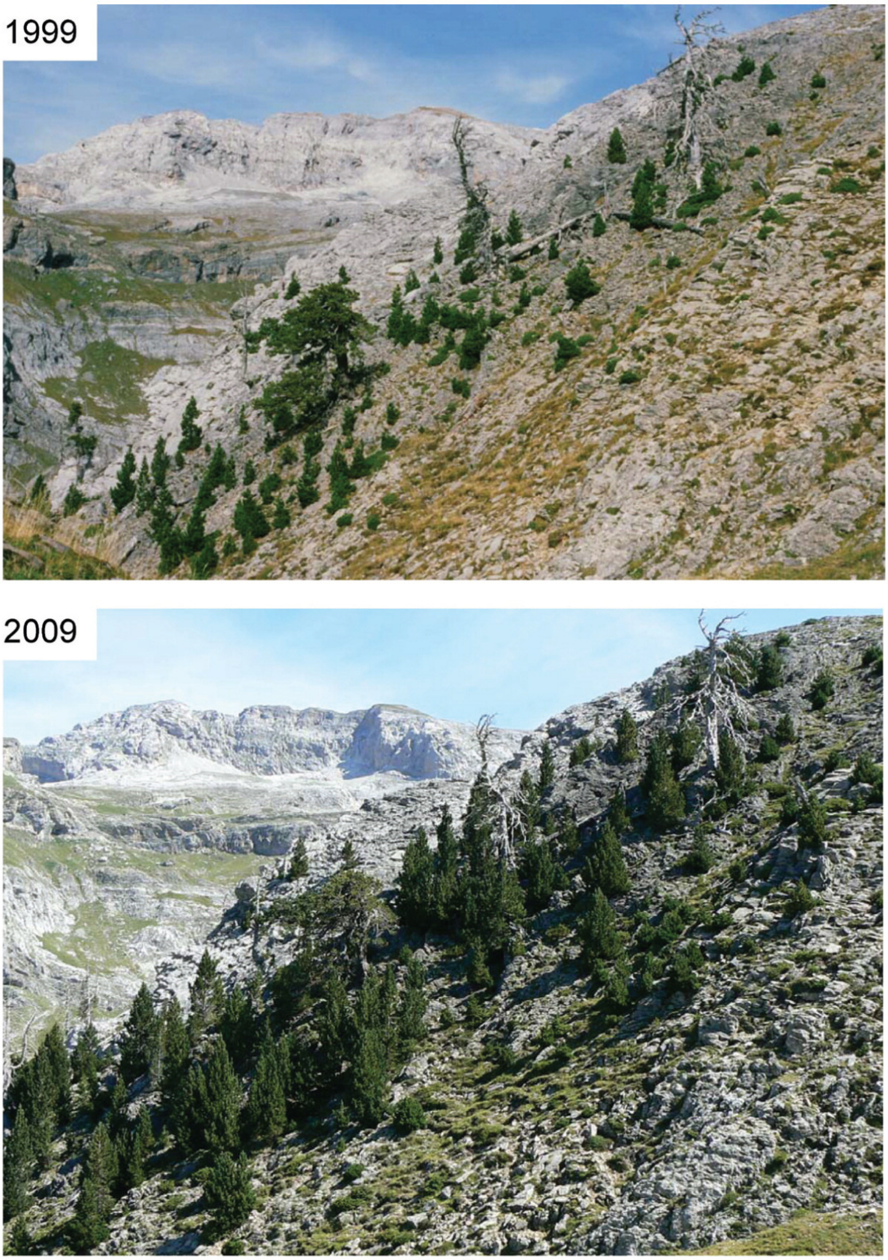

Figure 1.11: Tree encroachment at a Pyrenean treeline between 1999 and 2009 (Foratarruego, Central Spanish Pyrenees, Spain). Credit: Camarero et al. (2015).

generalists will be widely expanded (Albrich et al., 2020). Nevertheless, local effects of climate change on mountain forests can be heterogeneous due to the variability of current stand characteristics (Bircher, 2015), microclimatic conditions (Engler et al., 2011) and intrinsic spatial heterogeneity of climate change in mountain regions (Shafer et al., 2005).

1.2.4 Pyrenean mountain forests

Over half of the Pyrenees area is covered by forests (Price et al., 2011a). Pyrenean forests are classified into the temperate mountain systems of Europe, together with the Alps (FAO, 2012) (Figure 1.12). The overall temperate domain lies in a region where >10ºC is the average temperature from 4 to 8 months of the year. However, the temperate mountain systems share several characteristics of the boreal domain, as they are snow covered during a large part of the year, and often are also composed by conifer forests (de Rigo et al., 2016).

The vegetation zonation of the entire Pyrenean mountain system was described in Ninot et al. (2007) from a geobotanic point of view. A summary of its characteristics is following presented. The high mountain zone, or central core, is characterised by Boreo-Alpine flora. The surrounding area comprises one Atlantic territory, one Mediterranean and one Submediterranean area (Figure 1.13a). The cliseries show a gradual shift from the Atlantic to the Boreo-Alpine flora on most of the French northern side, as well as on the Iberian side in eastern Navarre and in mild northeastern Catalonia. In the rest of the Iberian southern side and in the Pre-Pyrenees, there is a complex transition from the Mediterranean lowlands, through the Sub-Mediterranean and Atlantic domain, to the Boreo-Alpine flora. An illustrative example of the most general associations along the altitudinal gradient on the Iberian side of the axial Pyrenees is shown in Figure 1.13b. Within the same belt, potential vegetation experience noticeable shifts depending on lithologic character of soils and exposition mainly, but also other factors such as topoclimates or continentality may induce variability. Focusing on dominant tree species of the potential forests of this mountain range, the coline belt (600–900 m a.s.l.) holds Atlantic mixed woodlands (*Quercus robur* or *Fraxinus excelsior* in cooler aspects and *Quercus petraea* or *Quercus humilis* in drier areas) and Mediterranean sclerophyllous forests (*Quercus rotundifolia* in the inland Mediterranean area and *Quercus ilex* on the Mediterranean maritime part

Figure 1.12: Ecological zonation of European forests elaborated by the Food and Agriculture Organisation of the United Nations (FAO). The Pyrenees mountain system is labelled. Credit: modified from FAO (2012).

of the chain). The submontane belt extends to 1110–1300(1500) m a.s.l. in the Iberian side and in the Pre-Pyrenees, and holds forests of marcescent oaks (*Quercus humilis*, *Q. faginea* and hybrids) and related pinewoods (*Pinus nigra* subsp. *salzmannii*, *Pinus sylvestris*). The montane belt, whose upper limit is at 1600–1700 m a.s.l. on north-facing slopes and 1700–1900 m a.s.l. on south-facing slopes, holds beechwoods of *Fagus sylvatica* and mixed forests of *F. sylvatica* and *Abies alba* (in areas with Atlantic influence or most humid places on the Iberian face), acidophilous oak woods (*Q. petraea*, common on the Atlantic side and restricted to acidic bedrocks of central and eastern Iberian face), pinewoods of *P. sylvestris* (on the Iberian side) and fir forests (of *A. alba* in areas with mild and subcontinental bioclimate were *F. sylvatica* is rare or absent). The subalpine belt is mainly the domain of the *Pinus uncinata* pinewoods, which extent to 2300–2500 m a.s.l. up to the treeline, while *A. alba* and a few deciduous trees can accompany it in the lower part of the belt. The upper edge of the subalpine belt gives way to a typical alpine mosaic with shrub krummholz pine (small-grown and deformed individuals encountered at the treeline ecotone), alpine scrublands and grasslands (tundra) (Camarero et al., 2000).

Therefore, Mountain pine (*Pinus uncinata* Ram.) or *pino negro* in Spanish forms the treelines in the Pyrenees and sets the upper limit of forests in the Iberian Peninsula (Bosch et al., 1992; Camarero, 1999; Cantegrel, 1983). The species name, *uncinata*, refers to the asymmetrical and hook-shaped scales present on the seed cones (Figure 1.14). It is treated either as an independent species or as a subespecies of the Dwarf Mountain pine (*Pinus mugo* Turra), i.e. *P. mugo* subsp. *uncinata* (Lewandowski et al., 2000). *P. uncinata* is native of the Pyrenees, Western Alps and some scattered populations in the NE Iberian Peninsula mountain ranges, and widely overlaps with *P. mugo* subsp. *mugo* in eastern Swizterland and western Austria (Figure 1.14). It is an evergreen, shade-intolerant, conifer that grows at high altitudes (Ruiz de la Torre et al., 1979). Mature individuals are 12–20 m height, showing straight trunks of 0.5–1 m in diameter. *P. uncinata* is able to hybridize with *P. sylvestris* where they co-occur, since *P. sylvestris* dominates at lower elevations than *P. uncinata* in the Pyrenees (Ruiz de la Torre et al., 1979). This pine species is long-lived and slow-growing (Bosch et al., 1992; Cantegrel, 1983). Its growing season starts at the end of May and ends in October, with major tree-ring formation occurring between May and July (Camarero et al., 1998). *P. uncinata* growth has been widely reported to be enhanced by warm springs and prior early autumn temperatures, while the influence of other climate variables may depend on local factors (Creus Novau & Puigdefábregas, 1976; Galván et al., 2014; Gutiérrez, 1991; Ruiz Flaño, 1989). The subalpine belt of the Pyrenees has been intensively deforested for centuries to extend

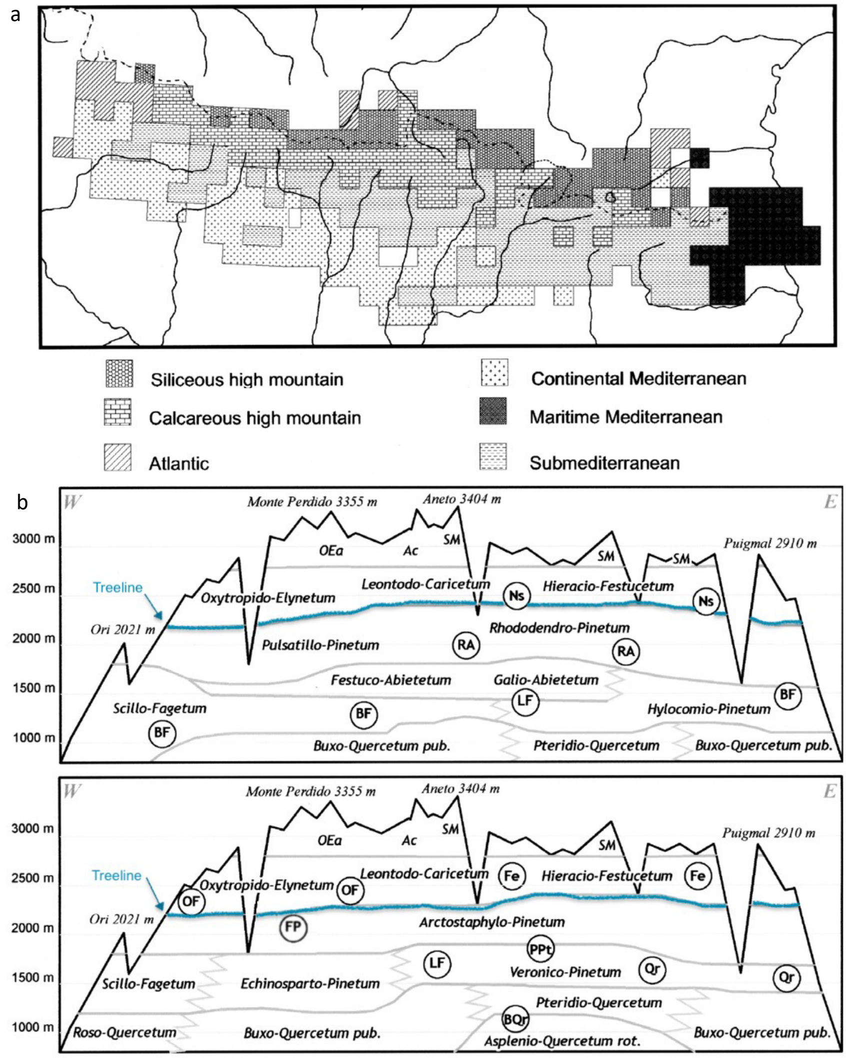

Figure 1.13: (a) Floristic territories of the Pyrenees. (b) Distribution of the main potential domains in the Iberian side of the axial Pyrenees on the north-facing slopes (top) and on south-facing slopes (bottom). OEa, Oxytropo-Elynetum var. of *Artemisia umbelliformis*; Ac, Androsacion ciliatae; SM, Saxifrago-Minuartietum sedoidis; Ns, Nardion strictae; RA, Rhododendro-Abietetum; BF, Buxo-Fagetum; LF, Luzulo-Fagetum; OF, Oxytropido-Festucetum; Fe, Festucion eskiae; FP, *Festuca scoparia-Pinus uncinata* community; PPt, Primulo-Pinetum teucrietosum; Qr, Quercion roboris; BQr, Buxo-Quercetum rotundifoliae. Blue lines indicate the treeline location in the mountain range. Credit: modified from Ninot et al. (2007).

the pasture surface, a process called *alpinisation*. This process was more pronounced in on the Atlantic face and in the valleys with softer relief of the

Figure 1.14: (a) Botanical illustration of *Pinus uncinata*. Credit: Philippe Bougeret, Plantes et Fleurs, Planche nº 13 (https://plantes.bougeret.fr). (b) Photography of some young *P. uncinata* individuals growing in the Central Spanish Pyrenees at 2100 m a.s.l. Credit: Sanmiguel-Vallelado, A. (c) Distribution map of *Pinus mugo* subespecies. Credit: The European Commission Joint Research Centre (Caudullo et al., 2017).

Iberian face, and during the Middle Ages (Ninot et al., 2007). Transhumance was the main deforestation factor in the subalpine belt and largely determined the altitudinal distribution of Pyrenean forests (García-Ruiz et al., 2020). The abandonment of traditional land use has enhanced forest recovery in the subalpine belt, through encroachment and densification, and these land-use changes have played a more important role than climate in driving forest dynamics at a landscape scale over the last decades (Améztegui et al., 2010; Camarero & Gutiérrez, 2004; Sanjuán et al., 2018).

1.3 Forest-snow interactions

It is estimated that about a ~19% of Northern Hemisphere snow cover overlaps boreal forests (Rutter et al., 2009) and accounts for 17% of global water storage (Güntner et al., 2007). Other areas at lower latitudes, as mid-latitude mountain regions, also hold snow-covered forests at least during a part of the year. Subsequently, in these areas were both elements co-occur, forest-snow feedbacks play a critical role in influencing snowpack dynamics, as well as in regulating tree growth and functioning.

1.3.1 Forest effects on snow processes

Forests differ from other vegetated sites in its complex structure, which varies in space (e.g. between patches or due to different tree heights) and time (e.g. successional dynamics). Most forested areas hold a mosaic of clearings (gaps) and denser patches. The snowpack depth and the timing and rate of ablation are very different between areas beneath the tree canopy and open areas. These differences are consequence of terrain characteristics, climate conditions, and their various and complex interactions also exert influence (Lundquist et al., 2013).

Snow accumulation differs significantly between forested and open areas because of interception, sublimation and wind redistribution processes (Pomeroy & Gray, 1995). Forest canopies can intercept large masses of snow and, as a result, usually less snow accumulates beneath the forest canopies than in forest openings (Golding & Swanson, 1978). The degree of difference in snow accu-

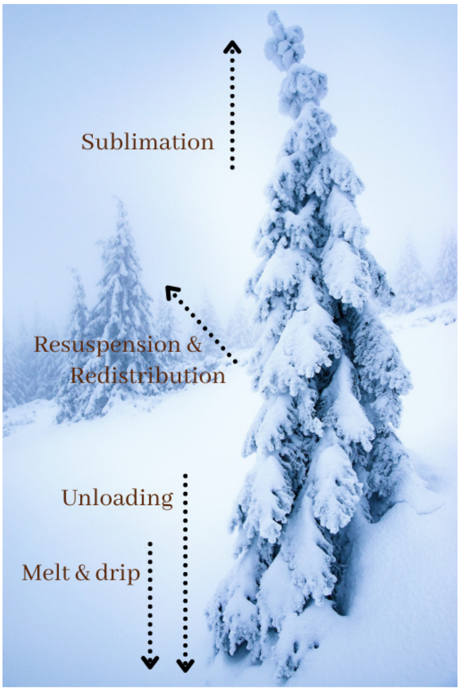

Figure 1.15: Possible pathways for intercepted snow by tree canopy.

mulation between forested and open areas is related to the size of the clearing (Golding & Swanson, 1986). Moreover, canopy interception efficiency depends on stand density, species composition, snowfall amount, temperature, canopy closure, wind speed, leaf area index, existing intercepted snow, and time since the last snowfall (Hedstrom & Pomeroy, 1998; Moore & McCaughey, 1997; Schneider et al., 2019). Not all intercepted snow reaches the ground (Figure 1.15). The intercepted snow at forest cover can follow different pathways: it may sublimate, melt, unload, or be resuspended and redistributed by wind (Pomeroy & Schmidt, 1993). Forest aerial biomass modifies surface roughness and, as a result, wind velocity is largely reduced within forest stands. As a result, usually greater snow accumulation occurs in downwind of forest areas (Hiemstra et al., 2006).

Alongside interception effects, the radiation characteristics of forest cover (trees are a large intercepting and radiating biomass) alters snow energy balance, and thus, the snow melting process (Geiger et al., 1965). Net solar radiation often dominates the snow energy balance during the melting season in conifer forests (Ellis et al., 2010), since the forest effectively decouples the above-canopy and sub-canopy atmospheres resulting in a large reduction of turbulent fluxes (Harding & Pomeroy, 1996). The incident solar radiation on snowpack is reduced by forest cover producing a shading effect, while the reflected solar radiation from the snow surface depends on deposited forest litter on and within snowpack which reduces its albedo (Melloh et al., 2001; Sicart et al., 2004). Moreover, the shortwave albedo of forest cover is low (0.10-0.15 in conifers), thus radiation absorption is high (Jeffrey, 1965). Radiation absorbed by forest cover is later dissipated as longwave radiation, being a major source of heat to snowpack in forested areas and near surroundings (Essery et al., 2008; Pomeroy et al., 2009).

Besides, subalpine forests structure and composition affect snow avalanches (that affect snow redistribution), even reducing the probability of avalanche disturbances in case of dense and large crown covered stands (Bebi et al., 2009).

1.3.2 Snow influences on forest growth and functioning

Snowpack dynamics affect soil microclimate throughout the year (Wilson et al., 2020), that ultimately may condition the growth of high-elevation forests in different ways. Scarce snow cover during winter promotes soil freeze that impacts negatively on root dynamics (Tierney et al., 2001), tree growth (Reinmann et al., 2019; Repo et al., 2008) and tree physiology (Comerford et al., 2013); in the end, complicating the ability of trees of taking water from soil and causing tissue damages. On the other hand, shallower snowpacks are related to earlier start of spring, and thus, longer growing seasons, through snowpack effects on soil temperature (Chapin & Körner, 2013). These conditions are related in turn to enhanced root production (Fukuzawa et al., 2021), promoted tree radial growth (Kirdyanov et al., 2003; Peterson & Peterson, 2011; Vaganov et al., 1999) and favoured encroachment (Fagre et al., 2003; Peterson et al., 2002). Leaf and shoot expansion for several subalpine tree species do not begin until complete snow depletion (Hansen-Bristow, 1986). Ultimately, although some studies have suggested that earlier snowmelt (which can led to longer growing seasons) could enhance carbon sequestration, other studies have pointed out that water supplied by the spring snowmelt is critical for subalpine forest carbon uptake and it is reduced during years with longer growing seasons, leading to less carbon sequestration (Hu et al., 2010; Monson et al., 2002). Snow melting contributes to soil moisture during growing season, which may exert a positive influence on seedling establishment, forest productivity and tree growth (Andrus et al., 2018; Hankin & Bisbing, 2021; Lubetkin et al., 2017; Trujillo et al., 2012). While its role varies among species and sites, it is more relevant in water-limited stands (Cooper et al., 2020).

Snow and wind storms can induce damage on mountain forests by causing leaf abrasion, breaking the stem and branches of trees inducing tree falling, mainly in those stands less heterogeneous and with more exposed crowns (Díaz-Yáñez et al., 2019; Martín-Alcón et al., 2010). Moreover, snow avalanches affect structure and composition of subalpine forests located in vulnerable places where avalanches can overwhelm several tens or hundreds of hectares (Bebi et al., 2009).

1.4 Objectives and justification

In main mid-latitude mountain areas, both snow and forests, constitute priority resources that have major economic and environmental roles (see Section 1.1 and Section 1.2). The Pyrenees are not an exception, where both elements coexists and interact in the altitudinal band comprised between 1600 and 2300–2500 m a.s.l., mostly comprising the subalpine belt. That forest-snow shared terrain accounts for the largest part of this mountain range, which only exceed 3000 m a.s.l. at some mountain summits. However, interactions between mountain forests and snowpack have yet to be fully addressed in the Pyrenees. Even less was known regarding forest-snow interactions response to the warm-up process that it is happening in this mountain range and it is expected to be accelerated in the following decades (Nogués Bravo et al., 2008).

The overall objective of this PhD Thesis is to deepen the knowledge on the forest-snow interactions in the Pyrenees, from an eco-hydrological perspective, through intensively monitoring of *Pinus uncinata* forests. It is a topic of high scientific interest, but it also involves results with potential applicability in forest and water resources management in the Pyrenees.

This overall objective is divided into three specific objectives, which are developed in the subsequently chapters of this manuscript coinciding with the research papers that compose this Thesis.

1. Firstly, this Thesis attemps to account for the uncertainty on the magnitude of forest effects on snowpack among nearby areas and during different years, and this can affect the representativeness of a study site and study period that is used for research. Since very few studies previously documented the different ways that forests modify the snowpack dynamics in the Pyrenees (Subsection 1.3.1), this first objective is a great potential to deepen understanding of forest-snow interactions in this region. The published research paper Sanmiguel-Vallelado et al. (2020) is featured in **Chapter 3**, and it highlights the similarities and differences in the spatial and temporal effects of *P. uncinata* forest cover on snowpack among nearby areas and during different snow seasons in the *Baños de Panticosa* experimental site.

2. Secondly, this Thesis attemps to discern how and where snow dynamics affects *P. uncinata* growth and functioning, which may help us understand future responses of Iberian mountain forests to forecasted hydroclimatic change. This influence had not been researched yet for *P. uncinata*, which sets the upper limit of forests in the Iberian Peninsula. This second objective was developed regionally and locally, and at two different temporal scales: inter- and intra-annually. The published research paper Sanmiguel-Vallelado et al. (2019) is featured in **Chapter 4**, and it contextualizes the associations between snow conditions and *P. uncinata* forests growth into a wider framework of space-time in the NE Iberian Peninsula mountains during the last decades. While the published research paper Sanmiguel-Vallelado et al. (2021) is featured in **Chapter 5**, and it aims to demonstrate how seasonal dynamics in snowpack characteristics modify microclimatic conditions (soil temperature and moisture) and tests if these modifications influ-

ence intra-annual growth and functioning of *P. uncinata* forests in the *Baños de Panticosa* experimental site.

3. Thirdly and lastly, this Thesis explores how forest cover can affect the snowpack sensitivity to changes in climate in the Pyrenees. Since climate mediates the forest effects on snowpack dynamics, we would expected that snowpacks in areas beneath forest canopy and in forest openings might respond differently to a changing climate. This third objective may allow us to anticipate future hydrological responses of forested mountain basins under climate change conditions. The published research paper Sanmiguel-Vallelado et al. (2022) is featured in **Chapter 6**, and aims to explore how changes in climate variables (air temperature and precipitation) can affect current forest-snow interactions in *P. uncinata* forests in the *Baños de Panticosa* experimental site.

References

Acar, R., Şenocak, S. & Şengül, S. (2009). Snow hydrology studies in the mountainous eastern part of Turkey. *2009 IEEE International Conference on Industrial Engineering and Engineering Management*, 1578–1582. https://doi.org/10.1109/IEEM.2009.5373102

Adam, J. C., Hamlet, A. F. & Lettenmaier, D. P. (2009). Implications of global climate change for snowmelt hydrology in the twenty-first century. *Hydrological Processes: An International Journal*, *23*(7), 962–972.

AghaKouchak, A., Cheng, L., Mazdiyasni, O. & Farahmand, A. (2014). Global warming and changes in risk of concurrent climate extremes: Insights from the 2014 California drought. *Geophysical Research Letters*, *41*(24), 8847–8852.

Agrawala, S. (2007). *Climate change in the European Alps: Adapting winter tourism and natural hazards management.* Organisation for Economic Cooperation and Development (OECD).

Albrich, K., Rammer, W. & Seidl, R. (2020). Climate change causes critical transitions and irreversible alterations of mountain forests. *Global Change Biology*, *26*(7). https://doi.org/10.1111/gcb.15118

Allen, C. D., Macalady, A. K., Chenchouni, H., Bachelet, D., McDowell, N., Vennetier, M., Kitzberger, T., Rigling, A., Breshears, D. D. & Hogg, E. T. (2010). A global overview of drought and heat-induced tree mortality reveals emerging climate change risks for forests. *Forest ecology and management*, *259*(4), 660–684.

Alonso-González, E., López-Moreno, J. I., Navarro-Serrano, F. M. & Revuelto, J. (2020b). Impact of North Atlantic Oscillation on the Snowpack in Iberian Peninsula Mountains. *Water*, *12*(1), 105. https://doi.org/10.3390/w12010105

Alonso-González, E., López-Moreno, J. I., Navarro-Serrano, F., Sanmiguel-Vallelado, A., Revuelto, J., Domínguez-Castro, F. & Ceballos, A. (2020a). Snow climatology for the mountains in the Iberian Peninsula using satellite imagery and simulations with dynamically downscaled reanalysis data. *International Journal of Climatology*, *40*(1), 477–491. https://doi.org/10.1002/joc.6223

Améztegui, A., Brotons, L. & Coll, L. (2010). Land-use changes as major drivers of mountain pine (Pinus uncinata Ram.) expansion in the Pyrenees. *Global Ecology and Biogeography*, *19*(5), 632–641. https://doi.org/10.1111/j.1466-8238.2010.00550.x

Anderson, B. T., McNamara, J. P., Marshall, H.-P. & Flores, A. N. (2014). Insights into the physical processes controlling correlations between snow distribution and terrain properties. *Water Resources Research*, *50*(6), 4545–4563. https://doi.org/10.1002/2013WR013714

Andrus, R. A., Harvey, B. J., Rodman, K. C., Hart, S. J. & Veblen, T. T. (2018). Moisture availability limits subalpine tree establishment. *Ecology*, *99*(3), 567–575. https://doi.org/10.1002/ecy.2134

Aoki, T., Aoki, T., Fukabori, M., Hachikubo, A., Tachibana, Y. & Nishio, F. (2000). Effects of snow physical parameters on spectral albedo and bidirectional reflectance of snow surface. *Journal of Geophysical Research: Atmospheres*, *105*(D8), 10219–10236.

Armstrong, R. L. & Brun, E. (2008). *Snow and climate: Physical processes, surface energy exchange and modeling*. Cambridge University Press.

Arndt, K. A., Lipson, D. A., Hashemi, J., Oechel, W. C. & Zona, D. (2020). Snow melt stimulates ecosystem respiration in Arctic ecosystems. *Global Change Biology*, *26*(9), 5042–5051. https://doi.org/10.1111/gcb.15193

Atmeh, K., Andruszkiewicz, A. & Zub, K. (2018). Climate change is affecting mortality of weasels due to camouflage mismatch. *Scientific Reports*, *8*(1), 1–7.

Band, L. E., Patterson, P., Nemani, R. & Running, S. W. (1993). Forest ecosystem processes at the watershed scale: Incorporating hillslope hydrology. *Agricultural and Forest Meteorology*, *63*(1-2), 93–126.

Barnett, T. P., Adam, J. C. & Lettenmaier, D. P. (2005). Potential impacts of a warming climate on water availability in snow-dominated regions. *Nature*, *438*(7066), 303–309. https://doi.org/10.1038/nature04141

Barrie, L. A. (1991). Snow Formation and Processes in the Atmosphere that Influence its Chemical Composition. In T. D. Davies, M. Tranter & H. G. Jones (Eds.), *Seasonal Snowpacks* (pp. 1–20). Springer. https://doi.org/10.1007/978-3-642-75112-7_1

Barry, R. & Gan, T. Y. (2011). *The Global Cryosphere: Past, Present and Future*. Cambridge University Press.

Barry, R. G. (1992). *Mountain weather and climate*. Routledge.

Barry, R. G. & Chorley, R. J. (2009). *Atmosphere, weather and climate*. Routledge.

Basler, D. & Körner, C. (2012). Photoperiod sensitivity of bud burst in 14 temperate forest tree species. *Agricultural and Forest Meteorology*, *165*, 73–81. https://doi.org/10.1016/j.agrformet.2012.06.001

Beaudin, L. & Huang, J.-C. (2014). Weather conditions and outdoor recreation: A study of New England ski areas. *Ecological Economics*, *106*, 56–68.

Bebi, P., Seidl, R., Motta, R., Fuhr, M., Firm, D., Krumm, F., Conedera, M., Ginzler, C., Wohlgemuth, T. & Kulakowski, D. (2017). Changes of forest cover and disturbance regimes in the mountain forests of the Alps. *Forest ecology and management*, *388*, 43–56. https://doi.org/10.1016/j.foreco.2016.10.028

Bebi, P., Kulakowski, D. & Rixen, C. (2009). Snow avalanche disturbances in forest ecosystems—State of research and implications for management. *Forest Ecology and Management*, *257*(9), 1883–1892. https://doi.org/10.1016/j.foreco.2009.01.050

Becken, S., Lama, A. K. & Espiner, S. (2013). The cultural context of climate change impacts: Perceptions among community members in the Annapurna Conservation Area, Nepal. *Environmental Development*, *8*, 22–37.

Beniston, M. (2003). Climatic change in mountain regions: A review of possible impacts. *Climate variability and change in high elevation regions: Past, present & future* (pp. 5–31). Springer.

Beniston, M., Farinotti, D., Stoffel, M., Andreassen, L. M., Coppola, E., Eckert, N., Fantini, A., Giacona, F., Hauck, C., Huss, M., Huwald, H., Lehning, M., López-Moreno, J.-I., Magnusson, J., Marty, C., Morán-Tejéda, E., Morin, S., Naaim, M., Provenzale, A., … Vincent, C. (2018). The European mountain cryosphere: A review of its current state, trends, and future challenges. *The Cryosphere*, *12*(2), 759–794. https://doi.org/10.5194/tc-12-759-2018

Biemans, H., Siderius, C., Lutz, A. F., Nepal, S., Ahmad, B., Hassan, T., von Bloh, W., Wijngaard, R. R., Wester, P., Shrestha, A. B. & Immerzeel, W. W. (2019). Importance of snow and glacier meltwater for agriculture on the Indo-Gangetic Plain. *Nature Sustainability*, *2*(7), 594–601.

Bircher, N. (2015). *To die or not to die: Forest dynamics in Switzerland under climate change* (Doctoral dissertation). ETH Zurich.

Blyth, S. (2002). *Mountain watch: Environmental change & sustainable developmental in mountains.* UNEP/Earthprint.

Bosch, O., Giné, L., Ramadori, E. D., Bernat, A. & Gutiérrez, E. (1992). Disturbance, age and size structure in stands of Pinus uncinata Ram. *Pirineos*, *140*, 5–14.

Breitsprecher, A. & Bethel, J. S. (1990). Stem-Growth Periodicity of Trees in a Tropical Wet Forest of Costa Rica. *Ecology*, *71*(3), 1156–1164. https://doi.org/10.2307/1937383

Bueno de Mesquita, C. P., Tillmann, L. S., Bernard, C. D., Rosemond, K. C., Molotch, N. P. & Suding, K. N. (2018). Topographic heterogeneity explains patterns of vegetation response to climate change (1972–2008) across a mountain landscape, Niwot Ridge, Colorado. *Arctic, Antarctic, and Alpine Research*, *50*(1), e1504492.

Butt, N. & Price, M. F. (2000). *Mountain people; forests, and trees: Strategies for balancing local management and outside interests*. The Food and Agriculture Organization (FAO).

Camarero, J. J. (1999). *Dinámica del límite altitudinal del bosque en los Pirineos y su relación con el cambio climático* (Doctoral dissertation). Ph. D. dissertation, University of Barcelona, Spain.

Camarero, J. J., García-Ruiz, J. M., Sangüesa-Barreda, G., Galván, J. D., Alla, A. Q., Sanjuán, Y., Beguería, S. & Gutiérrez, E. (2015). Recent and Intense Dynamics in a Formerly Static Pyrenean Treeline. *Arctic, Antarctic, and Alpine Research*, *47*(4), 773–783. https://doi.org/10.1657/AAAR0015-001

Camarero, J. J., Gazol, A., Galván, J. D., Sangüesa-Barreda, G. & Gutiérrez, E. (2015). Disparate effects of global-change drivers on mountain conifer forests: Warming-induced growth enhancement in young trees vs. CO_2 fertilization in old trees from wet sites. *Global Change Biology*, *21*(2), 738–749. https://doi.org/10.1111/gcb.12787

Camarero, J. J., Guerrero-Campo, J. & Gutiérrez, E. (1998). Tree-Ring Growth and Structure of Pinus uncinata and Pinus sylvestris in the Central Spanish Pyrenees. *Arctic and Alpine Research*, *30*(1), 1–10. https://doi.org/10.2307/1551739

Camarero, J. J. & Gutiérrez, E. (2004). Pace and pattern of recent treeline dynamics: Response of ecotones to climatic variability in the Spanish Pyrenees. *Climatic change*, *63*(1), 181–200.

Camarero, J. J., Sangüesa-Barreda, G., Montiel-Molina, C., Luelmo-Lautenschlaeger, R., Ortega, P., Génova, M. & López-Sáez, J. A. (2021). Historical Fires Induced Deforestation in Relict Scots Pine Forests during the Late 19th Century. *Fire*, *4*(2), 29. https://doi.org/10.3390/fire4020029

Camarero, J., Gutiérrez, E. & Fortin, M.-J. (2000). Spatial pattern of subalpine forest-alpine grassland ecotones in the Spanish Central Pyrenees. *Forest Ecology and Management*, *134*(1-3), 1–16. https://doi.org/10.1016/S0378-1127(99)00241-8

Cantegrel, R. (1983). Le pin à crochets pyrénéen: Biologie, biochimie, sylviculture. *Acta Biologica Montana*, *2*(3), 87–330.

Caudullo, G., Welk, E. & San-Miguel-Ayanz, J. (2017). Chorological maps for the main European woody species. *Data in Brief*, *12*, 662–666. https://doi.org/10.1016/j.dib.2017.05.007

Chapin, F. S. I. & Körner, C. (2013). *Arctic and alpine biodiversity: Patterns, causes and ecosystem consequences* (Vol. 113). Springer Science & Business Media.

Choi, G., Robinson, D. A. & Kang, S. (2010). Changing northern hemisphere snow seasons. *Journal of Climate*, *23*(19), 5305–5310.

Christner, B. C., Cai, R., Morris, C. E., McCarter, K. S., Foreman, C. M., Skidmore, M. L., Montross, S. N. & Sands, D. C. (2008). Geographic, seasonal, and precipitation chemistry influence on the abundance and activity of biological ice nucleators in rain and snow. *Proceedings of the National Academy of Sciences*, *105*(48), 18854–18859. https://doi.org/10.1073/pnas.0809816105

Cohen, J. (1994). Snow cover and climate. *Weather*, *49*(5), 150–156. https://doi.org/10.1002/j.1477-8696.1994.tb05997.x

Colbeck, S. C. (1973). Theory of metamorphism of wet snow.

Colbeck, S. C. (1982). An overview of seasonal snow metamorphism. *Reviews of Geophysics*, *20*(1), 45–61.

Comerford, D. P., Schaberg, P. G., Templer, P. H., Socci, A. M., Campbell, J. L. & Wallin, K. F. (2013). Influence of experimental snow removal on root and canopy physiology of sugar maple trees in a northern hardwood forest. *Oecologia*, *171*(1), 261–269.

Conedera, M., Colombaroli, D., Tinner, W., Krebs, P. & Whitlock, C. (2017). Insights about past forest dynamics as a tool for present and future forest management in Switzerland. *Forest Ecology and Management*, *388*, 100–112.

Cooper, A. E., Kirchner, J. W., Wolf, S., Lombardozzi, D. L., Sullivan, B. W., Tyler, S. W. & Harpold, A. A. (2020). Snowmelt causes different limitations on transpiration in a Sierra Nevada conifer forest. *Agricultural and Forest Meteorology*, *291*, 108089. https://doi.org/10.1016/j.agrformet.2020.108089

Creus Novau, J. & Puigdefábregas, J. (1976). Climatología histórica y dendocronología de Pinus Uncinata Ramond. *Cuadernos de investigación: Geografía e historia*, *2*(2), 17–30.

Cuny, H. E., Rathgeber, C. B. K., Frank, D., Fonti, P. & Fournier, M. (2014). Kinetics of tracheid development explain conifer tree-ring structure. *New Phytologist*, *203*(4), 1231–1241. https://doi.org/10.1111/nph.12871

Dale, V. H., Joyce, L. A., McNulty, S., Neilson, R. P., Ayres, M. P., Flannigan, M. D., Hanson, P. J., Irland, L. C., Lugo, A. E., Peterson, C. J., Simberloff, D., Swanson, F. J., Stocks, B. J. & Wotton, B. M. (2001). Climate Change and Forest Disturbances: Climate change can affect forests by altering the frequency, intensity, duration, and timing of fire, drought, introduced species, insect and pathogen outbreaks, hurricanes, windstorms, ice storms, or landslides. *BioScience*, *51*(9), 723–734. https://doi.org/10.1641/0006-3568(2001)051[0723:CCAFD]2.0.CO;2

Daloz, A. S., Mateling, M., L'Ecuyer, T., Kulie, M., Wood, N. B., Durand, M., Wrzesien, M., Stjern, C. W. & Dimri, A. P. (2020). How much snow falls in the world's mountains? A first look at mountain snowfall estimates in A-train observations and reanalyses. *The Cryosphere*, *14*(9), 3195–3207. https://doi.org/10.5194/tc-14-3195-2020

de Rigo, D., Houston Durrant, T., Caudullo, G. & Barredo, J. I. (2016). European forests: An ecological overview. *European Atlas of Forest Tree Species*. Publ. Off.

Decker, K. L. M., Wang, D., Waite, C. & Scherbatskoy, T. (2003). Snow Removal and Ambient Air Temperature Effects on Forest Soil Temperatures in Northern Vermont. *Soil Science Society of America Journal*, *67*(4), 1234–1242. https://doi.org/10.2136/sssaj2003.1234

Dedieu, J. P., Lessard-Fontaine, A., Ravazzani, G., Cremonese, E., Shalpykova, G. & Beniston, M. (2014). Shifting mountain snow patterns in a changing climate from remote sensing retrieval. *Science of The Total Environment*, *493*, 1267–1279. https://doi.org/10.1016/j.scitotenv.2014.04.078

Delpierre, N., Vitasse, Y., Chuine, I., Guillemot, J., Bazot, S., Rutishauser, T. & Rathgeber, C. B. K. (2016). Temperate and boreal forest tree phenology: From organ-scale processes to terrestrial ecosystem models. *Annals of Forest Science*, *73*(1), 5–25. https://doi.org/10.1007/s13595-015-0477-6

Díaz-Yáñez, O., Mola-Yudego, B. & González-Olabarria, J. R. (2019). Modelling damage occurrence by snow and wind in forest ecosystems. *Ecological Modelling*, *408*, 108741.

Dominé, F., Lauzier, T., Cabanes, A., Legagneux, L., Kuhs, W. F., Techmer, K. & Heinrichs, T. (2003). Snow metamorphism as revealed by scanning electron microscopy. *Microscopy Research and Technique*, *62*(1), 33–48. https://doi.org/10.1002/jemt.10384

Dorren, L. K., Berger, F., Imeson, A. C., Maier, B. & Rey, F. (2004). Integrity, stability and management of protection forests in the European Alps. *Forest ecology and management*, *195*(1-2), 165–176.

Dozier, J. (2011). Mountain hydrology, snow color, and the fourth paradigm. *Eos, Transactions American Geophysical Union*, *92*(43), 373–374. https://doi.org/10.1029/2011EO430001 _eprint: https://agupubs.onlinelibrary.wiley.com/doi/pdf/10.1029/2011EO430001

Einarsson, B. & Jónsson, S. (2010). The effect of climate change on runoff from two watersheds in Iceland. *Conference on Future Climate and Renewable Energy: Impacts, Risks and Adaptation*, 86.

Ellis, C., Pomeroy, J., T, B. & J, M. (2010). Simulations of snow accumulation and melt in needleleaf forest environments. *Hydrology and Earth System Sciences Discussions*, *14*. https://doi.org/10.5194/hess-14-925-2010

Engler, R., Randin, C. F., Thuiller, W., Dullinger, S., Zimmermann, N. E., Araújo, M. B., Pearman, P. B., Le Lay, G., Piedallu, C. & Albert, C. H. (2011). 21st century climate change threatens mountain flora unequally across Europe. *Global Change Biology*, *17*(7), 2330–2341.

Essery, R., Pomeroy, J., Ellis, C. & Link, T. (2008). Modelling longwave radiation to snow beneath forest canopies using hemispherical photography or linear regression. *Hydrological Processes: An International Journal*, *22*(15), 2788–2800.

Estreguil, C., Caudullo, G., De Rigo, D. & San-Miguel-Ayanz, J. (2013). Forest landscape in Europe: Pattern, fragmentation and connectivity. *EUR Scientific and Technical Research*, *25717*.

Evan, A. & Eisenman, I. (2021). A mechanism for regional variations in snowpack melt under rising temperature. *Nature Climate Change*. https://doi.org/10.1038/s41558-021-00996-w

Fagre, D. B., Peterson, D. L. & Hessl, A. E. (2003). Taking the Pulse of Mountains: Ecosystem Responses to Climatic Variability. In M. Beniston & H. F. Diaz (Eds.), *Climate Variability and Change in High Elevation Regions: Past, Present & Future* (pp. 263–282). Springer Netherlands. https://doi.org/10.1007/978-94-015-1252-7_13

Fairbanks, A. (1898). *The First Philosophers of Greece; an Edition and Translation of the Remaining Fragments of the Pre-Sokratic Philosophers, Together with a Translation of the More Important Accounts of Their Opinions Contained in the Early Epitomes of Their Works.* K. Paul, Trench, Trübner & Company, Limited.

FAO. (2012). Global ecological zones for FAO forest reporting: 2010 Update. *Forest Resources Assessment Working Paper 179.*

Fayad, A., Gascoin, S., Faour, G., López-Moreno, J. I., Drapeau, L., Page, M. L. & Escadafal, R. (2017). Snow hydrology in Mediterranean mountain regions: A review. *Journal of Hydrology*, *551*, 374–396. https://doi.org/10.1016/j.jhydrol.2017.05.063

Formozov, A. N. (1946). Snow cover as an integral factor of the environment and its importance in the ecology of mammals and birds. Fauna and Flora of the USSR. *New Ser. Zool.*, *5*, 1–152.

Freudiger, D., Kohn, I., Stahl, K. & Weiler, M. (2014). Large-scale analysis of changing frequencies of rain-on-snow events with flood-generation potential. *Hydrology and Earth System Sciences*, *18*(7), 2695–2709.

Fritts, H. (1976). *Tree Rings and Climate*. Elsevier.

Fukuzawa, K., Tateno, R., Ugawa, S., Watanabe, T., Hosokawa, N., Imada, S. & Shibata, H. (2021). Timing of forest fine root production advances with reduced snow cover in northern Japan: Implications for climate-induced change in understory and overstory competition. *Oecologia*, *196*(1), 263–273. https://doi.org/10.1007/s00442-021-04914-x

Fyfe, J. C., Derksen, C., Mudryk, L., Flato, G. M., Santer, B. D., Swart, N. C., Molotch, N. P., Zhang, X., Wan, H. & Arora, V. K. (2017). Large near-term projected snowpack loss over the western United States. *Nature communications*, *8*(1), 1–7.

Galván, J. D., Camarero, J. J. & Gutiérrez, E. (2014). Seeing the trees for the forest: Drivers of individual growth responses to climate in Pinus uncinata mountain forests. *Journal of Ecology*, *102*(5), 1244–1257. https://doi.org/10.1111/1365-2745.12268

García-Ruiz, J. M., López-Moreno, J. I., Vicente-Serrano, S. M., Lasanta–Martínez, T. & Beguería, S. (2011). Mediterranean water resources in a global change scenario. *Earth-Science Reviews*, *105*(3), 121–139. https://doi.org/10.1016/j.earscirev.2011.01.006

García-Ruiz, J. M., Tomás-Faci, G., Diarte-Blasco, P., Montes, L., Domingo, R., Sebastián, M., Lasanta, T., González-Sampériz, P., López-Moreno, J. I., Arnáez, J. & Beguería, S. (2020). Transhumance and long-term deforestation in the subalpine belt of the central Spanish Pyrenees: An interdisciplinary approach. *CATENA*, *195*, 104744. https://doi.org/10.1016/j.catena.2020.104744

Gascoin, S., Hagolle, O., Huc, M., Jarlan, L., Dejoux, J.-F., Szczypta, C., Marti, R. & Sánchez, R. (2015). A snow cover climatology for the Pyrenees from MODIS snow products. *Hydrology and Earth System Sciences*, *19*(5), 2337–2351. https://doi.org/10.5194/hess-19-2337-2015

Geiger, R., Aron, R. H. & Todhunter, P. (1965). *The Climate Near the Ground*. Harvard University Press.

Gilaberte-Búrdalo, M., López-Moreno, J. I., Morán-Tejeda, E., Jerez, S., Alonso-González, E., López-Martín, F. & Pino-Otín, M. R. (2017). Assessment of ski condition reliability in the Spanish and Andorran Pyrenees for the second half of the 20th century. *Applied Geography*, *79*, 127–142.

Gilbert, A., Vincent, C., Wagnon, P., Thibert, E. & Rabatel, A. (2012). The influence of snow cover thickness on the thermal regime of Tête Rousse Glacier (Mont Blanc range, 3200 m a.s.l.): Consequences for outburst flood hazards and glacier response to climate change. *Journal of Geophysical Research: Earth Surface*, *117*(F4). https://doi.org/10.1029/2011JF002258

Giorgi, F. (2006). Climate change hot-spots. *Geophysical Research Letters*, *33*(8). https://doi.org/10.1029/2006GL025734

Giorgi, F. & Lionello, P. (2008). Climate change projections for the Mediterranean region. *Global and Planetary Change*, *63*(2), 90–104. https://doi.org/10.1016/j.gloplacha.2007.09.005

Glushkova, M., Zhiyanski, M., Nedkov, S., Yaneva, R. & Stoeva, L. (2020). Ecosystem services from mountain forest ecosystems: Conceptual framework, approach and challenges. *Silva Balcanica*, *21*(1), 47–68. https://doi.org/10.3897/silvabalcanica.21.e54628

Golding, D. L. & Swanson, R. H. (1978). Snow accumulation and melt in small forest openings in Alberta. *Canadian Journal of Forest Research*, *8*(4), 380–388.

Golding, D. L. & Swanson, R. H. (1986). Snow distribution patterns in clearings and adjacent forest. *Water Resources Research*, *22*(13), 1931–1940. https://doi.org/10.1029/WR022i013p01931

Güntner, A., Stuck, J., Werth, S., Döll, P., Verzano, K. & Merz, B. (2007). A global analysis of temporal and spatial variations in continental water storage. *Water Resources Research*, *43*(5). https://doi.org/10.1029/2006WR005247

Gutiérrez, E. (1991). Climate tree-growth relationships for Pinus uncinata Ram. in the Spanish pre-Pyrenees. *Acta Oecologica*, *12*(2), 213–225.

Haeberli, W. & Whiteman, C. (2015). Chapter 1 - Snow and Ice-Related Hazards, Risks, and Disasters: A General Framework. In J. F. Shroder, W. Haeberli & C. Whiteman (Eds.), *Snow and Ice-Related Hazards, Risks and Disasters* (pp. 1–34). Academic Press. https://doi.org/10.1016/B978-0-12-394849-6.00001-9

Haines-Young, R. & Potschin, M. (2012). Common international classification of ecosystem services (CICES, Version 4.1). *European Environment Agency*, *33*, 17.

Hammond, J. C., Saavedra, F. A. & Kampf, S. K. (2018). Global snow zone maps and trends in snow persistence 2001–2016. *International*

Journal of Climatology, *38*(12), 4369–4383. https://doi.org/10.1002/joc.5674

Hankin, L. & Bisbing, S. (2021). Let it snow? Spring snowpack and microsite characterize the regeneration niche of high-elevation pines. *Journal of Biogeography*. https://doi.org/10.1111/jbi.14136

Hansen-Bristow, K. (1986). Influence of increasing elevation on growth characteristics at timberline. *Canadian Journal of Botany*, *64*(11), 2517–2523.

Hararuk, O., Campbell, E. M., Antos, J. A. & Parish, R. (2019). Tree rings provide no evidence of a CO2 fertilization effect in old-growth subalpine forests of western Canada. *Global Change Biology*, *25*(4), 1222–1234. https://doi.org/10.1111/gcb.14561

Harding, R. J. & Pomeroy, J. W. (1996). The energy balance of the winter boreal landscape. *Journal of Climate*, *9*(11), 2778–2787.

Hardy, J. P., Groffman, P. M., Fitzhugh, R. D., Henry, K. S., Welman, A. T., Demers, J. D., Fahey, T. J., Driscoll, C. T., Tierney, G. L. & Nolan, S. (2001). Snow depth manipulation and its influence on soil frost and water dynamics in a northern hardwood forest. *Biogeochemistry*, *56*(2), 151–174. https://doi.org/10.1023/A:1013036803050

Harsch, M. A. & Bader, M. Y. (2011). Treeline form - a potential key to understanding treeline dynamics: The causes of treeline form. *Global Ecology and Biogeography*, *20*(4), 582–596. https://doi.org/10.1111/j.1466-8238.2010.00622.x

Harsch, M. A., Hulme, P. E., McGlone, M. S. & Duncan, R. P. (2009). Are treelines advancing? A global meta-analysis of treeline response to climate warming. *Ecology letters*, *12*(10), 1040–1049.

He, W., Zhang, B., Zhao, F., Zhang, S., Qi, W., Wang, J. & Zhang, W. (2016). The Mass Elevation Effect of the Central Andes and Its Implications for the Southern Hemisphere's Highest Treeline. *Mountain Research and Development*, *36*(2), 213–221. https://doi.org/10.1659/MRD-JOURNAL-D-15-00027

Hedstrom, N. R. & Pomeroy, J. W. (1998). Measurements and modelling of snow interception in the boreal forest. *Hydrological Processes*, *12*(10-11), 1611–1625.

Hendrikx, J., Hreinsson, E. Ö., Clark, M. P. & Mullan, A. B. (2012). The potential impact of climate change on seasonal snow in New Zealand: Part I—an analysis using 12 GCMs. *Theoretical and Applied Climatology*, *110*(4), 607–618.

Hewlett, J. D. (1982). *Principles of forest hydrology*. University of Georgia press.

Hiemstra, C. A., Liston, G. E. & Reiners, W. A. (2006). Observing, modelling, and validating snow redistribution by wind in a Wyoming upper treeline landscape. *Ecological Modelling*, *197*(1), 35–51. https://doi.org/10.1016/j.ecolmodel.2006.03.005

Hock, R., Rasul, G., Adler, C., Cáceres, B., Gruber, S., Hirabayashi, Y., Jackson, M., Kääb, A., Kang, S. & Kutuzov, S. (2019). *High Mountain Areas: In: IPCC Special Report on the Ocean and Cryosphere in a Changing Climate*.

Holtmeier, F.-K. (2009). *Mountain Timberlines: Ecology, Patchiness, and Dynamics*. Springer Science & Business Media.

Hong, Z., Deguang, Z. & Huihui, L. (2002). Significance of Ecological Ethics of Cultural Tradition in Deity Mountain Forests. *Chinese Journal of Ecology*, *21*(4), 60–64.

Hoy, A., Katel, O., Thapa, P., Dendup, N. & Matschullat, J. (2016). Climatic changes and their impact on socio-economic sectors in the Bhutan Himalayas: An implementation strategy. *Regional Environmental Change*, *16*(5), 1401–1415.

Hu, J., Moore, D. J. P., Burns, S. P. & Monson, R. K. (2010). Longer growing seasons lead to less carbon sequestration by a subalpine forest. *Global Change Biology*, *16*(2), 771–783. https://doi.org/10.1111/j.1365-2486.2009.01967.x

Huggard, D. J. (1993). Effect of Snow Depth on Predation and Scavenging by Gray Wolves. *The Journal of Wildlife Management*, *57*(2), 382–388. https://doi.org/10.2307/3809437

Huggel, C., Carey, M. & Clague, J. J. (2015). *The high-mountain cryosphere*. Cambridge University Press.

Huning, L. S. & AghaKouchak, A. (2020). Global snow drought hot spots and characteristics. *Proceedings of the National Academy of Sciences*, *117*(33), 19753–19759. https://doi.org/10.1073/pnas.1915921117

Ibanez, I., Clark, J. S. & Dietze, M. C. (2009). Estimating colonization potential of migrant tree species. *Global Change Biology*, *15*(5), 1173–1188.

Intergovernmental Panel on Climate Change, ((2013). *Climate Change 2013 – The Physical Science Basis: Working Group I Contribution to the Fifth Assessment Report of the Intergovernmental Panel on Climate Change*. Cambridge University Press. https://doi.org/10.1017/CBO9781107415324

Janda, P., Trotsiuk, V., Mikoláš, M., Bače, R., Nagel, T. A., Seidl, R., Seedre, M., Morrissey, R. C., Kucbel, S. & Jaloviar, P. (2017). The historical disturbance regime of mountain Norway spruce forests in the Western

Carpathians and its influence on current forest structure and composition. *Forest Ecology and Management*, *388*, 67–78.

Jeffrey, W. W. (1965). Snow hydrology in the forest environment. *Proceedings of the Workshop Seminar: Snow Hydrology*, 1–19.

Jobbágy, E. G. & Jackson, R. B. (2000). Global BlackwellScience,Ltd controls of forest line elevation in the northern and southern hemispheres. *Global Ecology*, 16.

Johannessen, M. & Henriksen, A. (1978). Chemistry of snow meltwater: Changes in concentration during melting. *Water Resources Research*, *14*(4), 615–619. https://doi.org/10.1029/WR014i004p00615

Johnston, A. K. (1850). *The Physical Atlas of Natural Phenomena: Reduced from the Edition in Imperial Folio for the Use of Colleges, Academies and Families*. W. Blackwood.

Jones, H. G., Pomeroy, J. W., Walker, D. A. & Hoham, R. W. (2001). *Snow ecology: An interdisciplinary examination of snow-covered ecosystems*. Cambridge University Press.

Juez, C., Peña-Angulo, D., Khorchani, M., Regüés, D. & Nadal-Romero, E. (2021). 20-Years of hindsight into hydrological dynamics of a mountain forest catchment in the Central Spanish Pyrenees. *Science of The Total Environment*, *766*, 142610. https://doi.org/10.1016/j.scitotenv.2020.142610

Kapos, V., Rhind, J., Edwards, M., Price, M., Ravilious, C. & Butt, N. (2000). Developing a map of the world's mountain forests., Forests in sustainable mountain development: A state of knowledge report for 2000. *Task Force For. Sustain. Mt. Dev.*, 4–19.

Kappelle, M. (2004). TROPICAL FORESTS | Tropical Montane Forests. In J. Burley (Ed.), *Encyclopedia of Forest Sciences* (pp. 1782–1792). Elsevier. https://doi.org/10.1016/B0-12-145160-7/00175-7

Kaser, G., Großhauser, M. & Marzeion, B. (2010). Contribution potential of glaciers to water availability in different climate regimes. *Proceedings of the National Academy of Sciences*, *107*(47), 20223–20227. https://doi.org/10.1073/pnas.1008162107

Kerr, T., Clark, M., Hendrikx, J. & Anderson, B. (2013). Snow distribution in a steep mid-latitude alpine catchment. *Advances in Water Resources*, *55*, 17–24. https://doi.org/10.1016/j.advwatres.2012.12.010

Kirdyanov, A., Hughes, M., Vaganov, E., Schweingruber, F. & Silkin, P. (2003). The importance of early summer temperature and date of snow melt for tree growth in the Siberian Subarctic. *Trees*, *17*(1), 61–69. https://doi.org/10.1007/s00468-002-0209-z

Klein, G., Vitasse, Y., Rixen, C., Marty, C. & Rebetez, M. (2016). Shorter snow cover duration since 1970 in the Swiss Alps due to earlier snowmelt more than to later snow onset. *Climatic Change*, *139*(3), 637–649.

Klimeš, L. (2006). *Alpine Plant Life. Functional Plant Ecology of High Mountain Ecosystems.* JSTOR.

Kopytkovskiy, M., Geza, M. & McCray, J. E. (2015). Climate-change impacts on water resources and hydropower potential in the Upper Colorado River Basin. *Journal of Hydrology: Regional Studies*, *3*, 473–493.

Körner, C. (1998). A re-assessment of high elevation treeline positions and their explanation. *Oecologia*, *115*(4), 445–459.

Körner, C. (2003). The alpine life zone. *Alpine Plant Life* (pp. 9–20). Springer.

Körner, C. (2006). Significance of temperature in plant life. *Plant growth and climate change*, 48–69.

Körner, C. (2012). *Alpine treelines: Functional ecology of the global high elevation tree limits.* Springer Science & Business Media.

Körner, C., Paulsen, J. & Spehn, E. M. (2011). A definition of mountains and their bioclimatic belts for global comparisons of biodiversity data. *Alpine Botany*, *121*(2), 73–78. https://doi.org/10.1007/s00035-011-0094-4

Kozak, J. (2003). Forest cover change in the Western Carpathians in the past 180 years. *Mountain research and Development*, *23*(4), 369–375.

Kozlowski, T. T. & Pallardy, S. G. (1996). *Physiology of Woody Plants.* Elsevier.

Kudo, G. (1991). Effects of snow-free period on the phenology of alpine plants inhabiting snow patches. *Arctic and alpine research*, *23*(4), 436–443.

Kulakowski, D., Rixen, C. & Bebi, P. (2006). Changes in forest structure and in the relative importance of climatic stress as a result of suppression of avalanche disturbances. *Forest Ecology and Management*, *223*(1), 66–74. https://doi.org/10.1016/j.foreco.2005.10.058

Kulakowski, D., Seidl, R., Holeksa, J., Kuuluvainen, T., Nagel, T. A., Panayotov, M., Svoboda, M., Thorn, S., Vacchiano, G., Whitlock, C., Wohlgemuth, T. & Bebi, P. (2017). A walk on the wild side: Disturbance dynamics and the conservation and management of European mountain forest ecosystems. *Forest Ecology and Management*, *388*, 120–131. https://doi.org/10.1016/j.foreco.2016.07.037

LaChapelle, E. R. & Armstrong, R. L. (1977). *Temperature Patterns in an Alpine Snow Cover and Their Influence on Snow Metamorphism.*

(tech. rep.). Colorado University. Institue of Artic and Alpine Research. Boulder.

Leach, J. A. & Moore, R. D. (2014). Winter stream temperature in the rain-on-snow zone of the Pacific Northwest: Influences of hillslope runoff and transient snow cover. *Hydrology and Earth System Sciences*, *18*(2), 819–838. https://doi.org/10.5194/hess-18-819-2014

Lenoir, J., Gégout, J.-C., Dupouey, J.-L., Bert, D. & Svenning, J.-C. (2010). Forest plant community changes during 1989-2007 in response to climate warming in the Jura Mountains (France and Switzerland). *Journal of Vegetation Science*, *21*(5), 949–964.

Lewandowski, A., Boratyński, A. & Mejnartowicz, L. (2000). Allozyme investigations on the genetic differentiation between closely related pines—Pinus sylvestris, P. mugo, P. uncinata, and P. uliginosa (Pinaceae). *Plant Systematics and Evolution*, *221*(1), 15–24.

Li, D., Wrzesien, M. L., Durand, M., Adam, J. & Lettenmaier, D. P. (2017). How much runoff originates as snow in the western United States, and how will that change in the future? *Geophysical Research Letters*, *44*(12), 6163–6172.

Lionello, P., Malanotte-Rizzoli, P., Boscolo, R., Alpert, P., Artale, V., Li, L., Luterbacher, J., May, W., Trigo, R. & Tsimplis, M. (2006). *The Mediterranean climate: An overview of the main characteristics and issues*. Elsevier.

Loeffler, J., Anschlag, K., Baker, B., Finch, O.-D., Diekkrueger, B., Wundram, D., Schroeder, B., Pape, R. & Lundberg, A. (2011). Mountain ecosystem response to global change. *Erdkunde*, 189–213.

Löffler, J. (2007). The influence of micro-climate, snow cover, and soil moisture on ecosystem functioning in high mountains. *Journal of Geographical Sciences*, *17*(1), 3–19. https://doi.org/10.1007/s11442-007-0003-3

Logan, J. A., Régnière, J. & Powell, J. A. (2003). Assessing the impacts of global warming on forest pest dynamics. *Frontiers in Ecology and the Environment*, *1*(3), 130–137.

López-Moreno, J. I., Beniston, M. & García-Ruiz, J. M. (2008). Environmental change and water management in the Pyrenees: Facts and future perspectives for Mediterranean mountains. *Global and Planetary Change*, *61*(3), 300–312. https://doi.org/10.1016/j.gloplacha.2007.10.004

López-Moreno, J. I. & García-Ruiz, J. M. (2004). Influence of snow accumulation and snowmelt on streamflow in the central Spanish Pyrenees. *Hydrological Sciences Journal*, *49*(5), null–802. https://doi.org/10.1623/hysj.49.5.787.55135

López-Moreno, J. I., Gascoin, S., Herrero, J., Sproles, E. A., Pons, M., Alonso-González, E., Hanich, L., Boudhar, A., Musselman, K. N., Molotch, N. P., Sickman, J. & Pomeroy, J. (2017). Different sensitivities of snowpacks to warming in Mediterranean climate mountain areas. *Environmental Research Letters*, *12*(7), 074006. https://doi.org/10.1088/1748-9326/aa70cb

López-Moreno, J. I., Pomeroy, J. W., Alonso-González, E., Morán-Tejeda, E. & Revuelto, J. (2020). Decoupling of warming mountain snowpacks from hydrological regimes. *Environmental Research Letters*, *15*(11), 114006. https://doi.org/10.1088/1748-9326/abb55f

López-Moreno, J. I., Soubeyroux, J. M., Gascoin, S., Alonso-Gonzalez, E., Durán-Gómez, N., Lafaysse, M., Vernay, M., Carmagnola, C. & Morin, S. (2020). Long-term trends (1958–2017) in snow cover duration and depth in the Pyrenees. *International Journal of Climatology*, *40*(14), 6122–6136. https://doi.org/10.1002/joc.6571

López-Moreno, J. I., Beguería, S. & García-Ruiz, J. M. (2004). Storage regimes of the yesa reservoir, upper aragón river basin, central spanish pyrenees. *Environmental Management*, *34*, 508–515.

Lubetkin, K. C., Westerling, A. L. & Kueppers, L. M. (2017). Climate and landscape drive the pace and pattern of conifer encroachment into subalpine meadows. *Ecological Applications*, *27*(6), 1876–1887.

Lundquist, J. D., Dickerson-Lange, S. E., Lutz, J. A. & Cristea, N. C. (2013). Lower forest density enhances snow retention in regions with warmer winters: A global framework developed from plot-scale observations and modeling. *Water Resources Research*, *49*(10), 6356–6370. https://doi.org/10.1002/wrcr.20504

Macias-Fauria, M. & Johnson, E. A. (2013). Warming-induced upslope advance of subalpine forest is severely limited by geomorphic processes. *Proceedings of the National Academy of Sciences*, *110*(20), 8117–8122. https://doi.org/10.1073/pnas.1221278110

Magoun, A. J. & Copeland, J. P. (1998). Characteristics of wolverine reproductive den sites. *The Journal of wildlife management*, 1313–1320.

Mäkinen, H., Nöjd, P. & Saranpää, P. (2003). Seasonal changes in stem radius and production of new tracheids in Norway spruce. *Tree Physiology*, *23*(14), 959–968. https://doi.org/10.1093/treephys/23.14.959

Marqués, L., Peltier, D. M. P., Camarero, J. J., Zavala, M. A., Madrigal-González, J., Sangüesa-Barreda, G. & Ogle, K. (2021). Disentangling the Legacies of Climate and Management on Tree Growth. *Ecosystems*. https://doi.org/10.1007/s10021-021-00650-8

Martín-Alcón, S., González-Olabarría, J. & Coll, L. (2010). Wind and snow damage in the Pyrenees pine forests: Effect of stand attributes and location. *Silva Fennica*, *44*(3). https://doi.org/10.14214/sf.138

Maurer, G. E. & Bowling, D. R. (2014). Seasonal snowpack characteristics influence soil temperature and water content at multiple scales in interior western U.S. mountain ecosystems. *Water Resources Research*, *50*(6), 5216–5234. https://doi.org/10.1002/2013WR014452

Melloh, R. A., Hardy, J. P., Davis, R. E. & Robinson, P. B. (2001). Spectral albedo/reflectance of littered forest snow during the melt season. *Hydrological Processes*, *15*(18), 3409–3422. https://doi.org/10.1002/hyp.1043

Miehe, G., Miehe, S., Vogel, J., Co, S. & La, D. (2007). Highest Treeline in the Northern Hemisphere Found in Southern Tibet. *Mountain Research and Development*, *27*(2), 169–173. https://doi.org/10.1659/mrd.0792

Millar, C. I. & Stephenson, N. L. (2015). Temperate forest health in an era of emerging megadisturbance. *Science*, *349*(6250), 823–826. https://doi.org/10.1126/science.aaa9933

Millar, C. I., Westfall, R. D., Delany, D. L., King, J. C. & Graumlich, L. J. (2004). Response of Subalpine Conifers in the Sierra Nevada, California, U.S.A., to 20th-Century Warming and Decadal Climate Variability. *Arctic, Antarctic, and Alpine Research*, *36*(2), 181–200. https://doi.org/10.1657/1523-0430(2004)036[0181:ROSCIT]2.0.CO;2

Millennium Ecosystem Assessment, ((2005). *Ecosystems and Human Wellbeing: Synthesis* (Vol. 1). Island Press. Muller & Burkhard.

Monson, R. K., Turnipseed, A. A., Sparks, J. P., Harley, P. C., Scott-Denton, L. E., Sparks, K. & Huxman, T. E. (2002). Carbon sequestration in a high-elevation, subalpine forest. *Global Change Biology*, *8*(5), 459–478. https://doi.org/10.1046/j.1365-2486.2002.00480.x

Moore, C. A. & McCaughey, W. W. (1997). Snow accumulation under various forest stand densities at Tenderfoot Creek Experimental Forest, Montana, USA. *In: 65th Annual Meeting, Western Snow Conference: Joint Meeting with the 54th Annual Eastern Snow Conference and Canadian Geophysical Union.; 1997 May 4-8; Banff, Alberta, Canada. Brush Prairie, WA: Western Snow Conference. p. 42-51.*, 42–51.

Morán-Tejeda, E., López-Moreno, J. I. & Sanmiguel-Vallelado, A. (2017). Changes in climate, snow and water resources in the Spanish Pyrenees: Observations and projections in a warming climate. *High Mountain Conservation in a Changing World* (pp. 305–323). Springer.

Morán-Tejeda, E., Lorenzo-Lacruz, J., López-Moreno, J. I., Rahman, K. & Beniston, M. (2014). Streamflow timing of mountain rivers in Spain:

Recent changes and future projections. *Journal of hydrology*, *517*, 1114–1127.

Mote, P. W., Hamlet, A. F., Clark, M. P. & Lettenmaier, D. P. (2005). Declining mountain snowpack in western North America. *Bulletin of the American Meteorological Society*, *86*(1), 39–50. https://doi.org/10.1175/BAMS-86-1-39

Müller, M., Schwab, N., Schickhoff, U., Böhner, J. & Scholten, T. (2016). Soil Temperature and Soil Moisture Patterns in a Himalayan Alpine Treeline Ecotone. *Arctic, Antarctic, and Alpine Research*, *48*(3), 501–521. https://doi.org/10.1657/AAAR0016-004

Musselman, K. N., Addor, N., Vano, J. A. & Molotch, N. P. (2021). Winter melt trends portend widespread declines in snow water resources. *Nature Climate Change*, *11*(5), 418–424. https://doi.org/10.1038/s41558-021-01014-9

Mustonen, K.-R., Mykrä, H., Marttila, H., Sarremejane, R., Veijalainen, N., Sippel, K., Muotka, T. & Hawkins, C. P. (2018). Thermal and hydrologic responses to climate change predict marked alterations in boreal stream invertebrate assemblages. *Global Change Biology*, *24*(6), 2434–2446. https://doi.org/10.1111/gcb.14053

Mysterud, A. & Austrheim, G. (2014). Lasting effects of snow accumulation on summer performance of large herbivores in alpine ecosystems may not last. *Journal of Animal Ecology*, *83*(3), 712–719. https://doi.org/10.1111/1365-2656.12166

Navarro-Serrano, F., I. López-Moreno, J., Azorin-Molina, C., Alonso-González, E., Tomás-Burguera, M., Sanmiguel-Vallelado, A., Revuelto, J. & Beguería, S. (2018). Estimation of near-surface air temperature lapse rates over continental Spain and its mountain areas. *International Journal of Climatology*, *38*, 3233–3249. https://doi.org/10.1002/joc.5497

Nicolussi, K., Bortenschlager, S. & Körner, C. (1995). Increase in tree-ring width in subalpine Pinus cembra from the central Alps that may be CO2-related. *Trees*, *9*(4), 181–189. https://doi.org/10.1007/BF00195270

Niittynen, P., Heikkinen, R. K. & Luoto, M. (2018). Snow cover is a neglected driver of Arctic biodiversity loss. *Nature Climate Change*, *8*(11), 997–1001. https://doi.org/10.1038/s41558-018-0311-x

Ninot, J., Carrillo, E., Font, X., Carreras, J., Ferré, A., Masalles, R., Soriano, I. & Vigo, J. (2007). Altitude zonation in the Pyrenees. A geobotanic interpretation. *Phytocoenologia*, *37*(3-4), 371–398. https://doi.org/10.1127/0340-269X/2007/0037-0371

Nogués Bravo, D., Araújo, M. B., Lasanta, T. & López Moreno, J. I. (2008). Climate change in Mediterranean mountains during the 21st century. *Ambio*, *37*(4), 280–285. https://doi.org/10.1579/0044-7447(2008)37[280:ccimmd]2.0.co;2

Notarnicola, C. (2020). Hotspots of snow cover changes in global mountain regions over 2000–2018. *Remote Sensing of Environment*, *243*, 111781. https://doi.org/10.1016/j.rse.2020.111781

Nüsser, M. & Schmidt, S. (2017). Nanga Parbat revisited: Evolution and dynamics of sociohydrological interactions in the Northwestern Himalaya. *Annals of the American Association of Geographers*, *107*(2), 403–415.

O'Gorman, P. A. (2014). Contrasting responses of mean and extreme snowfall to climate change. *Nature*, *512*(7515), 416–418. https://doi.org/10.1038/nature13625

Oki, T. & Kanae, S. (2006). Global hydrological cycles and world water resources. *science*, *313*(5790), 1068–1072.

Oleksy, I. A., Beck, W. S., Lammers, R. W., Steger, C. E., Wilson, C., Christianson, K., Vincent, K., Johnson, G., Johnson, P. T. J. & Baron, J. S. (2020). The role of warm, dry summers and variation in snowpack on phytoplankton dynamics in mountain lakes. *Ecology*, *101*(10), e03132. https://doi.org/10.1002/ecy.3132

Pan, Y., Birdsey, R. A., Fang, J., Houghton, R., Kauppi, P. E., Kurz, W. A., Phillips, O. L., Shvidenko, A., Lewis, S. L., Canadell, J. G., Ciais, P., Jackson, R. B., Pacala, S. W., McGuire, A. D., Piao, S., Rautiainen, A., Sitch, S. & Hayes, D. (2011). A Large and Persistent Carbon Sink in the World's Forests. *Science*, *333*(6045), 988–993. https://doi.org/10.1126/science.1201609

Panayotov, M., Gogushev, G., Tsavkov, E., Vasileva, P., Tsvetanov, N., Kulakowski, D. & Bebi, P. (2017). Abiotic disturbances in Bulgarian mountain coniferous forests–An overview. *Forest Ecology and Management*, *388*, 13–28.

Paulsen, J. & Körner, C. (2014). A climate-based model to predict potential treeline position around the globe. *Alpine Botany*, *124*(1), 1–12. https://doi.org/10.1007/s00035-014-0124-0

Pedersen, S., Odden, M. & Pedersen, H. C. (2017). Climate change induced molting mismatch? Mountain hare abundance reduced by duration of snow cover and predator abundance. *Ecosphere*, *8*(3), e01722.

Pedrotti, F. (2012). *Plant and vegetation mapping*. Springer Science & Business Media.

Pedrotti, F. (2013). Mapping Vegetation Zones and Belts. In F. Pedrotti (Ed.), *Plant and Vegetation Mapping* (pp. 225–231). Springer. https://doi.org/10.1007/978-3-642-30235-0_10

Peña, L., Casado-Arzuaga, I. & Onaindia, M. (2015). Mapping recreation supply and demand using an ecological and a social evaluation approach. *Ecosystem Services*, *13*, 108–118.

Pepin, N., Bradley, R. S., Diaz, H. F., Baraër, M., Caceres, E. B., Forsythe, N., Fowler, H., Greenwood, G., Hashmi, M. Z. & Liu, X. D. (2015). Elevation-dependent warming in mountain regions of the world. *Nature climate change*, *5*(5), 424.

Périé, C. & de Blois, S. (2016). Dominant forest tree species are potentially vulnerable to climate change over large portions of their range even at high latitudes. *PeerJ*, *4*, e2218. https://doi.org/10.7717/peerj.2218

Peterson, D. W. & Peterson, D. L. (2011). Effects of climate on radial growth of subalpine conifers in the North Cascade Mountains. *Canadian Journal of Forest Research*. https://doi.org/10.1139/x94-247

Peterson, D. W., Peterson, D. L. & Ettl, G. J. (2002). Growth responses of subalpine fir to climatic variability in the Pacific Northwest. *Canadian Journal of Forest Research*, *32*(9), 1503–1517.

Pey, J., Revuelto, J., Moreno, N., Alonso-González, E., Bartolomé, M., Reyes, J., Gascoin, S. & López-Moreno, J. I. (2020). Snow Impurities in the Central Pyrenees: From Their Geochemical and Mineralogical Composition towards Their Impacts on Snow Albedo. *Atmosphere*, *11*(9), 937. https://doi.org/10.3390/atmos11090937

Pielmeier, C., Techel, F., Marty, C. & Stucki, T. (2013). Wet snow avalanche activity in the Swiss Alps–trend analysis for mid-winter season. *Proceedings of the International Snow Science Workshop, Grenoble and Chamonix*, 1240–1246.

Pomeroy, J. W. & Brun, E. (2001). Physical properties of snow. *Snow ecology: An interdisciplinary examination of snow-covered ecosystems*, *45*, 118.

Pomeroy, J. W. & Gray, D. M. (1995). Snowcover accumulation, relocation and management. *Bulletin of the International Society of Soil Science no*, *88*(2).

Pomeroy, J. W. & Li, L. (2000). Prairie and arctic areal snow cover mass balance using a blowing snow model. *Journal of Geophysical Research: Atmospheres*, *105*(D21), 26619–26634. https://doi.org/10.1029/2000JD900149

Pomeroy, J. W. & Schmidt, R. A. (1993). The use of fractal geometry in modelling intercepted snow accumulation and sublimation. *Proceedings of the Eastern Snow Conference*, *50*, 1–10.

Pomeroy, J. W., Marks, D., Link, T., Ellis, C., Hardy, J., Rowlands, A. & Granger, R. (2009). The impact of coniferous forest temperature on incoming longwave radiation to melting snow. *Hydrological Processes*, *23*(17), 2513–2525. https://doi.org/10.1002/hyp.7325

Pomeroy, J. W. (1988). *Wind transport of snow*. University of Saskatchewan.

Pompa-García, M., González-Cásares, M., Gazol, A. & Camarero, J. J. (2021). Run to the hills: Forest growth responsiveness to drought increased at higher elevation during the late 20th century. *Science of The Total Environment*, *772*, 145286. https://doi.org/10.1016/j.scitotenv.2021.145286

Price, M., Gratzer, G., Alemayehu Duguma, L., Kohler, T., Maselli, D. & Romeo, R. (2011a). Chapter 1: Why focus on the world's mountain forests? *Mountain Forests in a Changing World: Realizing Values, Adressing Challenges*. Food and Agriculture Organization of the United Nations (FAO).

Price, M., Gratzer, G., Alemayehu Duguma, L., Kohler, T., Maselli, D. & Romeo, R. (2011b). Chapter 2: Sources of water. *Mountain Forests in a Changing World: Realizing Values, Adressing Challenges*. Food and Agriculture Organization of the United Nations (FAO).

Price, M., Gratzer, G., Alemayehu Duguma, L., Kohler, T., Maselli, D. & Romeo, R. (2011c). Chapter 8: Climate change. *Mountain Forests in a Changing World: Realizing Values, Adressing Challenges*. Food and Agriculture Organization of the United Nations (FAO).

Price, M., Lysenko, I. & Gloersen, E. (2004). Delineating Europe's mountains. *Revue de géographie alpine*, *92*(2), 75–86.

Prislan, P., Čufar, K., Koch, G., Schmitt, U. & Gričar, J. (2013). Review of cellular and subcellular changes in the cambium. *IAWA Journal*, *34*(4), 391–407. https://doi.org/10.1163/22941932-00000032

Pulliainen, J., Luojus, K., Derksen, C., Mudryk, L., Lemmetyinen, J., Salminen, M., Ikonen, J., Takala, M., Cohen, J., Smolander, T. & Norberg, J. (2020). Patterns and trends of Northern Hemisphere snow mass from 1980 to 2018. *Nature*, *581*(7808), 294–298. https://doi.org/10.1038/s41586-020-2258-0

Qin, Y., Abatzoglou, J. T., Siebert, S., Huning, L. S., AghaKouchak, A., Mankin, J. S., Hong, C., Tong, D., Davis, S. J. & Mueller, N. D. (2020). Agricultural risks from changing snowmelt. *Nature Climate Change*, *10*(5), 459–465. https://doi.org/10.1038/s41558-020-0746-8

Rathgeber, C. B. K., Cuny, H. E. & Fonti, P. (2016). Biological Basis of Tree-Ring Formation: A Crash Course. *Frontiers in Plant Science*, *7*. https://doi.org/10.3389/fpls.2016.00734

Rathgeber, C. B., Decoux, V. & Leban, J.-M. (2006). Linking intra-tree-ring wood density variations and tracheid anatomical characteristics in Douglas fir (Pseudotsuga menziesii (Mirb.) Franco). *Annals of Forest Science*, *63*(7), 699–706.

Reinmann, A. B., Susser, J. R., Demaria, E. M. C. & Templer, P. H. (2019). Declines in northern forest tree growth following snowpack decline and soil freezing. *Global Change Biology*, *25*(2), 420–430. https://doi.org/10.1111/gcb.14420

Repo, T., Lehto, T. & Finér, L. (2008). Delayed soil thawing affects root and shoot functioning and growth in Scots pine. *Tree Physiology*, *28*(10), 1583–1591. https://doi.org/10.1093/treephys/28.10.1583

Rixen, C., Freppaz, M., Stoeckli, V., Huovinen, C., Huovinen, K. & Wipf, S. (2008). Altered snow density and chemistry change soil nitrogen mineralization and plant growth. *Arctic, Antarctic, and Alpine Research*, *40*(3), 568–575.

Robinson, D. A. & Frei, A. (2000). Seasonal variability of Northern Hemisphere snow extent using visible satellite data. *The Professional Geographer*, *52*(2), 307–315.

Rocca, M. E., Brown, P. M., MacDonald, L. H. & Carrico, C. M. (2014). Climate change impacts on fire regimes and key ecosystem services in Rocky Mountain forests. *Forest Ecology and Management*, *327*, 290–305. https://doi.org/10.1016/j.foreco.2014.04.005

Rosvold, J. (2016). Perennial ice and snow-covered land as important ecosystems for birds and mammals. *Journal of Biogeography*, *43*(1), 3–12. https://doi.org/10.1111/jbi.12609

Rudel, T. K., Coomes, O. T., Moran, E., Achard, F., Angelsen, A., Xu, J. & Lambin, E. (2005). Forest transitions: Towards a global understanding of land use change. *Global Environmental Change*, *15*(1), 23–31. https://doi.org/10.1016/j.gloenvcha.2004.11.001

Ruiz de la Torre, J., Ceballos y Fernández de Córdoba, L., Ceballos Jiménez, M. & Ruiz del Castillo y de Navascúes, J. (1979). *Árboles y arbustos de la españa peninsular*. Escuela Técnica Superior de Ingenieros de Montes, Sección de Publicaciones.

Ruiz Flaño, P. (1989). Análisis dendroclimático de" Pinus Uncinata Ramond" de la Sierra de Cebollera (Sistema Ibérico). *Cuadernos de investigación geográfica/Geographical Research Letters*, (15), 75–86.

Rutter, N., Essery, R., Pomeroy, J., Altimir, N., Andreadis, K., Baker, I., Barr, A., Bartlett, P., Boone, A., Deng, H., Douville, H., Dutra, E., Elder, K., Ellis, C., Feng, X., Gelfan, A., Goodbody, A., Gusev, Y., Gustafsson, D., . . . Yamazaki, T. (2009). Evaluation of forest snow processes models (SnowMIP2). *Journal of Geophysical Research: Atmospheres*, *114*(D6). https://doi.org/10.1029/2008JD011063

Saalfeld, S. T., McEwen, D. C., Kesler, D. C., Butler, M. G., Cunningham, J. A., Doll, A. C., English, W. B., Gerik, D. E., Grond, K., Herzog, P., Hill, B. L., Lagassé, B. J. & Lanctot, R. B. (2019). Phenological mismatch in Arctic-breeding shorebirds: Impact of snowmelt and unpredictable weather conditions on food availability and chick growth. *Ecology and Evolution*, *9*(11), 6693–6707. https://doi.org/10.1002/ece3.5248

Sadro, S., Sickman, J. O., Melack, J. M. & Skeen, K. (2018). Effects of climate variability on snowmelt and implications for organic matter in a high-elevation lake. *Water Resources Research*, *54*(7), 4563–4578.

Sanjuán, Y., Arnáez, J., Beguería, S., Lana-Renault, N., Lasanta, T., Gómez-Villar, A., Álvarez-Martínez, J., Coba-Pérez, P. & García-Ruiz, J. M. (2018). Woody plant encroachment following grazing abandonment in the subalpine belt: A case study in northern Spain. *Regional Environmental Change*, *18*(4), 1103–1115. https://doi.org/10.1007/s10113-017-1245-y

Sanmiguel-Vallelado, A., Camarero, J. J., Gazol, A., Morán-Tejeda, E., Sangüesa-Barreda, G., Alonso-González, E., Gutiérrez, E., Alla, A. Q., Galván, J. D. & López-Moreno, J. I. (2019). Detecting snow-related signals in radial growth of Pinus uncinata mountain forests. *Dendrochronologia*, *57*, 125622. https://doi.org/10.1016/j.dendro.2019.125622

Sanmiguel-Vallelado, A., Camarero, J. J., Morán-Tejeda, E., Gazol, A., Colangelo, M., Alonso-González, E. & López-Moreno, J. I. (2021). Snow dynamics influence tree growth by controlling soil temperature in mountain pine forests. *Agricultural and Forest Meteorology*, *296*, 108205. https://doi.org/10.1016/j.agrformet.2020.108205

Sanmiguel-Vallelado, A., López-Moreno, J. I., Morán-Tejeda, E., Alonso-González, E., Navarro-Serrano, F. M., Rico, I. & Camarero, J. J. (2020). Variable effects of forest canopies on snow processes in a valley of the central Spanish Pyrenees. *Hydrological Processes*, *34*, 2247–2262. https://doi.org/10.1002/hyp.13721

Sanmiguel-Vallelado, A., McPhee, J., Esmeralda Ojeda Carreño, P., Morán-Tejeda, E., Julio Camarero, J. & López-Moreno, J. I. (2022). Sensitivity of forest–snow interactions to climate forcing: Local variability in a Pyrenean valley. *Journal of Hydrology*, *605*, 127311. https://doi.org/10.1016/j.jhydrol.2021.127311

Sanmiguel-Vallelado, A., Morán-Tejeda, E., Alonso-González, E. & López-Moreno, J. I. (2017). Effect of snow on mountain river regimes: An example from the Pyrenees. *Frontiers of Earth Science*, *11*(3), 515–530. https://doi.org/10.1007/s11707-016-0630-z

Santeford, H. & Smith, J. (1974). Advanced concepts and techniques in the study of snow and ice resources. (ISBN-0-309-02235-5).

Schimel, J. P., Bilbrough, C. & Welker, J. M. (2004). Increased snow depth affects microbial activity and nitrogen mineralization in two Arctic tundra communities. *Soil Biology and Biochemistry*, *36*(2), 217–227. https://doi.org/10.1016/j.soilbio.2003.09.008

Schneider, E. E., Affleck, D. L. R. & Larson, A. J. (2019). Tree spatial patterns modulate peak snow accumulation and snow disappearance. *Forest Ecology and Management*, *441*, 9–19. https://doi.org/10.1016/j.foreco.2019.03.031

Schönenberger, W. & Brang, P. (2004). SITE-SPECIFIC SILVICULTURE | Silviculture in Mountain Forests. In J. Burley (Ed.), *Encyclopedia of Forest Sciences* (pp. 1085–1094). Elsevier. https://doi.org/10.1016/B0-12-145160-7/00228-3

Schöner, W., Koch, R., Matulla, C., Marty, C. & Tilg, A.-M. (2019). Spatiotemporal patterns of snow depth within the Swiss-Austrian Alps for the past half century (1961 to 2012) and linkages to climate change. *International Journal of Climatology*, *39*(3), 1589–1603. https://doi.org/10.1002/joc.5902

Schütz, C., Wallinger, M., Burger, R. & Füreder, L. (2001). Effects of snow cover on the benthic fauna in a glacier-fed stream: Effects of snow cover on stream fauna. *Freshwater Biology*, *46*(12), 1691–1704. https://doi.org/10.1046/j.1365-2427.2001.00852.x

Seibert, J., Jenicek, M., Huss, M. & Ewen, T. (2015). Snow and Ice in the Hydrosphere. *Snow and Ice-Related Hazards, Risks and Disasters* (pp. 99–137). Elsevier. https://doi.org/10.1016/B978-0-12-394849-6.00004-4

Seibert, J., Jenicek, M., Huss, M., Ewen, T. & Viviroli, D. (2021). Snow and ice in the hydrosphere. *Snow and ice-related hazards, risks, and disasters* (pp. 93–135). Elsevier.

Seidl, R., Schelhaas, M.-J., Rammer, W. & Verkerk, P. J. (2014). Increasing forest disturbances in Europe and their impact on carbon storage. *Nature Climate Change*, *4*(9), 806–810. https://doi.org/10.1038/nclimate2318

Senf, C. & Seidl, R. (2021). Mapping the forest disturbance regimes of Europe. *Nature Sustainability*, *4*(1), 63–70. https://doi.org/10.1038/s41893-020-00609-y

Serrano, F. M. N. & Moreno, J. I. L. (2017). Spatio-temporal analysis of snowfall events in the spanish Pyrenees and their relationship to atmospheric circulation. *Cuadernos de investigación geográfica / Geographical Research Letters*, (43), 233–254.

Serre, F. (1979). Résultats dendroclimatiques pour les Alpes méridionales françaises. *Colloque International Du Centre National d'Etudes Spatials "Evolution Des Atmoshperes Planétaires et Climatologie de La Terre"*, 381–386.

Sevruk, B. & Mieglitz, K. (2002). The effect of topography, season and weather situation on daily precipitation gradients in 60 Swiss valleys. *Water science and technology*, *45*(2), 41–48.

Shafer, S. L., Bartlein, P. J. & Whitlock, C. (2005). Understanding the spatial heterogeneity of global environmental change in mountain regions. *Global change and mountain regions* (pp. 21–30). Springer.

Sicart, J. E., Essery, R. L., Pomeroy, J. W., Hardy, J., Link, T. & Marks, D. (2004). A sensitivity study of daytime net radiation during snowmelt to forest canopy and atmospheric conditions. *Journal of Hydrometeorology*, *5*(5), 774–784.

Simpkins, G. (2018). Snow-related water woes. *Nature Climate Change*, *8*(11), 945–945. https://doi.org/10.1038/s41558-018-0330-7

Singh, P. (2001). *Snow and Glacier Hydrology*. Springer Science & Business Media.

Singh, P., Spitzbart, G., Hübl, H. & Weinmeister, H. W. (1997). Hydrological response of snowpack under rain-on-snow events: A field study. *Journal of Hydrology*, *202*(1-4), 1–20.

Skiles, S. M., Flanner, M., Cook, J. M., Dumont, M. & Painter, T. H. (2018). Radiative forcing by light-absorbing particles in snow. *Nature Climate Change*, *8*(11), 964–971. https://doi.org/10.1038/s41558-018-0296-5

Slatyer, R. A., Umbers, K. D. L. & Arnold, P. A. (2021). Ecological responses to variation in seasonal snow cover. *Conservation Biology*. https://doi.org/10.1111/cobi.13727
In press

Spandre, P., François, H., Verfaillie, D., Pons, M., Vernay, M., Lafaysse, M., George, E. & Morin, S. (2019). Winter tourism under climate change in the Pyrenees and the French Alps: Relevance of snowmaking as a technical adaptation. *The Cryosphere*, *13*(4), 1325–1347. https://doi.org/10.5194/tc-13-1325-2019

Speed, J. D. M., Austrheim, G., Hester, A. J. & Mysterud, A. (2010). Experimental evidence for herbivore limitation of the treeline. *Ecology*, *91*(11), 3414–3420. https://doi.org/10.1890/09-2300.1

Stadelmann, G., Bugmann, H., Wermelinger, B., Meier, F. & Bigler, C. (2013). A predictive framework to assess spatio-temporal variability of infestations by the European spruce bark beetle. *Ecography*, *36*(11), 1208–1217.

Steppuhn, H. (1981). Snow and agriculture. *Handbook of snow: Principles, processes, management and use* (pp. 60–125). Pergamon press.

Sterle, K., Jose, L., Coors, S., Singletary, L., Pohll, G. & Rajagopal, S. (2020). Collaboratively Modeling Reservoir Reoperation to Adapt to Earlier Snowmelt Runoff. *Journal of Water Resources Planning and Management*, *146*(1), 05019021. https://doi.org/10.1061/(ASCE)WR.1943-5452.0001136

Stevens-Rumann, C. S., Kemp, K. B., Higuera, P. E., Harvey, B. J., Rother, M. T., Donato, D. C., Morgan, P. & Veblen, T. T. (2018). Evidence for declining forest resilience to wildfires under climate change (F. Lloret, Ed.). *Ecology Letters*, *21*(2), 243–252. https://doi.org/10.1111/ele.12889

Stewart, I. T. (2009). Changes in snowpack and snowmelt runoff for key mountain regions. *Hydrological Processes: An International Journal*, *23*(1), 78–94.

Strasser, U., Bernhardt, M., Weber, M., Liston, G. E. & Mauser, W. (2008). Is snow sublimation important in the alpine water balance? *The Cryosphere*, *2*(1), 53–66.

Tatarinov, F. & Čermák, J. (1999). Daily and seasonal variation of stem radius in oak. *Annals of Forest Science*, *56*(7), 579–590. https://doi.org/10.1051/forest:19990705

Teich, M., Marty, C., Gollut, C., Grêt-Regamey, A. & Bebi, P. (2012). Snow and weather conditions associated with avalanche releases in forests: Rare situations with decreasing trends during the last 41years. *Cold Regions Science and Technology*, *83–84*, 77–88. https://doi.org/10.1016/j.coldregions.2012.06.007

Templer, P. H., Schiller, A. F., Fuller, N. W., Socci, A. M., Campbell, J. L., Drake, J. E. & Kunz, T. H. (2012). Impact of a reduced winter snowpack on litter arthropod abundance and diversity in a northern hardwood forest ecosystem. *Biology and Fertility of Soils*, *48*(4), 413–424. https://doi.org/10.1007/s00374-011-0636-3

Terzago, S., von Hardenberg, J., Palazzi, E. & Provenzale, A. (2014). Snowpack changes in the Hindu Kush–Karakoram–Himalaya from CMIP5 global climate models. *Journal of Hydrometeorology*, *15*(6), 2293–2313.

Theriault, J. M. & Stewart, R. E. (2008). Rain-Snow boundaries along mountainsides. *American Meteorological Society, 13th Conference on Mountain Meteorology.*

Tierney, G. L., Fahey, T. J., Groffman, P. M., Hardy, J. P., Fitzhugh, R. D. & Driscoll, C. T. (2001). Soil freezing alters fine root dynamics in a northern hardwood forest. *Biogeochemistry*, *56*(2), 175–190. https://doi.org/10.1023/A:1013072519889

Treml, V. & Chuman, T. (2015). Ecotonal dynamics of the altitudinal forest limit are affected by terrain and vegetation structure variables: An example from the Sudetes Mountains in Central Europe. *Arctic, Antarctic, and Alpine Research*, *47*(1), 133–146.

Trujillo, E., Molotch, N. P., Goulden, M. L., Kelly, A. E. & Bales, R. C. (2012). Elevation-dependent influence of snow accumulation on forest greening. *Nature Geoscience*, *5*(10), 705–709. https://doi.org/10.1038/ngeo1571

Vaganov, E. A., Hughes, M. K., Kirdyanov, A. V., Schweingruber, F. H. & Silkin, P. P. (1999). Influence of snowfall and melt timing on tree growth in subarctic Eurasia. *Nature*, *400*(6740), 149–151. https://doi.org/10.1038/22087

Van Mullem, J. A. & Garen, D. (2004). Chapter 11: Snowmelt. *United States Department of Agriculture (USDA). Natural Resources Conservation Service*, 27.

van Vuuren, D. P., Edmonds, J., Kainuma, M., Riahi, K., Thomson, A., Hibbard, K., Hurtt, G. C., Kram, T., Krey, V., Lamarque, J.-F., Masui, T., Meinshausen, M., Nakicenovic, N., Smith, S. J. & Rose, S. K. (2011). The representative concentration pathways: An overview. *Climatic Change*, *109*(1-2), 5–31. https://doi.org/10.1007/s10584-011-0148-z

Vannière, B., Colombaroli, D., Chapron, E., Leroux, A., Tinner, W. & Magny, M. (2008). Climate versus human-driven fire regimes in Mediterranean landscapes: The Holocene record of Lago dell'Accesa (Tuscany, Italy). *Quaternary Science Reviews*, *27*(11), 1181–1196. https://doi.org/10.1016/j.quascirev.2008.02.011

Vaughan, D. G., Comiso, J., Allison, I., Carrasco, J., Kaser, G., Kwok, R., Mote, P., Murray, T., Paul, F., Ren, J., Rignot, E., Solomina, O., Steffen, K. & Zhang, T. (2013). Observations: Cryosphere. In T. F. Stocker, D. Qin, G.-K. Plattner, M. M. B. Tignor, S. K. Allen, J. Boschung, A. Nauels, Y. Xia, V. Bex & P. M. Midgley (Eds.), *Climate change 2013. The physical science basis. Working group I Contribution to the fifth assessment report of the intergovernmental panel on climate change* (pp. 317–382). Cambridge University Press. https://doi.org/10.1017/CBO9781107415324.023

Vicuña, S., Garreaud, R. D. & McPhee, J. (2011). Climate change impacts on the hydrology of a snowmelt driven basin in semiarid Chile. *Climatic Change*, *105*(3), 469–488.

Villalba, R., Veblen, T. T. & Ogden, J. (1994). Climatic influences on the growth of subalpine trees in the Colorado Front Range. *Ecology*, *75*(5), 1450–1462.

Vittoz, P., Rulence, B., Largey, T. & Freléchoux, F. (2008). Effects of climate and land-use change on the establishment and growth of cembran pine (Pinus cembra L.) over the altitudinal treeline ecotone in the Central Swiss Alps. *Arctic, Antarctic, and Alpine Research*, *40*(1), 225–232.

Vogt, S. & Braun, M. (2004). Influence of glaciers and snow cover on terrestrial and marine ecosystems as revealed by remotely-sensed data, 15.

von Humboldt, A. & Bonpland, A. (1807). *Essai sur la géographie des plantes*. MAXTOR.

Walther, G.-R., Gritti, E. S., Berger, S., Hickler, T., Tang, Z. & Sykes, M. T. (2007). Palms tracking climate change. *Global Ecology and Biogeography*, *16*(6), 801–809. https://doi.org/10.1111/j.1466-8238.2007.00328.x

Wangchuk, K. & Wangdi, J. (2018). Signs of climate warming through the eyes of yak herders in northern Bhutan. *Mountain Research and Development*, *38*(1), 45–52.

Weih, M. & Karlsson, P. S. (2001). Growth response of Mountain birch to air and soil temperature: Is increasing leaf-nitrogen content an acclimation to lower air temperature? *New Phytologist*, *150*(1), 147–155. https://doi.org/10.1046/j.1469-8137.2001.00078.x
_eprint: https://nph.onlinelibrary.wiley.com/doi/pdf/10.1046/j.1469-8137.2001.00078.x

Weingartner, R., Schädler, B. & Hänggi, P. (2013). Auswirkungen der Klimaänderung auf die schweizerische Wasserkraftnutzung. *Geographica Helvetica*, *68*(4), 239–248. https://doi.org/10.5194/gh-68-239-2013

Westerling, A. L. (2016). Increasing western US forest wildfire activity: Sensitivity to changes in the timing of spring. *Philosophical Transactions of the Royal Society B: Biological Sciences*, *371*(1696), 20150178. https://doi.org/10.1098/rstb.2015.0178

Whitaker, A. C., Sugiyama, H. & Hayakawa, K. (2008). Effect of Snow Cover Conditions on the Hydrologic Regime: Case Study in a Pluvial-Nival Watershed, Japan 1. *JAWRA Journal of the American Water Resources Association*, *44*(4), 814–828.

Wieser, G. & Tausz, M. (2007). *Trees at their upper limit: Treelife limitation at the alpine timberline* (Vol. 5). Springer Science & Business Media.

Wilmking, M. & Juday, G. P. (2005). Longitudinal variation of radial growth at Alaska's northern treeline—recent changes and possible scenarios for the 21st century. *Global and Planetary Change*, *47*(2), 282–300. https://doi.org/10.1016/j.gloplacha.2004.10.017

Wilson, G., Green, M., Brown, J., Campbell, J., Groffman, P., Durán, J. & Morse, J. (2020). Snowpack affects soil microclimate throughout the year. *Climatic Change*, *163*(2), 705–722. https://doi.org/10.1007/s10584-020-02943-8

Winkler, D. E., Chapin, K. J. & Kueppers, L. M. (2016). Soil moisture mediates alpine life form and community productivity responses to warming. *Ecology*, *97*(6), 1553–1563.

Wipf, S. & Rixen, C. (2010). A review of snow manipulation experiments in Arctic and alpine tundra ecosystems. *Polar Research*, *29*(1), 95–109. https://doi.org/10.1111/j.1751-8369.2010.00153.x

Wu, Q. (2020). Season-dependent effect of snow depth on soil microbial biomass and enzyme activity in a temperate forest in Northeast China. *Catena*, *195*, 104760.

Zhang, T. (2005). Influence of the seasonal snow cover on the ground thermal regime: An overview. *Reviews of Geophysics*, *43*(4). https://doi.org/10.1029/2004RG000157

Chapter 2

Methodology

This section presents the materials and methods that were used to do this Thesis, allowing readers to evaluate the reliability and validity of the research. Firstly, the chosen methodological approach is explained. Secondly, the spatial context in which the research was carried out is described. Thirdly, the different environmental variables studied are presented. Fourthly, the way in which the data were collected is explained. Ultimately, the way in which the data were analyzed is described.

2.1 Methodological approach

Before describing what data were needed and where and how these data were collected, it is important to introduce the overall research design of this Thesis. Saunders and Tosey (2013) use the metaphor of the *Research Onion* to illustrate how the ultimate elements of the research (i.e. onion core) need to be considered in relation to other design elements (i.e. outer layers) (Figure 2.1). Research creates new knowledge. But, researcher's personal vision determines what constitutes acceptable knowledge and what are the suitable methods to obtain it. That is called the research philosophy and comprises the outermost layer of the *Research Onion.* Several views may be adopted depending of the field of knowledge in this regard. Since this Thesis is concerned with law–like generalisations such as cause and effect, the developed research is framed in the philosophy of the *positivism.* Positivism establishes that reality is stable and can be observed and described from an objective point of view, that is,

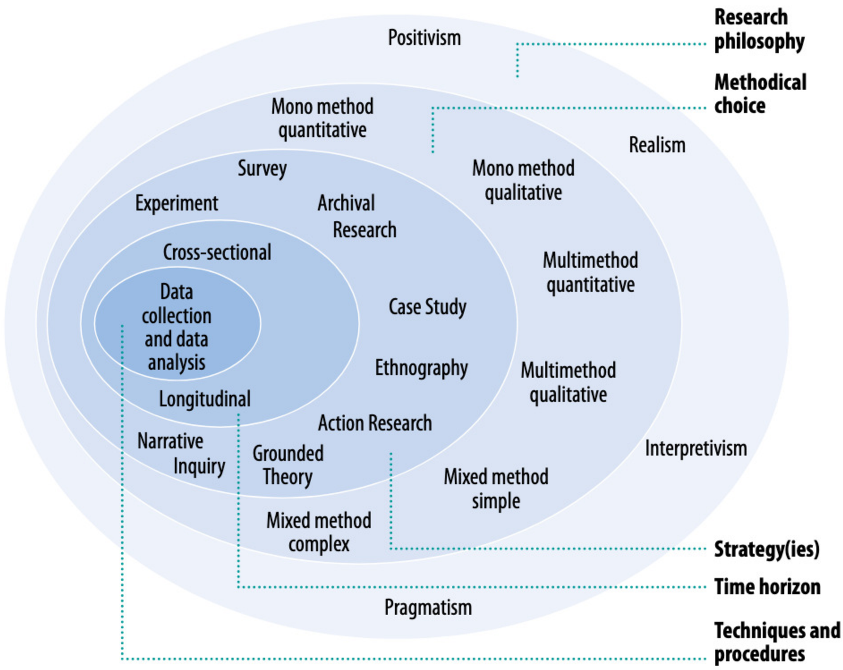

Figure 2.1: The Research Onion. Credit: Saunders and Tosey (2013).

without interfering with the phenomena that is being studied (Levin, 1988). To this end, this Thesis adopted the *scientific method* to propose hypotheses, via induction, based on previous observations that lead us to ask questions. Hypotheses were tested with highly–structured and measurable data, thus large samples of quantitative data and statistical testing were involved. In the end, hypotheses were refuted or rejected based on the experimental findings, which may entail a revision of the underlying theory. The following layer of the *Research Onion* addresses the methodological choice; including quantitative methods, qualitative methods or a mixture or both, such as the used in this Thesis. More specifically, it was used a *multimethod quantitative* design which implied more than one quantitative data collection technique with associate statistical analysis procedures, and following this, a *mixed method complex* design was used which comprised quantitative analyses techniques to analyze qualitative data, for example, to statistically compare the magnitude of different variables between different groups. This reflects the interdisciplinary approach followed in this Thesis, which comprised information, data, techniques, tools, perspectives, concepts and theories from several disciplines within the physical and life sciences (such as hydrology, forest ecology and climatology) to achieve the defined objectives. The next layer of the *Research Onion* includes the strategy or strategies followed within to answer a research question. The main methodologies used in this Thesis are field experiments, although part of it is based on simulations. It is important to note that boundaries between research strategies are permeable, as evidenced by the simulations carried out in this Thesis which were based on experimental data collected in the field. The time horizon in which the research is undertaken is determined by the final layer of the *Research Onion*, before reaching the core. In this Thesis, certain research questions were addressed at a particular time, and thus, in these cases the research could be considered *cross–sectional*. While in other cases, data from an extended period of time (e.g. 30 years) was needed to address the research question, and therefore, the research could be considered *longitudinal*.

The above presentation of the methodological approach followed in this Thesis will help to ensure that the data collection techniques and analysis procedures used, which I will describe below, are both appropriate and coherent.

2.2 Study areas

The main part of this Thesis was performed in a mountain valley (*Baños de Panticosa*) located in the central Spanish Pyrenees, while a minor part of it was carried out in a wider spatial context comprising the main NE Iberian Peninsula mountains. Therefore, the common context in which this Thesis is framed are the high mountains under the influence of the Mediterranean climate. The Mediterranean climate was already included in the Köppen (1936) classification of the different climates on Earth. This climate occurs in the regions around the Mediterranean Sea, but also in coastal areas of Central Chile, California, South Africa and Southwest Australia (Figure 2.2). All of these areas lie between about 30º and 45º latitude and at the western flank of continents. Mild wet winters and warm–to–hot summers with often little precipitation characterize the Mediterranean climate (Lionello et al., 2006). Focusing on the Mediterranean region, mountains cover 21% of its surface, occupying more than 50% of the land in many countries. In the case of Spain,

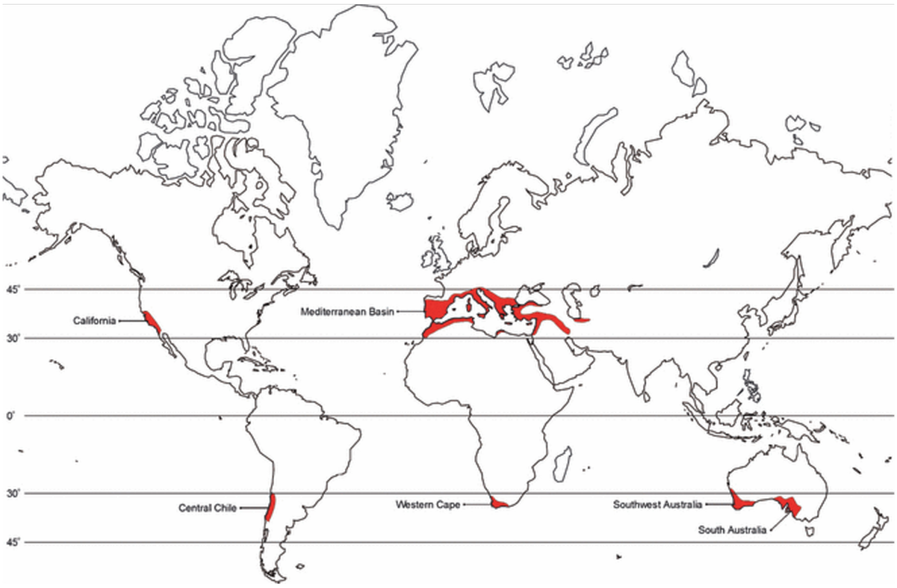

Figure 2.2: Areas under the influence of the Mediterranean climate (in red). Credit: Latron et al. (2009).

mountains cover 42% of the territory, and the mountains of the NE of the Iberian Peninsula constitute a large part of it. The complex morphology and topography of the Mediterranean region highly determine the oceanic and atmospheric circulation. The high mountain ranges that surround the Mediterranean sea produce sharp climate features that differ from the general climate. As a consequence, mean annual temperature is much lower in the Mediterranean mountains than in the lowlands, and annual rainfall is largely increased, although the characteristic summer drought period is maintained (Olcina, 2007). In those areas, precipitation during winter accounts more than 80% of the annual precipitation (November to March) and usually falls as snow, highly influencing related river regimes (Fayad et al., 2017). Although most population and economic activities are concentrated in the lowlands and coastal areas of the Mediterranean region, its mountains host ~10% of the total population (i.e. 66 million people), and critical water resources of lowlands and costs depend on mountain snow pools (d'Ostiani, 2004).

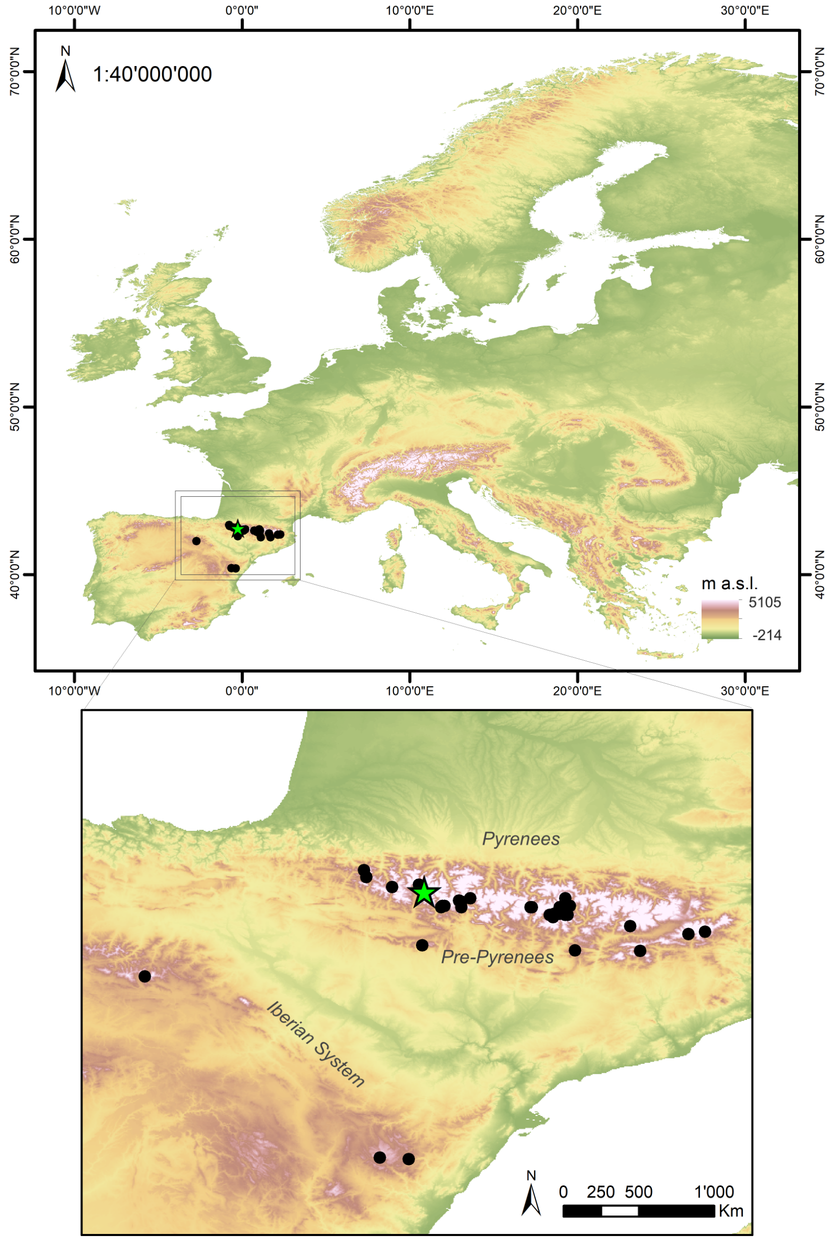

Figure 2.3: Location of the forest stands studied in this Thesis at the main mountains in the NE Iberian Peninsula. The black dots represent those sites analysed in Chapter 4, considering a regional scale. The green star highlights the location of the *Baños de Panticosa* experimental site, where the bulk of this Thesis (Chapters 3, 5 and 6) has been developed considering a local scale. Source of elevation data: European Digital Elevation model (EU-DEM v1.1) from Copernicus Land Monitoring Service, 25 m spatial resolution.

2.2.1 Regional scale: mountains in the NE Iberian Peninsula

The selection of this regional scale in this Thesis (Chapter 4) responds to the distribution of *Pinus uncinata* in the Iberian Peninsula. This pioneer, shade-intolerant and long-living pine species grows in the northeastern high mountains, mainly in the Pyrenees but also in some isolated and high areas in the Iberian System (see Figure 1.14). Furthermore, both mountain ranges host seasonal snowpacks every year, being in the Pyrenees deeper and longer lasting than in the Iberian System due to the latitudinal gradient, continentality, precipitation patterns and the higher elevation shown by the Pyrenees (Alonso-González et al., 2020a).

The Pyrenees is a West–East aligned mountain range and extends 450 km between the Mediterranean Sea and the Atlantic Ocean, over France, Andorra and Spain. This range reaches a maximum elevation of 3404 m a.s.l. (Aneto peak). The Atlantic climate strongly influences the westernmost Pyrenean edge and the northern side of the range, while Mediterranean conditions are widely shown by lower areas along the southern side. Moreover, orography produces contrasting conditions between the north side (Atlantic influence) and the central part of the southern side (Continental influence) through foehn winds (Ninot et al., 2017). The Spanish side of the Pyrenees extends southwards over secondary ranges known as the Pre–Pyrenees, where scattered *P. uncinata* populations grow. This lower mountain range acts as a transition between the Pyrenees and the flatter lowlands, although it shows peaks that may exceed 2000 m a.s.l. The Pre–Pyrenees are mainly formed of lime bedrock and show contrasting relief, where canyons and steep slopes are widespread. Their north–facing slopes receive a greater influence of Continental climate whilst the Mediterranean influence seems higher for south–facing slopes (Gutiérrez, 1991).

The Iberian System is located further inland on the Iberian Peninsula, and on the other side of the Ebro basin. This mountain range separates the Ebro basin from the Central Spanish Plateau along ∼600 km. It is aligned Northwest–Southeast and reaches a maximum elevation of 2314 m a.s.l. (Moncayo peak). This Thesis focused on the northwestern and southeastern extremes of the Iberian system where two relict populations of *P. uncinata* are located, being the southernmost distribution limit of this species in Europe. The northwestern extreme of the range shows greater Continental influence, while the greater Mediterranean influence is shown by the southeastern extreme (greater intensity of the summer drought) (Camarero & Gutiérrez, 2008).

In total, 36 pine forests stands were studied within these mountains based on the available tree-ring chronologies (Galván et al., 2012) and environmental conditions (Alonso-González et al., 2018) during the 1980–2010 period, covering the whole geographical distribution of this species in the Iberian Peninsula: 33 sites in the Pyrenees (3 of them in the Pre–Pyrenees) and 3 sites in the Iberian System (Figure 2.3). The sampled forests were 334 ± 108 years old and they were located between 1750 and 2451 m a.s.l. Please see Figure 1 and Table S1 in Chapter 4 for more details about the geography, topography, forest characteristics and average environmental conditions of sampled sites.

2.2.2 Local scale: *Baños de Panticosa* experimental site (Central Pyrenees)

The bulk of the research developed in this Thesis (Chapter 3 ,Chapter 5 and Chapter 6) took place at the *Baños de Panticosa* experimental site, which comprises a mountain valley located in the Spanish Central Pyrenees (Figure 2.3). The Central Pyrenees usually refers to the geographical part of the Pyrenees which extends approximately between the Somport mountain pass (in the West) and the Maladeta massif (in the East). The *Baños de Panticosa* valley constitutes the headwaters of the Caldarés river that drain to Gállego river, a main tributary of the Ebro river. The Continental climate is dominant in this place (Del Barrio et al., 1990). The bottom of the valley is located at 1630 m a.s.l., while the highest summits reach more than 3000 m a.s.l. *P. uncinata* dominates the landscape from the valley's bottom to 2300–2500 m a.s.l. A depth and long lasting seasonal snowpack is formed every year (from November to May–June) within the altitudinal range in which *P. uncinata* grows. These circumstances, together with the abrupt topography that induces contrasting aspects, slopes, microclimates, and forest structure within the valley, represent ideal characteristics for the study of forest–snow interactions at local scale under various environments. Another important reason for the selection of this study area was the ease of access by road, which was even viable during most of the winter, as well as, the dense network of hiking trails that permit access to diverse *P. uncinata* forests. The experimental site at the *Baños de Panticosa* valley consisted of four *P. uncinata* forest stands (38 $\pm$ 7 years old) located between 1674 and 2104 m a.s.l. with differing exposure, forest structure and microclimatology (Figure 2.4). One plot of approximately 450 m^2 was settled in each of the four forest stands. The plots were named based on their locations in the valley (from NE to SW) as plot 1, plot 2, plot 3 and plot 4. At each experimental plot, five *P. uncinata* individuals were monitored (2016–2018 period) as well as environmental conditions (2015–2020 period). Specific characteristics, including topography, forest structure and average environmental conditions of sampled sites during the study period are shown in Table 2 in Chapter 3, Table 1 in Chapter 5 and Table 1 in Chapter 6.

It is noteworthy to mention the complex logistics required for data collection in this study area all–year–round. To reach the studied forest stands from the bottom valley it was necessary to walk between 30 minutes and 1 hour and a half, which can take up to 2 hours if the snow conditions were inappropriate. The difference in altitude to reach each studied forest stand ranged from 33 to 474 m. This particular environment, and the fact that most of the field work was carried out during the snow season, boots, snowshoes and mountain skis were a must to access the studied forest stands, with the added difficulty of carrying the measurement equipment on the back. The time required just to get to the studied forest stands, added to the time required for maintenance of the installed devices and manual data collection, only allowed us to work on two sites per day. Therefore, each fieldwork campaign required spending two consecutive days in this study area. It should be noted that the choice of field work days, in order to ensure safe conditions for the staff involved, was conditioned by the mountain weather forecast[1] and the avalanche danger

[1]Weather mountain forecast for the Aragonese Pyrenees elaborated by the State Meteor-

Figure 2.4: (a) General view of the plots in the experimental site at the *Baños de Panticosa* valley during the snow–free season. The lake placed at the bottom of the valley, visible in both photographs, serves as a reference point. At left: southwest mountainside. At right: northeast mountain side. (b) Detail view of each of the plots during the snow season.

ological Agency (AEMET) (http://www.aemet.es/es/eltiempo/prediccion/montana?w=&p=arn1)

bulletin[2]. Furthermore, research group members were trained in avalanche terrain safety, acquiring the tools and knowledge necessary to operate safely in avalanche terrain (accreditation ACNA – Association for Snow and Avalanche Knowledge – Level 1).

2.3 Study variables

The following is a brief description of the main environmental variables that have been addressed in this Thesis. In the previous Chapter 1 the reader will find background information about the concepts outlined herein.

Snow–related data

Snowpack depth: A snowpack can be described in many different ways, but perhaps the simplest way is to quantify its depth. Snow depth is defined as the vertical distance from the snow surface to the ground and is reported in centimetres (cm).

Snow density: Density is defined as the amount of mass that an object has compared to its volume, and it is widely expressed in $kg \cdot m^{-3}$. On average, 1 m^3 of freshly–fallen snow has an average of $\sim$50 kg. However, the density of snow can vary by more than an order of magnitude as a function on formation conditions in the clouds, the atmospheric conditions during snowfall and the subsequent metamorphism after falling on the ground. The spatial variability of snow density is relatively small in comparison to snowpack depth (López-Moreno et al., 2013). Besides that, the measurement of snow density is much more difficult and time consuming than snow depth.

Snow Water Equivalent: The more relevant property of a snowpack from a hydrological point of view is the snow water equivalent (SWE). The SWE is defined as the amount of liquid water contained in the snowpack per unit ground surface area and may directly contribute to runoff. It is normally expressed in millimetres of water equivalent (mm) or $kg \cdot m^{-2}$ (Seibert et al.,

[2] Avalanche danger bulletin (in Spanish *Boletín de Peligro de Aludes, BPA*) for the valley of Canfranc elaborated by A Lurte (https://www.alurte.es/boletin.php).

2015). SWE, snowpack depth, snow density, and water density are directly related as is shown in Figure 2.5.

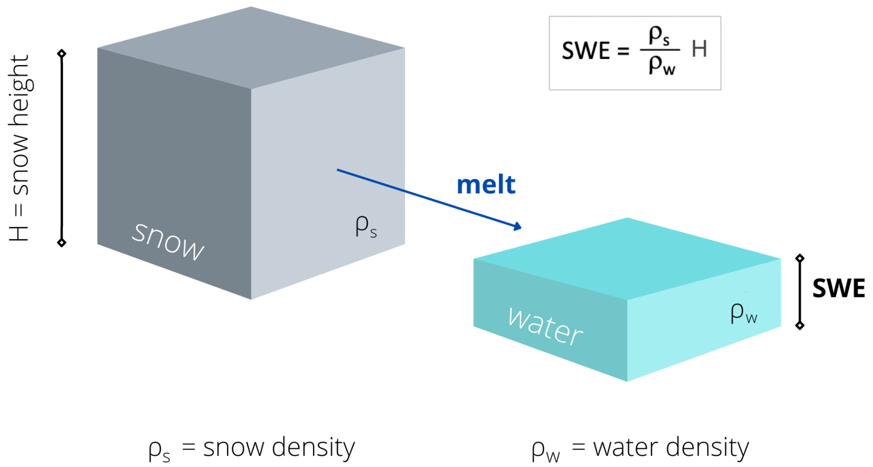

Figure 2.5: The Snow Water Equivalent (SWE) is a measure of the water content of the snow.

Snow energy fluxes: Snowpack can exchange energy with its surroundings, thus energy fluxes towards the snowpack mean gains and energy fluxes away from the snowpack mean losses. The snow energy balance (SEB) includes the following types of fluxes: incoming solar radiation, thermal radiation, sensible heat, latent heat, ground conduction and advected heat. They are expressed in $W \cdot m^{-2}$ in the International System of Units (SI).

Tree–related data

Tree–ring width: To assess long–term growth responses to environment it is necessary to perform retrospective analyses of tree–ring width chronologies. Based on the idea that trees form one ring per year, by coring a living tree and cross-dating and measuring tree–rings from the present backwards, it is possible to determine the year in which each ring was formed (i.e. tree–ring dating) and how much it grew wider. Thus, resulting cross–dated tree–ring width series can inform if past to current environmental conditions have been favorable or not for tree radial growth based on the thickening of tree rings.

Cell production or xylogenesis: The intra–annual xylem development involves a series of phases from cambial division onset to cell maturation, resulting in a new tree–ring. During the developmental stage, cells showed different shapes and stained with different colours when wood samples are processed in a laboratory, which makes it possible to differentiate between different cell types (Antonova & Stasova, 1993). The main characteristics of each type of cell are here listed: cambial cells have similar and small radial diameters and thin walls; radially elongating tracheids showed wider radial diameter and contain a protoplast enclosed by a thin primary wall; wall–thickening tracheids corresponded to the onset of secondary cell wall formation and were characterised by cell corner rounding; secondary walls glistened under polarised light and walls turned blue due to wall lignification; and mature cells did not contain cytoplasm and presented completely blue walls (Deslauriers et al., 2015; Rossi et al., 2006). The xylogenesis monitoring produces data on critical dates (e.g. onset of cell enlargement, timing of maximal growth rate, cessation of cell wall lignification), as well as derived variables that quantify rates of cell production (e.g. nº mature tracheids $\cdot$ day^{-1}) (De Micco et al., 2019). This information can be used to assess short–term ecophysiological responses to environment.

Stem radius variations: The study of stem radius variation throughout the year can provide useful information on tree growth process and water status. Thus, it is necessary to bear in mind that two processes occur simultaneously: (1) an irreversible stem expansion due to cell growth, and (2) a reversible shrinking and swelling of the stem induced by changes in the water balance of tissues (Kozlowski, 1972). These changes can be detected on a very short–term, even at hourly resolution. These data series are usually expressed as rates of stem radial increment in µm $\cdot$ day^{-1}.

Phenology of shoots and needles: This refers to the study of the temporal pattern of tissue allocation on apical meristems[3], which can provide useful information to establish relationships between the primary growth of trees and environmental conditions. Critical dates of shoot and needle elongation

[3]Meristems are regions of cells capable of division and growth in plants. Apical meristems are responsible for the vertical growth of trees (primary growth), while lateral meristems located in the cambium are responsible of trees thickening (secondary or radial growth).

(e.g. onset of elongation) can be visually tracked in the field, as well as, the elongation extent.

Non–structural carbohydrate (NSC) concentrations: Carbohydrates are products of the photosynthesis, which is the chemical combination of carbon dioxide and water by using the energy from the absorption of visible light. The structural carbohydrates (e.g. cellulose) are the building blocks for tree biomass used to form cell walls, and thus, to provide structural support for trees. Otherwise, the non–structural carbohydrates, mainly sugars and starch, are the major substrates for tree metabolism and growth, and can be used as osmolites for regulating turgor; that is, for tree functioning. The quantification of NSC (%) in tree tissues where carbohydrates are stored, such as sapwood (the part of living wood where sap flows) and needles, is widely used to link seasonal tree responses to environmental conditions (Blumstein & Hopkins, 2021; Peltier et al., 2021).

Forest structure: According to Smith (1993), the description of a forest structure may include measures of species composition, diversity, age–class distribution, stem height, stem diameter at breast height (dbh), basal area (proportion of the ground occupied by the stems, expressed in m^2 per ha), and tree density (number of trees per unit area). The sampled pine forests in this Thesis, characterised by being mono–especific, did not require the description of the first two measurements. Additionally, due to the nature of the studies that were carried out, it was of particular interest to determine: the canopy cover, which is the proportion of the forest floor covered by the vertical projection of the tree crowns expressed as a % (Korhonen et al., 2006), and the Leaf Area Index (LAI), which is the projected area of leaves over a unit of land ($m^2 \cdot m^{-2}$) (Waring & Running, 2007).

Climate–related data

Air Temperature: It refers to surface air temperature, generally measured at 1.25–2 m above ground, and here it is expressed in ºC. In mountainous areas, it shows a particularly complex relationship with altitude (Navarro-Serrano et al., 2018).

Air humidity: Humidity is the amount of water vapor present in the air. Air humidity is usually expressed as relative humidity (%), which indicates the amount of water vapor in the air at a given temperature relative to the maximum amount of water vapor that air can hold at that temperature.

Wind speed: Wind is caused by the movement of air following a pressure gradient, amongst other forces, as a result of differential heating of the Earth's surface. Wind speed is expressed in $m \cdot s^{-1}$ in SI units.

Total precipitation: Total precipitation refers to the amount of water reaching the ground at the weather station as rain, dew, hail or snow. It is expressed in mm, which is equivalent to $L \cdot m^{-2}$.

Global solar irradiance (GSI): Solar irradiance is the electromagnetic radiation from the Sun reaching Earth's surface described as power per unit area ($W \cdot m^{-2}$ in SI units). Global radiation, also called total incoming solar radiation at surface, includes that obtained directly from the solar disk, the diffuse radiation from the sky scattered through the atmosphere, and terrain contributions.

Potential solar irradiation: Solar irradiance is often integrated over a given time period in order to report the radiant energy emitted into the surrounding environment during that time period. This integrated solar irradiance is called solar irradiation, solar exposure, solar insolation, or insolation. It is expressed in $W \cdot h \cdot m^{-2}$. Potential solar irradiation refers to the estimated solar irradiation that could be received at surface. In this Thesis, it was considered interesting to estimate this variable in order to compare it with field measurements.

Soil–related data

Soil moisture: Soil moisture or soil water content is the amount of water, including the water vapor, in an unsaturated soil. One of the most widely used parameters for quantifying soil moisture is the volumetric water content (VWC), which is the ratio of volume of water to the unit volume of soil ($m^3 \cdot m^{-3}$). This Thesis focused on the surface soil moisture, considering the water that is in the upper 10–20 cm of soil.

Soil temperature: Here it refers to surface soil temperature (ºC), considering a depth of 10–20 cm from the top of soil.

2.4 Data acquisition proceedings

2.4.1 Field work

The bulk of the data used in this Thesis came from fieldwork carried out in both study areas: the main mountains in the NE Iberian Peninsula, and especially, the *Baños de Panticosa* experimental site. Given that the monitoring tasks carried out at the *Baños de Panticosa* experimental site changed throughout the study period, in Figure 2.6 is shown a graphical scheme of its temporal course. Photographs of the materials and methods used during that monitoring can be found in Figure 2.7 and Figure 2.8.

Snowpack depth was manually and semi–automatically measured at the *Baños de Panticosa* experimental site during three snow seasons (2015/16, 2016/17 and 2017/18), from the onset of snow accumulation (November) to the end of melting (May–June). Two different methods were adopted to collect data on snowpack depth; both are explained hereafter. The derived data were used in the preparation of Chapter 3, Chapter 5 and Chapter 6.

- Fixed snow poles, whose graduated marks (every 25 cm) could be read at a distance, were used to obtain permanent point measurements throughout the snow season. Three poles were placed in a forest opening (O), and five were placed beneath the forest canopy (F) at each plot. Snow poles were automatically photographed by time–lapse cameras (Bushnell, Trophy Cam, KS) several times a day. From the photographs, daily snow depth was subsequently extracted by image analysis, process which is subsequently described. Maintenance and data downloading of these facilities was carried out every 10–15 days during the snow season.
- Spatially distributed measurements of snow depth were done every 10–15 days using an extensible 1–cm–graduated snow depth probe (Snowmetrics Inc., Fort Collins, CO) that was manually inserted into the snowpack

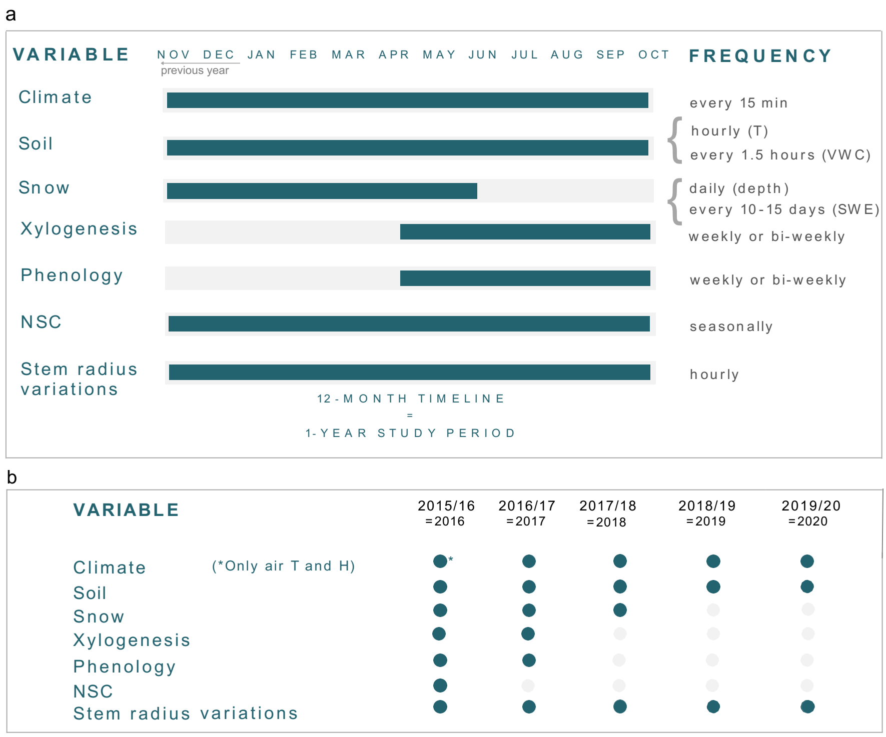

Figure 2.6: (a) Monitoring seasonality at the *Baños de Panticosa* experimental site throughout an annual period. The intra-annual period over which each variable (grouped by type) was measured is indicated by a dark bar. Note that each studied annual period does not correspond to a natural year, and comprised the last months of the previous year. (b) Monitoring period at the *Baños de Panticosa* experimental site. The inter-annual period over which each variable was measured is indicated by a dark dot. It is highlighted the different nomenclature used when naming each annual period according to the focus of the study: tree growing season (e.g. 2016) or snow seasons (e.g. 2015/16).

down to the ground surface. 10 O and 10 F sites were selected in a distributed manner at each plot in order to cover its entire surface, then 10 replicates were taken about 1 m apart per F–O site. Within F sites, measurements were taken from the tree trunks to the edge of the projections of the tree canopies to the ground, covering all aspects, to make sure that most of snowpack spatial variability was collected.

SWE was manually surveyed at the *Baños de Panticosa* experimental site during three snow seasons (2015/16, 2016/17 and 2017/18), from the onset of snow accumulation (November) to the end of melting (May–June).

Samples were taken every 10–15 days using a snow cylinder and scale (ETH core sampler, Swiss Federal Institute of Technology, Zurich) at snow pits dug down to the soil surface. One F and one O site were selected at each plot, where two replicates were collected per F–O site. Technical difficulties arose when trying to increase the number of locations for measurements of snowpack density during field work by digging snow pits, due to the time–consuming nature of the task in snowpacks as deep as the ones found here (maximum thickness found ~3 m). The derived data were used in the preparation of Chapter 3, Chapter 5 and Chapter 6.

Meteorological data was automatically monitored at the *Baños de Panticosa* experimental site all year round by means of two different devices, described below. The derived data were used in the preparation of Chapter 3, Chapter 5 and Chapter 6.

- One weather station (HOBO U30 NRC, Onset Co., Bourne, MA) was installed in an O site at each plot. Each one collected data on GSI[4], wind speed, air temperature and relative humidity every 15 min from October 2016 to June 2020. Maintenance and data downloading (HOBOware software, Onset Co., Bourne, MA) of facilities was carried out seasonally.

- One autonomous self–recording data–logger (Tinytag–Plus– 2; model TGP–4017, Gemini DataLoggers UK Ltd., Chichester, West Sussex, UK), that was equipped with a naturally ventilated radiation shield (Datamate ACS–5050 Weather Shield; Gemini DataLoggers UK Ltd., Chichester, West Sussex, UK), was installed at each forest stand hanging from a tree branch. They collected data on air temperature and relative humidity every 15 min from November 2015 to June 2020. In a previous test, paired data–loggers were installed at both F and O areas at each plot and the obtained series were compared, showing no significant differences between them. These sensors supported the data acquisition by meteorological stations. Maintenance and data downloading

[4]The installed pyranometers in HOBO weather stations present a spectral range from 0.3 to 1.1 µm. The shortwave radiation range is narrowly defined to include radiation with a wavelength between 0.2 µm and 3.0 µm. Thus, in addition to the fact that there is little radiation flux to the Earth's surface outside that range, in Chapter 6 the measured solar irradiance were considered as incoming shortwave radiation.

(Tinytag Explorer software, Gemini DataLoggers UK Ltd., Chichester, West Sussex, UK) of facilities was carried out seasonally.

Soil temperature and humidity data was automatically monitored at the *Baños de Panticosa* experimental site all year round from November 2015 to June 2020. Two different devices were used for that purpose, below described. The derived data were used in the preparation of Chapter 5 and Chapter 6.

- Four to six miniature temperature loggers (Thermochron iButton; DS–1922L model, Dallas Semiconductors, Texas, USA) were buried in the ground (at a depth of 10–20 cm) at each plot in a distributed manner, covering both F and O areas. They collected soil temperature data every hour. The dataloggers were wrapped with laboratory film and duct tape to prevent corrosion and tied to metallic picks to facilitate their later retrieval. Maintenance and data downloading (1–Wire Software, Maxim Integrated, CA, USA) of facilities was done seasonally.

- ECH2O probes (EC–5 model, Decagon Devices, Pullman, WA, USA) were installed in a distributed manner at each plot: two sensors were buried in the ground (at a depth of 10–20 cm) in F areas and two in O areas. They collected soil moisture data every 1.5 hours. The first month of measurements was discarded in order to ensure a proper settling time after field installation. Maintenance and data downloading (ECH2O Utility software, Decagon Devices, Pullman, WA, USA) of facilities was done seasonally.

Stem radius variations were automatically monitored every hour at the *Baños de Panticosa* experimental site all year round, from April 2016 to June 2020, by using stainless–steel band dendrometers (DR 26, EMS Brno, Czech Republic) (n = 10) installed on two or three *P. uncinata* individuals stems (at a height of ~150 cm) at each plot. The external layer of dead bark was previously removed. Maintenance and data downloading (Mini 32 software, EMS Brno, Czech Republic) of these facilities was done seasonally. The derived data were used in the preparation of Chapter 5.

Xylogenesis was manually monitored at the *Baños de Panticosa* experimental site during two years (2016 and 2017), since before the start of tree growth (April) to the end of the growing season (October). Two wood samples of 2 mm diameter and 15–20 mm length, called microcores, were collected weekly or bi–weekly from five *P. uncinata* individual at each plot. One of the samples was subsequently processed while the other was kept as a guarantee in case of sample loss during laboratory processing. Microcores were collected applying a Trephor® increment puncher at 1–1.5 m height on the individuals stems, following an ascending spiral pattern, and each sample was taken at least 5 cm from previous sampling points following the procedure reported in Deslauriers et al. (2015). Microcores were immediately fixed in 50% ethanol solution and stored at 5 ºC to preserve cells from degradation until to their further processing in the laboratory, later described. The derived data were used in the preparation of Chapter 5.

NSC concentrations in stem sapwood and young needles were manually monitored at the *Baños de Panticosa* experimental site in 2016. NSC concentrations were quantified in five *P. uncinata* individuals at each plot. Three apical shoots and one core, taken at breast height (1.3 m) with a Pressler increment borer (Haglöf, Sweden), were seasonally collected and stored at 5 ºC. The samples were then processed in the laboratory, as explained below. The derived data were used in the preparation of Chapter 5.

Phenology of shoots and needles were manually monitored at the *Baños de Panticosa* experimental site during 2016 and 2017, since before the start of tree growth (April) to the end of the growing season (October). Measurements were done weekly or bi–weekly with a ruler (1 mm precision) following Rossi et al. (2009) procedure. Five lower branches, from all exposures, were selected in five *P. uncinata* individuals at each plot. On the branches, the elongation of apical shoots was measured, and on each shoot, five developing needles were randomly selected and measured. The derived data were used in the preparation of Chapter 5.

Tree–ring width data series came from an updating of tree–ring chronologies from 36 forests sampled at the main mountains in the NE Iberian Peninsula and published by Galván et al. (2012). Thus, the related field work and subsequent laboratory processing (described later in this section) was carried out before the start of this Thesis by the mentioned research team. Cores were collected between 1994 and 2010 from 5 to 65 *P. uncinata* individuals randomly selected in each forest. Two or three cores were taken at breast height (1.3 m) with Pressler increment borers (Haglöf, Sweden) from each tree individuals. The derived data were used in the preparation of Chapter 4.

Forest structure was recorded in representative subplots of 15 × 15 m, considering one subplot per study plot, at the *Baños de Panticosa* experimental site. The diameter at breast height at the beginning of the study period (dbh0) was measured using tapes. Tree height was measured using clinometers. Canopy cover was estimated by measuring two crown projections (one perpendicular and one parallel to the slope line) in each pine, then two area values were calculated from these measurements. The cover area of each pine was expressed as a percentage of the subplot area. Finally, all individual canopy cover percentages were aggregated. Because the canopies of different individuals may overlap, the total cover may exceed 100%. Tree age was estimated from dbh0 values based on an age–dbh linear regression obtained in a nearby *P. uncinata* forest. Density was calculated by counting the number of pines per subplot and then dividing by the subplot area. Basal area of each stand was calculated by summing the individual basal areas of each pine and dividing by the subplot area. Individual basal areas were calculated by measuring the diameter of each pine at the breast height (1.3 m). LAI values were indirectly estimated from hemispherical photographs of the canopy, which were taken from the ground at the locations of the fixed snow poles using a fisheye lens. These forest structure data were used in the preparation of Chapter 3, Chapter 5 and Chapter 6. On the other hand, biometric (dbh and tree height) variables were recorded for each individual tree in sampled sites at the main mountains of the NE Peninsula using similar methods. These data were used in the preparation of Chapter 4.

2.4.2 Geographical Information System (GIS) data

Potential solar irradiation received by each plot was calculated using the Points Solar Radiation tool included in ArcGIS 9.3 software (ESRI, USA).

Figure 2.7: (a) Graduated fixed snow poles installed beneath the forest canopy in one of the studied plots at the *Baños de Panticosa* experimental site. (b) One of the time–lapse cameras installed to photograph the snow poles on a daily basis in order to obtain snow depth data. (c) Measuring SWE using a snow cylinder and scale (ETH core sampler) inside a snow pit. (d) Snow depth manually data collection using a graduated snow probe. (e) HOBO U30 NRC weather station registering solar irradiance and wind speed data. (f) Tinytag–Pus–2 data–logger inside a radiation shield registering air temperature and moisture data.

Figure 2.8: (a) Collecting microcores with a Trephor increment puncher to monitor xylogenesis. (b) One of the wood samples (microcore) fixed in ethanol solution. (c) Measuring shoot and needle elongation with a ruler to monitor tree phenology. (d) Installed dendrometer (DR 26, EMS Brno) registering stem radius variations. (e) Collecting cores with a Pressler increment borer to quantify sapwood NSC. (f) Soil moisture sensor (ECH2O probe). (g) Miniature temperature logger (Thermochron iButton). Credit of the image *a*: Centro Studi per l'Ambiente Alpino, Universita' degli Studi di Padova. Credit of the rest of images: Sanmiguel–Vallelado, A.

This tool calculates the total amount of radiation for particular locations and for specific time periods; in our case, studied plots in the *Baños de Panticosa* experimental site and over each month of the year. The calculation of potential solar irradiation are repeated for every location on the topographic surface, producing insolation maps for an entire geographic area. Digital Elevation Models of the analyzed area were required for calculations (source: IDEAragón–Infraestructura de Datos Espaciales de Aragón, https://idearagon.aragon.es/, 20 m resolution). Calculations were performed assuming clear–sky conditions (transmissivity value: 0.5)[5]. The derived data were used in the preparation of Chapter 3.

2.4.3 Image processing

To obtain daily data on snow depth from the photographs of the snow poles at the *Baños de Panticosa* experimental site, photographs were processed using ImageJ software (Rasband, 1997) following this process: (1) from a snow–free photograph of the poles of each plot, I measured in the ImageJ units the length of each pole, already knowing its real length in cm; (2) on each photograph taken during the snow season, I measured in the ImageJ units the length of each pole section above the surface of the snowpack; (3) by subtracting this last measurement–step 2–from the total length of the pole –step 1–, and converting the ImageJ units to cm, I obtained daily snow depth values for each pole. In case of doubt, the coloured graduation marks helped to determine the snow depth value for each pole. Using this methodology, we assumed an error of about $5 - 10$ cm in the measurement. The derived data were used in the preparation of Chapter 3, Chapter 5 and Chapter 6.

On the other hand, averaged LAI value for each plot at the *Baños de Panticosa* experimental site was extracted from hemispherical photographs using the Gap Light Analyzer software (Simon Fraser University, New York, USA). LAI 4 Ring variable was considered, which is the effective leaf area index

[5]Transmissivity is a property of the atmosphere that is expressed as the ratio of the energy reaching the Earth's surface to that which is received at the upper limit of the atmosphere (extraterrestrial). Values range from 0 (no transmission) to 1 (complete transmission). Typically observed values are 0.6 or 0.7 for very clear sky conditions and 0.5 for only a generally clear sky.

integrated over the zenith angles 0 to 60º (Stenberg et al., 1994). The derived data were used in the preparation of Chapter 6.

2.4.4 Data provided by governmental agencies

The Spanish State Meteorology Agency (AEMET) provided daily sum of total precipitation data during the study period, which were recorded by the 9451A AEMET's meteorological station located at the *Baños de Panticosa* experimental site (1630 m a.s.l.). This information on precipitation was supported by the nearby meteorological station (E235) operated by the Automated Hydrological Information System for the Basin of the Ebro River (SAIH) of the River Ebro Hydrographic Confederation (CHE). Moreover, daily maximum SWE series from 2008 to 2019 were provided by a tele–snow gauge operated by SAIH–CHE (N0004 Bachimaña). These data sets were used in the preparation of Chapter 6.

2.4.5 Laboratory procedures

To obtain tree–ring width data from collected cores at the studied forests stands located in the main mountains in the NE Iberian Peninsula, wood samples were air dried and sanded until tree–ring boundaries were clearly visible. Then, a LINTAB measuring device (Rinntech, Heidelberg, Germany) was used to measure at 0.01 mm resolution the ring widths. The individual ring width series were compared among coexisting trees of the same species and site in order to check the cross–dating quality, and for this purpose the COFECHA software (Holmes, 1983) was used. The resulting data are cross-dated tree–ring width (RWL) series, which were used in the preparation of Chapter 4. I would like to recall that tree–ring data series came from an updating of tree–ring chronologies published by Galván et al. (2012). Thus, the laboratory processing described above was carried out before the start of this Thesis by the mentioned research team.

To monitor xylogenesis from collected microcores at the *Baños de Panticosa* experimental site, wood samples were freezing and then transversally sectioned (15–20 µm thick) using a sliding microtome (Leica SM2010 R) with

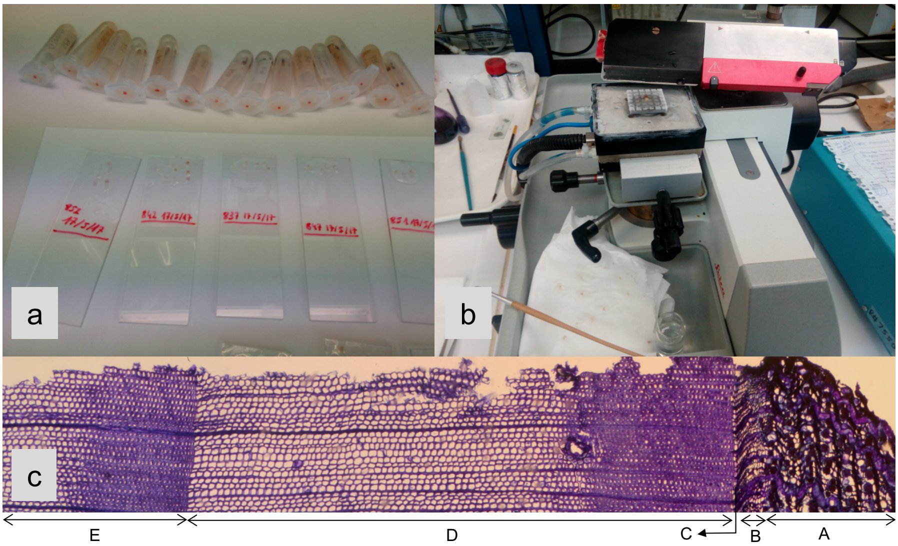

Figure 2.9: (a) Transversal microcore sections mounted on glass slides and stained. (b) A frozen microcore ready to be sliced using a sliding microtome (Leica SM2010 R). (c) Compiled image of one microcore section using a camera mounted on a light microscope (Olympus BH2). From right to left can be seen (A) the bark, (B) the cambium, (C) the first row of cells forming the incipient tree–ring, (D) the ring formed the previous year (darker rows of cells form the latewood and lighter rows form the earlywood), and finally (E) appears a part of the ring formed two years earlier.

temperature Controlled Freezing Stages for Microtomes (Physitemp BFS–30MP). Wood sections were mounted on glass slides, stained with 0.05% cresyl violet and fixed with Eukitt®. Then, sections were examined with visible and polarised light at 40–100x magnification, and photographs were taken when necessary using a digital camera mounted on a light microscope (Olympus BH2, Olympus, Hamburg, Germany). Samples usually comprised the preceding 4–5 rings alongside the developing ring with the cambial zone and adjacent phloem. The number of cambium cells, radially enlarging tracheids, wall–thickening tracheids and mature cells were counted and averaged on five radial lines per ring following Deslauriers et al. (2015) procedures. Photographs of the materials used during microcore processing at laboratory and the augmented view of one wood section can be found in Figure 2.9. The derived data were used in the preparation of Chapter 5.

To determine NSC concentrations in collected stem cores and needle samples at the *Baños de Panticosa* experimental site, procedures described in Sangüesa-Barreda et al. (2012) were followed. NSC measured after ethanol (80%) extraction is referred to as soluble sugars (SS), carbohydrates measured after enzymatic digestion in glucose equivalents are referred to as starch, and the sum of SS and starch is referred to as total NSC (TNC). The derived data were used in the preparation of Chapter 5.

2.4.6 Climatic modeling

Daily snow depth and temperature data from 1980 to 2010 for the studied sites at the main mountains in the NE Iberian Peninsula were extracted from a gridded meteorological dataset created by Alonso-González et al. (2018). The dataset was obtained by simulation from Weather Research and Forecasting (WRF; Skamarock et al. (2008)) model. The WRF model was driven by ERA-Interim (Berrisford et al., 2011) reanalysis and coupled offline with Factorial Snow Model (FSM 1.0; Essery (2015)), a physically based energy and mass balance snow model. WRF outputs were projected to the target elevation, and the new projected meteorological information was used as driving data of FSM. Part of this final dataset was used in the preparation of Chapter 4, representing one of its many possible applications, which comprises the whole Iberian Peninsula at different elevations from 1980 to 2014 and is freely available for download from Zenodo (https://doi.org/10.5281/zenodo.854618).

2.4.7 Hydrological modeling

Hourly SWE series and energy fluxes for each plot at the *Baños de Panticosa* experimental site were simulated from 2016/17 to 2019/20 snow seasons, distinguishing areas beneath the forest canopy (F) and forest openings (O). For that purpose, the Cold Regions Hydrological Model (CRHM; Pomeroy et al. (2007)) was used. SWE series and energy fluxes were outputs from the Snobal-CRHM and CanopyClearingGap modules. CRHM was fed by climate data registered at the *Baños de Panticosa* experimental site, mostly by our own weather stations, and part of it (precipitation data) provided by Governmental Agencies (AEMET and SAIH–CHE). The input dataset were transformed into CRHM observations using the CRHMr R package (Shook, 2016). The evaluation of model performance consisted of comparing the model outputs with observed daily SWE in F–O areas at each plot during the 2016/17 and 2017/18 snow seasons. Subsequently, a sensitivity analysis was performed to assess the response of forest effect on snow processes to changing climate conditions. To this end, SWE and energy fluxes were simulated under scenarios of combined increased temperature (from +1ºC to +4ºC) and varying precipitation (from -20% to +20%) following the future climate projections for the Mediterranean mountains and associate uncertainty (Knutti & Sedláček, 2013; Nogués Bravo et al., 2008). In total, 14 scenarios of perturbed climate conditions were simulated. CRHM outputs consisted on SWE and energy fluxes hourly series that were post–processed using the CRHMr R package (Shook, 2016) to obtain the maximum and mean value reached each day, respectively. It was tested whether the studied snow seasons were representative of a wider range of local snow conditions, by comparing them with the series obtained from a near tele–snow gauge operated by SAIH–CHE (N0004 Bachimaña). The derived data were used in the preparation of Chapter 6. In that chapter, the reader will find the particularities of the CRHM modelling platform, as well as the details about the model implementation and validation, the simulation process and the sensitivity analysis performed.

2.5 Data processing

Snow–related data

Daily snow depth series for each plot at the *Baños de Panticosa* experimental site, distinguishing F–O areas, were obtained after: (1) processing photographs from the monitoring system composed of time–lapse cameras and fixed snow poles, as previously described; (2) estimating missing data in the daily snow depth series obtained at each pole using a non–parametric iterative imputation method called missForest method[6] (Stekhoven & Buhlmann, 2012), which is implemented in the MissForest R package (Stekhoven, 2013); and (3) averaging daily snow depth series for the F–O poles at each experimental plot. These data series were used to estimate daily SWE series,

[6]The missForest method fits a Random Forest regression to the observed part and then predicts the missing parts of the input data (Breiman, 2001)

presented further and used in the preparation of Chapter 3, Chapter 5 and Chapter 6.

Daily snow density series for each plot at the *Baños de Panticosa* experimental site, distinguishing F–O areas, were obtained after: (1) averaging the SWE and depth values of the replicates taken in the manual measurements performed every 10–15 days in snow pits; (2) calculating the snowpack density from SWE and depth values using the following equation for each F–O area at each experimental plot:

$$\rho_s = \frac{SWE \cdot \rho_w}{H} \tag{2.1}$$

where ρ_s is the snow density, ρ_w is the water density and H is the snow height; and (3) estimating daily snow density series by linear interpolation between each pair of density measurements from consecutive surveys. These data series were required to estimate two types of SWE series, below presented (daily and spatially distributed), and used in the preparation of Chapter 3, Chapter 5 and Chapter 6.

Daily SWE series for each plot at the *Baños de Panticosa* experimental site, distinguishing F–O areas, were inferred from data on daily snow depth and estimated daily snow density using the equation 2.1. Therefore, these data series can be considered estimations. Only data in a continuous snowpack period were considered, i.e. from the first day of 14 or more consecutive days with snow on the ground to the last date with a snow record. Daily rates of snow accumulation (positive values) and melting (negative values) were calculated from daily SWE series by performing first–order differencing, day–by–day. Finally, forest effects on snow processes were calculated as a percentage (increase or decrease) comparing F–O data on snowpack duration, cumulative SWE, and accumulation and melting rates (annual medians). This dataset was used in the preparation of Chapter 3, Chapter 5 (where data from F and O areas were averaged to obtain a single representative value for each plot) and Chapter 6.

Spatially distributed SWE series with ∼biweekly temporal resolution for each plot at the *Baños de Panticosa* experimental site, distinguishing F–O areas, were obtained after: (1) averaging the snowpack depth values of the replicates taken in the distributed measurements manually performed every 10–15 days using a snow probe; and (2) inferring SWE values from these data on snow depth and calculated snowpack density of each survey day using the equation 2.1. Series of spatial CV of SWE were obtained from spatially distributed SWE series by calculating the ratio of the standard deviation to the mean value of SWE of each F–O area at each experimental plot (averaging the 10 sites measured at each F–O area). Finally, forest effects on cumulative SWE and SWE CV were calculated as a percentage comparing obtained values in F–O areas (annual median). This dataset was used in the preparation of Chapter 3.

Indices describing seasonal snow conditions were calculated from daily snow depth series obtained by WRF-FSM simulations for the studied sites located at the main mountains in the NE Iberian Peninsula, including: average November snow depth, average February snow depth and average March snow depth. These indices aimed to reflect previous autumn, winter and spring snow conditions, respectively, based on the cumulative nature of snow (López-Moreno, 2005). These data series were used in the preparation of Chapter 4.

Indices describing annual snow conditions were calculated from daily SWE series obtained by CRHM simulations (in some cases performed under climate–forced conditions) for each plot at the *Baños de Panticosa* experimental site, distinguishing F–O areas. Calculated annual snow indices included: accumulation onset (i.e. date of first day having SWE $>$ 5 mm), melt out date (i.e. last date having SWE $>$ 5 mm), snow duration (i.e. number of days annually having SWE $>$ 5 mm; López-Moreno et al. (2020)), peak SWE (i.e. maximum annual amount of SWE), peak SWE date, and the annual median melting rate. In turn, from the obtained snow indices, I calculated: (1) the relative change of snow indices under combined temperature and precipitation perturbed scenarios with respect to observed conditions; and (2) the forest effects on snow processes as a percentage (increase or decrease) of snow indices magnitude. This dataset was used in the preparation of Chapter 6.

Series of dimensionless ring–width indices (RWI) were obtained for the studied sites located at the main mountains in the NE Iberian Peninsula from RWL series by removing age or size trends and temporal autocorrelation using the ARSTAN V. 44 software (Cook, 1985). Residual or pre-whitened RWI series were obtained by removing long–term trends of ring–width data fitting negative linear functions, followed by 30–year cubic smoothing splines, and then by eliminating the first–order autocorrelation of the resulting residuals. After that, individual series were averaged by using a bi–weight robust mean for each site. These mean site RWI series were used in the preparation of Chapter 4.

Daily rates of mature tracheid production for each studied forest stand at the *Baños de Panticosa* experimental site were obtained from data on xylem development. Firstly, and following Camarero et al. (1998) and Rossi et al. (2003) methodologies, the Gompertz function was used to model the increase in the number of mature tracheids at plot level. It is defined in Cheng and Gordon (2000) as:

$$Y = A \cdot exp[-e^{(\beta - k \cdot t)}] \tag{2.2}$$

where Y is the weekly cumulative sum of mature cells (sum of earlywood and latewood mature tracheids), A is the upper growth asymptote, β is the x–axis placement parameter, k is the rate of change parameter, and t is the time in day–of–year (DOY). For this purpose, there was used the non–linear regression tools included in the growth–models R package (Rodriguez Perez, 2013). Secondly, resulting Gompertz–adjusted series were limited to the main *P. uncinata* growing season period from April–May to October (Camarero et al., 1998). Finally, first–order differences were calculated between the values of two consecutive days of the Gompertz–adjusted series to obtain daily rates of mature tracheid production. Apart from that, some annual indices were calculated from these resulting series, including: production of mature tracheids, maturation onset, maturation cessation, maturation duration, maximum rate of mature tracheid development, and timing of maximum rate of mature tracheid development; details on their calculation can be found in

Table A.1 of Chapter 5. These datasets were used in the preparation of Chapter 5.

Daily rates of radial increment were calculated for each studied *P. uncinata* individual at the *Baños de Panticosa* experimental site from data on hourly stem perimeter variations, considering a daily approach, and following these steps: (1) collected data on stem perimeter variations were transformed into radial changes, assuming that stems were circular in shape, and knowing the initial diameter of the trunk at the beginning of the study (dbh0); (2) the dendrometeR package (van der Maaten et al., 2016) was used to obtain daily maximum radius series; (3) resulting series were limited to the main *P. uncinata* growing season period (April–May to October)(Camarero et al., 1998) and set to 0 on April 1 every season (except in 2016, when the series were set to 0 the May 1 due to data availability); (4) Gompertz functions were adjusted to daily maximum radius series at plot level following the procedure described in the previous paragraph; and (5) first–order differences were calculated between the values of two consecutive days of the Gompertz–adjusted series to obtain daily rates of mature radial increment. Apart from that, some annual indices were calculated from these resulting series, including: total stem radial increment, stem radial increment onset, stem radial increment cessation, stem radial increment duration, maximum rate of radial increment, and timing of maximum rate of radial increment; details on their calculation can be found in Table A.1 of Chapter 5. This dataset was used in the preparation of Chapter 5.

Annual indices describing shoot and needle pheonology were calculated for each studied *P. uncinata* individual at the *Baños de Panticosa* experimental site from data on shoot and needle elongation. Calculated indices include: onset of shoot elongation (i.e. first day when an increment in shoot length was recorded after dormancy), shoots final length (i.e. maximum shoot length value recorded), onset of needle elongation (i.e. first day when an increment in needle length was recorded after dormancy), and needle final length (i.e. maximum needle length value recorded). This dataset was used in the preparation of Chapter 5.

Climate–related data

Climate series (including air temperature, relative humidity, wind speed, global solar irradiation and precipitation) were obtained from several weather stations located at each plot in the *Baños de Panticosa* experimental site, as previously mentioned. Less than 1% of the data were outliers caused by errors in sensor measuring, and they were removed. Missing data were estimated using the previously mentioned missForest method. Hourly and daily average series at each experimental plot were calculated, except in the case of precipitation data which was only available for the valley bottom by a AEMET weather station (1630 m a.s.l.). Climate data registered by another meteorological station operated by us (apart from the stations installed at each plot) located at the valley bottom, and the SAIH–CHE meteorological station, were included in the data imputation process. These data series were used in the preparation of Chapter 3, Chapter 5 and Chapter 6.

Indices describing monthly average temperatures were calculated from daily mean temperature series obtained by WRF–FSM simulations for the studied sites located at the main mountains in the NE Iberian Peninsula, including: November mean temperature, February mean temperature, November–February mean temperature, December–February mean temperature, January–February mean temperature, May mean temperature, March–May mean temperature and April–May mean temperature. These data were used in the preparation of Chapter 4.

Indices describing annual energy conditions were calculated from daily energy fluxes series obtained by CRHM simulations (in some cases performed under climate–forced conditions) for each plot at the *Baños de Panticosa* experimental site, distinguishing F–O areas. From these CRHM outputs, the annual average values from October to June were calculated. In turn, from the obtained annual energy fluxes values, I calculated: (1) the relative change of annual values of energy fluxes under temperature perturbed scenarios, with respect to observed conditions; and (2) the forest effects on snow energy content as a percentage (increase or decrease) in energy fluxes indices magnitude. This dataset was used in the preparation of Chapter 6.

Soil temperature and humidity data

Soil series (including temperature and moisture) were obtained for each plot at the *Baños de Panticosa* experimental site, distinguishing F–O areas, using automatic devices. Less than 1% of the data were outliers caused by errors in sensor measuring, and they were removed. In Chapter 5, missing values in the soil temperature and moisture series were filled using the missForest method (previously detailed), and data from F and O areas were averaged to obtain a single representative value for each plot. In Chapter 6, missing values in the soil temperature series were filled by linear or spline interpolation using the function *interpolate* included in the CRHMr R package (Shook, 2016).

All data processing was performed using R statistical software (Team, 2020)

2.6 Statistical analyses

Normality tests were often a first step when analyzing data since many subsequent statistical analyses have normality as an assumption, and if analyzed data do not meet that requirement, a different statistical approach will be needed. The Shapiro–Wilk test was used to examine if data of the analyzed variables followed a normal or gaussian distribution. The null hypothesis considered in this test is that a variable is normally distributed in some population. If p-value $< \alpha$ this hypothesis was rejected and thus, it was conclude that the analyzed variable was not normally distributed. In the opposite case (p-value $> \alpha$), this hypothesis was accepted and therefore it was conclude that the analyzed variable was normally distributed. These tests were done considering a significance level (α) of 0.05.

Correlations were used to determine the statistical association between pairs of continuous variables. Firstly, the relationship between each pair of variables was visually examined by means of scatterplots. Then, the strength and the direction of the relationship were quantified using a linear correlation coefficient. Prior to this, and when necessary, variables were detrended to prevent spurious correlation[7]. Two types of correlation coefficients were used in this

[7] A spurious correlation describes a relationship between two variables that seems to

Thesis: when data of the analyzed variables were normally distributed, the Pearson coefficient was used; in the opposite case, the non–parametric Spearman coefficient was calculated. Hypothesis tests of the significance of the correlation coefficient were used to decide if the calculated correlation coefficients were close to zero (H_0 or null hypothesis) or significantly different from zero (H_1 or alternative hypothesis). Thus, when the p-value obtained from these test was less than α, H_0 was rejected and H_1 was accepted, concluding that there was a significant linear relationship between the two analyzed variables. In the opposite case (p-value $> \alpha$), H_0 was accepted, concluding that the two analyzed variables were not linearly correlated. These tests were done considering a significance level (α) of 0.05. In Chapter 3, correlation tests were used to determine the influence of environmental variables on the detected effects of forests at the *Baños de Panticosa* experimental site. In Chapter 4, correlation tests were used to explore the variations of tree growth responses to snow conditions along biogeographical gradients at the main mountains in the NE Iberian Peninsula. In Chapter 5, were used to determine (1) the temporal variability of the linear soil VWC response to snowmelt, (2) the influence of snowpack duration on soil temperature over time, and (3) intra–annual microclimate effects on tree growth at the *Baños de Panticosa* experimental site.

Partial correlations only differ from the above-mentioned correlations in that they control for the effect of one or more other continuous variables called covariates. This analysis is used to avoid the misleading results that can be obtained when a correlation coefficient is calculated between two variables but there is another variable that is related to both of them. In Chapter 4, partial correlations were calculated between RWI series and snow depth data by partially removing the effects of air temperature, because the aim was to infer the pure effect of snow on tree growth at the studied sites located in the main mountains in the NE Iberian Peninsula. Similar to the above, hypothesis tests were done for calculating the partial correlations, which considered the non–parametric Spearman coefficient since the data distribution

have a cause–and–effect connection, but in reality they are absolutely uncorrelated. This correlation without causation is induced by a *third factor*, such us a common trend exhibited by both analyzed variables.

of the analyzed variables was not normal. These tests were done considering a significance level (α) of 0.05. Prior to this, snow and temperature variables were detrended to prevent spurious correlation.

Simple linear regressions were used to model the relationship between two continuous variables in which one variable (the predictor or independent variable) may explain the variability of other variable (the response or dependent variable) by fitting a linear equation to data. They can then be used to predict changes in the response variable for a given change in the predictor value. As mentioned, this type of models assumes that the relationship between the predictor and response variable is linear. The regression line describes how much the mean response of Y values changes when the X variable does, and it takes this form:

$$Y = \beta_0 + \beta_1 \cdot X + \epsilon \tag{2.3}$$

where Y represents the response variable, X is the predictor variable, β_0 is the Y when X is 0 or the intercept, β_1 is the estimated regression coefficient which represents the change in Y relative to a one unit change in X, and ϵ is the residual term which represents the deviations of the Y values from their the mean response (i.e. the line). R^2 statistic, called coefficient of determination, measures how well data fit the regression model. More specifically, it determines the proportion of variance in the response variable that can be explained by the predictor variable. In Chapter 5, the relationships between snow melting and soil VWC were modeled by means of simple linear regressions at the *Baños de Panticosa* experimental site to investigate influences of snowpack on soil moisture.

Polynomial regressions are one option to model a nonlinear relationship between above-mentioned predictor and response variables by fitting a polynomial equation to data. The fitted curve takes this form:

$$Y = \beta_0 + \beta_1 \cdot X + \beta_2 \cdot X^2 + ... + \beta_h \cdot X^h + \epsilon \tag{2.4}$$

where h refers to the degree of the polynomial. In Chapter 5, the relationships between SWE and soil temperature were modeled by means of polynomial regressions at the *Baños de Panticosa* experimental site to investigate influences of snowpack on soil temperature.

Multiple linear regressions model the relationships between two or more predictor variables (covariates) and a response variable by fitting a linear equation to data. The basic approach is the same as the one introduced above in the case of the simple linear regressions, but the equation takes another form:

$$Y = \beta_0 + \beta_1 \cdot X_1 + \beta_2 \cdot X_2 + ... + \beta_n \cdot X_n + \epsilon \tag{2.5}$$

where n are the distinct number of predictor variables. Caution must be taken, because when increasing the number of predictor variables in the model, the R^2 will increase reaching a maximum R^2 value ($R^2 = 1$) when the number of covariates equals the number of observations - 1. Therefore, in multiple regression a common goal is to determine which predictor variables contribute significantly to explaining the variability in the response variable. In this Thesis, I used the stepwise regression as a variable selection method. This method tests together various combinations of variables, and allows to introduce variables that substantially improve the model by rejecting those that may be redundant. The first step will identify the best one-variable model, and subsequent steps will identify the best two-variable, three-variable, etc. models. Training models were compared using the Akaike Information Criterion (AIC) value considering the smaller AIC, which points to the most parsimonious model (i.e. a model that achieves a maximised R^2 using as few explanatory variables as possible) (Burnham & Anderson, 2003). The MuMIn R package (Barton & Barton, 2018) was used to perform an automated model selection. In Chapter 4, stepwise linear regressions were used to infer whether the snow depth or temperature conditions were the best predictors of RWI at the studied sites located in the main mountains of the NE Iberian Peninsula.

Principal component analysis (PCA) is a multivariate method that reduces the dimensionality of large data sets while preserving as much information (variability) as possible. The objective is to obtain a reduced number of new uncorrelated variables (called principal components, PCs) that are lineal combinations of the original variables and keep much of the variance contained in them (Jolliffe, 2005). A PCA involves five steps: (1) variable standardisation; (2) covariance matrix computation to identify correlations between variables; (3) eigenvalues and eigenvectors computation from the covariance matrix to identify the PCs of the data set; (4) selection of the PCs we decide to keep based on the Kaiser criterion, preserving those with eigenvalues greater than 1 (Kaiser, 1974); and (5) classification of the original variables into the selected PCs by following the maximum loading rule. PCA results were graphically represented as vectors, indicating (i) the direction in which the value of the vector increases, and (ii) the correlation magnitude among vectors and between vectors and component axes (low angles correspond to high correlations). In Chapter 5, PCAs were performed to identify the most influencing microclimate variables (i.e. climate, snow and soil conditions) on xylogenesis and tree radial increment at the *Baños de Panticosa* experimental site.

To detect statistical differences among groups, that is, to determine if two or more data samples are different from one another in a statistically significant manner, two different tests were used depending on the number of groups considered. In case of comparing three or more groups, I used the Kruskal–Wallis test, which is the non–parametric equivalent one-way ANOVA, for testing if samples were originated from the same distribution. In case of comparing two groups, I used the non–parametric Wilcoxon test, which is often described as the non–parametric version of the two–sample t–test. The Dunn test was used for post–hoc pairwise test to determine which groups differed from each other when results from a Kruskal–Wallis test were statistically significant, since both tests use the same rankings of the data. The null hypothesis of all of these tests is that the data distributions of the compared groups do not differ. Therefore, when the p-value obtained from the test was less than α, H_0 was rejected and it was concluded that the analyzed groups statistically deferred from each other. A significance level (α) of 0.05 was considered. All three mentioned tests were non–parametric since the assumption of normality in data distribution within the groups of analyzed variables was not always met. In Chapter 3, the Wilcoxon test was used to detect the significance of observed different snow conditions between F and O areas, which allow to detect several forest effects on snowpack at the *Baños de Panticosa* experimental site. In the same chapter, the Kruskal–Wallis test was used to assess whether there were statistically significant differences in the detected effects of forests on snowpack among plots, snow seasons, and periods in the snow seasons at the same study site. In Chapter 4, the Kruskal–Wallis test was used to identify statistically significant different tree growth responses to snow conditions among groups of sites along biogeographical gradients at the studied sites located in the main mountains of the NE Iberian Peninsula. In Chapter 5, the Kruskal–Wallis test was used to assess whether there were statistically significant differences in certain analyzed variables (i.e. air and soil temperatures, soil VWC, and NSC concentrations) among plots or years at the *Baños de Panticosa* experimental site. In Chapter 6, the Wilcoxon test was used to detect the significance of obtained differences between F and O areas in snow conditions and their sensitivity under different scenarios of perturbed climate at the *Baños de Panticosa* experimental site.

Trend analyses quantify and explain monotonic trends in a data set over time. Here, it is important to note that there are two main kinds of trends: a gradual change over time in one direction (monotonic trend) and an abrupt shift at a specific point in time (step trend). Thus, linear trends are a type of monotonic trends. In this Thesis, the statistical importance of trends in analyzed time series was evaluated using the non–parametric Mann–Kendall test (Kendall & Gibbons, 1975; Mann, 1945), since the data did not conform to a normal distribution. The null hypothesis of this test is that data do not follow a trend on time, while the alternative hypothesis affirms that there is a monotonic trend. However, that trend can be positive (i.e. an upward monotonic trend) or negative (i.e. a downward monotonic trend). The Mann–Kendall test was used in conjunction with the Theil–Sen's slope estimator (Sen, 1968; Thiel, 1950), which computes the magnitude of the statistically significant trend detected. The Theil–Sen's slope estimator is a non–parametric technique for estimating the slope of the fitted line to sample points in the plane (i.e. linear regression) by choosing the median of all slopes between paired values. Trend analyses were carried out using the zyp R package (Bronaugh et al., 2009), which includes a trend–free pre–whitening method for removing serial autocorrelation. In Chapter 3, trend analyses were used to detect and quantify trends of the effects of forests on snowpack during the study period at the *Baños de Panticosa* experimental site. In Chapter 4, trends in RWL and snow data series analyses were analyzed at the studied sites located in the main mountains of the NE Iberian Peninsula following these methods to quantify and explain the change over time in snow conditions and tree radial growth.

All statistical analyses were performed using R statistical software (Team, 2020).

References

Alonso-González, E., López-Moreno, J. I., Gascoin, S., García-Valdecasas Ojeda, M., Sanmiguel-Vallelado, A., Navarro-Serrano, F., Revuelto, J., Ceballos, A., Esteban-Parra, M. J. & Essery, R. (2018). Daily gridded datasets of snow depth and snow water equivalent for the Iberian Peninsula from 1980 to 2014. *Earth System Science Data*, *10*(1), 303–315.

Alonso-González, E., López-Moreno, J. I., Navarro-Serrano, F., Sanmiguel-Vallelado, A., Revuelto, J., Domínguez-Castro, F. & Ceballos, A. (2020a). Snow climatology for the mountains in the Iberian Peninsula using satellite imagery and simulations with dynamically downscaled reanalysis data. *International Journal of Climatology*, *40*(1), 477–491. https://doi.org/10.1002/joc.6223

Antonova, G. F. & Stasova, V. V. (1993). Effects of environmental factors on wood formation in Scots pine stems. *Trees*, *7*(4), 214–219.

Barton, K. & Barton, M. (2018). MuMIn: Multi-model inference.

Berrisford, P., Dee, D., Poli, P., Brugge, R., Fielding, K., Fuentes, M., Kållberg, P., Kobayashi, S., Uppala, S. & Simmons, A. (2011). The ERA-Interim archive version 2.0, shinfield park. *Reading*, *1*, 23.

Blumstein, M. & Hopkins, R. (2021). Adaptive variation and plasticity in non-structural carbohydrate storage in a temperate tree species. *Plant, Cell & Environment*, *44*(8), 2494–2505. https://doi.org/10.1111/pce.13959
_eprint: https://onlinelibrary.wiley.com/doi/pdf/10.1111/pce.13959

Breiman, L. (2001). Random forests. *Machine learning*, *45*(1), 5–32.

Bronaugh, D., Werner, A. & Bronaugh, M. D. (2009). Package 'zyp'.

Burnham, K. P. & Anderson, D. R. (2003). *Model selection and multimodel inference: A practical information-theoretic approach.* Springer Science & Business Media.

Camarero, J. J., Guerrero-Campo, J. & Gutiérrez, E. (1998). Tree-Ring Growth and Structure of Pinus uncinata and Pinus sylvestris in the Central Spanish Pyrenees. *Arctic and Alpine Research*, *30*(1), 1–10. https://doi.org/10.2307/1551739

Camarero, J. J. & Gutiérrez, E. (2008). La respuesta del crecimiento de" Pinus Uncinata" al clima en poblaciones relictas del sistema ibérico. *Zubía*, (20), 61–96.

Cheng, C. & Gordon, I. L. (2000). The Richards function and quantitative analysis of germination and dormancy in meadowfoam (Limnanthes alba). *Seed Science Research*, *10*(3), 265–277.

Cook, E. R. (1985). *A time series analysis approach to tree ring standardization*. The University of Arizona
PhD Dissertation.

De Micco, V., Carrer, M., Rathgeber, C. B., Julio Camarero, J., Voltas, J., Cherubini, P. & Battipaglia, G. (2019). From xylogenesis to tree rings: Wood traits to investigate tree response to environmental changes. *IAWA Journal*, *40*(2), 155–182. https://doi.org/10.1163/22941932-40190246

Del Barrio, G., Creus, J. & Puigdefábregas, J. (1990). Thermal seasonality of the high mountain belts of the Pyrenees. *Mountain Research and Development*, 227–233.

Deslauriers, A., Rossi, S. & Liang, E. (2015). Collecting and processing wood microcores for monitoring xylogenesis. *Plant Microtechniques and Protocols* (pp. 417–429). Springer.

d'Ostiani, L. F. (2004). *Watershed Management: A Key Component of Rural Development in the Mediterranean Region* (tech. rep.). FAO. Rome.

Essery, R. (2015). A factorial snowpack model (FSM 1.0). *Geoscientific Model Development*, *8*(12), 3867–3876. https://doi.org/10.5194/gmd-8-3867-2015

Fayad, A., Gascoin, S., Faour, G., López-Moreno, J. I., Drapeau, L., Page, M. L. & Escadafal, R. (2017). Snow hydrology in Mediterranean mountain regions: A review. *Journal of Hydrology*, *551*, 374–396. https://doi.org/10.1016/j.jhydrol.2017.05.063

Galván, J. D., Camarero, J. J., Sangüesa-Barreda, G., Alla, A. Q. & Gutiérrez, E. (2012). Sapwood area drives growth in mountain conifer forests. *Journal of Ecology*, *100*(5), 1233–1244. https://doi.org/10.1111/j.1365-2745.2012.01983.x

Gutiérrez, E. (1991). Climate tree-growth relationships for Pinus uncinata Ram. in the Spanish pre-Pyrenees. *Acta Oecologica*, *12*(2), 213–225.

Holmes, R. L. (1983). Computer-Assisted Quality Control in Tree-Ring Dating and Measurement. *Tree-Ring Bulletin*, *43*, 69–78.

Jolliffe, I. (2005). Principal component analysis. *Encyclopedia of statistics in behavioral science*.

Kaiser, H. F. (1974). An index of factorial simplicity. *Psychometrika*, *39*(1), 31–36.

Kendall, M. & Gibbons, J. (1975). Rank correlation methods, 1970. *Griffin, London*.

Knutti, R. & Sedláček, J. (2013). Robustness and uncertainties in the new CMIP5 climate model projections. *Nature Climate Change*, *3*(4), 369–373.

Köppen, W. (1936). Das geographische system der klimat. *Handbuch der klimatologie*, 46.

Korhonen, L., Korhonen, K., Rautiainen, M. & Stenberg, P. (2006). Estimation of forest canopy cover: A comparison of field measurement techniques. *Silva Fennica*, *40*(4). https://doi.org/10.14214/sf.315

Kozlowski, T. T. (1972). Shrinking and swelling of plant tissues. *Water deficits and plant growth*, *3*, 1–64.

Latron, J., Llorens, P. & Gallart, F. (2009). The Hydrology of Mediterranean Mountain Areas. *Geography Compass*, *3*(6), 2045–2064. https://doi.org/10.1111/j.1749-8198.2009.00287.x

Levin, W. C. (1988). *Sociological ideas: Concepts and applications*. Wadsworth Publishing.

Lionello, P., Malanotte-Rizzoli, P., Boscolo, R., Alpert, P., Artale, V., Li, L., Luterbacher, J., May, W., Trigo, R. & Tsimplis, M. (2006). *The Mediterranean climate: An overview of the main characteristics and issues*. Elsevier.

López-Moreno, J. I., Soubeyroux, J. M., Gascoin, S., Alonso-Gonzalez, E., Durán-Gómez, N., Lafaysse, M., Vernay, M., Carmagnola, C. & Morin, S. (2020). Long-term trends (1958–2017) in snow cover duration and depth in the Pyrenees. *International Journal of Climatology*, *40*(14), 6122–6136. https://doi.org/10.1002/joc.6571

López-Moreno, J. I. (2005). Recent variations of snowpack depth in the Central Spanish Pyrenees. *Arctic, Antarctic, and Alpine Research*, *37*(2), 253–260.

López-Moreno, J. I., Fassnacht, S. R., Heath, J. T., Musselman, K. N., Revuelto, J., Latron, J., Morán-Tejeda, E. & Jonas, T. (2013). Small scale spatial variability of snow density and depth over complex alpine terrain: Implications for estimating snow water equivalent. *Advances in water resources*, *55*, 40–52.

Mann, H. B. (1945). Nonparametric tests against trend. *Econometrica: Journal of the econometric society*, 245–259.

Navarro-Serrano, F., I. López-Moreno, J., Azorin-Molina, C., Alonso-González, E., Tomás-Burguera, M., Sanmiguel-Vallelado, A., Revuelto, J. & Beguería, S. (2018). Estimation of near-surface air temperature lapse rates over continental Spain and its mountain areas. *International Journal of Climatology*, *38*, 3233–3249. https://doi.org/10.1002/joc.5497

Ninot, J. M., Carrillo, E. & Ferré, A. (2017). The Pyrenees. In J. Loidi (Ed.), *The Vegetation of the Iberian Peninsula: Volume 1* (pp. 323–366). Springer International Publishing. https://doi.org/10.1007/978-3-319-54784-8_8

Nogués Bravo, D., Araújo, M. B., Lasanta, T. & López Moreno, J. I. (2008). Climate change in Mediterranean mountains during the 21st century. *Ambio*, *37*(4), 280–285. https://doi.org/10.1579/0044-7447(2008)37[280:ccimmd]2.0.co;2

Olcina, A. G. (2007). Mediterranean and subtropical climatic elements. *Boletín de la AGEN º*, *44*, 351–354.

Peltier, D. M. P., Guo, J., Nguyen, P., Bangs, M., Gear, L., Wilson, M., Jefferys, S., Samuels-Crow, K., Yocom, L. L., Liu, Y., Fell, M. K., Auty, D., Schwalm, C., Anderegg, W. R. L., Koch, G. W., Litvak, M. E. & Ogle, K. (2021). Temporal controls on crown nonstructural carbohydrates in southwestern US tree species. *Tree Physiology*, *41*(3), 388–402. https://doi.org/10.1093/treephys/tpaa149

Pomeroy, J. W., Gray, D. M., Brown, T., Hedstrom, N. R., Quinton, W. L., Granger, R. J. & Carey, S. K. (2007). The cold regions hydrological model: A platform for basing process representation and model structure on physical evidence. *Hydrological Processes*, *21*(19), 2650–2667. https://doi.org/10.1002/hyp.6787

Rasband, W. (1997). ImageJ.

Rodriguez Perez, D. (2013). Growthmodels: Nonlinear Growth Models.

Rossi, S., Deslauriers, A. & Anfodillo, T. (2006). Assessment of Cambial Activity and Xylogenesis by Microsampling Tree Species: An Example at the Alpine Timberline. *IAWA Journal*, *27*(4), 383–394. https://doi.org/10.1163/22941932-90000161

Rossi, S., Deslauriers, A. & Morin, H. (2003). Application of the Gompertz equation for the study of xylem cell development. *Dendrochronologia*, *21*(1), 33–39.

Rossi, S., Rathgeber, C. B. K. & Deslauriers, A. (2009). Comparing needle and shoot phenology with xylem development on three conifer species in Italy. *Annals of Forest Science*, *66*(2), 206–206. https://doi.org/10.1051/forest/2008088

Sangüesa-Barreda, G., Linares, J. C. & Camarero, J. J. (2012). Mistletoe effects on Scots pine decline following drought events: Insights from within-tree spatial patterns, growth and carbohydrates. *Tree Physiology*, *32*(5), 585–598. https://doi.org/10.1093/treephys/tps031

Sanmiguel-Vallelado, A., Camarero, J. J., Gazol, A., Morán-Tejeda, E., Sangüesa-Barreda, G., Alonso-González, E., Gutiérrez, E., Alla, A. Q., Galván, J. D. & López-Moreno, J. I. (2019). Detecting snow-related signals in radial growth of Pinus uncinata mountain forests. *Dendrochronologia*, *57*, 125622. https://doi.org/10.1016/j.dendro.2019.125622

Sanmiguel-Vallelado, A., Camarero, J. J., Morán-Tejeda, E., Gazol, A., Colangelo, M., Alonso-González, E. & López-Moreno, J. I. (2021). Snow dynamics influence tree growth by controlling soil temperature in mountain pine forests. *Agricultural and Forest Meteorology*, *296*, 108205. https://doi.org/10.1016/j.agrformet.2020.108205

Sanmiguel-Vallelado, A., López-Moreno, J. I., Morán-Tejeda, E., Alonso-González, E., Navarro-Serrano, F. M., Rico, I. & Camarero, J. J. (2020). Variable effects of forest canopies on snow processes in a valley of the central Spanish Pyrenees. *Hydrological Processes*, *34*, 2247–2262. https://doi.org/10.1002/hyp.13721

Sanmiguel-Vallelado, A., McPhee, J., Esmeralda Ojeda Carreño, P., Morán-Tejeda, E., Julio Camarero, J. & López-Moreno, J. I. (2022). Sensitivity of forest–snow interactions to climate forcing: Local variability in a Pyrenean valley. *Journal of Hydrology*, *605*, 127311. https://doi.org/10.1016/j.jhydrol.2021.127311

Saunders, M. & Tosey, P. (2013). The layers of research design. *Rapport*, (Winter), 58–59.

Seibert, J., Jenicek, M., Huss, M. & Ewen, T. (2015). Snow and Ice in the Hydrosphere. *Snow and Ice-Related Hazards, Risks and Disasters* (pp. 99–137). Elsevier. https://doi.org/10.1016/B978-0-12-394849-6.00004-4

Sen, P. K. (1968). Estimates of the regression coefficient based on Kendall's tau. *Journal of the American statistical association*, *63*(324), 1379–1389.

Shook, K. (2016). CRHMr: Pre- and post- processing for the Cold Regions Hydrological Modelling (CRHM) platform.

Skamarock, W. C., Klemp, J. B., Dudhia, J., Gill, D. O., Barker, D. M., Wang, W. & Powers, J. G. (2008). A description of the Advanced Research WRF version 3. NCAR Technical note-475+ STR.

Smith, T. J. (1993). Forest structure. *Tropical mangrove ecosystems* (pp. 101–101). American Geophysical Union.

Stekhoven, D. J. (2013). missForest: Nonparametric missing value imputation using random forest.

Stekhoven, D. J. & Buhlmann, P. (2012). MissForest–non-parametric missing value imputation for mixed-type data. *Bioinformatics*, *28*(1), 112–118. https://doi.org/10.1093/bioinformatics/btr597

Stenberg, P., Linder, S., Smolander, H. & Flower-Ellis, J. (1994). Performance of the LAI-2000 plant canopy analyzer in estimating leaf area index of some Scots pine stands. *Tree Physiology*, *14*(7-8-9), 981–995.

Team, R. C. (2020). *R: A language and environment for statistical computing. R Foundation for Statistical Computing, Vienna, Austria.*

Thiel, H. (1950). A rank-invariant method of linear and polynomial regression analysis, Part 3. *Proceedings of Koninalijke Nederlandse Akademie van Weinenschatpen a*, *53*, 1397–1412.

van der Maaten, E., van der Maaten-Theunissen, M., Smiljanić, M., Rossi, S., Simard, S., Wilmking, M., Deslauriers, A., Fonti, P., von Arx, G. & Bouriaud, O. (2016). dendrometeR: Analyzing the pulse of trees in R. *Dendrochronologia*, *40*, 12–16.

Waring, R. H. & Running, S. W. (2007). CHAPTER 2 - Water Cycle. In R. H. Waring & S. W. Running (Eds.), *Forest Ecosystems (Third Edition)* (pp. 19–57). Academic Press. https://doi.org/10.1016/B978-012370605-8.50007-4

Chapter 3

Variable effects of forest canopies on snow processes in a valley of the central Spanish Pyrenees

This article was published in:

Sanmiguel-Vallelado, A., López-Moreno, J. I., Morán-Tejeda, E., Alonso-González, E., Navarro-Serrano, F. M., Rico, I. & Camarero, J. J. (2020). Variable effects of forest canopies on snow processes in a valley of the central Spanish Pyrenees. *Hydrological Processes*, *34*, 2247–2262. https://doi.org/10.1002/hyp.13721

Authors thank WILEY for the permission to present here the article in its entirely.

Received: 30 July 2019 | Accepted: 3 February 2020

DOI: 10.1002/hyp.13721

RESEARCH ARTICLE

WILEY

Variable effects of forest canopies on snow processes in a valley of the central Spanish Pyrenees

Alba Sanmiguel-Vallelado[1] | Juan I. López-Moreno[1] | Enrique Morán-Tejeda[2] | Esteban Alonso-González[1] | Francisco M. Navarro-Serrano[1] | Ibai Rico[3] | J. Julio Camarero[1]

[1]Department of Geoenvironmental Processes and Global Change, Pyrenean Institute of Ecology, IPE-CSIC, Zaragoza, Spain

[2]Department of Geography, University of the Balearic Islands, Palma de Mallorca, Spain

[3]Department of Geography, Prehistory and Archaeology, University of the Basque Country, Vitoria-Gasteiz, Spain

Correspondence
Alba Sanmiguel-Vallelado, Department of Geoenvironmental Processes and Global Change, Pyrenean Institute of Ecology, IPE-CSIC, Avda. Montañana 1005, 50059 Zaragoza, Spain.
Email: albasv@ipe.csic.es

Funding information
Ministerio de Educación, Cultura y Deporte, Grant/Award Number: FPU16/00902; Ministry of Economy and Competitiveness, Grant/Award Numbers: CGL2017-82216-R, CGL2014-52599-P; Ministry of Education, Culture and Sports, Grant/Award Numbers: FPU15, FPU16

Abstract

Snowpacks and forests have complex interactions throughout the large range of altitudes where they co-occur. However, there are no reliable data on the spatial and temporal interactions of forests with snowpacks, such as those that occur in nearby areas that have different environmental conditions and those that occur during different snow seasons. This study monitored the interactions of forests with snowpacks in four forest stands in a single valley of the central Spanish Pyrenees during three consecutive snow seasons (2015/2016, 2016/2017 and 2017/2018). Daily snow depth data from time-lapse cameras were compared with snow data from field surveys that were performed every 10–15 days. These data thus provided information on the spatial and temporal changes of snow–water equivalent (SWE). The results indicated that forest had the same general effects on snowpack in each forest stand and during each snow season. On average, forest cover reduced the duration of snowpack by 17 days, reduced the cumulative SWE of the snowpack by about 60% and increased the spatial heterogeneity of snowpack by 190%. Overall, forest cover reduced SWE total accumulation by 40% and the rate of SWE accumulation by 25%. The forest-mediated reduction of the accumulation rate, in combination with the occasional forest-mediated enhancement of melting rate, explained the reduced duration of snowpacks beneath forest canopies. However, the magnitude and timing of certain forest effects on snowpack had significant spatial and temporal variations. This variability must be considered when selecting the location of an experimental site in a mountainous area, because the study site should be representative of surrounding areas. The same considerations apply when selecting a time period for study.

KEYWORDS

mountain forest, snowpack, spatial and temporal variability, SWE

1 | INTRODUCTION

The snowpack of a mountain plays a fundamental role in several ecological and hydrological processes, in that it provides water for forest growth, and it also affects the water cycles and economies of mid-latitude mountainous regions (Barnett, Adam, & Lettenmaier, 2005; Beniston, 2012; Jones, Pomeroy, Walker, & Hoham, 2001; Pulliainen et al., 2017). Such is the case in the Mediterranean basin, in which winter snow dynamics influence the streamflow of many rivers (Darwish et al., 2015; Gil'ad & Bonne, 1990; López & Justribó, 2010; López-Moreno & García-Ruiz, 2004; Morán-Tejeda, Lorenzo-Lacruz, López-Moreno, Rahman, & Beniston, 2014; N'da et al., 2016; Sanmiguel-Vallelado, Morán-Tejeda, Alonso-González, & López-Moreno, 2017), and water from spring snowmelt is an essential resource in the lower watersheds, which are drought-prone regions (Ceballos-Barbancho, Morán-Tejeda, Luengo-Ugidos, & Llorente-Pinto, 2008; García-Ruiz, López-Moreno, Vicente-Serrano, & Lasanta–Martínez, & Beguería, 2011; López-Moreno et al., 2014).

The variable climate of the mountainous headwaters induces high inter- and intra-annual variability in snowpack characteristics (i.e., distribution, depth, density and snow–water equivalent [SWE]; Fayad et al., 2017). The characteristics of the snowpack also depend on interactions between topography and forest cover (Huerta, Molotch, & McPhee, 2019; Jenicek, Pevna, & Matejka, 2018; Jost, Weiler, Gluns, & Alila, 2007). Forest cover reduces snow accumulation on the ground because the tree canopies intercept some of the snowfall (Storck, Lettenmaier, & Bolton, 2002). Thus, the snowpack is smaller in forested areas than open sites (Moeser, Stähli, & Jonas, 2015; Veatch, Brooks, Gustafson, & Molotch, 2009). Snow that is intercepted by the forest canopy may return to the atmosphere by sublimation or may reach the ground as it melts or by direct mass release (Storck, 2000). The efficiencies of canopy interception and subsequent process depend on local climate and forest structure (Varhola, Coops, Weiler, & Moore, 2010). Furthermore, forest cover influences snow melt by altering the energy balance (Nakai, Sakamoto, Terajima, Kitamura, & Shirai, 1999). For example, forested areas have reduced turbulent heat transfer because of their reduced wind speeds (Marks, Kimball, Tingey, & Link, 1998; Yamazaki & Kondo, 1992). The forest canopy can also reduce energy inputs by shading the snowpack from solar radiation (Ellis, 2011; Musselman, Molotch, & Brooks, 2008) and the snowpack beneath a canopy receives increased long-wave radiation from trees (Pomeroy et al., 2009), which have higher rates of emissivity than the atmosphere (Essery, Pomeroy, Ellis, & Link, 2008; Lawler & Link, 2011). In addition, litter on the snow surface (needles, leaves, etc.) can increase the net radiation during the melting period due to a reduction in the snow albedo (Hardy, Melloh, Robinson, & Jordan, 2000).

The Pyrenees, a mountain range located in the transition of the temperate-continental Atlantic-Eurosiberian and mild-dry Mediterranean climate, has a snowpack above 1,600 m a.s.l. that usually lasts until late spring (López-Moreno et al., 2010). In the central Spanish part of this range, the dominant trees in the subalpine forests are mountain pine (*Pinus uncinata* Ram.) from 1,600 to 2,500 m a.s.l. and Scots pine (*Pinus sylvestris* L.) from 1,200 to 1,900 m a.s.l. (de la Torre & Ceballos, 1979). Therefore, snowpack and forests interact at altitudes of 1,600 to 2,500 m a.s.l. Most of the Pyrenees are in this altitudinal band, and elevations only occasionally exceed 3,000 m a.s.l. However, few studies have examined the impact of forest on snow in the Spanish Pyrenees, despite the climatically transitional nature of this range, which could make it vulnerable to dry conditions in a warmer future (López-Moreno & Latron, 2008a; López-Moreno & Latron, 2008b; Revuelto, López-Moreno, Azorin-Molina, Alonso-González, & Sanmiguel-Vallelado, 2016). Examination of the impact of the forest canopy on snow processes in the Pyrenees will improve our understanding of hydrological responses to future hydroclimatic changes (climate warming) in this region (El Kenawy, López-Moreno, & Vicente-Serrano, 2012; López-Moreno et al., 2010; Morán-Tejeda et al., 2014).

Previous studies have documented the different ways that snowpacks and forests interact at different altitudinal ranges in mid-latitude mountain ranges (Huerta et al., 2019; Jenicek et al., 2018; Lundquist, Dickerson-Lange, Lutz, & Cristea, 2013). However, there is uncertainty on the magnitude of these interactions among nearby areas and during different years, and this can affect the representativeness of a study site and study period that is used for research. Thus, the location of the experimental site and time span of the study are key considerations when undertaking research on a mountain area and designing the experimental setup. To account for this uncertainty, it is necessary to have reliable data on the spatial and temporal variability of snow–forest interactions under contrasting environmental conditions.

This study assessed the sources of uncertainty in the magnitude of interactions among nearby areas and during different years by determining which characteristics of the forest–snow interactions remained constant and which varied among different nearby areas and during different consecutive snow seasons. Our purpose was to highlight the similarities and differences in the spatial and temporal effects of forest on snowpack. Thus, we used a snow monitoring initiative based on ground data that were developed in the central Spanish Pyrenees to compare forest openings (O) and areas beneath forest canopy (F). The specific objectives of this study were to: (a) identify and quantify the influences of forest canopies on the duration of snowpacks, amount of SWE, SWE distribution and SWE accumulation and melting rates in the study area; (b) identify similarities and differences in the effects of forest canopies on the snowpacks of four nearby forest stands and during three consecutive snow seasons, in which there were different snow and climatic characteristics; and (c) determine the representativeness of the selected experimental setup, based on results from localized daily estimations of SWE and spatially distributed SWE measurements across each plot every 10–15 days.

2 | DATA AND METHODS

2.1 | Experimental setting

This study was performed in the central Spanish Pyrenees, in the northeastern Iberian Peninsula (Figure 1a). The selected valley is Balneario de Panticosa, which constitutes the headwaters of the Caldarés River, a Pyrenean tributary. The experimental area consists of four forest stands that have different elevations (1,674 to 2,104 m a.s.l.), exposure, forest structure and climatology because of the abrupt topography in this area (Figure 1b). There was one plot of

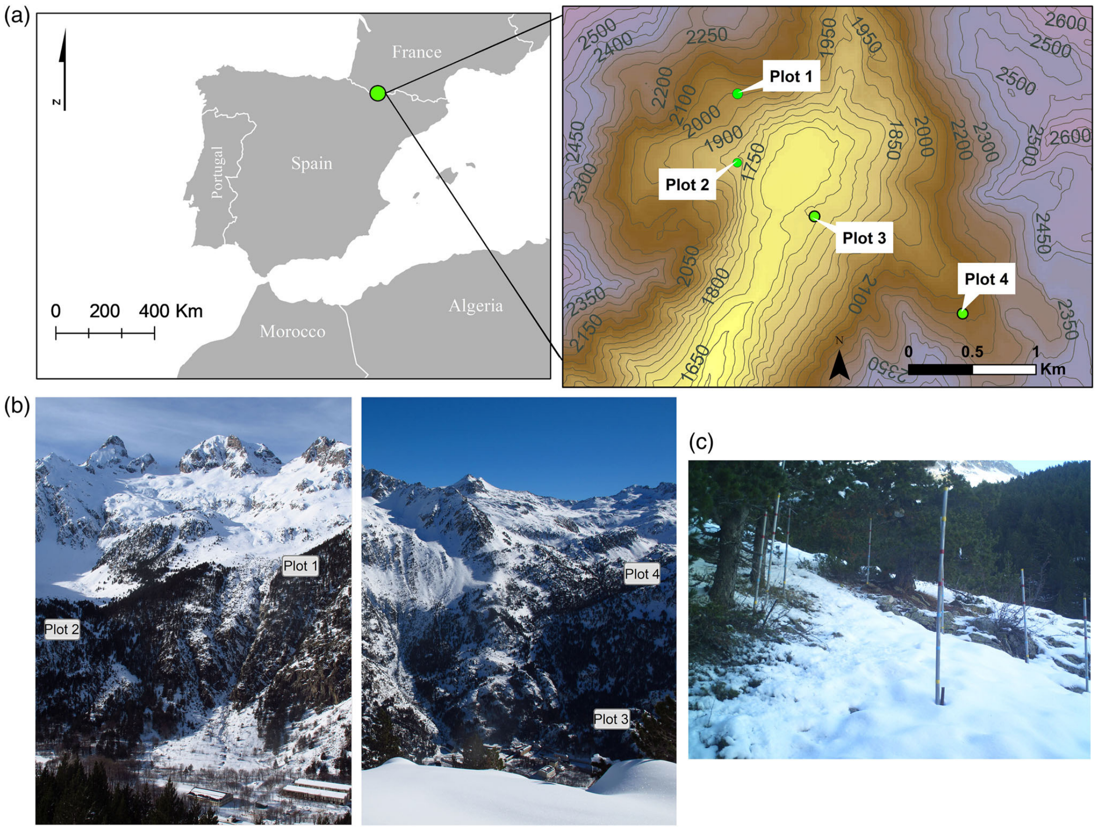

FIGURE 1 (a) Left: Study location (Balneario de Panticosa) in the Spanish Pyrenees. Right: Location of the experimental plots in the Balneario de Panticosa Valley (orthophoto source: PNOA 1:25,000 n°145). (b) General view of the experimental plots in situ. (c) Example of the semi-automatic snow depth monitoring system in plot 2, based on time-lapse cameras and snow poles

approximately 450 m^2 in each of the four forest stands. The plots were designated based on their locations in the valley (from NE to SW) as plot 1, plot 2, plot 3 and plot 4 (Figure 1a). The studied forest stands mainly consisted of *P. uncinata*, although plot 3 also contained *P. sylvestris*.

2.2 | Meteorological data

Global solar irradiance (GSI) and wind speed series were obtained from an automatic weather station (HOBO U30 NRC, Onset Co., Bourne, MA) that was located at forest openings within each plot. These were installed in November 2016, so GSI and wind speed data were not available during the first snow season (2015/2016), but they were available during the other two snow seasons (2016/2017 and 2017/2018). Measurements were recorded every 15 min. Potential irradiation received by each plot was calculated using the Points Solar Radiation tool implemented in ArcGIS 9.3 software (ESRI, USA). This tool allows calculation of the amount of radiant energy for specific time periods (monthly) and specific locations (plots). These calculations were performed under clear-sky conditions (transmissivity: 0.5) and were based on a 20 m resolution digital elevation model (source: IDEAragón–Infraestructura de Datos Espaciales de Aragón, https://idearagon.aragon.es/). Air temperature and humidity series were obtained using autonomous self-recording data-loggers (Tinytag-Plus-2; model TGP-4017, Gemini DataLoggers UK Ltd., Chichester, West Sussex, UK) that were equipped with naturally ventilated radiation shields (Datamate ACS-5050 Weather Shield; Gemini DataLoggers UK Ltd., Chichester, West Sussex, UK). One data-logger was installed at each forest stand, and measurements were recorded every 15 min during the three snow seasons.

2.3 | Forest structure

The structure of the forest stand of each plot was characterized by measuring the following variables in representative subplots of 15 × 15 m (1 subplot per study plot):

- Canopy cover (%): Canopy cover refers to the proportion of the forest floor covered by the vertical projection of the tree crowns (Korhonen, Korhonen, Rautiainen, & Stenberg, 2006). For estimation, two crown projections (one perpendicular and one parallel to the slope line) were measured in each pine. Two area values were calculated from these measurements and were then averaged for each pine. The cover area of each pine was expressed as a percentage of the subplot area. Finally, all individual canopy cover percentages were aggregated. Because the canopies of different individuals may overlap, the total cover may exceed 100%.
- Density (trees per ha): Number of pines per unit area.
- Basal area (m^2 per ha): Proportion of the ground occupied by the pine stems. The diameter of each tree was measured at 1.3 m above the bare ground surface, the area was calculated, and the individual basal areas were then summed and divided by the subplot area.

2.4 | Snow monitoring

Snow data were collected during three snow seasons (2015/2016, 2016/2017 and 2017/2018), from the onset of snow accumulation (November) to the end of melting (May/June). This provided the following data series:

- Snowpack density: SWE was manually surveyed every 10–15 days using a snow cylinder and scale (ETH core sampler, Swiss Federal Institute of Technology, Zurich) at snow pits dug at two single locations in each plot, one in a forest opening (O) and one below the forest canopy (F). Two replicates per F–O site were collected. Snow density was calculated from the collected data using the equation:

$$\rho_s = \frac{SWE \cdot \rho_w}{H}$$

where ρ_s is snowpack density (kg m^{-3}), SWE is the measured equivalent water of the snowpack (m), H is measured snowpack depth (m) and ρ_w is water density (kg m^{-3}). Daily snow density series were estimated by linear interpolation between each pair of density measurements from consecutive surveys.
- Spatially distributed SWE series: Snow depth was manually measured every 10–15 days. In total, 200 depth measurements were taken using a snow depth probe (Snowmetrics Inc., Fort Collins, CO) that covered the entire area of each plot (about 450 m^2), clustered in 10 forest openings (O) and 10 sites beneath forest canopy (F), with 10 replicates per F–O site. The samples consisted of 10 replicates (about 1 m apart) that had homogeneous distributions in each F–O site. Within F sites, effort was made to collect most of the snowpack spatial variability caused by canopy cover. Thus, measurements were taken from the tree trunks to the edge of the projections of the tree canopies to the ground, covering all aspects. Spatially distributed SWE series for F–O sites (Figure S1) were inferred from spatially distributed snow depth measurements and density values (described above).
- Daily SWE series: Eight fixed snow poles and time-lapse cameras were used to measure snow depth each day at several spots in a single representative location of each plot (Bushnell, Trophy Cam, KS) (Figure 1c). Three poles were placed in a forest opening, and five were placed beneath the forest canopy. Daily snow depth series for each pole were manually extracted from collected photographs using ImageJ software (Rasband, 1997). Missing data were estimated at each pole using the missForest method (Stekhoven & Bühlmann, 2012), which is implemented in the MissForest R package (Stekhoven, 2013). This is a nonparametric iterative imputation method that accounts for missing data based on Random Forests (Breiman, 2001). For each variable, the missForest method fits a Random Forest regression to the observed part, and then predicts the missing parts of the input data. The algorithm proceeds iteratively until a stopping criterion is met or a user-specified maximum number of iterations are achieved. Average daily snow depth series for the F–O poles at each experimental plot were calculated. The estimated daily SWE series for the F–O poles at each experimental plot (Figure 2) were inferred from data on daily snow depth and estimated daily snow density (described above).

Daily records provided high temporal resolution data, but were restricted to small areas; spatially distributed measurements had low temporal resolution, but provided an overview of snowpack characteristics for the whole plot and allow quantification of spatial variability. Use of both data sources allowed determination of whether continuous local data are representative of a larger neighbouring area at the plot scale.

2.5 | Statistical analyses

Some derived variables were calculated from the SWE series (Table 1). The Wilcoxon test was used to detect the significance of differences in the cumulative SWE and derived variables between forest canopy areas (F) and forest openings (O). Comparisons were only performed when snowpack was present in both areas. When a forest effect was detected (i.e., statistically significant differences in the variables at F and O areas), the increase or decrease of a variable associated with the forest canopy relative to the original variable was calculated as a percentage. The Kruskal–Wallis test and then the Wilcoxon test were used to assess whether there were statistically significant differences in the detected effects of forests among plots, snow seasons, main accumulation periods and main melting periods.

The Mann–Kendall test was used to detect trends of the effects of forests during each snow season, and the Theil-Sen slope estimator was used to compute the magnitude of this trend. Trend analyses were carried out using the zyp package (Bronaugh & Consortium, 2019), which includes a trend-free pre-whitening method for removing serial autocorrelation. Spearman correlations were calculated to determine the influence of environmental variables on the detected effects of forests.

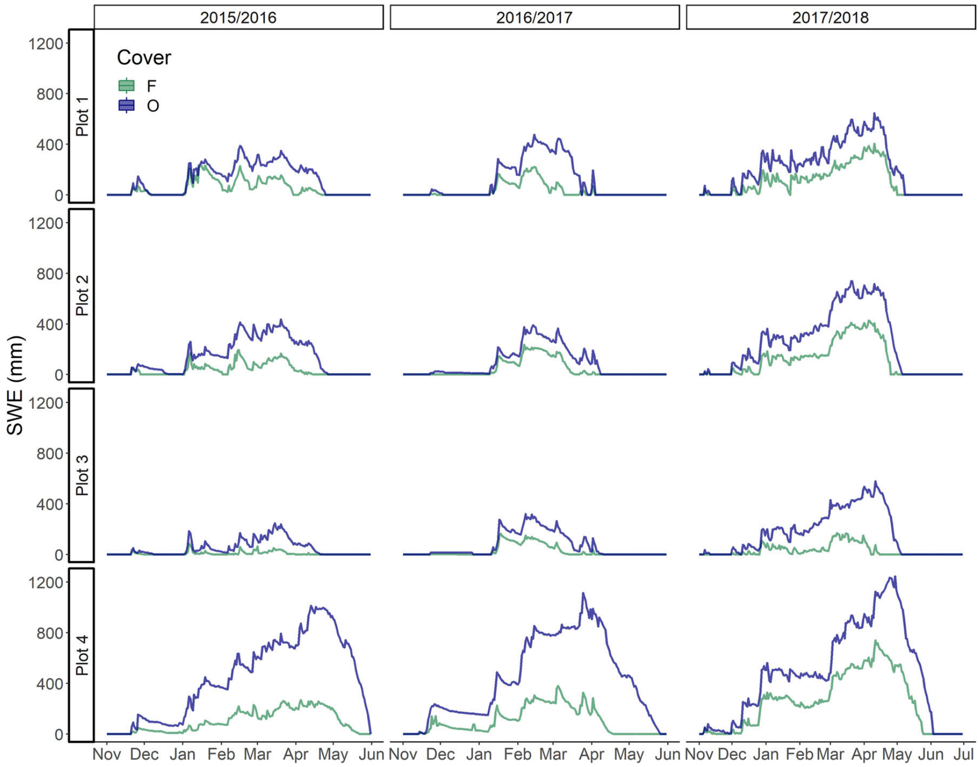

FIGURE 2 Daily snow–water equivalent at each experimental plot and each snow season in areas beneath forest canopies (F, green lines) and in forest openings (O, blue lines)

TABLE 1 Criteria used for statistical analysis (top) and derived variables calculated from SWE series (bottom)

Criteria for statistical analysis		Description	
Continuous snowpack[a]	Start	Date of the first day of 14 or more consecutive days with snow on the ground	
	End	Last date with a snow record	
	Duration	Time between the start and end dates	
Main accumulation period		Date of continuous snowpack start to the date of peak SWE	
Main melt period		Date of peak SWE to the end of the continuous snowpack	
Days of accumulation[b]		SWE difference between consecutive days >0	
Days of melting[b]		SWE difference between consecutive days <0	
Derived variables		**Source of data**	**Description**
Spatial CV[c]		Spatially distributed SWE series	Ratio of the SD to the mean value of SWE of each survey day
Accumulation rates		Daily SWE series	Positive values obtained when performing first-order differencing, day-by-day. Units: mm day^{-1}
Melting rates		Daily SWE series	Negative values obtained when performing first-order differencing, day-by-day. Units: mm day^{-1}

Abbreviations: CV, coefficient of variation; SWE, snow–water equivalent.
[a]Only data in a continuous snowpack period were considered.
[b]Assuming that the main processes in SWE gain and loss were snowfall and snow melting, although other processes may have contributed (e.g., snow redistribution by wind).
[c]For each area, CV shows the extent of spatial variability in relation to the SWE average.

TABLE 2 Average values of forest structure, topography and climatology in the four plots

Plot	Elevation (m a.s.l.)	Aspect	Slope (°)	Canopy cover (%)	Density (indiv ha^{-1})	Basal area (m^2 ha^{-1})	DJF T (°C)	March SD (cm)	RH (%)	Wind speed (m s^{-1})	MAM potential irradiation (1,000 W h m^{-2})	MAM measured GSI (W m^{-2})
1	2,008	S	29.4	156	1,689	45.1	−0.44	101.4	70.0	0.04	165.3	154.4
2	1,814	E	20.4	85	844	13.7	−0.43	113.9	69.3	0.40	129.6	167.6
3	1,674	W	9.3	119	533	35.3	0.29	78.8	68.9	0.49	140.2	192.7
4	2,104	NE	22.7	29	356	26.6	−1.95	246.5	66.9	0.78	122.6	195.1

Note: The source of climate data is in Section 2.2. The methods used to obtain forest structure data are in Section 2.3. The methods used to obtain snow data are in Section 2.4.
Abbreviations: DJF T, winter mean air temperature from December to February; March SD, average snow depth in March; RH, average relative humidity for the whole snow season (November to May); Wind speed, average for the whole snow season (November to May); MAM potential irradiation, average from March to May; MAM measured GSI, average global solar irradiation from March to May.
Source of data: daily records in forest openings.

None of the analysed variables had normal distributions (Shapiro–Wilk test: $p < .05$), so non-parametric methods were used in all analyses. The criteria considered for statistical analysis are in Table 1. The results commented below are all statistically significant ($p < .05$). Both significant and insignificant results can be seen in the respective tables. All analyses were performed using R statistical software (R Core Team, 2018).

3 | RESULTS

3.1 | Characteristics of the plots

Table 2 shows the major topographic and climatic characteristics of the forests in each plot. Plot 1 had the greatest tree density, canopy cover and basal area per ha, and its forest openings were rather small. Plot 1 was also the steepest plot and mostly faced southward, so it could potentially receive the greatest amount of solar radiation. However, actual measurements indicated that the forest openings in plot 1 received the least radiation and also had the lowest wind speed values (close to 0) because of the sheltering effects of trees. Plot 2 had a relatively dense forest and the smallest basal area per ha. Its exposure was mostly eastward, and its winter temperatures and March snow depth were similar to those of plot 1 (intermediate among all plots). Plot 3 had the lowest elevation, was the flattest plot, and it faced westward. This plot had a relatively high canopy-cover and received a relatively high irradiance. Plot 3 also had the highest winter temperatures and the thinnest snowpacks. Plot 4 had the highest elevation and faced northeastward. This plot had the lowest tree density and amount of canopy-covered forest, so it could potentially receive the least amount of solar irradiation. However, measurements indicated this plot had the largest irradiance, as well as the greatest wind speeds, the coldest winter temperatures and the deepest snowpacks.

3.2 | Characteristics of the snow seasons

The study area had notable interannual variability in snow accumulation and melting from 2015 to 2018 (Table 3; Figure 2). The longest snow season was 2017/2018, and this season had the largest SWE peak values. Snow accumulation started much earlier and ended much later during this snow season, and the shortest melt period occurred afterwards. In contrast, the 2016/2017 snow season was the shortest. Heavy snowfalls occurred, as indicated by the magnitude of the SWE peak, but snow accumulation occurred over a short period of time, and was followed by a long melt period. In 2015/2016, a smaller snow accumulation was recorded but the duration of snow cover was longer than in 2016/2017.

3.3 | Effects of forest on snowpack duration

Snow disappeared 17 ± 10 days earlier when it was beneath forest canopies than in forest openings, on average (Table 4). Plot 3 had the greatest forest-mediated reduction in snow duration, and plot 1 had the least. Plot 4 had the greatest interannual variability in forest-mediated reduction of snow duration. The 2016/2017 snow season had the strongest forest-mediated reduction of snow duration.

3.4 | Effects of forest on snowpack distribution: cumulative SWE

Daily measurements showed there was significantly less SWE beneath forest canopies than in forest openings (Figure 3a). Forest reduced the cumulative SWE by an average of 64.2 ± 10.8% (Figure 3b). The magnitude of this forest effect varied significantly among snow seasons and among plots (Table 4). Forest had the greatest effect in plot 3, and the smallest effect in plot 1. This forest effect was significantly stronger during 2015/2016 and significantly weaker during 2017/2018 and was also greater during the main melting period than the main accumulation period (73.8 ± 15.4% vs. 59.4 ± 13.1%). In most cases, this forest effect significantly decreased when near the SWE peak, but increased towards the end of the melting period (Table 5; Figure 4).

Spatially distributed measurements also showed a significantly lower SWE beneath forest canopies than in forest openings

TABLE 3 Characteristics of the three snow seasons

Snow season	Plot	Date of accumulation onset	Date of SWE peak	SWE peak (mm)	Date at end of melt	Days of SWE accumulation	Days of SWE melting	Continuous snowpack duration (days)
2015/2016	1	2 January	16 February	388.7	24 April	46	69	114
	2	21 November	20 March	436.2	26 April	121	38	158
	3	2 January	15 March	247.0	20 April	74	37	110
	4	21 November	13 April	1,012.7	30 May	145	48	192
2016/2017	1	10 January	14 February	476.3	23 March	36	38	73
	2	23 November	13 February	390.0	8 April	83	55	137
	3	11 January	7 February	318.7	10 April	28	63	90
	4	14 November	25 March	1,113.7	25 May	132	62	193
2017/2018	1	1 December	10 April	645.4	7 May	131	28	158
	2	1 December	20 March	738.8	5 May	110	47	156
	3	1 December	11 April	578.3	5 May	132	25	156
	4	5 November	29 April	1,245.2	2 June	176	35	210

Note: The methods used to obtain snow data are in Sections 2.4 and 2.5.
Source of data: daily records in forest openings.

TABLE 4 Average effects of forests ± SDs among snow seasons (top) and among plots (bottom)

	Forest effects							
	Reduction in snow duration (days)	Decrease in cumulative SWE (%)						
Season or Plot		DS	DM	Increase of SWE CV (%)	Decrease in rate of SWE accumulation (%)	Increase in rate of SWE accumulation (%)	Decrease in melting rate of SWE (%)	Increase in melting rate of SWE (%)
2015/2016	11 ± 7	69.8 ± 12.0^{a}	61.6 ± 11.3 ^{a}	148.0 ± 93.3 ^{a}	55.8 ± 7.6 ^{a}	31.7 ± 18.7	57.3 ± 2.5 ^{a}	54.9 ± 10.4
2016/2017	26 ± 8	63.5 ± 6.5 ^{a}	46.8 ± 8.6 ^{a}	112.2 ± 60.2 ^{b}	56.4 ± 4.2 ^{b}	30.3 ± 30.0	47.1 ± 1.8 ^{a}	47.1 ± 14.7
2017/2018	14 ± 10	59.3 ± 12.9 ^{a}	62.3 ± 10.1	309.7 ± 95.7 ^{a,b}	47.6 ± 7.3 ^{a,b}	48.7 ± 16.8	53.8 ± 9.5 ^{a}	54.3 ± 20.0
Plot 1	10 ± 8	56.8 ± 6.2 ^{a}	51.0 ± 11.0 ^{a}	215.2 ± 92.4 ^{a}	48.6 ± 3.6 ^{a,c}	55.5 ± 17.7	52.2 ± 4.2	54.0 ± 3.4 ^{a}
Plot 2	15 ± 6	60.1 ± 7.5 ^{a}	55.9 ± 8.0 ^{b}	101.2 ± 114.5 ^{a,b,c}	50.3 ± 6.7 ^{b}	24.6 ± 20.2	48.6 ± 6.3 ^{a,b}	51.6 ± 26.1 ^{b}
Plot 3	26 ± 5	73.4 ± 9.3 ^{a}	63.7 ± 20.2 ^{a,b,c}	274.4 ± 162.4 ^{b}	59.3 ± 5.0 ^{a,b}	28.7 ± 34.6	57.6 ± 9.4 ^{a}	61.4 ± 9.0 ^{c}
Plot 4	18 ± 16	66.5 ± 14.6 ^{a}	56.9 ± 6.6 ^{c}	169.2 ± 66.4 ^{c}	55.0 ± 10.0 ^{c}	38.2 ± 10.6	52.6 ± 6.9 ^{b}	41.4 ± 8.9 ^{a,b,c}

Note: Daily SWE series (DS) were used to determine the effect of forest on snowpack duration and accumulation and melting rates of SWE. Spatially distributed SWE measurements (DM) were used to determine the effect of forest on the SWE CV. Both sources of data were used to determine the effect of forest on the cumulative SWE. Identical superscript letters in the same column indicate significant differences for snow seasons or plots (Wilcoxon test, $p < .05$).

(Figure S2a). Similarly, the overall forest-mediated reduction in cumulative SWE was 56.9 ± 11.8% (Figure S2b). The magnitude of this forest effect varied significantly among snow seasons and among plots (Table 4). This forest effect was significantly greater in plot 3 than in the other plots and was also significantly greater during the main melting periods than the main accumulation periods (68.3 ± 11.2% vs. 51.2 ± 16.1%).

3.5 | Effect of forest on snowpack distribution: SWE coefficient of variation

Spatially distributed measurements showed that the SWE spatial coefficient of variation (CV) was significantly greater beneath the forest canopies than in forest openings (0.5 ± 0.2 *vs.* 0.2 ± 0.1; Figure 5a and Table 6). On average, forest increased the SWE CV by 190.0 ± 118.0% (Figure 5b). The magnitude of this effect varied significantly among snow seasons and among plots (Table 4). Thus, the forest in plot 2 had the smallest effect on the SWE CV, and forests during the 2017/2018 snow season had the greatest effect on the SWE CV. There were no statistically significant differences in the effects of forest on the SWE CV between the main accumulation and melting periods.

3.6 | Effect of forest on accumulation and melting rates of SWE

Based on daily series, there was a significantly lower accumulation rate of SWE beneath the canopies relative to forest openings (Figure 6a).

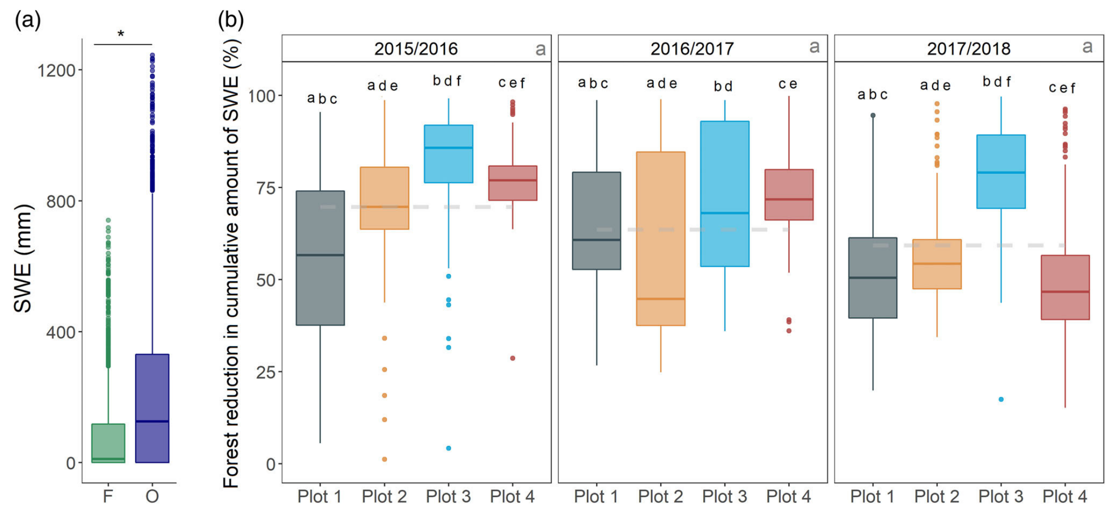

FIGURE 3 (a) Cumulative snow–water equivalent (SWE) in areas beneath forest canopies (F) and in forest openings (O). (b) Reduction of SWE in forested areas. Box indicates 25% and 75% percentiles; central line represents the median; whiskers indicate 1.5 × interquartile range (IQR); and points indicate outliers (>1.5 × IQR and <3 × IQR). Dashed lines: averages of each plot during each snow season. Statistical differences between plots, snow seasons and covers are indicated by same letters or an asterisk (Wilcoxon test, $p < .05$). *Source of data*: daily records

TABLE 5 Mann–Kendall linear trends in the intra-annual change of forest-mediated reduction in the cumulative SWE in each plot

Period	Snow season	Plot 1	Plot 2	Plot 3	Plot 4
Before SWE peak	2015/2016	0.14*	0.11*	0.17*	−0.21
	2016/2017	−0.10	−0.15*	−0.40*	−0.03
	2017/2018	−0.30*	−0.28*	−0.06	−0.24*
After SWE peak	2015/2016	0.27*	0.54*	0.43*	0.55*
	2016/2017	0.10	0.56*	0.60*	0.73*
	2017/2018	0.22	0.51*	*NA*	0.60*

*$p < .05$.
Source of data: daily records.

Overall, forest reduced SWE accumulation by 40.3 ± 13.5% when considering all accumulation days. Analysis of snowmelt indicated there were significantly lower melting rates of SWE beneath the canopies than in forest openings (Figure 6b). Overall, forest also reduced SWE melting by 25.1 ± 9.9% when considering all melting days. On average, a forest had a 70.4 ± 59.8% greater effect on accumulation than melting (Figure 6c). This imbalance was greatest in plot 3 and smallest in plot 1.

Forest cover reduced the SWE accumulation rate on 84.5% of the days when accumulation occurred. If only these days were considered, forest reduced the SWE accumulation rate by 53.30 ± 7.2% (Figure 7a). The magnitude of this forest effect varied significantly between snow seasons and among plots (Table 4). During the 2017/2018 snow season, this forest effect was significantly weaker. Plot 1 had the smallest forest-mediated reduction in accumulation rate, and plot 3 had the greatest. The forest-mediated reduction in accumulation rate was significantly greater after the SWE peak than before the SWE peak (59.7 ± 13.6% vs. 52.2 ± 8.0%). There were no significant intra-annual trends in the forest-mediated effect on accumulation rate (Table 7).

The rates of SWE accumulation were only occasionally greater beneath the forest canopies (occurring on 15.5% of accumulation days), and the mean increase was 37.5 ± 21.2% (Figure S3a). However, the magnitude of this effect had no significant variations among snow seasons, among plots or within snow seasons (Table 4).

Forest canopies reduced the melting rates of SWE on 73.6% of the days when melting occurred. When considering these days alone, forest canopies reduced the melting rates of SWE by 52.7 ± 6.8% on average (Figure 7b). The magnitude of this forest effect varied significantly between snow seasons and among plots (Table 4). During the 2016/2017 snow season, this forest effect was significantly weaker, and during the 2015/2016 snow season, it was significantly stronger. Plot 2 had the smallest forest-mediated reduction in melting rate. There were no statistically significant differences in the forest-mediated reduction in melting rate during periods before and after the SWE peak. The effect of forest on melting rate significantly increased from the SWE peak towards the end of the snow depletion in three plots (Table 7).

The rate of SWE melting was greater beneath forest canopies on 26.4% of the days when melting occurred, and the mean increase on

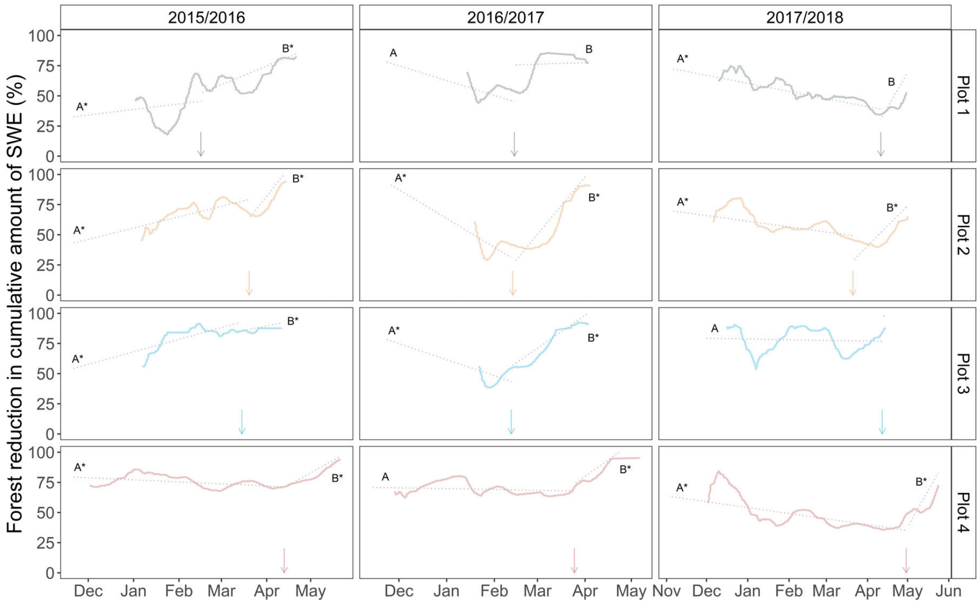

FIGURE 4 Temporal changes in the effect of forest on reducing cumulative of snow–water equivalent (SWE). Continuous lines: moving means for each plot over a 20-day period; dashed lines: general linear adjustments according to the main period of accumulation (A) and melting (B). Arrows indicate the date of peak of SWE. Statistically significant Mann–Kendall linear trends (p < .05) are indicated by asterisks. Table 5 provides related statistics. *Source of data*: daily records

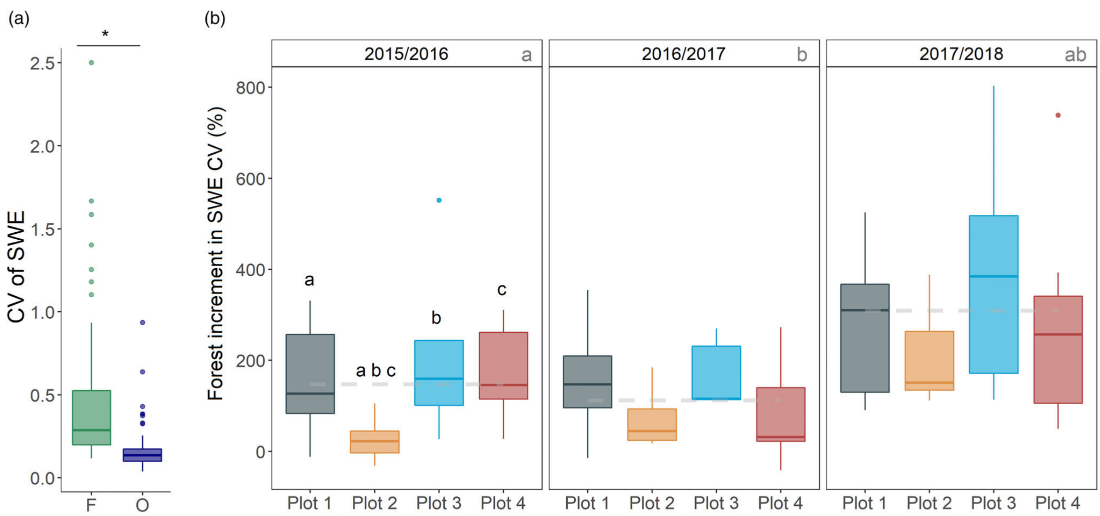

FIGURE 5 (a) Snow–water equivalent (SWE) coefficients of variation in areas beneath forest canopies (F) and in forest openings (O). (b) Changes of SWE variability in forested areas. Box plots, dashed lines and statistical differences are as described in Figure 3. *Source of data*: spatially distributed measurements from field surveys

these days was 37.5 ± 21.2% (Figure S3b). The magnitude of this effect varied significantly among plots, but not between snow seasons (Table 4). The effect was significantly weaker in plot 4 than the other plots. The forest-mediated increase in melting rate was significantly larger after than before the SWE peak (63.2 ± 18.3% vs. 47.5 ± 17.7%).

3.7 | Role of environmental variables on intra-annual variability of effects of forests on snowpack

Several environmental factors influenced the effects of forests on the rate of accumulation of SWE, melting and the SWE CV (Table 8). The strongest effect was a reduction of SWE accumulation by forest canopies and snowfall magnitudes, with significant correlations in all plots. As a result, the reduced rate of SWE accumulation by forest canopy was greater during seasons with less snowfall. We also observed larger SWE CVs beneath the canopy generally occurred when the snowpack was thinner, with significant correlations in plot 1. Similarly, the forest-mediated reduction of melting rate of SWE was lower when the snowpack was thicker, with significant correlations in plots 1 and 3. Higher irradiance increased the forest-mediated reduction in melting rate, but this only occurred after the SWE peak, and these correlations were only significant in plots 3 and 4. Higher temperatures significantly reduced the forest-mediated reduction in melting rates in plots 1 and 2.

TABLE 6 Absolute SWE CV values in forest openings (O) and beneath forest canopy (F) areas (average ± SDs)

Season or plot	O	F
2015/2016	0.2 ± 0.1	0.4 ± 0.3
2016/2017	0.2 ± 0.1	0.4 ± 0.2
2017/2018	0.1 ± 0.0	0.6 ± 0.2
Plot 1	0.2 ± 0.1	0.5 ± 0.2
Plot 2	0.2 ± 0.1	0.4 ± 0.2
Plot 3	0.2 ± 0.1	0.7 ± 0.4
Plot 4	0.1 ± 0.0	0.3 ± 0.1

4 | DISCUSSION

This study examined the spatial and temporal changes of the interactions of forests and snowpacks, and identified characteristics that varied and those that remained constant. The results highlight the need to consider spatial and temporal sources of uncertainty when undertaking research in a mountain area, in particular when designing the experimental setup and selecting the location and time span of a study.

4.1 | Spatial and temporal sources of uncertainty

Topographic factors, such as elevation, aspect and slope, can affect snowpack accumulation, insolation, air and soil temperatures, and other important factors (Hungerford, Nemani, Running, & Coughlan, 1989; Sartz, 1972). Consequently, the different topography of the plots we studied meant they had different microclimates, snowpack regimes and forest characteristics (Table 2). However, our results indicated the effects of forest on snow processes were generally the same in all plots. Local topography and vegetation cover strongly affect snow accumulation, distribution and melting in forested areas (Duyar, 2018; Jost et al., 2007). We found significant spatial variability among our four forest stands in terms of the magnitude of certain influences. In contrast, the typically high temporal variability of climate in mountainous headwaters induces high inter- and intra-annual variability in snowpack characteristics (Fayad et al., 2017). Consequently, the three snow seasons that we examined had different snowpack regimes (Table 3). Forests had the same basic effects on snowpack during all three snow seasons, but the magnitude of certain effects varied among snow seasons. Previous research indicated that

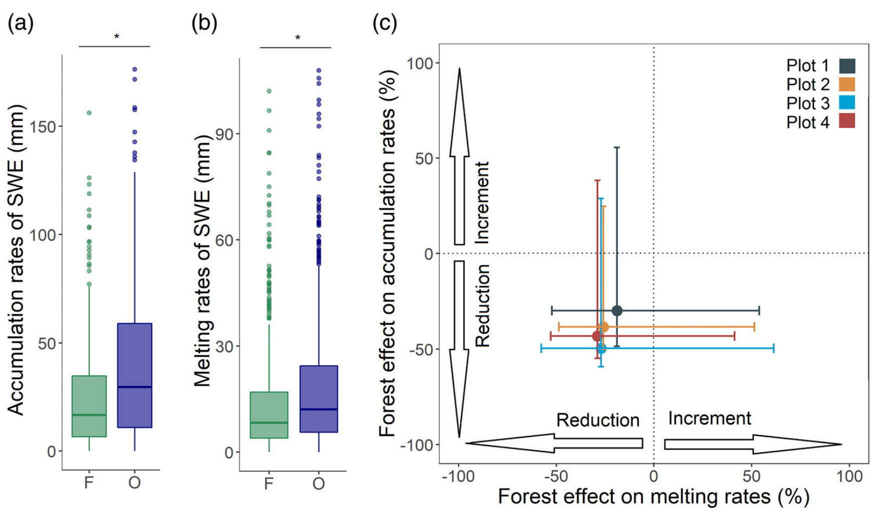

FIGURE 6 (a) Accumulation and (b) melting rates of snow–water equivalent in areas beneath forest canopies (F) and in forest openings (O). Statistical differences are indicated by asterisks (Wilcoxon test, $p < .05$). (c) Effect of forest on accumulation rates and on melting rates. Dots: overall forest effect; whiskers: mean increase and mean decrease. *Source of data*: daily records

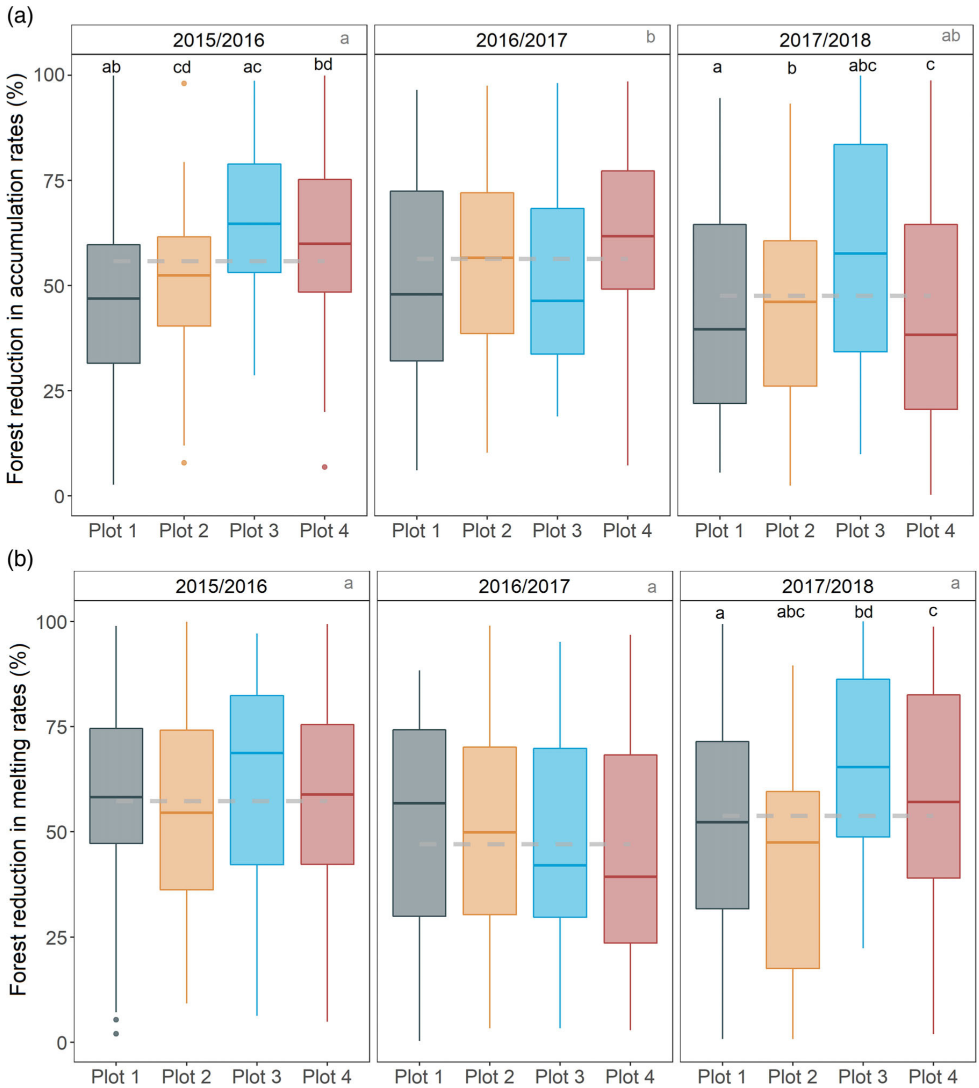

FIGURE 7 Effect of forest on reducing the rate of accumulation (a) and melting (b). Significant differences among plots and snow seasons are indicated by the same letters (Wilcoxon test, p < .05). Boxes and dashed lines are as described in Figure 3. *Source of data*: daily records

such variability is related to differences in the intensity of snowfall, accumulated snowpack, timing of accumulation and melting events and other climatic conditions (López-Moreno & Latron, 2008a; López-Moreno & Stähli, 2008; Mellander, Laudon, & Bishop, 2005).

4.2 | Effects of forest canopy on snowpack distribution

We found that forest canopies had a large effect in reducing the cumulative SWE of snowpack (average from daily records: 64.2%, average from spatially distributed measurements: 56.9%); in contrast, previous studies reported mean reductions in the range of 40–50% (Jenicek et al., 2018; Jost et al., 2007; López-Moreno & Latron, 2008b; Lundberg, Nakai, Thunehed, & Halldin, 2004; Musselman et al., 2008; Revuelto, López-Moreno, Azorin-Molina, & Vicente-Serrano, 2015; Winkler, Spittlehouse, & Golding, 2005). We found that the magnitude of the forest effect significantly varied among plots and was greatest in plot 3 and weakest in plot 1. Plot 3 is at the lowest elevation, had the warmest temperatures, and the shallowest snowpacks, and therefore received the least amount of snow. Boon (2009) reported that when the amount of snow is small, forest usually has a greater impact on snow accumulation (Boon, 2009). This is consistent with our results (Table 7), which showed that forest had the

TABLE 7 Mann–Kendall linear trends in the intra-annual changes of forest-mediated reduction in the SWE rates of accumulation and melting in each plot

Type of forest-mediated reduction	Period	Snow season	Plot 1	Plot 2	Plot 3	Plot 4
Accumulation rate	Before SWE peak	2015/2016	−0.09	0.21	0.13	−0.09
		2016/2017	−0.23	−0.10	−0.12	−0.16
		2017/2018	−0.12	−0.16	0.03	−0.01
	After SWE peak	2015/2016	−0.16	0.43	−0.40	0.20
		2016/2017	0.06	0.51*	−0.03	*NA*
		2017/2018	−0.33	−0.33	*NA*	*NA*
Melting rate	Before SWE peak	2015/2016	*NA*	*NA*	*NA*	−0.17*
		2016/2017	−0.21	−0.01	−0.04	0.12
		2017/2018	−0.11	−0.10	−0.11	0.18*
	After SWE peak	2015/2016	0.24	0.36*	−0.05	0.37*
		2016/2017	0.17	0.05	0.20	0.46*
		2017/2018	−0.27	0.08	−1.00	−0.12

*$p < .05$.
Source of data: daily records.

TABLE 8 Spearman correlation coefficients for the relationships between forest effects and environmental variables in each plot

Forest effects	Environmental variables	Plot 1	Plot 2	Plot 3	Plot 4
Increase of SWE CV	Snow depth	−0.63*	0.01	−0.04	−0.26
Decrease in rates of SWE accumulation	Daily snow accumulation	−0.57*	−0.54*	−0.62*	−0.42*
Decrease in rates of SWE melting	Snow depth	−0.23*	−0.06	−0.26*	−0.05
Decrease in rates of SWE melting	Global solar irradiance (†)	0.01	0.03	0.39*	0.33*
Decrease in rates of SWE melting	Air temperature	−0.13*	−0.23*	0.05	0.10*

*$p < .01$.
†Significant correlations only occurred during the main melting period (after SWE peak).

greatest impact on cumulative SWE at plot 3. Plot 1 had a dense canopy with very small forest openings; consequently, its trees had a sheltering effect on the forest openings, and the forest cover had a greater influence than in other plots. This meant that the effect of forest on reducing cumulative SWE was smallest in plot 1.

The magnitude of the effects of forest also varied significantly among the snow seasons. As noted above, previous studies reported that the effect of forest cover increases as snowpack depth decreases (Boon, 2009;López-Moreno & Latron, 2008b; Revuelto et al., 2015). In agreement, we found that the 2015/2016 snow season, when snow accumulation was lowest, forest had the greatest effect on reducing cumulative SWE; the 2017/2018 snow season, when snow accumulation was greatest, forest had the weakest effects. The same reasoning explains the intra-annual variability for this effect: forest caused a significantly greater reduction in cumulative SWE after the SWE peak (main melting period) than before it, and this effect was greater towards the end of the snow season. These results are similar to previous findings of studies in the Pyrenees (López-Moreno & Latron, 2008b; Revuelto et al., 2015).

Our study confirms the results of previous research (López-Moreno & Latron, 2008a; Talbot et al., 2006; Winkler & Moore, 2006), in that areas with forest cover had increased (190.0% on average) small-scale spatial variability of snowpack thickness compared to open areas. The magnitude of this effect of significantly varied among plots and snow seasons, but there was no significant intra-annual variability.

4.3 | Effects of forest canopy on snow accumulation and melting rates

The interception of snow by forest canopies explains why daily accumulation rates were greater in forest openings (53.3% on average), consistent with previous research (Garvelmann, Pohl, & Weiler, 2013; Hedstrom & Pomeroy, 1998; Lundberg et al., 2004; Stähli, Jonas, & Gustafsson, 2009). The magnitude of the forest-mediated reduction in accumulation rate significantly varied among plots, among snow seasons, and within each snow season. This effect was significantly greater in plot 3, which had the least snowfall, and weaker during 2017/2018 and during the main accumulation period of each year, periods that had greater snowfall. Thus, our observations indicated that the forest-mediated reduction in SWE accumulation rate was inversely related to the amount of snowfall (Table 7). This is because trees have a limited capacity of snow interception (Boon, 2009; Keller & Strobel, 1982; López-Moreno & Latron, 2008a; Mellander et al., 2005; Revuelto et al., 2016). Enhancement of the SWE accumulation rate beneath the forest canopy was infrequent (15.5% of accumulation days). This may be because there was a delayed snow loading from the forest canopy on days with no snowfall, or because wind released some of the intercepted snow. The magnitude of this unusual forest-mediated increase in the SWE accumulation rate did not vary significantly among plots, among snow seasons or within snow seasons.

Our analysis of snow melting indicated that forest reduced the melting rate of SWE by 52.7% on average. Many previous studies also reported that forest canopies reduce the snow ablation rate by attenuating solar radiation, because they reflect incoming shortwave radiation back to the atmosphere (Ellis, 2011; Jenicek et al., 2018; López-Moreno & Stähli, 2008; Molotch et al., 2009; Musselman et al., 2008; Musselman, Pomeroy, & Link, 2015; Pomeroy, Fang, & Ellis, 2012; Revuelto et al., 2015; Schnorbus & Alila, 2013; Sicart et al., 2004). We found that the magnitude of this effect varied significantly among plots and snow seasons. The low irradiance in plot 2 may explain why the forest there had the weakest effect on melting rate, in agreement with the previous observations of Sicart et al. (2004) and Musselman et al. (2015). Although we did not find significant differences in the magnitude of this effect when comparing the main accumulation and main melting periods, it was greater near the end of the ablation period. This is likely because the level of incoming solar radiation is a function of the time of year (shortwave) and air temperature (longwave) (Lundquist et al., 2013).

In addition, during early summer, the solar angle is higher and the amount of incoming radiation blocked by the forest canopy is therefore greater relative to open areas. This is because of enhanced shading compared to earlier in the season (Lundquist et al., 2013; Schnorbus & Alila, 2013). Thus, towards the end of the snow season, when the irradiance is greater, the enhanced shading was responsible for the greater effect of forest on snow melting (Table 7). It is also worth mentioning that on 26.4% of days with SWE melting we observed higher ablation rates beneath forest canopies than in forest openings. Longwave emission from evergreen conifers, enhanced by warmer temperatures, can increase melting beneath a forest canopy (Davis et al., 1997; Essery et al., 2008; López-Moreno & Stähli, 2008; Lundquist et al., 2013; Sicart et al., 2004). The most common effect of forest that we observed was reduced melting rate, thus suggesting that the effect of shadowing by the forest canopy exceeded the effect of release of longwave radiation from trees. The magnitude of this forest-mediated increase in the melting rate of SWE varied significantly among plots and within years, but not among snow seasons. The forest in plot 4, which had the lowest temperatures, had the weakest effect on SWE melting rate. Lundquist et al. (2013) reported similar observations.

4.4 | Effects of forest canopy on snowpack duration

We observed a shorter duration of snowpack beneath forest canopies (more than 2 weeks on average). This may be explained by forest variations among plots and among snow seasons. Lundquist et al. (2013) reported similar results for regions with warm winters; their average December–January–February temperatures were higher than -1°C, and this value was $-0.63 \pm 0.94^{\circ}$C in our study area. These researchers argued that the forest canopy enhanced longwave radiation and this was the main driver for earlier snow depletion in forested areas, especially during winter. However, we only occasionally observed a forest-mediated increase in the melting rate in our forest stands, as mentioned above. Thus, our observations are consistent with those of Lundquist et al., but only to a limited extent. The shorter duration of snowpacks beneath forest canopies in our study can be mostly explained by the more intense forest-mediated reduction in accumulation (40.3% on average) than on melting (25.1% on average), when considering the overall effect of forest on all days of accumulation and melting together. Dickerson-Lange et al. (2017) also reported a greater effect of forest on accumulation than melting in several mountainous forests of the Pacific Northwest in the United States.

4.5 | Study limitations and future research

We only studies four forest stands over three snow seasons, thus limiting our ability to definitively identify the different roles of climate, topography and forest characteristics on the observed variability in forest–snow interactions. It is difficult to increase the number of study plots when using manual or semi-automated measurements because of the significant manual labour required in the field. Thus, further research is needed to better quantify the influence of these factors on the observed variability of forest–snow interactions. We also experienced technical difficulties when trying to increase the number of locations for measurements of snowpack density during field work by digging snow pits. Because snowpack density has spatial variation, this could contribute to uncertainty in these measurements.

We analysed the effect of forest on the cumulative SWE using two sources of SWE data—SWE daily estimations and spatially distributed SWE measurements. The results from both data sources were similar in magnitude, and indicated similar spatial and temporal variability in the effect of forest on snow. Therefore, our experimental design, which employed intensive field work during 3 years, daily SWE estimations at snow poles, and bi-weekly spatially distributed measurements, confirmed that accurate local data could be representative of a larger area at the plot scale. The combination of such field measurements with spatially distributed modelling of energy and mass balance of snow (Bair, Davis, & Dozier, 2018; Liu et al., 2019) and emerging techniques of measurements based on airborne LIDAR (Laser Imaging Detection and Ranging) or UAVs (Unmanned Aerial Vehicle) (Bühler, Adams, Bösch, & Stoffel, 2016; Currier et al., 2019; Mazzotti et al., 2019; Painter et al., 2016; Webster & Jonas, 2018) will be key to obtaining reliable large-scale results in the future.

5 | CONCLUSIONS

1. We found that forest canopies reduced the duration and cumulative SWE of snowpacks, and increased small-scale spatial

variability relative to forest openings. Forest canopies also reduced the accumulation rate and melting rate of the SWE. In addition, there was a more intense forest-mediated reduction of SWE accumulation than SWE melting and this, in combination with the occasional enhancement of SWE melting, was responsible for the earlier snow depletion beneath forest canopies.

2. Forests had the same general effects on snowpacks in all four of our forest stands and during all three snow seasons. However, the magnitude of these effects varied significantly among the forest stands (despite their proximity) and among different snow seasons. We also observed an intensification during the main period of melting (from the SWE peak to complete snow depletion) for certain forest effects. Thus, the magnitude and timing of the effects of forest on snowpack had significant spatial and temporal variations among plots in the same valley. This finding highlights the need to consider the effects of forests as a source of uncertainty when undertaking research in mountain areas, when designing field experiments and when selecting the location of the experimental site and time span of a study.
3. Our experimental design provided localized daily estimations of SWE and spatially distributed measurements of SWE across each plot every 10–15 days. This approach allowed verification that local data were representative of a larger area at the plot scale.

ACKNOWLEDGEMENTS

This study was supported by the projects: "Bosque, nieve y recursos hídricos en el Pirineo ante el cambio global" funded by Fundación Iberdrola, and IBERNIEVE [CGL2014-52599-P] and HIDROIBERNIEVE [CGL2017-82216-R] funded by the Spanish Ministry of Economy and Competitiveness. A. Sanmiguel-Vallelado and F. Navarro-Serrano were supported by pre-doctoral University Professor Training grants [FPU16/00902, FPU15/00742] funded by the Spanish Ministry of Education, Culture and Sports. E. Alonso-González was supported by a pre-doctoral FPI grant [BES-2015-071466] funded by the Spanish Ministry of Economy and Competitiveness. We thank Dr Maite Gartzia for kindly providing the potential solar radiation data series. We also sincerely thank colleagues, friends and relatives who helped during the field surveys.

DATA AVAILABILITY STATEMENT

The data recorded during this study are available from the corresponding author upon reasonable request.

ORCID

Alba Sanmiguel-Vallelado https://orcid.org/0000-0001-6884-1728

REFERENCES

Bair, E. H., Davis, R. E., & Dozier, J. (2018). Hourly mass and snow energy balance measurements from Mammoth Mountain, CA USA, 2011–2017. *Earth System Science Data*, *10*(1), 549–563. https://doi.org/10.5194/essd-10-549-2018

Barnett, T. P., Adam, J. C., & Lettenmaier, D. P. (2005). Potential impacts of a warming climate on water availability in snow-dominated regions. *Nature*, *438*(7066), 303–309. https://doi.org/10.1038/nature04141

Beniston, M. (2012). Impacts of climatic change on water and associated economic activities in the Swiss Alps. *Journal of Hydrology*, *412–413*, 291–296. https://doi.org/10.1016/j.jhydrol.2010.06.046

Boon, S. (2009). Snow ablation energy balance in a dead forest stand. *Hydrological Processes*, *23*(18), 2600–2610. https://doi.org/10.1002/hyp.7246

Breiman, L. (2001). Random Forests. *Machine Learning*, *45*(1), 5–32.

Bronaugh, D., & Consortium, A. W. (2019). zyp: Zhang + Yue-Pilon Trends Package (Version 0.10-1.1). Available at https://CRAN.R-project.org/package=zyp

Bühler, Y., Adams, M. S., Bösch, R., & Stoffel, A. (2016). Mapping snow depth in alpine terrain with unmanned aerial systems (UASs): Potential and limitations. *The Cryosphere*, *10*(3), 1075–1088. https://doi.org/10.5194/tc-10-1075-2016

Ceballos-Barbancho, A., Morán-Tejeda, E., Luengo-Ugidos, M. Á., & Llorente-Pinto, J. M. (2008). Water resources and environmental change in a Mediterranean environment: The south-west sector of the Duero river basin (Spain). *Journal of Hydrology*, *351*(1), 126–138. https://doi.org/10.1016/j.jhydrol.2007.12.004

Currier, W. R., Pflug, J., Mazzotti, G., Jonas, T., Deems, J. S., Bormann, K. J., … Spaete, L. (2019). Comparing aerial LIDAR observations with terrestrial LIDAR and snow-probe transects from NASA's 2017 SnowEx campaign. *Water Resources Research*, *55*, 6285–6294. https://doi.org/10.1029/2018WR024533

Darwish, T., Shaban, A., Portoghese, I., Vurro, M., Khadra, R., Saqallah, S., … Amacha, N. (2015). Inducing Water Productivity from Snow Cover for Sustainable Water Management in Ibrahim River Basin, Lebanon. *British Journal of Applied Science & Technology*, *5*(3), 233–243. https://doi.org/10.9734/BJAST/2015/13777

Davis, R. E., Hardy, J. P., Ni, W., Woodcock, C., McKenzie, J. C., Jordan, R., & Li, X. (1997). Variation of snow cover ablation in the boreal forest: A sensitivity study on the effects of conifer canopy. *Journal of Geophysical Research: Atmospheres*, *102*(D24), 29389–29395. https://doi.org/10.1029/97JD01335

Dickerson-Lange, S. E., Gersonde, R. F., Hubbart, J. A., Link, T. E., Nolin, A. W., Perry, G. H., … Lundquist, J. D. (2017). Snow disappearance timing is dominated by forest effects on snow accumulation in warm winter climates of the Pacific Northwest, United States. *Hydrological Processes*, *31*(10), 1846–1862. https://doi.org/10.1002/hyp.11144

Duyar, A. (2018). The effects of forest canopy cover and altitude on snow accumulation and melting in the upper watersheds. *Fresenius Environmental Bulletin*, *27*(12), 9642–9649.

El Kenawy, A., López-Moreno, J. I., & Vicente-Serrano, S. M. (2012). Trend and variability of surface air temperature in northeastern Spain (1920–2006): Linkage to atmospheric circulation. *Atmospheric Research*, *106*, 159–180. https://doi.org/10.1016/j.atmosres.2011.12.006

Ellis, C. R. (2011). *Radiation and snowmelt dynamics in mountain forests*. Ph. D. thesis, University of Saskatchewan, Saskatchewan, Canada.

Essery, R., Pomeroy, J., Ellis, C., & Link, T. (2008). Modelling longwave radiation to snow beneath forest canopies using hemispherical photography or linear regression. *Hydrological Processes*, *22*(15), 2788–2800. https://doi.org/10.1002/hyp.6930

Fayad, A., Gascoin, S., Faour, G., López-Moreno, J. I., Drapeau, L., Page, M. L., & Escadafal, R. (2017). Snow hydrology in Mediterranean mountain regions: A review. *Journal of Hydrology*, *551*, 374–396. https://doi.org/10.1016/j.jhydrol.2017.05.063

García-Ruiz, J. M., López-Moreno, J. I., Vicente-Serrano, S. M., Lasanta–Martínez, T., & Beguería, S. (2011). Mediterranean water resources in a global change scenario. *Earth-Science Reviews*, *105*(3), 121–139. https://doi.org/10.1016/j.earscirev.2011.01.006

Garvelmann, J., Pohl, S., & Weiler, M. (2013). From observation to the quantification of snow processes with a time-lapse camera network. *Hydrology and Earth System Sciences*, *17*(4), 1415–1429. https://doi.org/10.5194/hess-17-1415-2013

Gil'ad, D., & Bonne, J. (1990). The snowmelt of Mt. Hermon and its contribution to the sources of the Jordan River. *Journal of Hydrology*, *114*(1), 1–15. https://doi.org/10.1016/0022-1694(90)90072-6

Hardy, J. P., Melloh, R., Robinson, P., & Jordan, R. (2000). Incorporating effects of forest litter in a snow process model. *Hydrological Processes*, *14*(18), 3227–3237. https://doi.org/10.1002/1099-1085(20001230)14:18<3227::AID-HYP198>3.0.CO;2-4

Hedstrom, N. R., & Pomeroy, J. W. (1998). Measurements and modelling of snow interception in the boreal forest. *Hydrological Processes*, *12* (10–11), 1611–1625. https://doi.org/10.1002/(SICI)1099-1085(199808/09)12:10/11<1611::AID-HYP684>3.0.CO;2-4

Huerta, M. L., Molotch, N. P., & McPhee, J. (2019). Snowfall interception in a deciduous Nothofagus forest and implications for spatial snowpack distribution. *Hydrological Processes*, *33*(13), 1818–1834. https://doi.org/10.1002/hyp.13439

Hungerford, R. D., Nemani, R. R., Running, S. W., & Coughlan, J. C. (1989). *MTCLIM: A mountain microclimate simulation model*. Research Paper INT-RP-414. Ogden, UT: U.S. Department of Agriculture, Forest Service, Intermountain Research Station. 52 pp. https://doi.org/10.2737/INT-RP-414

Jenicek, M., Pevna, H., & Matejka, O. (2018). Canopy structure and topography effects on snow distribution at a catchment scale: Application of multivariate approaches. *Journal of Hydrology and Hydromechanics*, *66* (1), 43–54. https://doi.org/10.1515/johh-2017-0027

Jones, H. G., Pomeroy, J. W., Walker, D. A., & Hoham, R. W. (2001). *Snow ecology: An Interdisciplinary examination of snow-covered ecosystems*. Cambridge, UK: Cambridge University Press.

Jost, G., Weiler, M., Gluns, D. R., & Alila, Y. (2007). The influence of forest and topography on snow accumulation and melt at the watershed-scale. *Journal of Hydrology*, *347*(1), 101–115. https://doi.org/10.1016/j.jhydrol.2007.09.006

Keller, H. M., & Strobel, T. (1982). Water and nutrient discharge during snowmelt in subalpine areas. In J. W. Glen (Ed.), *Hydrological aspects of alpine and high-mountain areas*. Wallingford: IAHS Publication IAHS Press; 331–341.

Korhonen, L., Korhonen, K. T., Rautiainen, M., & Stenberg, P. (2006). Estimation of forest canopy cover: a comparison of field measurement techniques. *Silva Fennica*, *40*(4), 577–588. https://doi.org/10.14214/sf.315

Lawler, R. R., & Link, T. E. (2011). Quantification of incoming all-wave radiation in discontinuous forest canopies with application to snowmelt prediction. *Hydrological Processes*, *25*(21), 3322–3331. https://doi.org/10.1002/hyp.8150

Liu, Y., Zhang, P., Nie, L., Xu, J., Lu, X., & Li, S. (2019). Exploration of the snow ablation process in the semiarid region in China by combining site-based measurements and the Utah energy balance model: A case study of the Manas River basin. *Water*, *11*(5), 1058. https://doi.org/10.3390/w11051058

López, R., & Justribó, C. (2010). The hydrological significance of mountains: A regional case study, the Ebro River basin, northeast Iberian Peninsula. *Hydrological Sciences Journal*, *55*(2), 223–233. https://doi.org/10.1080/02626660903546126

López-Moreno, J. I., & García-Ruiz, J. M. (2004). Influence of snow accumulation and snowmelt on streamflow in the central Spanish Pyrenees. *Hydrological Sciences Journal*, *49*(5), 787–802. https://doi.org/10.1623/hysj.49.5.787.55135

López-Moreno, J. I., & Latron, J. (2008a). Spatial heterogeneity in snow water equivalent induced by forest canopy in a mixed beech–fir stand in the Pyrenees. *Annals of Glaciology*, *49*, 83–90. https://doi.org/10.3189/172756408787814951

López-Moreno, J. I., & Latron, J. (2008b). Influence of canopy density on snow distribution in a temperate mountain range. *Hydrological Processes*, *22*(1), 117–126. https://doi.org/10.1002/hyp.6572

López-Moreno, J. I., & Stähli, M. (2008). Statistical analysis of the snow cover variability in a subalpine watershed: Assessing the role of topography and forest interactions. *Journal of Hydrology*, *348*(3), 379–394. https://doi.org/10.1016/j.jhydrol.2007.10.018

López-Moreno, J. I., Vicente-Serrano, S. M., Moran-Tejeda, E., Zabalza, J., Lorenzo-Lacruz, J., & García-Ruiz, J. M. (2010). Impact of climate evolution and land use changes on water yield in the Ebro basin. *Hydrology and Earth System Sciences*, *15*, 311–322. https://doi.org/10.5194/hess-15-311-2011 Discussions, 7(2), 2651–2681. https://doi.org/10.5194/hessd-7-2651-2010

López-Moreno, J. I., Zabalza, J., Vicente-Serrano, S. M., Revuelto, J., Gilaberte, M., Azorin-Molina, C., … Tague, C. (2014). Impact of climate and land use change on water availability and reservoir management: Scenarios in the Upper Aragón River, Spanish Pyrenees. *Science of the Total Environment*, *493*, 1222–1231. https://doi.org/10.1016/j.scitotenv.2013.09.031

Lundberg, A., Nakai, Y., Thunehed, H., & Halldin, S. (2004). Snow accumulation in forests from ground and remote-sensing data. *Hydrological Processes*, *18*(10), 1941–1955. https://doi.org/10.1002/hyp.1459

Lundquist, J. D., Dickerson-Lange, S. E., Lutz, J. A., & Cristea, N. C. (2013). Lower forest density enhances snow retention in regions with warmer winters: A global framework developed from plot-scale observations and modeling: Forests and snow retention. *Water Resources Research*, *49*(10), 6356–6370. https://doi.org/10.1002/wrcr.20504

Marks, D., Kimball, J., Tingey, D., & Link, T. (1998). The sensitivity of snowmelt processes to climate conditions and forest cover during rain-on-snow: A case study of the 1996 Pacific Northwest flood. *Hydrological Processes*, *12*(10–11), 1569–1587. https://doi.org/10.1002/(SICI)1099-1085(199808/09)12:10/11<1569::AID-HYP682>3.0.CO;2-L

Mazzotti, G., Currier, W. R., Deems, J. S., Pflug, J. M., Lundquist, J. D., & Jonas, T. (2019). Revisiting snow cover variability and canopy structure within forest stands: Insights from airborne LIDAR data. *Water Resources Research*, *55*, 6198–6216. https://doi.org/10.1029/2019WR024898

Mellander, P. E., Laudon, H., & Bishop, K. (2005). Modelling variability of snow depths and soil temperatures in Scots pine stands. *Agricultural and Forest Meteorology*, *133*(1), 109–118. https://doi.org/10.1016/j.agrformet.2005.08.008

Moeser, D., Stähli, M., & Jonas, T. (2015). Improved snow interception modeling using canopy parameters derived from airborne LiDAR data. *Water Resources Research*, *51*(7), 5041–5059. https://doi.org/10.1002/2014WR016724

Molotch, N. P., Brooks, P. D., Burns, S. P., Litvak, M., Monson, R. K., McConnell, J. R., & Musselman, K. N. (2009). Ecohydrological controls on snowmelt partitioning in mixed-conifer sub-alpine forests. *Ecohydrology*, *2*(2), 129–142. https://doi.org/10.1002/eco.48

Morán-Tejeda, E., Lorenzo-Lacruz, J., López-Moreno, J. I., Rahman, K., & Beniston, M. (2014). Streamflow timing of mountain rivers in Spain: Recent changes and future projections. *Journal of Hydrology*, *517*, 1114–1127. https://doi.org/10.1016/j.jhydrol.2014.06.053

Musselman, K. N., Molotch, N. P., & Brooks, P. D. (2008). Effects of vegetation on snow accumulation and ablation in a mid-latitude sub-alpine forest. *Hydrological Processes*, *22*(15), 2767–2776. https://doi.org/10.1002/hyp.7050

Musselman, K. N., Pomeroy, J. W., & Link, T. E. (2015). Variability in shortwave irradiance caused by forest gaps: Measurements, modelling, and implications for snow energetics. *Agricultural and Forest Meteorology*, *207*, 69–82. https://doi.org/10.1016/j.agrformet.2015.03.014

N'da, A. B., Bouchaou, L., Reichert, B., Hanich, L., Ait Brahim, Y., Chehbouni, A., … Michelot, J. L. (2016). Isotopic signatures for the assessment of snow water resources in the Moroccan high Atlas mountains: Contribution to surface and groundwater recharge. *Environmental Earth Sciences*, *75*(9), 755. https://doi.org/10.1007/s12665-016-5566-9

Nakai, Y., Sakamoto, T., Terajima, T., Kitamura, K., & Shirai, T. (1999). Energy balance above a boreal coniferous forest: A difference in turbulent fluxes between snow-covered and snow-free canopies. *Hydrological Processes*, *13*(4), 515–529. https://doi.org/10.1002/(SICI)1099-1085(199903)13:4<515::AID-HYP712>3.0.CO;2-J

Painter, T. H., Berisford, D. F., Boardman, J. W., Bormann, K. J., Deems, J. S., Gehrke, F., … Winstral, A. (2016). The Airborne Snow Observatory: Fusion of scanning LIDAR, imaging spectrometer, and physically-based modeling for mapping snow water equivalent and snow albedo. *Remote Sensing of Environment*, *184*, 139–152. https://doi.org/10.1016/j.rse.2016.06.018

Pomeroy, J. W., Marks, D., Link, T., Ellis, C., Hardy, J., Rowlands, A., & Granger, R. (2009). The impact of coniferous forest temperature on incoming longwave radiation to melting snow. *Hydrological Processes*, *23*(17), 2513–2525. https://doi.org/10.1002/hyp.7325

Pomeroy, J., Fang, X., & Ellis, C. (2012). Sensitivity of snowmelt hydrology in Marmot Creek, Alberta, to forest cover disturbance. *Hydrological Processes*, *26*(12), 1891–1904. https://doi.org/10.1002/hyp.9248

Pulliainen, J., Aurela, M., Laurila, T., Aalto, T., Takala, M., Salminen, M., … Vesala, T. (2017). Early snowmelt significantly enhances boreal springtime carbon uptake. *Proceedings of the National Academy of Sciences*, *114*(42), 11081–11086. https://doi.org/10.1073/pnas.1707889114

R Core Team. (2018). *R: A language and environment for statistical computing*. Vienna: R Foundation for Statistical Computing.

Rasband, W. S. (1997). *ImageJ*. Bethesda, MD: US National Institutes of Health.

Revuelto, J., López-Moreno, J. I., Azorin-Molina, C., & Vicente-Serrano, S. M. (2015). Canopy influence on snow depth distribution in a pine stand determined from terrestrial laser data: Canopy influence on snow depth distribution. *Water Resources Research*, *51*(5), 3476–3489. https://doi.org/10.1002/2014WR016496

Revuelto, J., López-Moreno, J. I., Azorin-Molina, C., Alonso-González, E., & Sanmiguel-Vallelado, A. (2016). Small-scale effect of pine stand pruning on snowpack distribution in the Pyrenees Observed with a terrestrial laser scanner. *Forests*, *7*(8), 166. https://doi.org/10.3390/f7080166

Ruiz de la Torre, J., & Ceballos, L. (1979). *Árboles y Arbustos de la España Peninsular*. Madrid: ETSI de Montes. 512 pp. ISBN 84-600-84-600.

Sanmiguel-Vallelado, A., Morán-Tejeda, E., Alonso-González, E., & López-Moreno, J. I. (2017). Effect of snow on mountain river regimes: An example from the Pyrenees. *Frontiers of Earth Science*, *11*(3), 515–530. https://doi.org/10.1007/s11707-016-0630-z

Sartz, R. S. (1972). *Effect of topography on microclimate in southwestern Wisconsin*. USDA Forest Service Research Paper NC-74, North Central Forest Experiment Station, St. Paul, MN.

Schnorbus, M., & Alila, Y. (2013). Peak flow regime changes following forest harvesting in a snow-dominated basin: Effects of harvest area, elevation, and channel connectivity. *Water Resources Research*, *49*(1), 517–535. https://doi.org/10.1029/2012WR011901

Sicart, J. E., Essery, R. L. H., Pomeroy, J. W., Hardy, J., Link, T., & Marks, D. (2004). A sensitivity study of daytime net radiation during snowmelt to forest canopy and atmospheric conditions. *Journal of Hydrometeorology*, *5*(5), 774–784. https://doi.org/10.1175/1525-7541(2004)005<0774:ASSODN>2.0.CO;2

Stähli, M., Jonas, T., & Gustafsson, D. (2009). The role of snow interception in winter-time radiation processes of a coniferous sub-alpine forest. *Hydrological Processes*, *23*(17), 2498–2512. https://doi.org/10.1002/hyp.7180

Stekhoven, D. J. (2013). missForest: Nonparametric missing value imputation using random forest (Version 1.4). https://CRAN.R-project.org/package=missForest

Stekhoven, D. J., & Bühlmann, P. (2012). MissForest – Nonparametric missing value imputation for mixed-type data. *Bioinformatics*, *28*(1), 112–118.

Storck, P. (2000). *Trees, snow and flooding: An investigation of forest canopy effects on snow accumulation and melt at the plot and watershed scales in the Pacific Northwest*. Water Resources Series, Tech. Rep. 161, Department of Civil and Environmental Engineering, University of Washington, 176 pp.

Storck, P., Lettenmaier, D. P., & Bolton, S. M. (2002). Measurement of snow interception and canopy effects on snow accumulation and melt in a mountainous maritime climate, Oregon, United States. *Water Resources Research*, *38*(11), 5-1–5-16. https://doi.org/10.1029/2002WR001281

Talbot, J., Plamondon, A. P., Lévesque, D., Aubé, D., Prévos, M., Chazalmartin, F., & Gnocchini, M. (2006). Relating snow dynamics and balsam fir stand characteristics, Montmorency Forest, Quebec. *Hydrological Processes*, *20*(5), 1187–1199. https://doi.org/10.1002/hyp.5938

Varhola, A., Coops, N. C., Weiler, M., & Moore, R. D. (2010). Forest canopy effects on snow accumulation and ablation: An integrative review of empirical results. *Journal of Hydrology*, *392*(3), 219–233. https://doi.org/10.1016/j.jhydrol.2010.08.009

Veatch, W., Brooks, P. D., Gustafson, J. R., & Molotch, N. P. (2009). Quantifying the effects of forest canopy cover on net snow accumulation at a continental, mid-latitude site. *Ecohydrology*, *2*(2), 115–128. https://doi.org/10.1002/eco.45

Webster, C., & Jonas, T. (2018). Influence of canopy shading and snow coverage on effective albedo in a snow-dominated evergreen needleleaf forest. *Remote Sensing of Environment*, *214*, 48–58.

Winkler, R. D., & Moore, R. D. (2006). Variability in snow accumulation patterns within forest stands on the interior plateau of British Columbia, Canada. *Hydrological Processes*, *20*(17), 3683–3695. https://doi.org/10.1002/hyp.6382

Winkler, R. D., Spittlehouse, D. L., & Golding, D. L. (2005). Measured differences in snow accumulation and melt among clearcut, juvenile, and mature forests in southern British Columbia. *Hydrological Processes*, *19*(1), 51–62. https://doi.org/10.1002/hyp.5757

Yamazaki, T., & Kondo, J. (1992). The snowmelt and heat balance in snow-covered forested areas. *Journal of Applied Meteorology*, *31*(11), 1322–1327. https://doi.org/10.1175/1520-0450(1992)031<1322:TSAHBI>2.0.CO;2

SUPPORTING INFORMATION

Additional supporting information may be found online in the Supporting Information section at the end of this article.

How to cite this article: Sanmiguel-Vallelado A, López-Moreno JI, Morán-Tejeda E, et al. Variable effects of forest canopies on snow processes in a valley of the central Spanish Pyrenees. *Hydrological Processes*. 2020;1–16. https://doi.org/10.1002/hyp.13721

Supporting information

Figure S1. Snow-water equivalent (SWE) at each experimental plot and each snow season in areas beneath forest canopies (F, green lines) and in forest openings (O, blue lines). Confidence intervals: mean ± standard deviation. Source of data: spatially distributed measurements from field surveys.

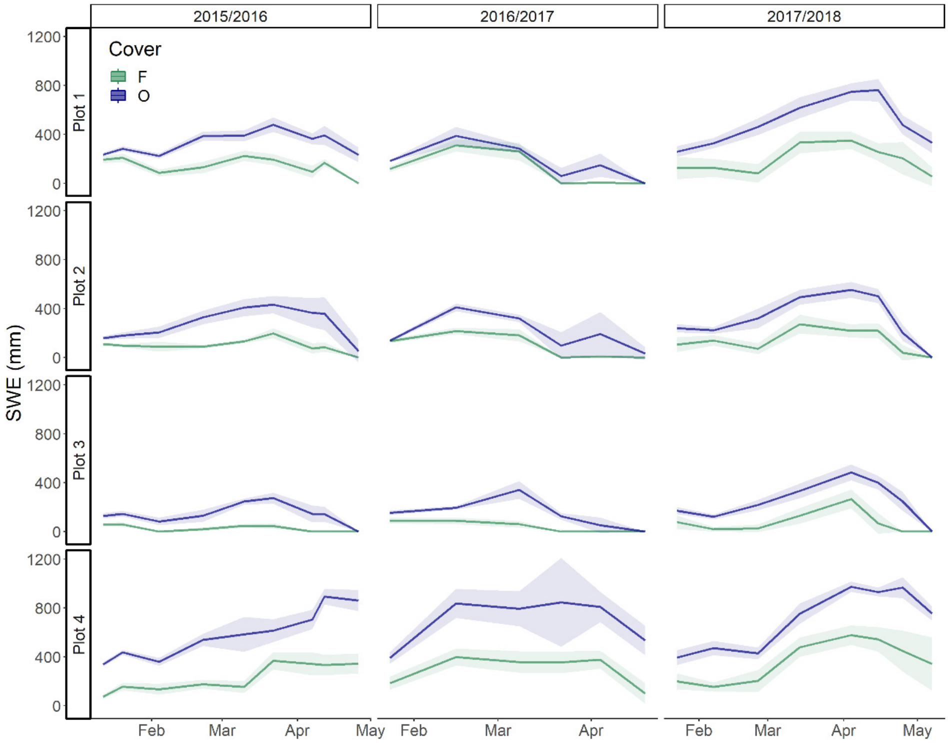

Figure S2. (a) Cumulative SWE in areas beneath forest canopies (F) and in forest openings (O). (b) Reduction of SWE in forested areas. Box indicates 25% and 75% percentiles; central line represents the median; whiskers indicate 1.5×interquartile range (IQR); and points indicate outliers (>1.5×IQR and <3×IQR). Dashed lines: averages of each plot during each snow season. Statistical differences between plots, snow seasons, and covers are indicated by same letters or an asterisk (Wilcoxon test, $p < 0.05$). Source of data: spatially distributed measurements from field surveys.

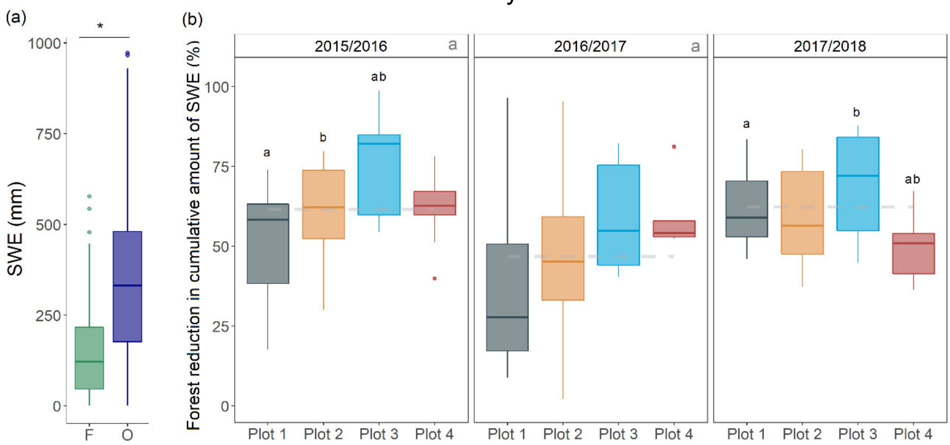

Figure S3. Effect of forest on reducing the rate of accumulation (a) and melting (b). Significant differences among plots and snow seasons are indicated by the same letters (Wilcoxon test, $p < 0.05$). Boxes and dashed lines are as described in Figure S2. Source of data: daily records.

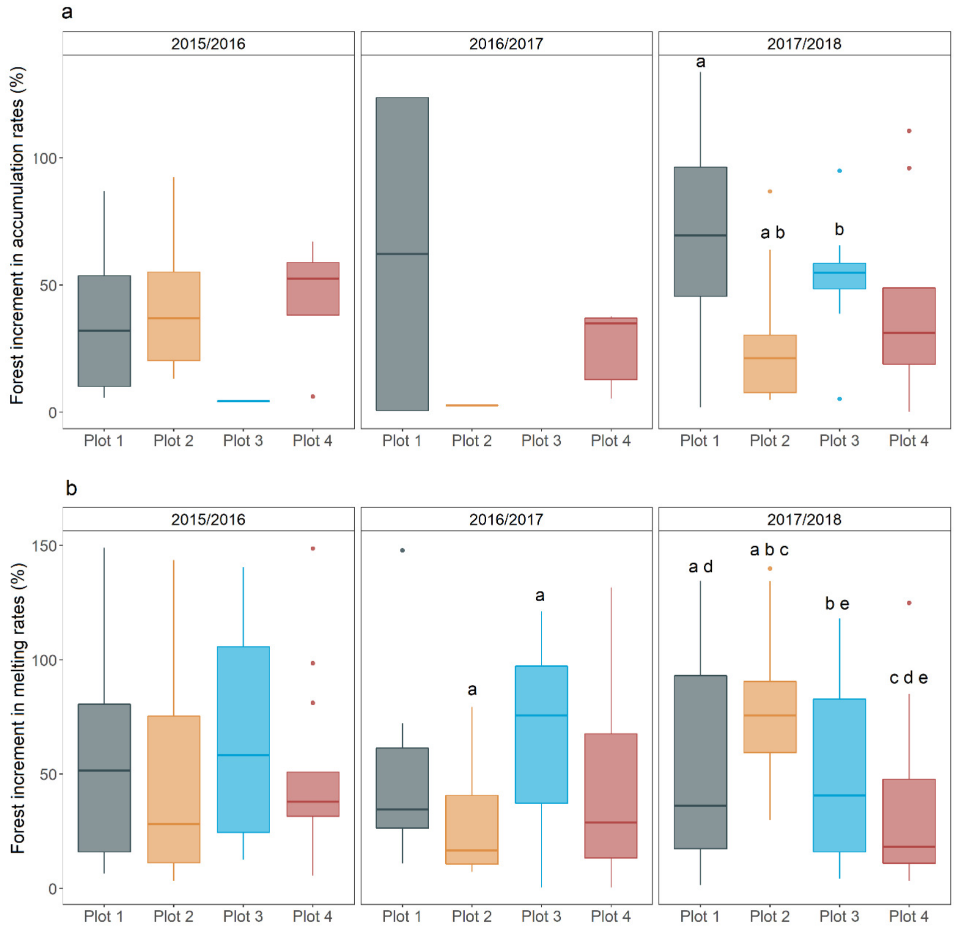

Chapter 4

Detecting snow-related signals in radial growth of *Pinus uncinata* mountain forests

This article was published in:

Sanmiguel-Vallelado, A., Camarero, J. J., Gazol, A., Morán-Tejeda, E., Sangüesa-Barreda, G., Alonso-González, E., Gutiérrez, E., Alla, A. Q., Galván, J. D. & López-Moreno, J. I. (2019). Detecting snow-related signals in radial growth of Pinus uncinata mountain forests. *Dendrochronologia*, *57*, 125622. https://doi.org/10.1016/j.dendro.2019.125622

Authors thank ELSEVIER for the permission to present here the article in its entirely.

Dendrochronologia 57 (2019) 125622

Contents lists available at ScienceDirect

Dendrochronologia

journal homepage: www.elsevier.com/locate/dendro

Detecting snow-related signals in radial growth of *Pinus uncinata* mountain forests

Alba Sanmiguel-Vallelado[a,*], J. Julio Camarero[a], Antonio Gazol[a], Enrique Morán-Tejeda[b], Gabriel Sangüesa-Barreda[c,a], Esteban Alonso-González[a], Emilia Gutiérrez[d], Arben Q. Alla[e], J. Diego Galván[f], Juan Ignacio López-Moreno[a]

[a] *Pyrenean Institute of Ecology, IPE-CSIC, Avda. Montañana 1005, 50059, Zaragoza, Spain*
[b] *Department of Geography, University of the Balearic Islands, Carr. de Valldemossa km 7.5, 07122, Palma de Mallorca, Spain*
[c] *Área de Botánica, Departamento de Ciencias Agroforestales, EiFAB, iuFOR-Universidad de Valladolid, Campus Duques de Soria, 42004, Soria, Spain*
[d] *Dept. Biologia Evolutiva, Ecologia i Ciències Ambientals, Univ. Barcelona, Av. Diagonal 643, 08028, Barcelona, Spain*
[e] *Fakulteti i Shkencave Pyjore, Universiteti Bujqësor i Tiranës, 1029, Tirana, Albania*
[f] *Ionplus AG. Lerzenstrasse 12, 8953, Dietikon, Switzerland*

ARTICLE INFO

Keywords:
Dendroecology
Tree-ring width
Snowpack
Subalpine forests
Pyrenees

ABSTRACT

Climate warming is responsible for observed reduction in snowpack depth and an earlier and faster melt-out in many mountains of the Northern Hemisphere. Such changes in mountain hydroclimate could negatively affect productivity and tree growth in high-elevation forests, but few studies have investigated how and where recent warming trends and changes in snow cover influence forest growth. A network comprising 36 high-elevation *Pinus uncinata* forests was sampled in the NE Iberian Peninsula, mainly across the Spanish Pyrenees, using dendrochronology to relate tree radial growth to a detailed air temperature and snow depth data. Radial growth was negatively influenced by a longer winter snow season and a higher late-spring snowpack depth. Notably, the effect of snow on tree growth was found regardless the widely reported positive effect of growing-season air temperatures on *P. uncinata* growth. No positive influence of moisture from spring snowmelt on annual growth of *P. uncinata* was detected in sampled forests. Tall trees showed a lower growth responsiveness to snow than small trees. Decreasing trends in winter and spring snow depths were detected at most Pyrenean forests, suggesting that the growth of high-elevation *P. uncinata* forests can beneficiate for a shallower and of shorter duration snowpack associated with warmer conditions. However, water-limited sites located on steep slopes or on rocky substrates, with poor soil-water holding capacity, could experience drought stress because of early depleted snow-related soil moisture.

1. Introduction

Mountain forests are particularly susceptible to climatic variation because low temperatures typically limit radial growth and productivity near the uppermost edge of tree distribution ranges (Körner, 2012). Recent warming trends have induced shifts in tree recruitment (Smithers et al., 2018; Sangüesa-Barreda et al., 2018) and have enhanced radial growth (Innes, 1991; Tardif et al., 2003; Camarero et al., 2015a; Zhuang et al., 2017), excepting few sites were warming have induced some drought stress (Camarero et al., 2015c; Galvön et al., 2015). Most studies have focused on the direct effects of rising temperatures on tree growth (e.g. Del Barrio et al., 1990; Gutiérrez, 1991; Tardif et al., 2003; Andreu et al., 2007; Galván et al., 2014; Camarero et al., 2017; Franke et al., 2017; D'Orangeville et al., 2018; Sanchez-Salguero et al., 2018; Wang et al., 2019). Research focused on the indirect effects of climate warming, such as the influence of snow dynamics on forest productivity, is still scarce (Vaganov et al., 1999; Kirdyanov et al., 2003; Helama et al., 2013; Watson and Luckman, 2016; Carlson et al., 2017).

Snow accumulation requires a combination of precipitation and low temperatures to initiate snowfall and persistent below-zero temperatures to sustain the snowpack (Beniston et al., 2011; López-Moreno et al., 2011). Due to the high sensitivity of snow cover to seasonal temperatures (Morán-Tejeda et al., 2013a), a warmer climate can easily impact the process of snow accumulation/melting (Beniston, 2003). An increase in winter temperature leads to a precipitation shift from snow

* Corresponding author.
E-mail address: albasv@ipe.csic.es (A. Sanmiguel-Vallelado).

https://doi.org/10.1016/j.dendro.2019.125622
Received 26 February 2019; Received in revised form 30 May 2019; Accepted 30 July 2019
Available online 03 August 2019
1125-7865/

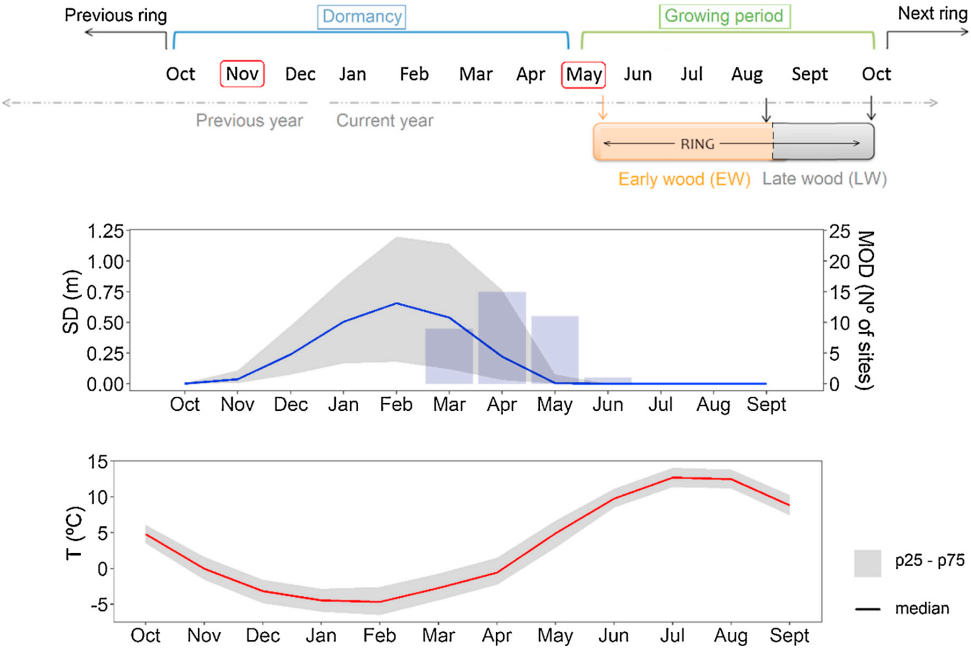

Fig. 1. Top panel: Timing of *P. uncinata* tree-ring formation based on Camarero et al. (1998). Red boxes indicate the most influencing months to *P. uncinata* radial growth by temperature (Tardif et al., 2003; Galván et al., 2014). Bottom panels: monthly median snow depth (SD, blue line), melt-out date frequency (MOD, bars) and monthly median temperature (T, red line) of sampled sites in NE Iberian Peninsula from 1980 to 2009 hydrological years. Shaded areas show the 25–75 percentile ranks.

towards rain, and warmer spring conditions induce earlier and faster snowpack melting (Morán-Tejeda et al., 2014). Reduced snowpack depth and duration have been reported in the main mid-latitude mountain ranges (López-Moreno, 2005; Marty, 2008; McCabe and Wolock, 2009; Beniston, 2012; Morán-Tejeda et al., 2013a) including Mediterranean (drought-prone) areas such as the Pyrenees (Morán-Tejeda et al., 2017).

Snow dynamics may influence forest growth (e.g., Kirdyanov et al., 2003). Early snowfalls in the autumn may shorten the growing season and lead to a reduction in the assimilation of carbohydrates, and this can negatively affect growth in the following year (Carlson et al., 2017). A lack of snow cover during the winter can cause premature yellowing and shedding of needles of shrubby krummholz individuals during cold and dry winters and repeated freeze-thaw cycles (winter drought), reducing growth in the following spring (Helama et al., 2013; Camarero et al., 2015b). Larger snow accumulation and a longer snowmelt period may negatively affect tree radial growth by slowing the increase of soil temperature, delaying the growing period, and thus shortening the growing season (Vaganov et al., 1999; Kirdyanov et al., 2003; Watson and Luckman, 2016). On the other hand, snowmelt effects on soil moisture have been reported to positively influence tree growth during the next growing season (St. George, 2014; Watson and Luckman, 2016). All these observations suggest that the radial growth of trees can be related to winter snowpack, melt-out date and spring snow depth.

In the main mountains of the NE Iberian Peninsula (Pyrenees, Pre-Pyrenees, Iberian System), increasing trends in mean temperatures and an increment in precipitation variability have been observed during the second half of the 20th century (López-Moreno et al., 2010; El Kenawy et al., 2011). Such consequent water stress increase may also limit tree growth in high-elevation forests (Tardif et al., 2003; Andreu et al., 2007). Nevertheless, high-elevation mountain pine (*Pinus uncinata*) forests and treelines are forecasted to show enhanced growth during the late 21st century due to a longer and warmer growing season (Sánchez-Salguero et al., 2012; Camarero et al., 2017). Climate warming has also affected mountain hydrology and influences the accumulation, duration and melt-out of snow, leading to a shallow snowpack or a longer snow-free season (Morán-Tejeda et al., 2013a, 2013b). Discerning how and where snow dynamics affects forest growth may help us understand future responses of mountain forests to forecasted hydroclimatic change.

The main hypothesis of the present study is that snowpack depth and duration influence radial growth of high-elevation *P. uncinata* forests. It was expected that snow cover affects tree radial growth, in addition to the widely reported temperature effects on growth (Gutiérrez, 1991; Rolland and Schueller, 1994; Camarero et al., 1998). It was also expected that there would be greater impact of snowpack depth and duration on growth in high-elevation forests with a shorter growing season, since elevation indirectly controls the effects of climate on *P. uncinata* growth by modifying growing season air temperature (Tardif et al., 2003; Galván et al., 2014). These hypotheses were tested by analyzing the radial growth of a *P. uncinata* dendrochronological network in the main mountain ranges of NE Iberia in relation to snow cover conditions at site level. The specific objectives of the present study were: (1) to evaluate the associations between snow conditions and radial-growth variability of *P. uncinata* forests; (2) to explore the influence of biogeographical patterns and tree characteristics on tree growth responses to snow depth; and (3) to estimate and compare the temporal evolution of radial growth and snow trends for the 1980–2010 period.

2. Materials and methods

2.1. Study species

The mountain pine (*Pinus uncinata* Ram.) is a long-lasting and light-demanding conifer, which shows a wide ecological tolerance regarding

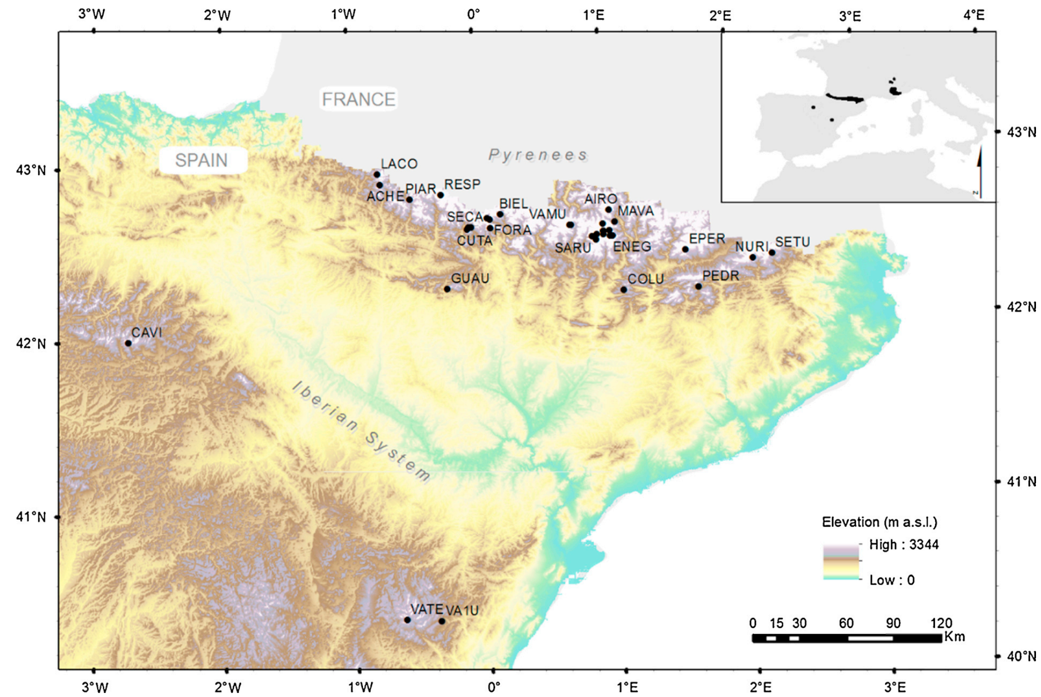

Fig. 2. Map of sampled mountain *P. uncinata* sites in NE Iberian Peninsula (black dots, see sites' codes in Table S1) and distribution of the study species in Europe (inset, top right).

topography (slope, aspect, elevation) and soil type (Cantegrel, 1983) and forms high-elevation forests. The natural habitat of *P. uncinata* includes central and southwest European mountains, while its southern geographical limit is reached in the Iberian System (Spain). It is dominant in the subalpine belt of the central and eastern Pyrenees (1800–2500 m a.s.l.). Its growing season starts at the end of May and ends in October, with major growth rates occurring from the end of May to July (Camarero et al., 1998). Warm autumn and spring temperatures before and during tree-ring formation enhance *P. uncinata* radial growth, whereas summer precipitation during the growing season is the main positive climate driver of growth in certain xeric sites located in the Pre-Pyrenees and southern Iberian System (Gutiérrez, 1991; Camarero et al., 1998; Tardif et al., 2003; Andreu et al., 2007; Galván et al., 2014). The timing of *P. uncinata* tree-ring formation is schematized in Fig. 1.

2.2. Study sites

The 36 studied forests are located in the main mountain ranges of the NE Iberian Peninsula (Fig. 2): 33 are located in the Pyrenees, (3 of them in the Pre-Pyrenees, the Pyrenees' foothills), and the other 3 sites are located in the Iberian System. Two of the sites sampled in the southern Iberian system (VATE, VA1U) constitute the southernmost distribution limit of the species in Europe. Sampled sites cover the whole geographical distribution of the species in the Iberian Peninsula. The elevation of the sampled sites ranges from 1750 to 2451 m a.s.l. and the mean slope of the terrain is $35^{\circ} \pm 16^{\circ}$ (see Table S1 in the Supplementary Material). Mean diameter at breast height (dbh) measured at 1.3 m of sampled trees is 66 ± 7 cm, and their age is 334 ± 108 years on average (Table S1).

The location of the Pyrenees, between the Atlantic Ocean on the west side and the Mediterranean Sea in the east, causes a fast climatic transition, while the Central Pyrenees shows a greater continental influence (Del Barrio et al., 1990). In the western areas, most of the annual precipitation falls during the cold winter season, whereas precipitation falls mainly during spring and autumn in the east (Del Barrio et al., 1990). Air temperature changes depend on elevation with -5.17 °C km^{-1} being the mean temperature lapse rate across the Pyrenees (Navarro-Serrano et al., 2018). The annual 0 °C isotherm is located at 2900 m a.s.l. (Del Barrio et al., 1990), whereas it falls to 1600 m a.s.l. between December and April, establishing the lower limit of the seasonal snowpack (López-Moreno et al., 2011). Snow accumulation also shows a correlation to Atlantic–Mediterranean proximity and distance from the main divide of the mountain range (Revuelto et al., 2012). Monthly mean values of temperature, snow depth and melt-out date from1980 to 2009 hydrological years for all sampled sites are presented in Fig. 1.

2.3. Dendrochronological data

Dendrochronological data correspond to an updating of data from 36 forests sampled and published by Galván et al. (2012, 2014). Wood samples were collected between 1994 and 2010 from 5 to 65 dominant individual trees of different sizes and ages, randomly selected in each site. From each tree, two or three cores were taken at 1.3 m height with Pressler increment borers. The sapwood length was measured in the field, and topographic (elevation, slope and aspect) and biometric (dbh and tree height) variables were also recorded for each individual tree.

Wood samples were air dried and sanded until tree-ring boundaries were clearly visible. Then, they were visually cross-dated and measured at 0.01 mm resolution using a LINTAB measuring device (Rinntech, Heidelberg, Germany). Cross-dating quality was checked using the program COFECHA (Holmes, 1983) by comparing the individual ring-width series among coexisting trees of the same species. Finally, cross-dated tree-ring width (RWL) series were obtained.

Dimensionless ring-width indices (RWI) series were obtained by removing age or size trends and temporal autocorrelation to reflect growth response to climate. Residual RWIs were obtained by removing long-term trends of ring-width data fitting negative linear functions, followed by 30-year cubic smoothing splines, and then by eliminating the first-order autocorrelation of the resulting residuals using the software ARSTAN V. 44 (Cook, 1985). A bi-weight robust mean was then computed to obtain residual or pre-whitened chronologies (mean site series) for each site, which were used in subsequent analyses.

2.4. Climatic and snow data

Daily snow depth (SD) and temperature data (T) for the studied sites were extracted from a gridded meteorological dataset obtained by simulation from Weather Research and Forecasting (WRF; Skamarock et al., 2008) model. The WRF model was driven by ERA-Interim (Berrisford et al., 2011) reanalysis and coupled offline with Factorial Snow Model (FSM 1.0; Essery, 2015), a physically based energy and mass balance snow model. WRF outputs were projected to the target elevation, using hygrobarometric formulas and lapse rates and the new projected meteorological information as driving data of FSM. The methodology to develop the snow dataset and its validation is shown in Alonso-González et al. (2018).

Several annual snow indices were created from the daily snow data as indicators of specific snow conditions all year round, based on Fig. 1:

- Average November snow depth (Nov SD) as previous autumn snow conditions indicator.
- Average February snow depth (Feb SD) as winter snow conditions indicator.
- Average May snow depth (May SD) as spring snow conditions indicator.

The selection of these monthly SD values for representing snow seasonal conditions is based on the cumulative nature of snow. Thus, the snow depth value at the end of the season will be representative of the accumulated snow and the meteorological conditions of the previous months (e.g. López-Moreno, 2005; Morán-Tejeda et al., 2016). Snow indices were not highly correlated with each other, showing an average coefficient of correlation lower than $r_s = 0.55$ (Spearman Rho). Variables were detrended prior to the correlation analyses. Correlation coefficients (r_s) were: 0.48 for Nov SD–Feb SD, 0.33 for Nov SD–May SD and 0.54 for Feb SD–May SD.

Given that snow depth conditions of a given month are highly influenced by the temperature of previous months, the following monthly aggregations (averages) of temperature data were computed for statistical analyses: November mean temperature (Nov T), February mean temperature (Feb T), November-December-January-February mean temperature (Nov-Feb T), December-January-February mean temperature (Dec-Feb T), January-February mean temperature (Jan-Feb T), May mean temperature (May T), March-April-May mean temperature (Mar-May T), April-May mean temperature (Apr-May T).

2.5. Statistical analyses

We searched for snowpack effects on subsequent tree-ring development, considering the period from November (previous to tree-ring formation) to May, based on snow cover presence at the sampled forests (Fig. 1).

The growing-season air temperature is a major and widely reported determinant of *P. uncinata* growth (Gutiérrez, 1991; Rolland and Schueller, 1994; Camarero et al., 1998; Tardif et al., 2003; Andreu et al., 2007; Galván et al., 2014). However, temperature also determines the large variability of snowpack among elevations (López-Moreno, 2005; Morán-Tejeda et al., 2013b). Because the aim was to control the temperature effect on growth (RWI) and infer the pure effect of snow, the computed snow indices from the influence of temperature were isolated. This was done by considering the aforementioned snow depth and temperature indices as predictors of RWI by means of stepwise linear regressions. First, Spearman non-parametric correlations (r_s) were computed between the snow depth indices (Nov SD, Feb SD, May SD) and the whole set of temperature monthly aggregations. Temperature aggregations that best correlated with snow indices were November T, Jan-Feb T and Mar-May T for Nov SD, Feb SD and May SD (See Supplementary Material Table S2). These best-correlated temperature aggregations, together with mean May temperature, because its influence on tree growth is widely reported as the most important (e.g., Tardif et al., 2003) and the snow depth indices were then used as predictors in the stepwise linear models (Eq. 1). The stepwise model allows introduction of variables that substantially improve the model by rejecting those that may be redundant. This prevents greatly autocorrelated variables from being included in the model and allowed us to infer whether the snow depth indices or temperature indices were the best predictors of RWI. Linear models were performed individually for each site, as well as a regional model for the whole set of sites. The models can be formulated as follows:

$$y = \beta_0 + \beta_1 x_1 + \beta_2 x_2 + \cdots + \beta_n x_n + \varepsilon \qquad (1)$$

where, y is the response variable (i.e. RWI values), β_0 is the intercept, x_1 to x_n are the predictors (i.e., snow depth and temperature indices), β_1 to β_n are the estimated partial regression coefficients and ε is the error. The models were compared using the Akaike Information Criterion (AIC) value; the smaller the AIC, the better the fit (most parsimonious model) since it penalizes complex models (Burnham and Anderson, 2003). Only the best model for each site and the one run for the whole set of sites are shown in the results, including the following information: the explained variance (adjusted R^2), the statistical significance (p) and the partial coefficients of the regressions. Automated model selection was performed with the MuMIn package (Barton and Barton, 2018) of the R language version 3.1.0 (R Core Team, 2014).

Additionally, partial correlations using the Spearman coefficient were calculated between RWI and SD indices by partially removing the effects of temperature (Table S2). Non-parametric methods were used, since not all analyzed variables had normal distributions (Shapiro–Wilk test, $p < 0.05$). Snow and temperature variables were previously detrended.

Variations of tree growth responses to snow conditions along biogeographical gradients for a subset of sites where a snow index was the best predictor in the aforementioned stepwise models were investigated. The following variables were considered: latitude, longitude, slope, elevation of the terrain, dbh, tree height, sapwood and tree age (Table S1), and annual maximum snow depth (Max SD) (as an indicator of site differences in snow accumulation). Statistically significant different responses among groups of sites whose models selected the same best predictor using the non-parametric Kruskal-Wallis test were identified along gradients. Non-parametric Spearman correlations were calculated, considering the amount of radial growth variance explained by snow variables (adjusted R^2 from the stepwise models) as the dependent variable and biogeographical gradients as independent variables. Complementary correlation analyses were done using partial correlation coefficients between tree growth and snow depth as dependent variables (in Supplementary Material Fig. S3).

Trend analysis for tree-ring width (RWL series) as well as for snow indices was performed using the Mann-Kendall test and Theil-Sen's slope estimator for computing the magnitude of the trend, considering a subset of sites where any snow – growth significant relationship was previously found. Trend analysis was carried out using the zyp package in R language (Bronaugh et al., 2009), which includes a trend-free pre-whitening method for removing serial autocorrelation.

RWI and RWL series were shorter than the snow series at some sites. Thus, all analyses were performed for the longest common period available, for example, from 1981 to last formed tree-ring measured

Table 1
Statistical parameters of stepwise linear models between radial growth (response variable RWI) and snow and temperature indices (predictors) in each site, for all sites (All sites), and for all statistically significant sites (Sig sites). See sites codes in Table S1 and Fig. 2.

Site	N	Coefficients								Adjusted R^2	p
		Intercept	Nov SD	Feb SD	May SD	Nov T	May T	Jan-Feb T	Mar-May T		
ACHE*	30	0.99			**−0.15**					0.11	0.041
AIRO*	16	1.00			**−0.16**			0.04		0.50	0.019
BIEL*	16	1.01			**−4.30**					0.20	0.046
BLLA	30	0.99					0.03	**0.03**		0.25	0.098
CAVI	30	1.01	**−0.36**	−0.07		0.02				0.16	0.090
COLU	30									–	
CONU*	14	0.99	**−0.77**	−0.11	−0.56				−0.08	0.81	0.001
CORT	30	1.00			**−1.80**					0.08	0.072
CUTA	17	1.00				**−0.03**				0.17	0.058
EAMI*	29	1.00			**−0.55**					0.23	0.005
EGER*	30	0.99			**−0.17**			0.02		0.21	0.019
ELLA	29									–	
ENEG*	29	0.99			**−0.32**	−0.02				0.26	0.006
EPER*	17	0.99						**0.07**		0.44	0.002
FORA	29									–	
GUAU	30									–	
LACO	19									–	
LEST	13	1.00		**−0.29**						0.18	0.084
MAVA*	17	1.00						**0.09**		0.29	0.016
MIRA	29	1.00							**0.05**	0.10	0.055
MIRE*	18	0.99		**−0.18**						0.19	0.041
MONE	29	1.00		−0.08	**−1.36**					0.19	0.082
NURI*	21	0.99				−0.03		**0.05**		0.42	0.005
PEDR	26	1.00						**0.03**		0.10	0.063
PIAR	14	1.01						**0.04**		0.21	0.059
RATE	29	0.99	**0.76**							0.06	0.109
RESP	30	1.00			**−0.04**					0.08	0.071
SAMA*	16	0.98						**0.08**		0.20	0.047
SARU*	15	1.00		**−0.27**						0.25	0.034
SECA	29									–	
SETU	19									–	
SOBR	29									–	
TESO*	15	0.97						**0.08**		0.28	0.024
VA1U*	26	1.00	1.77		**−2.83**					0.17	0.030
VAMU*	14	1.02		**−0.23**						0.35	0.015
VATE*	26	0.99							**0.08**	0.15	0.028
All sites	–	0.99	**0.08**		−0.03	−0.01	0.01	0.01	−0.01	0.05	0.00
Sig sites	–	0.99			**−0.13**	−0.01	0.02	0.01	−0.01	0.13	0.00

N: data series length starting from 1981 (years). Statistically significant sites (model $p < 0.05$) are followed by*. The best predictor for each model (site) is indicated in bold characters. Hyphen indicates null models (any significant predictor).

(number of available years for each one is indicated in Table S1).

3. Results

3.1. Growth responses to snow variables

Stepwise linear models (Table 1) pointed out snow indices as main predictors of *P. uncinata* radial growth in 47% of sites (17 out of 36 sites; with 11 out of the 17 showing a statistically significant model). These 17 sites (Fig. 3) were selected and used in later analyses. Average explained variance by models in these sites was 24% (30% for statistically significant models). The site in which predictors explained the larger variance of RWI was CONU (adjusted $R^2 = 0.81$; Table 1). May SD was the best predictor in 64% of sites where snow indices were the most important predictors and their models were statistically significant (Fig. 4). It was followed by Feb SD (selected in 27% of these sites) and Nov SD (only selected in one of these 11 sites). All snow indices negatively influenced radial growth (RWI) in all sites, except for Nov SD, which positively influenced tree radial growth in VA1U site.

In total, 17% of statistically significant models (6 out of 36 sites) pointed out temperature indices as main predictors of *P. uncinata* radial growth. Jan-Feb T was selected as the best predictor of RWI in 5 out of 6 of these sites, and Mar–May T was selected in only one site.

For the regional model, which takes into account all of the 36 site-chronologies combined (Table 1, bottom), Nov SD was selected as the most important predictor (despite it only explained 5% of the total variance). When a subset of statistically significant sites was included in the general model, May SD was the most important predictor again explaining 13% of the total growth variance.

Complementary to stepwise linear models, partial correlations also noted the prevalence of Feb SD, with respect to the other two snow indices, in terms of influencing radial growth of *P. uncinata* (Table S3 and Fig. S1, Supplementary Material). Most sites (67%) showed a Feb SD negative influence on radial growth (mean $r_s = -0.34$; SD = 0.18), being five of them statistically significant. For May SD, one site showed statistically significant partial correlation with radial growth.

3.2. Influence of biogeographical patterns and tree characteristics on growth responses to snow depth

Tree characteristics determined the response of growth to snow (Fig. 5a). The presence of small trees strengthen the linkage between snow and growth in sites where a snow index was the main driver of RWI ($r_s = -0.61, p = 0.03$) (Fig. 5b). It was observed that sites where a snow index was the statistically significant main driver of *P. uncinata* radial growth were mostly located in the Pyrenees (at western and central area of this mountain range), with the exception of one forest stand located in the southern Iberian System (VA1U) (Fig. S2). May SD

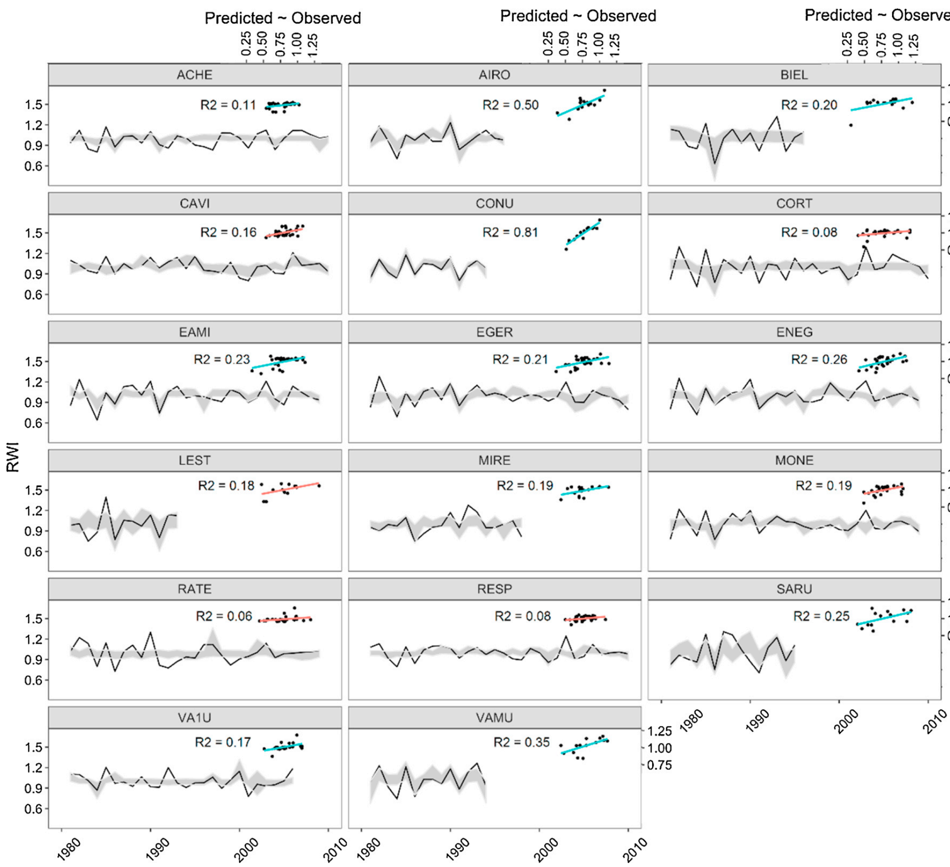

Fig. 3. Tree-ring width indices (RWI, lines) and confidence intervals (shaded areas) stepwise linear models for selected sites. Scatter plots show correlatios between observed and RWI values (right y-axes) predicted by the model (adjusted R^2), and its statistical significance (red: not significant; blue: significant, $p < 0.05$).

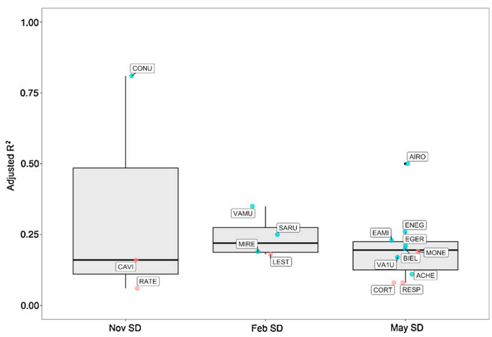

Fig. 4. Tree-growth variance (adjusted R^2) explained by stepwise linear models for selected sites. Values are displayed aggregated by best model predictor (snow indices only). Sites related to each model are labelled. Statistical significance of models is represented in red ($p > 0.05$) and blue ($p < 0.05$) colors. See sites codes in Table S1 and Fig. 2.

was the main RWI predictor across the Pyrenees and also in the southern Iberian System site.

Additional biogeographical analyses based on growth-snow partial correlations showed that greater and statistically significant negative snow influence on tree growth was found in high-elevation sites (Nov SD index) and sites with bigger tree dbh (Feb SD index) (Fig. S3).

3.3. Tree radial growth and snow indices trend analysis

Five of thirteen forests presented statistically significant RWL trends, only one of them showed a positive slope for RWL trend while all the others showed a negative slope (Fig. 6b; Fig. S4). There were found statistically significant trends for May SD and Feb SD variables, in 35% and 12% of sites where snow index was the main driver of *P. uncinata* radial growth respectively, but nor for Nov SD. All these statistically significant snow trends show negative slopes.

A statistically significant correlation was found between growth trends (RWL) and snow (Feb SD) trends ($r_s = -0.68$; $p = 0.01$) (Fig. 6a). From the regional perspective, only in the Pyrenees there were found statistically significant trends in snow variables (all of them with negative coefficients as mentioned above).

4. Discussion

There is evidence that previous snow cover conditions influence *P. uncinata* tree-ring formation, in addition to the widely reported growing season air temperature effects, as hypothesized. The used methodology allowed us to infer the pure effect of snow on tree-ring growth by controlling the temperature influence on snowpack evolution. First, the most correlated monthly temperature aggregations to snow indices

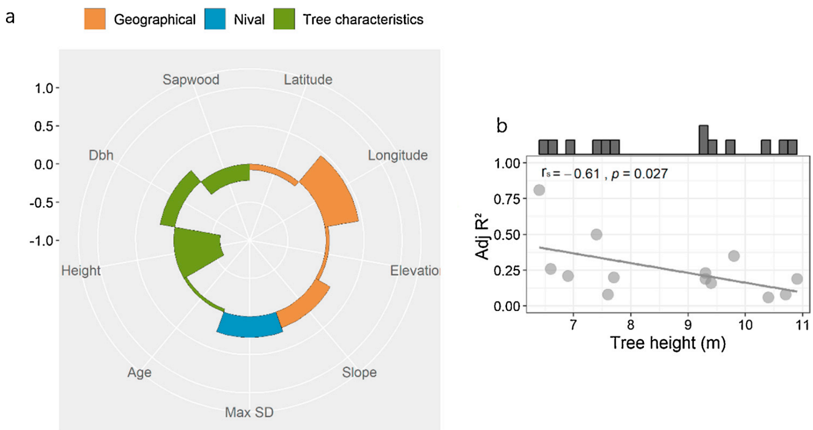

Fig. 5. (a) Effects of geographical, nival gradients and tree influences on growth-snow variance (adjusted R^2) established by Spearman correlations (r_s). The southern Iberian System sites were omitted in latitude analyses. (b) Scatterplot of single obtained statistically significant correlation between growth-snow variance and biogeographical gradients (tree height) ($p < 0.05$). Histograms show sites frequency of distribution along this gradient.

were detected (Table S2), including other key temperature indices (May T) for *P. uncinata* growth; second, both temperature and snow indices were taken into account as predictors in radial growth stepwise linear models and by using partial correlations as complementary analyses. Similar procedures were used in Carlson et al. (2017) and Helama et al. (2013). Results provide additional information about the effects of climate on high-elevation *P. uncinata* radial growth. Previous studies showed that radial growth of *P. uncinata* was mainly limited by growing-season air temperature (Rolland and Schueller, 1994; Camarero et al., 1998; Tardif et al., 2003; Andreu et al., 2007; Galván et al., 2014) and, only in certain drought-prone sites, by low early summer precipitation (Andreu et al., 2007; Galván et al., 2014).

The influence of snow cover on radial growth had not been researched for *P. uncinata*, but it has been researched for other species of Pinaceae (Walsh et al., 1994; Kirdyanov et al., 2003; Helama et al., 2013; Watson and Luckman, 2016; Carlson et al., 2017; Franke et al., 2017; Appleton and George S., 2018; Fkiri et al., 2018; Legendre-Fixx et al., 2018; Truettner et al., 2018). In this study, almost half the sampled forests in the main mountain ranges of the NE Iberian Peninsula showed certain snow-growth interaction (most of them were statistically significant).

The date of cambial initiation is a key factor for climate-growth associations. This date is related to the date when snowmelt occurs (Kirdyanov et al., 2003) and, consequently, with snow accumulation throughout the winter. The presence of abundant snowpack in late spring may induce a late melt-out and, as a result, a delay in the onset of the *P. uncinata* growing season because the persistent snow cover may cool the soil (Kirdyanov et al., 2003; Helama et al., 2013). This would explain the dominant negative spring snow (May SD index) influence on *P. uncinata* annual growth found in this study (Table 1, Fig. 4). In

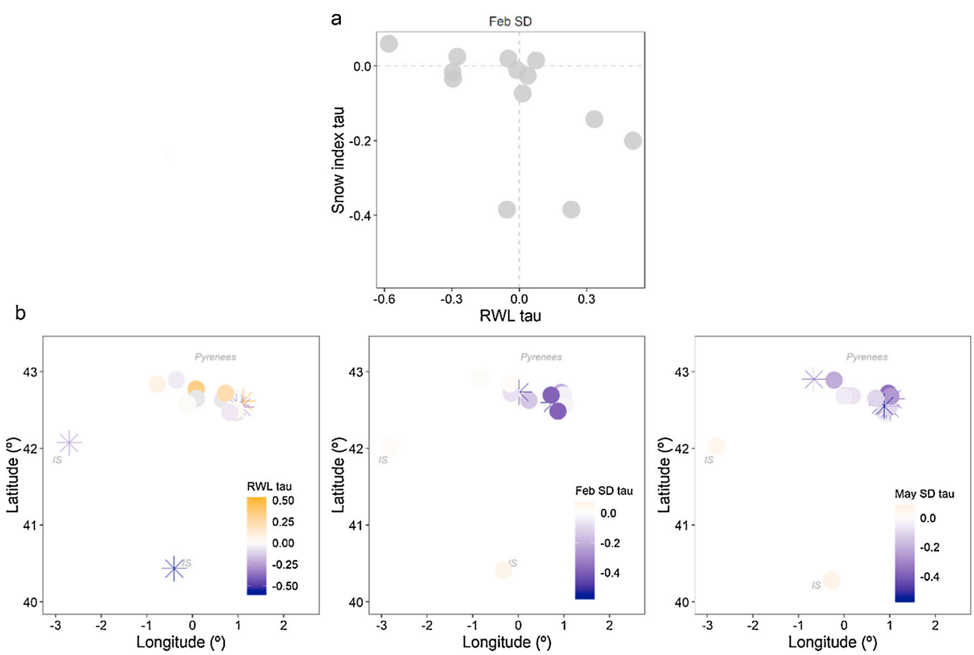

Fig. 6. (a) Mann-Kendall linear trends (tau) for tree-ring width (RWL) and Feb SD snow index of selected sites from 1981 to last year with data (see series' lengths in Table S1) and (b) geographical representation of trend analyses results. Pyrenees and Iberian System (IS) locations are indicated.

this regard, Franke et al. (2017) reported that the average monthly snow cover during the current year's May correlated negatively with *P. sylvestris* chronologies. Likewise, northern conifers showed delayed cambial activity when snow melt was delayed in the beginning of the growing season (Vaganov et al., 1999; Kirdyanov et al., 2003). Previous studies of *P. uncinata* have demonstrated that this pine species is negatively affected by the preceding growing-season low air temperatures because the onset of cambial activity is triggered by a typical rise in temperature during spring (Tardif et al., 2003; Galván et al., 2014). Since no positive relation was found between May SD snow index and RWI series in the performed models, we cannot report that moisture from spring snowmelt promotes annual growth of *P. uncinata* in sampled forests. The positive influence of snow on tree growth, explained by a moisture-limitation, widely reported in more arid places as well as in large snow accumulation areas (St. George, 2014; Watson and Luckman, 2016; Carlson et al., 2017), was not detected in the few possible drought-prone sites (Pre-Pyrenees and southern Iberian System) sampled in this study. Winter precipitation is less likely to contribute to the soil moisture reservoir used by trees during the following growing season if spring precipitation is abundant and shows low year-to-year variability as is the case. Spring rainfalls would introduce an extra source of water that would sum up to the water from snowmelt, and thus, the positive influence of snow on tree growth based on moisture-limitation was not detected.

As discussed above, large winter snow accumulation likely produces larger snow presence in spring and this, in turn, causes a delayed meltout. It is not easy to isolate the impact of winter snow on radial growth, compared to that of late spring snow, because they both are related; however, we did observe that May SD was selected 60% more than Feb SD as best predictor of RWI in the performed models (Table 1). In this regard, Watson and Luckman (2016) evidenced a relation between larger snow accumulation and delays in *P. ponderosa* and *Pseudotsuga menziesii* growing seasons in some regions of Canada. Fkiri et al. (2018) also reported that winter snow is a major factor limiting growth of *P. nigra* in NW Tunisia. Other studies, however, pointed to a positive influence of winter snowfall on tree-ring growth due to snowmelt waters may constitute much of the available resource to trees during the beginning of the following growing season (St. George, 2014).

A possible explanation for the scarce influence of preceding November snow conditions on growth observed in our study is that occasional early-season snowfalls before November did not contribute to overall autumn snow accumulation, thus it was relegated to accumulation occurred in the season last month. As a consequence, small snowpacks were found in November. Furthermore, this late autumn snow depth accumulation has a minor influence on the presence of late spring snow (Nov SD and May SD indices were not correlated, $r_s = 0.33$), which was pointed out in this study as the most important seasonal snow component influencing *P. uncinata* growth. Contrary to our results, Carlson et al. (2017) in *P. albicaulis* forests and Helama et al. (2013) in *P. sylvestris* forests detected significant negative effects of autumn snowfall and autumn snow depth on radial growth, respectively. The early snowfall in autumn and soil cooling can be related to the cessation and shortening of the growing season (Carlson et al., 2017). In this instance, other physiological tree processes are affected: among others, (1) the reduction of photosynthate storage for the following year growth resumption (Fritts, 1976), (2) the reduction of mycorrhizal activity (Peterson and Peterson, 1994), and (3) the inhibition of carbon transfer into radial growth and later carbon storage for the following year (Hoch and Körner, 2003). Moreover, previous studies have demonstrated that *P. uncinata* is sensitive to previous November low temperatures, when synthesis and storage of carbohydrates can affect later radial growth (Tardif et al., 2003; Galvön et al., 2014).

Evidence of tree characteristics' influence on the snow-radial growth relationship was found. Smaller trees showed to be more sensitive to snow effects (Fig. 5b), which could be due to a more efficient hydraulic functioning (Galván et al., 2012) or to a lower influence of snowpack on microclimate and phenology in the case of tall trees. Zhu et al. (2015) reported that large trees have higher recovery rates from snow damage than smaller trees. With regard to geographical distribution of snow-growth interactions, in the Pyrenean sites (central and western areas) occurred almost all of the significant snow-growth correlations, but also the negative snow-growth influence was detected in the drier Iberian System site. Any snow influence on *P. uncinata* growth was found in the Pre-Pyrenees or eastern Pyrenees sampled sites. Previous studies (Tardif et al., 2003; Galván et al., 2014) have demonstrated that elevation plays a major role in *P. uncinata* radial growth-index responses to climate. Galván et al. (2014) observed an elevation pattern regarding temperature: November temperature conditions during the year prior to tree-ring formation influence *P. uncinata* growth mainly in mid-elevation sites, whereas at higher elevations, growth was more dependent on May temperature conditions during the year of tree-ring formation. However, no statistical significant relation was found regarding the elevation gradient determine whether *P. uncinata* radial growth is influenced by a specific snow index. Thought results from partial correlation analyses indicate that the main negative snow influences on tree growth were found at higher elevations (Fig. S3), this study did not produce sufficient evidence to confirm our initial hypothesis. We expected that upper and therefore colder forest sites could be the most sensitive to snow-growth influences. The decrease in near-surface air temperature produced by an increase in elevation (Navarro-Serrano et al., 2018) was suggested to limit the maximum elevation of tree growth due to a short growing season (Körner, 2012). Consequently, snow conditions could be expected to be the most limiting factor for radial growth at high elevations which further reduces *P. uncinata* growth period, especially linked to late spring snow cover. But more detailed information on elevational gradients of snow features are needed to test it.

Significant and decreasing trends were detected in winter and spring snow depths along the Pyrenees (although trend coefficients are very dependent on the selected study period), similar to other main mid-latitude mountain ranges (López-Moreno, 2005; Marty, 2008; McCabe and Wolock, 2009; Beniston, 2012; Morön-Tejeda et al., 2013a; Buisán et al., 2015) (Fig. 6b). A significant and negative response of *P. uncinata* growth to the negative trends in winter snow was found (Fig. 6a), but it was not ubiquitous. Thus, trends of *P. uncinata* growth were not consistent through all forests, thought almost all the statistically significant coefficients found were negative (only there was one increasing growth trend). This may be related, however, to the length of the radial growth data series. Overall results suggest that *P. uncinata* radial growth could benefit from the predicted shallower snowpack in these mountain ranges (López-Moreno, 2005; Morán-Tejeda et al., 2013a) over the next decades by a prolongation of the growing season, especially in high elevation forests. Likewise, climatic warming is expected to promote forest growth in the Pyrenees in a similar way (Tardif et al., 2003). However, growth could be declined in some dry sites where the amount of soil water available to trees in the growing season relates to the previous months' snowpack (Pederson et al., 2011). Therefore, in xeric sites, a shallower snowpack due to warmer temperatures could lead to limited soil water content in spring and reduce growth (Walsh et al., 1994; Truettner et al., 2018). It has been reported that these thermal stress sites are dependent on early summer precipitation (Richter et al., 1991; Andreu et al., 2007; Galván et al., 2014), but this has not been observed so far in our studied sites. This may be related to limitation in the data used in this study. The length of the radial growth data series was not consistent throughout the sampled sites, ranging from 30 to 13 years of available data per sampled forest. The temperature and snow depth data were a product of a climate simulation with the WRF model, with a spatial resolution (10 x 10 km) that could be too coarse to represent their real spatial variability on the complex terrains of the forests. The regional nature of this study prevented consideration with finer-scale climatic observations.

This study seeks to further research with higher spatial and temporal resolution data, including in-situ climatic and snow cover records, and other environmental variables (such as soil moisture, wind, and solar radiation) in order to improve understanding of how snow-growth relations occur in *P. uncinata* mountain forests.

5. Conclusions

Radial growth of *P. uncinata* forests is affected by snow cover depth, independent of the widely reported effect of growing season air temperature on their wood formation. *P. uncinata* growth is negatively influenced by a larger winter and late spring snowpack depth. Geographical and topographical gradients and some tree characteristics as height explained differences in snow–growth relationships. This study suggests that a future shallower and more transitory snowpack in the studied mountains may benefit the growth of *P. uncinata* over the next decades, although a few forests could experience warming-induced drought stress.

Funding

This study was funded by the Spanish Ministry of Economy and Competitiveness [grant numbers CGL2014-52599-P (IBERNIEVE), CGL2017-82216-R (HIDROIBERNIEVE)]. A. Sanmiguel-Vallelado is supported by a University Professor Training grant [grant number FPU16/00902] funded by the Spanish Ministry of Education, Culture and Sport.

Acknowledgements

We thank all management personnel and forest guards connected to the National Parks or protected areas sampled in this study for their support. We also thank AEMET and CHE for providing climate data.

Appendix A. Supplementary data

Supplementary data associated with this article can be found, in the online version, at https://doi.org/10.1016/j.dendro.2019.125622.

References

Alonso-González, E., López-Moreno, J.I., Gascoin, S., García-Valdecasas Ojeda, M., Sanmiguel-Vallelado, A., Navarro-Serrano, F., Revuelto, J., Ceballos, A., Esteban-Parra, M.J., Essery, R., 2018. Daily gridded datasets of snow depth and snow water equivalent for the Iberian Peninsula from 1980 to 2014. Earth Syst. Sci. Data Discuss. 10, 303–315. https://doi.org/10.5194/essd-10-303-2018.

Andreu, L., Gutiérrez, E., Macias, M., Ribas, M., Bosch, O., Camarero, J.J., 2007. Climate increases regional tree-growth variability in Iberian pine forests. Glob. Change Biol. Bioenergy 13, 804–815. https://doi.org/10.1111/j.1365-2486.2007.01322.x.

Appleton, S.N., St. George, S., 2018. High-elevation mountain hemlock growth as a surrogate for cool-season precipitation in Crater Lake National Park. USA. Dendrochronologia 52, 20–28. https://doi.org/10.1016/j.dendro.2018.09.003.

Barton, K., Barton, M.K., 2018. Package 'MuMIn.' Model Selection and Model Averaging Based on Information Criteria. R package version 3.5.1. R Foundation for Statistical Computing, Vienna, Austria.

Beniston, M., 2003. Climatic change in mountain regions: a review of possible impacts. Climate Variability and Change in High Elevation Regions: Past, Present & Future. Springer, pp. 5–31.

Beniston, M., 2012. Is snow in the Alps receding or disappearing? Wiley Interdiscip. Rev. Clim. Change 3, 349–358. https://doi.org/10.1002/wcc.179.

Beniston, M., Uhlmann, B., Goyette, S., Lopez-Moreno, J.I., 2011. Will snow-abundant winters still exist in the Swiss Alps in an enhanced greenhouse climate? Int. J. Climatol. 31, 1257–1263. https://doi.org/10.1002/joc.2151.

Berrisford, P., Dee, D., Poli, P., Brugge, R., Fielding, K., Fuentes, M., Kallberg, P., Kobayashi, S., Uppala, S., Simmons, A., 2011. The ERA-Interim archive version 2.0. ERA Rep. Ser. 23.

Bronaugh, D., Werner, A., Bronaugh, M.D., 2009. Package 'zyp.' CRAN Repos.

Buisán, S.T., Saz Sánchez, M.A., López-Moreno, J.I., 2015. Spatial and temporal variability of winter snow and precipitation days in the western and central Spanish Pyrenees. Int. J. Climatol. 35, 259–274. https://doi.org/10.1002/joc.3978.

Burnham, K.P., Anderson, D.R., 2003. Model Selection and Multimodel Inference: a Practical Information-theoretic Approach. Springer Science & Business Media.

Camarero, J.J., Gazol, A., Galván, J.D., Sanguesa-Barreda, G., Gutiérrez, E., 2015a. Disparate effects of global-change drivers on mountain conifer forests: warming-induced growth enhancement in young trees vs. CO_2 fertilization in old trees from wet sites. Glob. Change Biol. Bioenergy 21, 738–749. https://doi.org/10.1111/gcb.12787.

Camarero, J.J., Gazol, A., Sancho-Benages, S., Sanguesa-Barreda, G., 2015b. Know your limits? Climate extremes impact the range of Scots pine in unexpected places. Ann. Bot. 116, 917–927. https://doi.org/10.1093/aob/mcv124.

Camarero, J.J., Gazol, A., Tardif, J.C., Conciatori, F., 2015c. Attributing forest responses to global-change drivers: limited evidence of a CO2-fertilization effect in Iberian pine growth. J. Biogeogr.y 42, 2220–2233.

Camarero, J.J., Guerrero-Campo, J., Gutiérrez, E., 1998. Tree-ring growth and structure of *Pinus uncinata* and *Pinus sylvestris* in the Central Spanish Pyrenees. Arct. Alp. Res. 30, 1–10.

Camarero, J.J., Linares, J.C., García-Cervigón, A.I., Batllori, E., Martínez, I., Gutiérrez, E., 2017. Back to the future: the responses of alpine treelines to climate warming are constrained by the current ecotone structure. Ecosystems 20, 683–700. https://doi.org/10.1007/s10021-016-0046-3.

Cantegrel, R., 1983. Le Pin à crochets pyrénéen: biologie, biochimie, sylviculture. Acta Biol. Mont. 2, 87–330.

Carlson, K.M., Coulthard, B., Starzomski, B.M., 2017. Autumn snowfall controls the annual radial growth of centenarian whitebark pine (Pinus albicaulis) in the southern Coast Mountains, British Columbia, Canada. Arct. Antarct. Alp. Res. 49, 101–113. https://doi.org/10.1657/AAAR0016-033.

Cook, E.R., 1985. A time series analysis approach to tree ring standardization (dendrochronology, forestry, dendroclimatology, autoregressive process). Dissertation. The University of Arizona.

D'Orangeville, L., Houle, D., Duchesne, L., Phillips, R.P., Bergeron, Y., Kneeshaw, D., 2018. Beneficial effects of climate warming on boreal tree growth may be transitory. Nat. Commun. 9 (1), 3213. https://doi.org/10.1038/s41467-018-05705-4.

Del Barrio, G., Creus, J., Puigdefábregas, J., 1990. Thermal seasonality of the high mountain belts of the Pyrenees. Res. Dev. 227–233.

El Kenawy, A., López-Moreno, J.I., Vicente-Serrano, S.M., 2011. Recent trends in daily temperature extremes over northeastern Spain (1960–2006). Nat. Hazards Earth Syst. Sci. Discuss. 11, 2583–2603. https://doi.org/10.5194/nhess-11-2583-2011.

Essery, R., 2015. A factorial snowpack model (FSM 1.0). Geosci. Model. Dev. Discuss. 8 (12), 3867–3876. https://doi.org/10.5194/gmd-8-3867-2015.

Fkiri, S., Guibal, F., Fady, B., Khorchani, A.E., Khaldi, A., Khouja, M.L., Nasr, Z., 2018. Tree-rings to climate relationships in nineteen provenances of four black pines subspecies (Pinus nigra Arn.) growing in a common garden from Northwest Tunisia. Dendrochronologia 50, 44–51. https://doi.org/10.1016/j.dendro.2018.05.001.

Franke, A.K., Bräuning, A., Timonen, M., Rautio, P., 2017. Growth response of Scots pines in polar-alpine tree-line to a warming climate. For. Ecol. Manag. 399, 94–107. https://doi.org/10.1016/j.foreco.2017.05.027.

Fritts, H.C., 1976. Tree rings and climate. Acad. San Diego Calif. 567.

Galván, D.J., Büntgen, U., Ginzler, C., Grudd, H., Gutiérrez, E., Labuhn, I., Camarero, J.J., 2015. Drought-induced weakening of growth-temperature associations in high-elevation Iberian pines. Glob. Planet. Change 95–106 Ch. 124.

Galván, J.D., Camarero, J.J., Gutiérrez, E., 2014. Seeing the trees for the forest: drivers of individual growth responses to climate in *Pinus uncinata* mountain forests. J. Ecol. 102, 1244–1257. https://doi.org/10.1111/1365-2745.12268.

Galván, J.D., Camarero, J.J., Sangüesa-Barreda, G., Alla, A.Q., Gutiérrez, E., 2012. Sapwood area drives growth in mountain conifer forests. J. Ecol. 100, 1233–1244. https://doi.org/10.1111/j.1365-2745.2012.01983.x.

Gutiérrez, E., 1991. Climate-tree-growth relationships for *Pinus uncinata Ram.* In the Spanish pre-Pyrenees. Acta Oecol. 12, 213–225.

Helama, S., Mielikainen, K., Timonen, M., Herva, H., Tuomenvirta, H., Venalainen, A., 2013. Regional climatic signals in Scots pine growth with insights into snow and soil associations. Dendrobiology 70, 27–34. https://doi.org/10.12657/denbio.070.003.

Hoch, G., Körner, C., 2003. The carbon charging of pines at the climatic treeline: a global comparison. Oecologia 135, 10–21. https://doi.org/10.1007/s00442-002-1154-7.

Holmes, R.L., 1983. Computer-assisted Quality Control in Tree-ring Dating and Measurement. Tree-Ring Bull.

Innes, J.L., 1991. High-altitude and high-latitude tree growth in relation to past, present and future global climate change. Holocene 1, 168–173. https://doi.org/10.1177/095968369100100210.

Kirdyanov, A., Hughes, M., Vaganov, E., Schweingruber, F., Silkin, P., 2003. The importance of early summer temperature and date of snow melt for tree growth in the Siberian Subarctic. Trees 17, 61–69. https://doi.org/10.1007/s00468-002-0209-z.

Körner, C., 2012. Alpine Treelines: Functional Ecology of the Global High Elevation Tree Limits. Springer.

Legendre-Fixx, M., Anderegg, L.D.L., Ettinger, A.K., HilleRisLambers, J., 2018. Site- and species-specific influences on sub-alpine conifer growth in Mt. Rainier National Park, USA. Forests 9, 1. https://doi.org/10.3390/f9010001.

López-Moreno, J.I., 2005. Recent variations of snowpack depth in the Central Spanish Pyrenees. Arct. Antarct. Alp. Res. 37, 253–260 https://doi.org/10.1657/1523-0430(2005)037[0253:RVOSDI]2.0.CO;2.

López-Moreno, J.I., Morán-Tejeda, E., Vicente Serrano, S.M., Lorenzo-Lacruz, J., García-Ruiz, J.M., 2011. Impact of climate evolution and land use changes on water yield in the Ebro basin. Hydrol. Earth Syst. Sci. Discuss. 15, 311–322. https://doi.org/10.5194/hess-15-311-2011.

López-Moreno, J.I., Vicente-Serrano, S.M., Angulo-Martínez, M., Beguería, S., Kenawy, A., 2010. Trends in daily precipitation on the northeastern Iberian Peninsula, 1955–2006. Int. J. Climatol. 30, 1026–1041. https://doi.org/10.1002/joc.1945.

Marty, C., 2008. Regime shift of snow days in Switzerland. Geophys. Res. Lett. 35, L12501. https://doi.org/10.1029/2008GL033998.

McCabe, G.J., Wolock, D.M., 2009. Recent declines in western US snowpack in the context of twentieth-century climate variability. Earth Interact. 13, 1–15. https://doi.org/10.1175/2009EI283.1.

Morán-Tejeda, E., Herrera, S., López-Moreno, J.I., Revuelto, J., Lehmann, A., Beniston, M., 2013Ea. Evolution and frequency (1970–2007) of combined temperature–-precipitation modes in the Spanish mountains and sensitivity of snow cover. Reg. Environ. Change 13, 873–885. https://doi.org/10.1007/s10113-012-0380-8.

Morán-Tejeda, E., López-Moreno, J.I., Stoffel, M., Beniston, M., 2016. Rain-on-snow events in Switzerland: recent observations and projections for the 21st century. Clim. Chang. Res. Lett. 71, 111–125. https://doi.org/10.3354/cr01435.

Morán-Tejeda, E., López-Moreno, J.I., Beniston, M., 2013Eb. The changing roles of temperature and precipitation on snowpack variability in Switzerland as a function of altitude. Geophys. Res. Lett. 40, 2131–2136. https://doi.org/10.1002/grl.50463.

Morán-Tejeda, E., López-Moreno, J.I., Sanmiguel-Vallelado, A., 2017. Changes in climate, snow and water resources the Spanish pyrenees: observations and projections in a warming climate. In: Catalan, J., Ninot, J.M., Aniz, M.M. (Eds.), High Mountain Conservation in a Changing World. Springer, pp. 305–323.

Morán-Tejeda, E., Lorenzo-Lacruz, J., López-Moreno, J.I., Rahman, K., Beniston, M., 2014. Streamflow timing of mountain rivers in Spain: recent changes and future projections. J. Hydrol. 517, 1114–1127. https://doi.org/10.1016/j.jhydrol.2014.06.053.

Navarro-Serrano, F., López-Moreno, I., J, Azorin-Molina, C, Alonso-González, E, Tomás-Burguera, M, Sanmiguel-Vallelado, A, Revuelto, J, Beguería, Vicente-Serrano, S.M., 2018. Estimation of near-surface air temperature lapse rates over continental Spain and its mountain areas. Int. J. Climatol. 38, 3233–3249. https://doi.org/10.1002/joc.5497.

Pederson, G.T., Gray, S.T., Woodhouse, C.A., Betancourt, J.L., Fagre, D.B., Littell, J.S., Watson, E., Luckman, B.H., Graumlich, L.J., 2011. The unusual nature of recent snowpack declines in the North American Cordillera. Science 333, 332–335. https://doi.org/10.1126/science.1201570.

Peterson, D.W., Peterson, D.L., 1994. Effects of climate on radial growth of subalpine conifers in the North Cascade Mountains. Can. J. For. Res. 24, 1921–1932. https://doi.org/10.1139/x94-247.

R Core Team, 2014. R: a Language and Environment for Statistical Computing. R Foundation for Statistical Computing, Vienna, Austria.

Revuelto, J., López-Moreno, J.I., Morán Tejeda, E., Fassnacht, S., Serrano, V., Martín, S., 2012. Variabilidad interanual del manto de nieve en el pirineo: tendencias observadas y su relación con índices de teleconexión durante el periodo 1985-2011. In: Rodríguez, C., Ceballos, A., González, N., Morán-Tejeda, E., Pacheco, S., Hernández, A. (Eds.), Cambio Climático. Extremos e impactos. Asociación Española de Climatología, Salamanca, pp. 613–621.

Richter, K., Eckstein, D., Holmes, R.L., 1991. The dendrochronological signal of pine trees (*Pinus* spp.) in Spain. Tree-Ring Bull. 51, 1–13.

Rolland, C., Schueller, J.F., 1994. Relationships between mountain pine and climate in the French Pyrenees (Font-Romeu) studied using the radiodensitometrical method. Pirineos 143, 55–70. https://doi.org/10.3989/pirineos.1994.v143-144.156.

Sanchez-Salguero, R., Camarero, J., Gutiérrez, E., Gazol, A., Sangüesa-Barreda, G., Moiseev, P., Linares, J., 2018. Climate warming alters age-dependent growth sensitivity to temperature in eurasian alpine treelines. Forests 9, 688. https://doi.org/10.3390/f9110688.

Sánchez-Salguero, R., Navarro-Cerrillo, R.M., Swetnam, T.W., Zavala, M.A., 2012. Is drought the main decline factor at the rear edge of Europe? The case of southern Iberian pine plantations. For. Ecol. Manage. 271, 158–169. https://doi.org/10.1016/j.foreco.2012.01.040.

Sangüesa-Barreda, G., Camarero, J.J., Esper, J., Galván, J.D., Büntgen, U., 2018. A millennium-long perspective on high-elevation pine recruitment in the Spanish central Pyrenees. Can. J. For. Res. 1113, 1108–1113.

Skamarock, W.C., Klemp, J.B., Dudhia, J., Gill, D.O., Barker, D.M., Dudha, M.G., Huang, X., Wang, W., Powers, Y., 2008. A Description of the Advanced Research WRF Version 3. NCAR Tech. Note NCAR/TN-475 + STR. https://doi.org/10.5065/D68S4MVH.

Smithers, B.V., North, M.P., Millar, C.I., Latimer, A.M., 2018. Leap frog in slow motion: divergent responses of tree species and life stages to climatic warming in Great Basin subalpine forests. Glob. Change Biol. Bioenergy 24, 442–457. https://doi.org/10.1111/gcb.13881.

St. George, S., 2014. An overview of tree-ring width records across the Northern Hemisphere. Quat. Sci. Rev. 95, 132–150. https://doi.org/10.1016/j.quascirev.2014.04.029.

Tardif, J., Camarero, J.J., Ribas, M., Gutiérrez, E., 2003. Spatiotemporal variability in tree growth in the Central Pyrenees: climatic and site influences. Ecol. Monogr. 73, 241–257. https://doi.org/10.1890/0012-9615(2003)073[0241:SVITGI]2.0.CO;2.

Truettner, C., Anderegg, W.R.L., Biondi, F., Koch, G.W., Ogle, K., Schwalm, C., Litvak, M.E., Shaw, J.D., Ziaco, E., 2018. Conifer radial growth response to recent seasonal warming and drought from the southwestern USA. For. Ecol. Manage. 418, 55–62. https://doi.org/10.1016/j.foreco.2018.01.044.

Vaganov, E.A., Hughes, M.K., Kirdyanov, A.V., Schweingruber, F.H., Silkin, P.P., 1999. Influence of snowfall and melt timing on tree growth in subarctic Eurasia. Nature 400, 149–151. https://doi.org/10.1038/22087.

Walsh, S.J., Butler, D.R., Allen, T.R., Malanson, G.P., 1994. Influence of snow patterns and snow avalanches on the alpine treeline ecotone. J. Veg. Sci. 5, 657–672. https://doi.org/10.2307/3235881.

Wang, X., Pederson, N., Chen, Z., Lawton, K., Zhu, C., Han, S., 2019. Recent rising temperatures drive younger and southern Korean pine growth decline. Sci. Total Environ. 649, 1105–1116. https://doi.org/10.1016/j.scitotenv.2018.08.393.

Watson, E., Luckman, B.H., 2016. An investigation of the snowpack signal in moisture-sensitive trees from the Southern Canadian Cordillera. Dendrochronologia 38, 118–130. https://doi.org/10.1016/j.dendro.2016.03.008.

Zhu, L., Zhou, T., Chen, B., Peng, S., 2015. How does tree age influence damage and recovery in forests impacted by freezing rain and snow? Sci. China Life Sci. 58, 472–479. https://doi.org/10.1007/s11427-014-4722-2.

Zhuang, L., Axmacher, J.C., Sang, W., 2017. Different radial growth responses to climate warming by two dominant tree species at their upper altitudinal limit on Changbai Mountain. J. For. Res. 28, 795–804. https://doi.org/10.1007/s11676-016-0364-5.

Supplementary data

Table S1. *Pinus uncinata* sampled sites and their geographical, topographical, ecological and nival characteristics. Values are means ± standard deviation.

Mountain range	Site (code)	Analysed years	Latitude N (º)	Longitude –W, +E (º)	Elevation (m a.s.l.)	Slope (º)	dbh (cm)	Age (years)	Max SD (m)
	Acherito (ACHE)	30	42.89	-0.75	1850	–	–	–	2.31 ± 0.61
	Airoto (AIRO)	16	42.70	1.03	2300	47 ± 29	58.5 ± 13.5	288 ± 10[illegible]	2.54 ± 0.70
	Bielsa (BIEL)	16	42.70	0.18	2000	88 ± 4	45.1 ± 9.[illegible]	270 ± 67	1.14 ± 0.36
	Barranc de Llacs (BLLA)	30	42.53	0.92	2250	44 ± 38	71.7 ± 20.0	616 ± 17[illegible]	2.65 ± 0.86
	Conangles (CONU)	14	42.62	0.73	2106	43 ± 15	56 ± 14.5	318 ± 11[illegible]	1.94 ± 0.61
	Corticelles-Delluí (CORT)	30	42.56	0.93	2269	24 ± 17	83.1 ± 28.8	509 ± 17[illegible]	1.26 ± 0.47
	Las Cutas (CUTA)	17	42.62	-0.08	2150	20 ± 5	33.3 ± 8.[illegible]	129 ± 16	1.31 ± 0.49
	Estany d'Amitges (EAMI)	29	42.58	0.98	2390	40 ± 21	69 ± 26.0	355 ± 10[illegible]	1.51 ± 0.59
	Estany Gerber (EGER)	30	42.62	0.98	2268	15 ± 15	53.5 ± 14.6	426 ± 14[illegible]	2.24 ± 0.64
Pyrenees	Estany de Lladres (ELLA)	29	42.55	1.05	2120	35 ± 12	52.1 ± 9.[illegible]	313 ± 12[illegible]	1.03 ± 0.54
	Estany Negre (ENEG)	29	42.55	1.03	2451	35 ± 18	71 ± 26.0	411 ± 18[illegible]	1.68 ± 0.66
	Estanys de la Pera (EPER)	17	42.45	1.61	2360	30 ± 0	65.2 ± 11.0	339 ± 11[illegible]	0.94 ± 0.39
	Foratarruego (FORA)	29	42.62	0.10	2031	37 ± 11	49.5 ± 18.3	433 ± 50	1.83 ± 0.83
	Larra (LACO)	19	42.95	-0.77	1750	38 ± 24	46.4 ± 14.0	350 ± 10[illegible]	1.90 ± 0.53
	La Estiva (LEST)	13	42.68	0.08	2000	–	–	–	1.10 ± 0.32
	Mata de València (MAVA)	17	42.63	1.07	2019	19 ± 10	43.2 ± 3.[illegible]	237 ± 72	1.65 ± 0.58
	Mirador (MIRA)	29	42.58	0.98	2180	33 ± 18	55.1 ± 25.8	401 ± 13[illegible]	1.06 ± 0.41
	Mirador del Rey (MIRE)	18	42.63	-0.07	1980	25 ± 10	53.3 ± 15.3	117 ± 18	0.94 ± 0.29
	Monestero (MONE)	29	42.56	0.98	2280	28 ± 13	64.4 ± 16.1	346 ± 11[illegible]	1.28 ± 0.49
	Vall de Núria (NURI)	21	42.38	2.13	2075	–	–	–	0.49 ± 0.27

	Pic d'Arnousse (PIAR)	14	42.80	-0.52	1940	32 ± 4	65.4 ± 5.1	248 ± 83	2.80 ± 0.67
	Ratera (RATE)	29	42.58	0.98	2170	40 ± 5	28.3 ± 8.1	380 ± 146	1.04 ± 0.40
	Respomuso (RESP)	30	42.82	-0.28	2350	70 ± 19	49.5 ± 15.1	280 ± 83	4.61 ± 1.17
	Sant Maurici (SAMA)	16	42.58	0.98	1933	16 ± 15	38.2 ± 5.7	204 ± 23	0.67 ± 0.22
	Sarradé (SARU)	15	42.55	0.89	1950	–	–	–	1.65 ± 0.51
	Senda de Cazadores (SECA)	29	42.63	-0.05	2247	49 ± 12	60.9 ± 16.5	337 ± 145	1.60 ± 0.76
	Setcases (SETU)	19	42.40	2.28	2080	–	–	–	0.68 ± 0.35
	Sobrestivo (SOBR)	29	42.67	0.10	2296	38 ± 2	61.7 ± 17.5	341 ± 97	2.06 ± 0.88
	Tessó de Son (TESO)	15	42.58	1.03	2239	42 ± 14	74.5 ± 18.8	346 ± 202	1.15 ± 0.37
	Vall de Mulleres (VAMU)	14	42.62	0.72	1800	34 ± 13	69 ± 26.0	437 ± 184	1.27 ± 0.35
Pre-Pyrenees	Cap de Boumort (COLU)	30	42.23	1.12	1915	–	–	–	0.35 ± 0.22
	Guara (GUAU)	30	42.28	-0.25	1790	–	–	–	0.62 ± 0.32
	Pedraforca (PEDR)	26	42.23	1.70	2100	–	–	–	0.69 ± 0.37
Iberian System	Vinuesa (CAVI)	30	42.00	-2.73	2050	21 ± 1	85.6 ± 23.0	368 ± 148	1.31 ± 0.39
	Valdelinares (VATE-VA1U)	26	40.37	-0.37	1955	10 ± 5	63.8 ± 12.4	214 ± 107	0.57 ± 0.32

Table S2. Coefficients from Spearman correlations (r_s) between snow indices and temperature monthly aggregations. Arrow indicates which monthly aggregation of temperature is best correlated to each snow index and is then used in further analysis.

Temperature indices	Snow indices		
	Nov SD	Feb SD	May SD
Nov T	-0.34** ←		
Feb T		-0.63**	
Nov-Feb T		-0.57**	
Dec-Feb T		-0.63**	
Jan-Feb T		-0.64** ←	
May T			-0.55**
Mar-May T			-0.57** ←
Apr-May T			-0.56**

Values followed by ** are statistically significant at $p < 0.01$.

Table S3. Correlation coefficients from partial correlations calculated between tree-ring width and snow indices.

Site	Nº analysed years	Spearman correlations coefficients (r_s)		
		Nov SD	Feb SD	May SD
ACHE	30	-0.09	-0.27	-0.22
AIRO	16	-0.24	-0.23	-0.41
BIEL	16	0.32	-0.34	-0.12
BLLA	30	0.09	-0.09	-0.13
CAVI	30	-0.23	-0.35	-0.33
COLU	30	0.01	0.14	0.03
CONU	14	-0.06	-0.78**	-0.51
CORT	30	-0.02	-0.26	-0.18
CUTA	17	-0.30	0.01	0.07
EAMI	29	0.14	-0.23	0.03
EGER	30	0.05	-0.29	-0.38*
ELLA	29	0.19	0.21	-0.16
ENEG	29	0.06	-0.23	-0.12
EPER	17	-0.45	-0.56*	0.09
FORA	29	0.15	0.06	0.20
GUAU	30	0.13	0.17	0.06
LACO	19	0.22	-0.25	-0.31
LEST	13	0.14	-0.31	0.31
MAVA	17	0.17	0.08	0.15
MIRA	29	0.06	-0.23	-0.05
MIRE	18	-0.05	-0.47	0.37
MONE	29	0.02	-0.26	-0.21
NURI	21	0.11	-0.13	0.09
PEDR	26	0.04	-0.21	-0.25
PIAR	14	0.32	0.07	0.28
RATE	29	0.33	0.12	-0.24
RESP	30	-0.15	-0.15	-0.27
SAMA	16	0.33	0.05	-0.43
SARU	15	-0.06	-0.54*	-0.12
SECA	29	0.26	0.25	0.10
SETU	19	-0.15	0.07	-0.11
SOBR	29	-0.09	-0.29	-0.08
TESO	15	-0.01	-0.63*	-0.18
VA1U	26	0.34	0.06	0.07
VAMU	14	0.19	-0.71**	0.10
VATE	26	0.18	-0.34	-0.15

Values followed by * and ** are statistically significant at $p < 0.05$ and $p < 0.01$, respectively. Note that data length differs between sites.

Figure S1. Partial correlation coefficients (Spearman, r_s) calculated between tree-ring width and snow indices. Sites where a statistically significant correlation was found are labelled. Statistical significance of models is represented in red ($p > 0.05$) and blue ($p < 0.05$) colors.

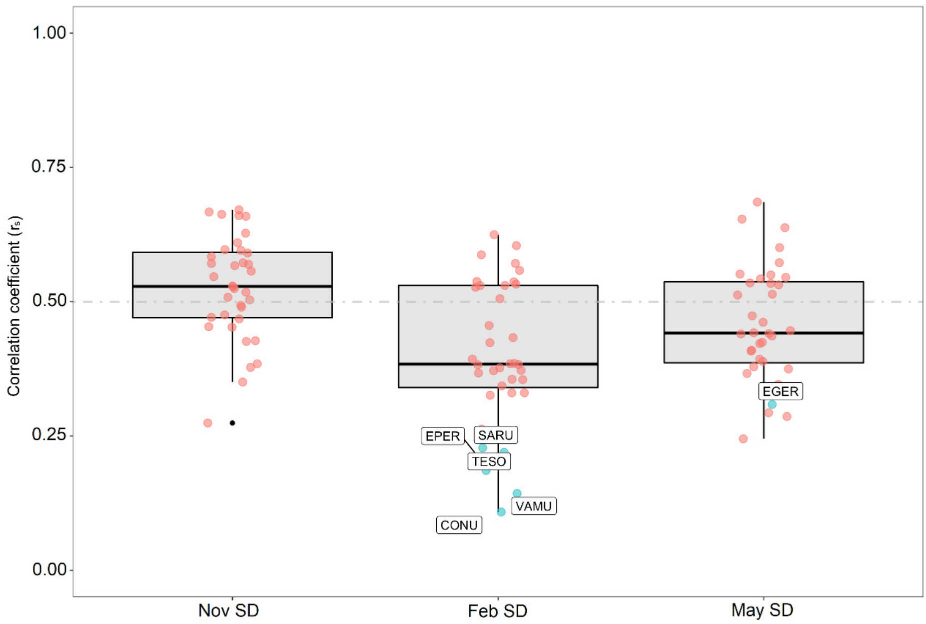

Figure S2. Latitude, longitude and elevation distribution patterns for groups of sites with the same RWI main drivers. Pre-Pyrenees (Pre-Pyr) and Iberian System (IS) locations are indicated where applicable. NA indicates sites whose selected model was null. Stars indicate sites whose selected model was statistically significant ($p < 0.05$).

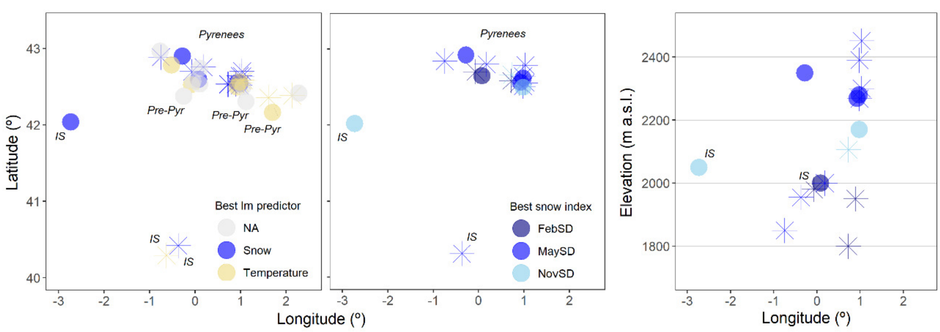

Figure S3. (a) Effect of geographical, nival gradients and tree influences on growth-snow partial correlations (Spearman correlations, r_s). The southern Iberian System sites were omitted in latitude analyses. (b) Scatterplots of statistically significant correlations (p < 0.05) obtained between growth-snow partial correlations and biogeographical gradients. Histograms show sites frequency of distribution along gradients.

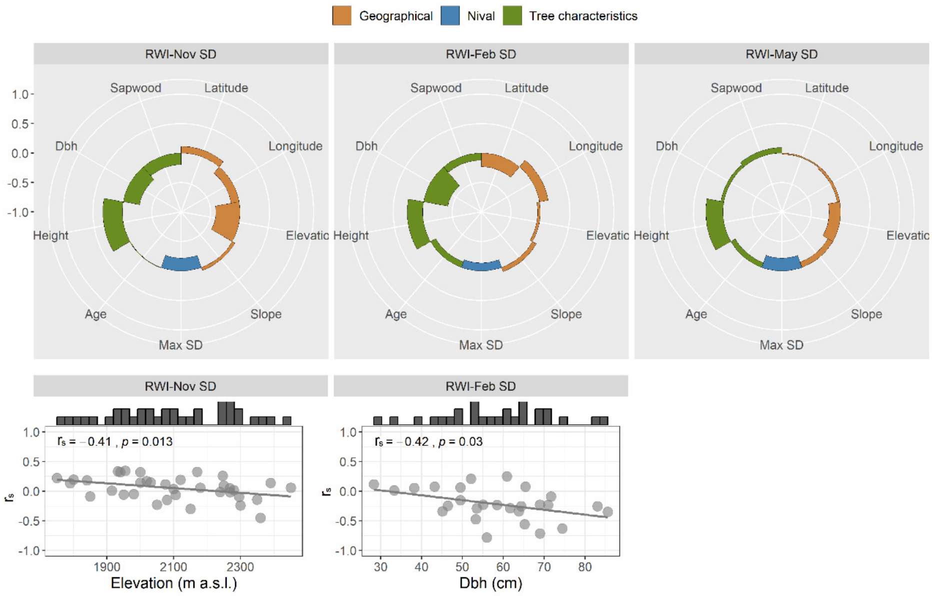

Figure S4. Theil-Sen's slopes (variable's units in mm·year^{-1}) for tree-ring width (RWL) and snow indices trends of selected sites from 1981 to last year with data (series' lengths are shown after site codes). Statistically significant values at p < 0.05 are represented with stars. Blank values in RWL mean data is not available for these sites.

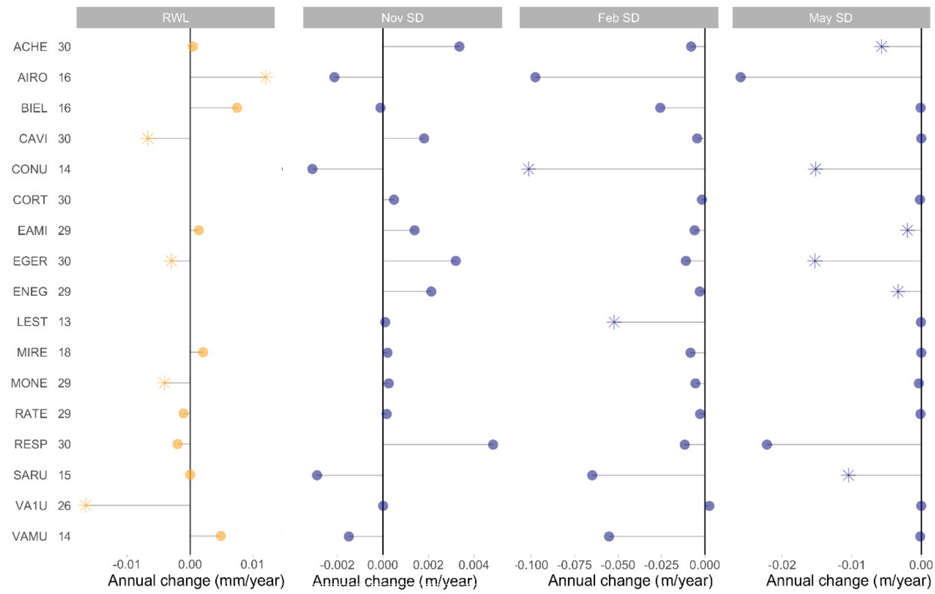

Chapter 5

Snow dynamics influence tree growth by controlling soil temperature in mountain pine forests

This article was published in:

Sanmiguel-Vallelado, A., Camarero, J. J., Morán-Tejeda, E., Gazol, A., Colangelo, M., Alonso-González, E. & López-Moreno, J. I. (2021). Snow dynamics influence tree growth by controlling soil temperature in mountain pine forests. *Agricultural and Forest Meteorology*, *296*, 108205. https://doi.org/10.1016/j.agrformet.2020.108205

Authors thank ELSEVIER for the permission to present here the article in its entirely.

Agricultural and Forest Meteorology 296 (2021) 108205

Contents lists available at ScienceDirect

Agricultural and Forest Meteorology

journal homepage: www.elsevier.com/locate/agrformet

Snow dynamics influence tree growth by controlling soil temperature in mountain pine forests

Alba Sanmiguel-Vallelado[a,*], J. Julio Camarero[a], Enrique Morán-Tejeda[b], Antonio Gazol[a], Michele Colangelo[a,c], Esteban Alonso-González[a], Juan Ignacio López-Moreno[a]

[a] Pyrenean Institute of Ecology, CSIC (Spanish Research Council), Avda. Montañana 1005, 50059 Zaragoza, Spain
[b] Department of Geography, University of the Balearic Islands, Carr. de Valldemossa km 7.5, 07122 Palma de Mallorca, Spain
[c] School of Agricultural, Forest, Food and Environmental Sciences, University of Basilicata, viale dell'Ateneo Lucano 10, 85100 Potenza, Italy

ARTICLE INFO

Keywords:
Pyrenees
snow cover
soil temperature
subalpine forests
tree growth
xylogenesis

ABSTRACT

Snow dynamics are key to understanding tree growth in mountain forests and future response to climate change. However, precise monitoring of microclimate conditions and variables related to tree growth and functioning are lacking. To advance on those issues, snow cover and microclimate conditions, tree phenology, xylogenesis, intra-annual radial growth and the concentration of sapwood and needle non-structural carbohydrates were intensively monitored in four *Pinus uncinata* forests along an altitudinal gradient over three years in a Pyrenean valley (NE Spain). Snow dynamics exerted strong influence on soil temperature and moisture, particularly before and during the early growing season. Soil temperature was the most relevant microclimate variable during the overall xylogenesis, mainly influencing the production of mature tracheids. Large snow accumulation resulted in later snow depletion and a consequent delay in soil warming onset. Low soil temperatures in the spring, related to prolonged snow persistence, retarded cambial reactivation and led to lower growth rate. Despite strong spatial variability among plots, wood production was determined by snow dynamics in three out of the four studied plots. This study highlights the major role played by early and late growing season soil temperatures on radial growth of mountain conifers. The results of this study suggest that a future shallower and more transitory snowpack in the studied forests, together with warmer soil and air temperatures, may increase radial growth and productivity of similar mid-latitude, young mountain forests.

1. Introduction

Climate plays a major role as driver of forest productivity, stem wood formation and radial growth (Babst et al., 2019). In mountainous areas, regional climate is greatly controlled by topographic complexity (elevation, aspect, slope) and also by the presence of forest patches, resulting in the creation of large microclimatic variability (Albrich et al., 2020; Dan Moore et al., 2005). In cold, high-elevation forests and alpine treelines, low air and soil temperatures limit tree growth by shortening the growing season and reducing growth rates (Körner, 2012). There is a minimal air temperature threshold for cambial activity of many conifers around 5°C (Rossi et al., 2008). Air temperatures can also impact tree growth by retarding or accelerating snowmelt (Barnett et al., 2005). Snow dynamics have been reported to influence forest productivity, radial growth and xylogenesis in subalpine and subarctic forest ecosystems (Carlson et al., 2017; Helama et al., 2013). A deep snowpack, together with low air temperatures, can delay the melt-out date, resulting in later soil warming, delayed root growth and cambial onset, thus reducing growth (Kirdyanov et al., 2003; Rossi et al., 2011; Vaganov et al., 1999). Other studies, however, have not found that soil temperature strongly influences stem growth and, in such cases, air temperature was considered to be the main factor limiting xylogenesis (D'Orangeville et al., 2013; Lupi et al., 2012; Rossi et al., 2007). Additionally, snowmelt enhances water infiltration into deep soils (Woelber et al., 2018) and can positively influence tree growth by reducing soil moisture-limitation in seasonally dry mountain areas from mid to low latitudes (St. George, 2014; Watson and Luckman, 2016; Zhang et al., 2019).

Mountain forests from mid to high latitudes, where growth is mainly controlled by low temperatures, are very exposed to climate warming (Albrich et al., 2020). Rising air temperatures are expected to promote tree growth by extending the growing season and increasing growth rates (Camarero et al., 2017; Zhang et al., 2017). A likely shallower shorter-lived snowpack in mid-latitude mountain ranges

* Corresponding author.
E-mail address: albasv@ipe.csic.es (A. Sanmiguel-Vallelado).

https://doi.org/10.1016/j.agrformet.2020.108205
Received 12 June 2020; Received in revised form 24 September 2020; Accepted 28 September 2020

(Beniston, 2012; McCabe and Wolock, 2009; Morán-Tejeda et al., 2017; López-Moreno et al., 2017) will allow the soil temperature to rise earlier in the year, consequently prolonging the growing season. However, a shorter-lived snowpack may also lead to less available snowmelt water at the end of spring, intensifying periods of water shortage in drought-prone regions such as the Mediterranean mountains (Pederson et al., 2011; Truettner et al., 2018).

Understanding how snow dynamics affect tree grow in mountain forests will allow us to anticipate their future responses to forecasted climate change. That is especially relevant in the Spanish Pyrenees, which is a mountain range located in the transition of temperate-continental Atlantic-Eurosiberian and dry Mediterranean climate influences (Del Barrio et al., 1990; El Kenawy et al., 2011; López-Moreno et al., 2010; Morán-Tejeda et al., 2017). This study investigates how seasonal dynamics in snowpack characteristics modify microclimatic conditions (soil temperature and moisture) and tests if these modifications influence intra-annual growth and functioning in Mountain pine (*Pinus uncinata*). For that purpose, microclimate conditions, shoot and needle phenology, xylogenesis, radial growth, sapwood and needle non-structural carbohydrate (NSC) concentrations were monitored in four *P. uncinata* forests situated along altitudinal gradients over three consecutive years in a Pyrenean valley. The objectives of the study were (1) to determine the extent to which small-scale variations in soil temperature and moisture are influenced by snowpack magnitude and duration; (2) to characterize seasonal growth and functioning in *P. uncinata*; and (3) to analyze the influence of intra-annual snow dynamics on *P. uncinata* growth through snowpack contribution to microclimate. The main hypothesis is that snow dynamics influence intra-annual growth patterns through their impact on soil temperature and moisture.

2. Data and methods

2.1. Study species

The Mountain pine (*Pinus uncinata* Ram.) is a long-lived and shade-intolerant conifer which dominates in high-elevation areas of the Pyrenees, western Alps, and Iberian System (Cantegrel, 1983). Spain's geographical distribution is limited to the subalpine forests of the Pyrenees (1600 - 2500 m) and to two isolated populations in the Iberian System, where it reaches its southern distribution limit (Ruiz de la Torre and Ceballos, 1979). *P. uncinata* begins to form the annual tree ring in April-May and ends growing in October, with main growth peaks from May to July (Camarero et al., 1998). A positive effect of warm air temperatures during the autumn before ring formation and during the growing season has been widely reported in tree-ring studies. (Andreu et al., 2007; Camarero et al., 1998; Galván et al., 2014; Tardif et al., 2003). In addition, there is evidence that a preceding abundant snowpack negatively influences *P. uncinata* radial growth at inter-annual scale (Sanmiguel-Vallelado et al., 2019).

2.2. Study site

The study was performed in the central Spanish Pyrenees (Figure 1a), where climate is continental (Del Barrio et al., 1990). The experimental setting comprised four forest stands located in the Balneario de Panticosa valley (Figure 1b); all stands have different elevations (from 1674 to 2104 m a.s.l.), exposure, forest structure and microclimatology because of the complex topography in this area (see Table 1 and Figure 1c). During the study period, the average annual sum of precipitation registered in the valley bottom (1630 m) was 1493 mm. In each forest an experimental plot of approximately 450 m^2 was designed. The plots were labeled (plot 1, plot 2, plot 3 and plot 4) based on their locations in the valley (from N to S). *P. uncinata* dominates the studied stands, although plot 3 contained a few individual *Pinus sylvestris* L. At each experimental plot, five young individual *P. uncinata* were monitored and their diameter at breast height (Dbh_0) and full height were measured using tapes and clinometers, respectively.

2.3. Data collection

A graphical description of the monitoring procedures and measures variables is shown in Figure A.1.

2.3.1. Microclimate data

Air temperature (T) and humidity (H) series were obtained using dataloggers (Tinytag-Plus-2; model TGP-4017, Gemini DataLoggers UK Ltd., Chichester, West Sussex, UK) that were equipped with naturally ventilated radiation shields (Datamate ACS-5050 Weather Shield; Gemini DataLoggers UK Ltd., Chichester, West Sussex, UK). One datalogger was installed at each plot stand, hanging from a tree branch, and measurements were recorded every 15 minutes from November 2015 to December 2018.

The soil temperature (T soil) series was obtained using miniature temperature loggers (Thermochron iButton; DS-1922L model, Dallas Semiconductors, Texas, USA). Four to six dataloggers were installed at each studied forest stand in a distributed manner, covering both forest openings and beneath forest canopy areas. The dataloggers were wrapped with laboratory film and duct tape to prevent corrosion, tied to metallic picks to facilitate their later retrieval, and buried in the ground at a depth of 10 – 20 cm. Soil temperature data were collected every hour from November 2015 to December 2018.

The soil moisture series was obtained using ECH_2O probes (EC-5 model, Decagon Devices, Pullman, WA, USA). Soil moisture sensors were installed in a distributed manner at each plot: two sensors were installed in forest openings and two beneath forest canopy areas. Sensors were buried in the ground at a depth of 10 - 20 cm. Volumetric water content (VWC) of soil was registered by the ECH_2O datalogger every 1.5 hours from November 2015 to December 2018. The first month of measurements was discarded in order to ensure a proper settling time after field installation.

Snowpack data were collected from November 2015 to June 2018. Each year comprised snow data collected from the onset of snow accumulation to the end of melting. The snow depth series was obtained from automatic time-lapse cameras (Bushnell, Trophy Cam, Kansas, USA) shooting every day at eight fixed snow poles at each plot: three poles were placed in an open area and five were placed beneath the forest canopy at each plot. Photographs were processed using ImageJ software (Rasband, 1997) to manually obtain a daily snow depth series. The average daily snow depth series for the set of poles at each experimental plot was calculated. Snow Water Equivalent (SWE) was manually surveyed every 10 to 15 days using a snow cylinder and scale (ETH core sampler, Swiss Federal Institute of Technology, Zurich) at snow pits dug at two single locations in each plot, one in a forest opening and one below the forest canopy. Two replicates per location were collected. Snow density data was calculated from SWE collected data using the equation (Eq. 1):

$$\rho_s = \frac{SWE \cdot \rho_w}{H} \tag{1}$$

where ρ_s is the snowpack density ($kg \cdot m^{-3}$), SWE is the measured equivalent water of the snowpack (m), *H* is the measured snowpack depth (m), and ρ_w is the assumed water density ($kg \cdot m^{-3}$). Daily snow density series were estimated by linear interpolation between each pair of density measurements from consecutive surveys. Daily SWE series for the set of poles at each experimental plot were inferred from data on daily snow depth and estimated daily snow density. The methodology to obtain the snow dataset is described in Sanmiguel-Vallelado et al. (2020).

2.3.2. Stem radius variations

Changes in stem perimeter were monitored on two to three

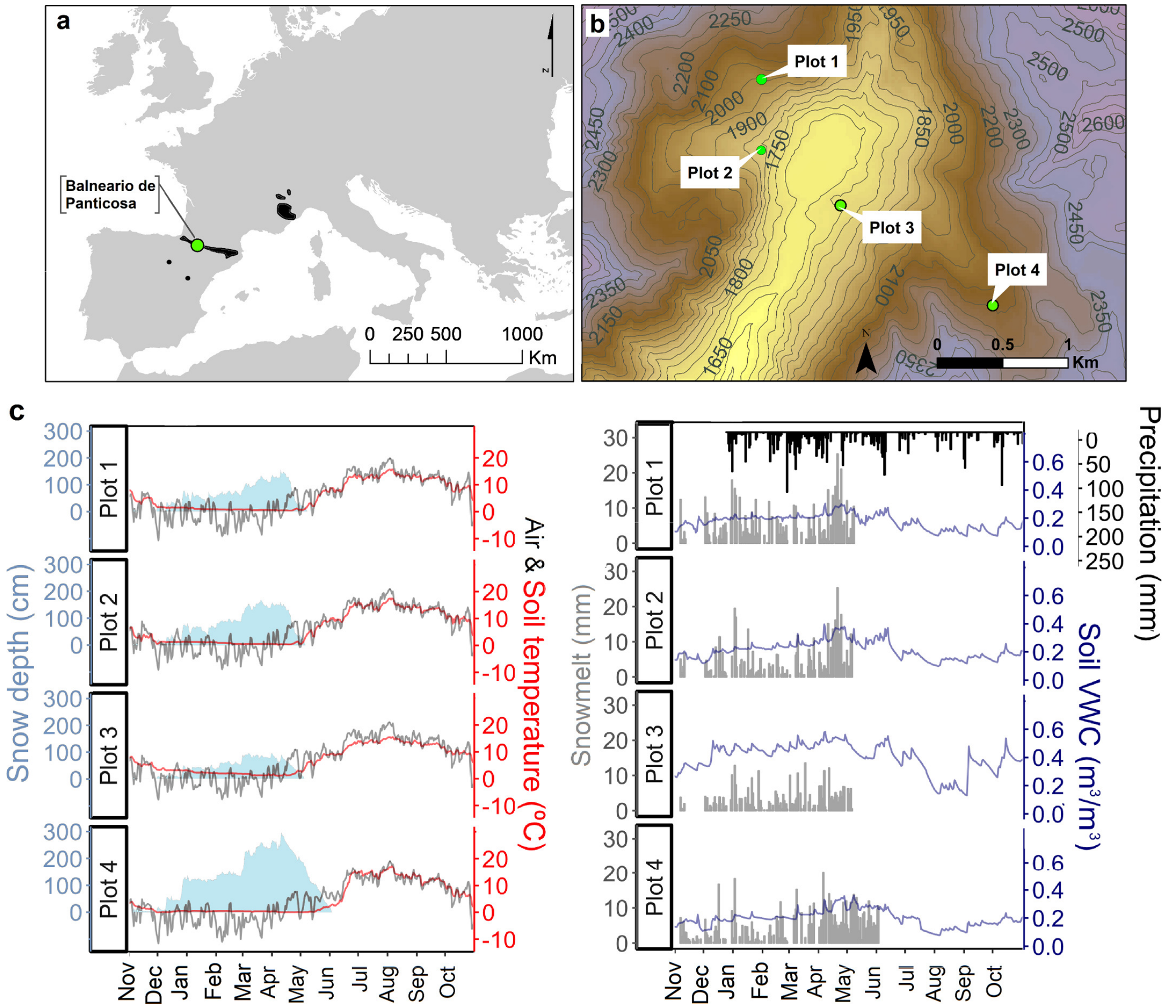

Figure 1. (a) Distribution of the study species (*Pinus uncinata*) in Europe (black areas) and location of the study area location (Balneario de Panticosa) in the Spanish Pyrenees (green dot). (b) Location of the experimental plots in the study valley. (c) On the left: daily time series of snow depth (light blue areas), mean soil temperature (red lines) and mean air temperature (grey lines) by plot during 2018. On the right: daily time series of snow melting rates (grey bars), mean soil VWC (blue lines), and precipitation sum (black bars) by plot during 2018. Precipitation data source was a meteorological station located in the study area at 1630 m a.s.l. (note that this series contained NA periods).

individual *P. uncinata* at each plot, using stainless-steel band dendrometers (DR 26, EMS Brno, Czech Republic). Dendrometers (n = 10) were installed at a height of ~ 150 cm on the individual stems. The external layer of dead bark was previously removed. Hourly stem perimeter variations data (1 µm resolution) were collected from April 2016 to December 2018 and transformed into radial changes, assuming a circular shape of the stem and measuring the diameter at breast height (1.3 m) at the beginning of the study (Dbh_0). Data downloading

Table 1
Topography, microclimate conditions, tree characteristics, and forest structure in the four plots. Mean ± standard deviations are presented.

Plot	Elevation (m a.s.l.)	Aspect	Slope (°)	DJF air T (°C)	TGS air T (°C)	Max SD (cm)	MAM GSI (W•m − 2)	Dbh0 (cm)	Height (m)	Age (years)†	Density (indiv•ha − 1)	Basal area (m2•ha − 1)
1	2008	S	29.4	-0.5	11.1	133.2	154	20.4 ± 4.0	9.2 ± 0.3	38 ± 6	1689	45.1
2	1814	E	20.4	-0.4	11.4	169.3	168	18.8 ± 4.6	8.6 ± 1.2	35 ± 7	844	13.7
3	1674	W	9.3	0.3	12.2	95.3	193	22.4 ± 2.9	9.5 ± 1.1	42 ± 4	533	35.3
4	2104	NE	22.7	-2.0	10.3	260.4	195	20.2 ± 4.0	9.1 ± 0.3	37 ± 6	356	26.6

Abbreviations: DJF T, winter mean air temperature from December to February; TGS, Thermal Growing Season (see 2.4 section); Max SD, maximum snow depth; MAM GSI, average global solar irradiation from March to May; Dbh_0, diameter at breast height at the beginning of the study. Note: The methods used to obtain stand structure data were described in Sanmiguel-Vallelado et al., (2020). (†) Tree age was estimated from Dbh_0 values based on an age-Dbh linear regression constructed in a nearby *P. uncinata* forest.

(Mini 32 software, EMS Brno, Czech Republic) was done seasonally (i.e. four times per year, every three months).

2.3.3. Xylogenesis

To study xylogenesis (xylem phenology and development), wood samples (microcores of 2 mm diameter and 15-20 mm length) were collected from five individual *P. uncinata* at each plot to monitor wood formation. Microcores (n = 20) were taken weekly or bi-weekly from May to October during 2016 and 2017. The individuals were punched with a Trephor® increment puncher at 1-1.5 m height, following an ascending spiral pattern, and each sample was taken at least 5 cm from previous sampling points (Deslauriers et al., 2015). The samples usually contained the preceding 4–5 rings and the developing ring with the cambial zone and adjacent phloem. Microcores were immediately fixed in 50% ethanol solution and preserved.

Transversal wood sections (15-20 µm thick) were obtained using a sliding microtome (Leica SM2010 R) with temperature Controlled Freezing Stages for Microtomes (Physitemp BFS-30MP), which allowed freezing the samples for optimal sectioning. Sections were mounted on glass slides, stained with 0.05% cresyl violet and fixed with Eukitt®. The mounted and fixed sections were examined with visible and polarized light within 10–30 min of staining. Images of sections were first taken at 40–100x magnification, using a digital camera mounted on a light microscope (Olympus BH2, Olympus, Hamburg, Germany). We counted and averaged, on five radial lines per ring, the number of cambium cells, radially enlarging tracheids, wall-thickening tracheids and mature cells (Camarero et al., 2010; Deslauriers et al., 2015). Images allowed verifying cell counts and distinguishing earlywood (EW) and latewood (LW) tracheids according to their lumen and cell wall thickness, distinguishing earlywood from latewood tracheids as a function of their radial lumen diameter and wall thickness following (Denne, 1989). In the developmental stage, cells showed different shapes and stained with different colors (Antonova and Stasova, 1993); cambial cells had similar and small radial diameters and thin walls; radially elongating tracheids showed a wider radial diameter and contained a protoplast enclosed by a thin primary wall; wall-thickening tracheids corresponded to the onset of secondary cell wall formation and were characterized by cell corner rounding; secondary walls glistened under polarized light and walls turned blue due to wall lignification; and mature cells did not contain cytoplasm and presented completely blue walls.

2.3.4. Shoot and needle phenology

Following the procedure reported in Rossi et al. (2009) the dynamics of shoot and needle growth on five individual *P. uncinata* were monitored at each experimental plot. Shoot and needle measurements were taken weekly or bi-weekly from May to October during 2016 and 2017. Five lower branches, from all exposures, were selected on each tree. On the branches, the developing apical shoots were measured with a ruler (1 mm precision). On each shoot, five developing needles were randomly selected and measured.

2.3.5. Non-structural carbohydrate concentrations

Non-structural carbohydrate (NSC) concentrations were quantified in stem sapwood and young needles of stems from individual five *P. uncinata* at each experimental plot. Three apical shoots and one core, taken at breast height (1.3 m) with Pressler increment borers (Gestern, Germany), were seasonally collected from selected trees in 2016. The concentrations of soluble sugars (SS) and starch (as non-soluble sugars NS) were measured in current-year needles and stem sapwood. Following Sangüesa-Barreda et al. (2012), SS were extracted with 80% ethanol solution and a colorimetric approach to determine their concentration. The undissolved fraction of carbohydrates after ethanol extraction was enzymatically reduced to glucose and then analyzed, as in Palacio et al. (2007). NSC measured after ethanol extraction is referred to as SS; carbohydrates measured after enzymatic digestion in glucose equivalents are referred to as starch; and the sum of SS and starch is referred to as total NSC (TNC).

2.4. Data analyses

From the raw microclimate series, a few (<1%) outliers caused by errors in sensor measuring were removed. Missing data were estimated using a non-parametric iterative imputation method called missForest (Stekhoven and Buhlmann, 2012), which is implemented in the MissForest R package (Stekhoven, 2013). For each variable, the missForest method fits a Random Forest regression to the observed part and then predicts the missing parts of the input data (Breiman, 2001). Average daily series at each experimental plot were calculated. Data from forest openings and beneath forest canopy areas were averaged for SWE, soil temperature and soil moisture series. Snowmelt was calculated by first-order differencing from SWE daily series. Only snow data in a continuous snowpack period were considered; that is, from the date of the first day of 14 or more consecutive days with snow on the ground (i.e. snow accumulation onset) to the last date with a snow record (i.e. melt-out date). Air warming onset was defined as the day when the 7-day running mean air T reached a threshold of 5°C after the date of minimum air T, because 5°C is the minimal temperature threshold for cambial activity of many conifers (Rossi et al., 2008). Soil warming onset was determined the same way, with the soil temperature series. Therefore, the most favorable thermal growing season (TGS) comprises the period when air temperatures overcome the 5°C threshold. Snowmelt infiltration in soil was assumed when there was a rise of 0.01 $m^3 \cdot m^{-3} \cdot day^{-1}$ of soil VWC (Harpold et al., 2015).

Regressions at plot level (i) were performed between monthly sums of snowmelt and monthly averages of soil VWC and (ii) between monthly averages of SWE and soil T to investigate influences of snowpack on soil conditions. Linear and polynomial adjustments were done, respectively. The linear soil VWC response to snowmelt allowed inference of temporal variability of this relationship by performing correlation analysis between snowmelt weekly sums and soil VWC weekly averages, grouping by month and plot. The influence of snow duration on soil T over time was determined by performing correlation analysis between the melt-out date and the (current and following) monthly average values of soil temperature by plot and year.

From xylem development data, the increase in the number of mature tracheids was modelled at plot level with a Gompertz function (Eq. 2) (Zeide, 1993) using the non-linear regression procedure included in the growthmodels R package (Rodriguez Perez, 2013), following Camarero et al. (1998) and Rossi et al. (2003).

$$Y = A^{*}\exp[-\exp(\beta - k^{*}t)] \qquad (2)$$

where Y is the weekly cumulative sum of mature cells (sum of earlywood and latewood mature tracheids), A is the upper growth asymptote, β is the x-axis placement parameter, k is the rate of change parameter, and t is the time in day-of-year (DOY). Adjusted functions were again limited to the main *P. uncinata* growing season period (Camarero et al., 1998). Daily rates of mature tracheids production (Number of mature tracheids $\cdot day^{-1}$) were estimated by first-order differencing the values of two consecutive days of the Gompertz-adjusted series.

For the stem radius variations data series, calculating daily mean and maximum values allows removal of the effect of temperature and soil moisture fluctuations on stem diameter changes over daily periods (Deslauriers et al., 2007). However, a daily approach was preferred because the temporal resolution of most available microclimate variables was not high enough to perform further analysis for selecting a stem cycle approach. Dendrometer raw data were processed using the dendrometeR package (van der Maaten et al., 2016) to obtain the daily maximum radius series. Dendrometer data was delimited to the main *P. uncinata* growing period (Camarero et al., 1998), and was set to 0 on April 1 every season (in 2016 the series was set to 0 the May 1 due to data availability). Gompertz functions were adjusted to daily maximum radius series at plot level following the procedure described above (Eq. 2). Daily rates of radial increment (µm•day^{-1}) were estimated by first-order differencing the values of two consecutive days of the Gompertz-adjusted series. Some annual indices were extracted from mature tracheid production, stem radial increment and phenology data to characterize tree growth (see Table A.1).

Intra-annual microclimate effects on tree growth were examined by performing correlation analyses between weekly averages of microclimate variables and weekly maximum growth rates. Correlations were grouped by month and plot. Additionally, principal component analyses (PCA) were performed to identify the most representative microclimate variables of tree growth rates during the whole growing period. The first PCA was performed using weekly microclimate averages and maximum rates of mature tracheid production; the second PCA was performed using weekly microclimate averages and maximum rates of radial increment. A set of non-correlated variables (principal components, PCs) was obtained; these were linear combinations of the original variables (Jolliffe, 2002). The number of PCs selected in each PCA was based on the Kaiser criterion (Kaiser, 1974), preserving those with eigenvalues > 1. The original variables were classified into the selected PCs by following the maximum loading rule. Original variables were represented as vectors, indicating (i) the direction in which the value of the vector increases, and (ii) the correlation magnitude among vectors and between vectors and component axes (low angles correspond to high correlations).

The non-parametric Kruskal-Wallis test was used to assess whether there were statistically significant differences in certain variables among plots or years, (i.e. air and soil temperatures, soil VWC, and NSC concentrations). This test was selected because the assumption of normality in data distribution within the groups of analyzed variables was not always met (Shapiro-Wilk test: $p < 0.05$). If the Kruskal–Wallis test was significant, the Dunn test post-hoc analysis was performed to determine which groups differed from each other. In correlations, Pearson coefficients were calculated when data distribution of the analyzed variables was normal (Shapiro-Wilk test: $p > 0.05$), otherwise, Spearman coefficients were calculated. All analyses were performed using R statistical software (R Core Team, 2018).

3. Results

3.1. Influence of snowpack on microclimate

Snow accumulation occurred from November to January, whereas the snow melt-out dates occurred throughout April and May (DOY 122 ± 21; average value ± SDs among all years and plots), with a snow cover lasting 143 ± 39 days (Table A.2). Snow accumulation usually peaked in mid-March (DOY 74 ± 25), reaching maximum depths of 120 ± 67 cm. Larger snow accumulation involved later melt-out dates (r = 0.91, $p < 0.05$) (Figure A.2) and a longer duration of annual snow cover (r = 0.87, $p < 0.05$). More variability in snowpack duration and magnitude was found among plots (CV = 0.24, CV = 0.50) than among years (CV = 0.16, CV = 0.29).

Soil temperatures were highly influenced by snowpack magnitude during the snow-covered period. Both variables presented a non-linear relationship (Figure A.3); thus, snow presence induced soil cooling until insulation. Snowpacks with more than a 65 cm depth (on average) insulated the ground from winter air temperatures and, consequently, freezing of the soil surface was very rare. On average, soil temperature was 3.3°C higher than air temperature during winter. During spring, the snowpack also insulated the ground; in this case, soil temperature was on average 2.8°C lower than air temperature. Soil warming onset occurred in early May (DOY 125 ± 22), 4 ± 8 days after the melt-out date, and 26 ± 23 days after air warming onset (early April; DOY 99 ± 24) (Table A.2). Soil warming onset differed among plots (SD = 18 days), contrary to air warming onset (SD = 6 days). Soil warming onset was driven by the melt-out date (r = 0.94, $p < 0.05$; Figure A.2). May and June soil temperature was negatively influenced by melt-out date (Figure A.3). There were lagged effects (1 – 2 months) of snow persistence on soil temperature (in May r = -0.76, $p < 0.05$; in June r = -0.71, $p < 0.05$). Soil temperature also was correlated to air temperature during these months (in May: r = 0.69, $p < 0.05$; in June: r = 0.66, $p < 0.05$). From July onwards, soil temperature was mostly correlated to air temperature.

Soil water infiltration occurred during all snow-covered periods. Soil VWC peaked in late April (DOY 120 ± 17), 46 ± 36 days after the SWE peak, either before (2 ± 28 days) or after (23 ± 27 days) the melt-out date (Table A.2). No significant correlation was found in timing or magnitude between the soil VWC and SWE peaks. Positive relationships were found between snowmelt and soil VWC on a monthly scale (Figure A.4), being more frequent in Plot 1. This influence was stronger when larger melt occurred, i.e. in April and May (Figure A.4). No statistically significant correlations were found when lagged effects (1 or 2 months) of snowmelt on soil moisture were analyzed (data not shown).

Different microclimatic conditions were observed across plots and years (Table 1; Table A.2). Plot 4 showed the longest and thickest snowpacks, and the coldest air and soil temperatures during winter and TGS. Plot 3 showed the shortest and shallowest snowpacks, the warmest winter air temperature and TGS, and the highest soil VWC all year round. Plots 1 and 2 presented similar winter temperature and March snow depth. Plot 2 showed the warmest soil temperature during TGS. Plot 1 showed the lowest soil VWC values during TGS and reached the minimum soil VWC values earlier. In 2018, the longest and deepest snowpack, and the largest soil VWC and air humidity values during TGS were reached. In 2016, significantly warmer air and soil TGS temperatures were observed, whilst during 2017 the opposite was found. In 2017, the shortest snow season and, as a result, the earliest melt-out dates were observed.

3.1. uncinata radial-growth characterization

Stem radial increment lasted on average 91 ± 44 days; it began in mid-May (DOY 130 ± 15) and finished in August (DOY 221 ± 33) (Figure 2a; Table 2). Overall, the annual stem radial increment was 1.0 ± 0.7 mm. More variability in the duration of the radial increment period was found among plots (CV = 0.40) than among years (CV = 0.23). More variability in seasonal radial change was also found among plots (CV = 0.75) than among years (CV = 0.21). Based on estimated daily rates of stem radial increment (Figure 2b, Table 2), growth peaked in mid-June (DOY 162 ± 9). Again, more variability was found in the magnitude of maximum rates of radial increment among plots (CV = 0.49) than among years (CV = 0.22).

In 2018, the duration of the radial increment period was longer, the radial increment was higher and rates of radial increment were the lowest, followed by 2017. The maximum rates occurred earlier in 2017 than in other years. Plot 4 showed the longest radial increment periods, the highest and latest rates of radial increment and the largest total radial increment; followed primarily by plot 3. Plot 1 showed the lowest values for the mentioned variables.

The onset of tracheid formation, i.e. when the first enlarging tracheids were formed, occurred in mid-May (Figure 3a). The number of radially enlarging tracheids peaked from mid-May to late June. Tracheid maturation ended in October, when the thickening phase finished. Based on Gompertz models adjusted to the cumulative sum of mature cells, the estimated timing of growth season differed slightly from the previously noted (Figure 3b). The formation of mature tracheids started in early June (DOY 160 ± 7) and finished in October (DOY 286 ± 20) (Table 2). Maximum rates of production of mature tracheids (0.57 ± 0.28 cells day^{-1}) occurred in mid-July (DOY 202 ± 20)

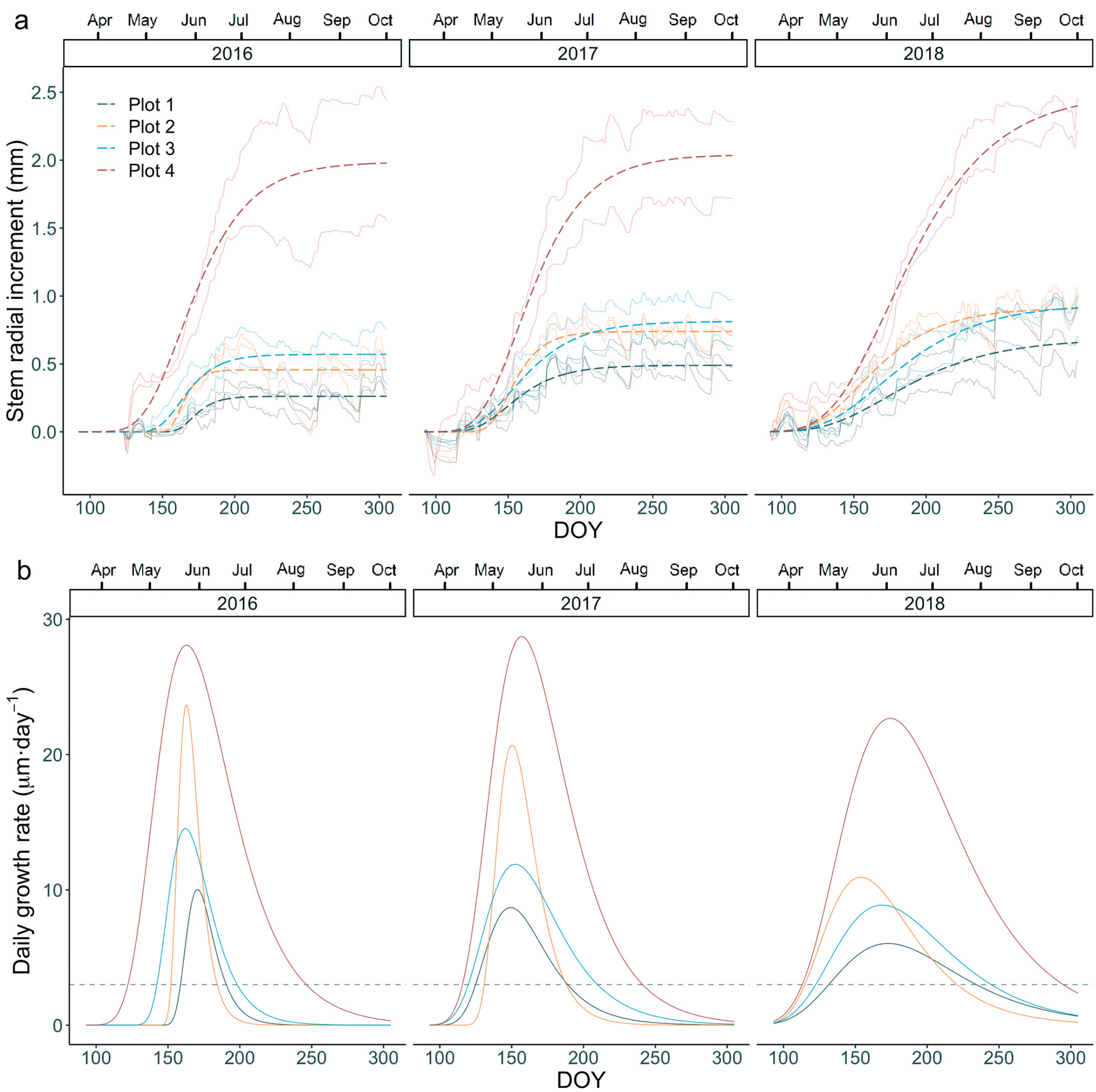

Figure 2. (a) Time series of stem daily maximum radius by tree (solid lines) and same series adjusted to Gompertz function at plot level (dashed lines) during 2016, 2017 and 2018. (b) Estimated daily rates of stem radial increment by plot during 2016, 2017 and 2018. Timing is represented by the day of the year (DOY). Dashed lines in the bottom panels represent daily growth rates equal to 3 μm•day^{-1}.

(Figure 3c). A high variability was found in the magnitude of maximum rates of production of mature tracheids among plots (CV = 0.51), but not among years (CV = 0.17).

The production of mature tracheids started and peaked earlier in 2017 but lasted longer in 2016 (Figure 3c). Plot 4 showed the longest period of production of mature tracheids, and the highest production rate, followed by plot 3, whereas plot 1 showed the lowest values for the mentioned variables.

3.2. Needle and shoot phenology

In 2016, the onset of shoot elongation occurred earlier (May) than in 2017 (early June). A 55% smaller shoot length was reached in 2016 than in 2017 (Figure A.5.). For needles, the onset of elongation occurred later in 2016 (late June) than in 2017 (early June). A 15% longer needle was formed in 2016. The highest shoot and needle growth rates took place in plot 1, whilst the smallest rates were observed in plot 4.

3.3. Needle and sapwood non-structural carbohydrate (NSC) concentrations

Sapwood SS and starch concentrations peaked in October, whereas needle SS concentrations peaked in August or before (April, June). Needle starch concentrations peaked in June (plots 1 and 2), April (plot

Table 2
Growth characteristics considering stem radius increment and production of mature tracheids. Average values during 2016, 2017 and 2018 at each plot are shown.

		Stem radius increment						Mature tracheids					
Year	Plot	Total radial increment (mm•y − 1)	Onset (DOY)	Cessation (DOY)	Duration (days)	Max rate (µm•d − 1)	Timing of max rate (DOY)	Cell production (N° mature trach•y − 1)	Onset (DOY)	Cessation (DOY)	Duration (days)	Max rate (n° mat trach•d − 1)	Timing of max rate (DOY)
2016	1	0.26	159	191	32	10	171	30	163	297	134	0.23	221
	2	0.46	153	185	32	24	163	25	162	285	123	0.28	201
	3	0.57	143	199	56	15	162	70	162	302	140	0.62	222
	4	1.99	123	247	124	28	163	90	172	305	133	0.89	228
2017	1	0.49	125	189	64	9	149	21	161	246	85	0.42	182
	2	0.74	131	189	58	21	150	32	155	282	127	0.41	190
	3	0.81	120	210	90	12	153	35	151	272	121	0.76	172
	4	2.04	116	242	126	29	157	78	153	298	145	0.97	197
2018	1	0.69	132	235	103	6	173	–	–	–	–	–	–
	2	0.91	115	221	106	11	154	–	–	–	–	–	–
	3	0.94	123	245	122	9	169	–	–	–	–	–	–
	4	2.50	114	295	181	23	174	–	–	–	–	–	–

3) or October (plot 4). In 2016, maximum NSC concentrations in needles were reached in April in plot 4, June in plot 2 and August in plots 1 and 3 (Table 3). In sapwood, maximum TNC were reached in all plots in October. There was no significant difference in needle and sapwood NSC concentrations among plots.

3.4. Microclimate influences on growth

Soil temperature was the microclimate variable most related to xylogenesis during June (when the first mature tracheids were observed) and September (during the final phase of tracheid maturation) (Figure 4a). The positive influence of soil temperature on growth mainly occurred throughout the entire spring. Soil temperatures (7-day mean) were 10.4 ± 1.4 °C and 7.9 ± 2.8 °C when the first and last mature tracheids were formed, respectively. A later soil warming onset can delay and therefore shorten the growing season, and this was related to a lower growth rate (see Figure A.6). This was observed in 3 out of the 4 studied plots, with plot 4 not showing this relationship. Air temperature showed positive correlations to xylem development rates in May, when the first radially enlarging tracheids were detected. Air and soil temperatures (7-day mean) were 6.1 ± 3.1 °C and 5.6 ± 3.6 °C, respectively, when the first radially enlarging tracheids were observed. Mostly negative correlations of xylem development rates with soil VWC were found during September and during the spring in plot 4. An exception was the positive correlation found in plot 1 with April soil VWC.

For radial increment rates, air temperature was the variable that most related to these rates during May in all plots (Figure 4b). In most plots, soil temperatures were also relevant to the onset of stem radial increment. Air and soil temperatures (7-day means) were 8.4 ± 4.5 °C and 5.9 ± 4.7 °C respectively, when the stem radial increment began. July air H and July-August soil VWC were positively correlated to stem radial increment rates in all plots. Maximum radial increment rates occurred about 10 days earlier (± 9 days) than maximum day length.

The first principal component (PC1) of the first PCA explained 55.3% of the variability (Table A.3). Air T, soil T and xylem development rates spread along the PC1 axis increasing in same direction, while soil VWC increased in the opposite direction. Rates of production of mature tracheids were highly and positively related to soil temperature, followed by air temperature (Figure 5a). As air H spread along the second principal component (PC2), explaining only a small percentage of variability (18.16 %), its influence on formation of mature tracheids was low. The PC1 of the second PCA, performed considering all microclimate variables and radial increment rates, explained 49.9% of the variability. All microclimate variables spread along the PC1 axis, where air and soil T increased in the opposite direction of air H and soil VWC (Table A.3). Radial increment rates spread alone along the PC2 axis (22.1 %). Among microclimate variables, soil VWC was related to radial increment rates (Figure 5b), followed by air H.

4. Discussion

Evidence has been presented to show how snow dynamics influence seasonal growth dynamics by influencing soil temperature in mountain forests. Soil temperature was the microclimate variable most relevant to the production of mature tracheids, highly influencing timing (onset and cessation) and resulting growth rates. As snowpack duration determines soil warming at the beginning of the growing season, a larger and more lasting snowpack induces a retarded cambial reactivation and is related to lower growth rates. Hence, this study at intra-annual scale, confirms what Sanmiguel-Vallelado et al. (2019) found at inter-annual scale in a tree-ring network of *P. uncinata* forests. The results provide additional information about the effects of climate and soil temperature and humidity conditions on radial growth

The winter snow accumulation, the time of melt-out date, the onset of the growing season and the growth rates were strongly interrelated (Helama et al., 2013; Kirdyanov et al., 2003). In this study it was observed that larger snow accumulation involved later snow depletion that, in connection with lower spring air temperatures, produced a delay in soil warming onset and in tracheid maturation. Therefore, the most limiting factor to xylem development found in this study was low soil temperature in June. On the one hand, the soil cooling induced by snow presence can be explained by the effects of high snow albedo and high latent heat due to snowmelt is a heat sink (Zhang, 2005). On the other hand, low soil temperatures had been reported to inhibit root activity (Alvarez-Uria and Körner, 2007), which could explain an indirect effect on cambium reactivation in the spring, since roots provide water and nutrients to meristems such as the cambium. Several potential physiological mechanisms by which cool soils may limit conifer growth have been described in the literature. Kozlowski (1964) suggested that trees cannot uptake water through their roots and initiate hydraulic and metabolic processes until snowpacks wane to a threshold at which soil temperatures increase and viscosity decreases. CO_2 uptake was decreased at low root temperatures and appeared to be influenced by the pattern of nitrogen translocation (Vapaavuori et al., 1992). In cold substrates (< 5°C), root growth in *P. sylvestris* has been found to be constrained by plasma membrane H + -ATPase (PM-ATPase) transport, which has multiple functions in cell growth (Iivonen et al., 1999). Furthermore, Peterson and Peterson (2001) suggest that increased cloudiness, associated with cool springs and late-lying snowpacks, could reduce solar radiation and increase the frequency of photoinhibition following cold nights.

The highest correlation between air temperature and xylem development rates in most plots was found when the first radially enlarging tracheids were formed. By this time, the observed mean air temperature (6°C) is similar to the 5°C minimal air temperature threshold proposed by Rossi et al. (2008) for conifers from cold sites. Previous tree-ring studies demonstrated that low air temperatures during the growing

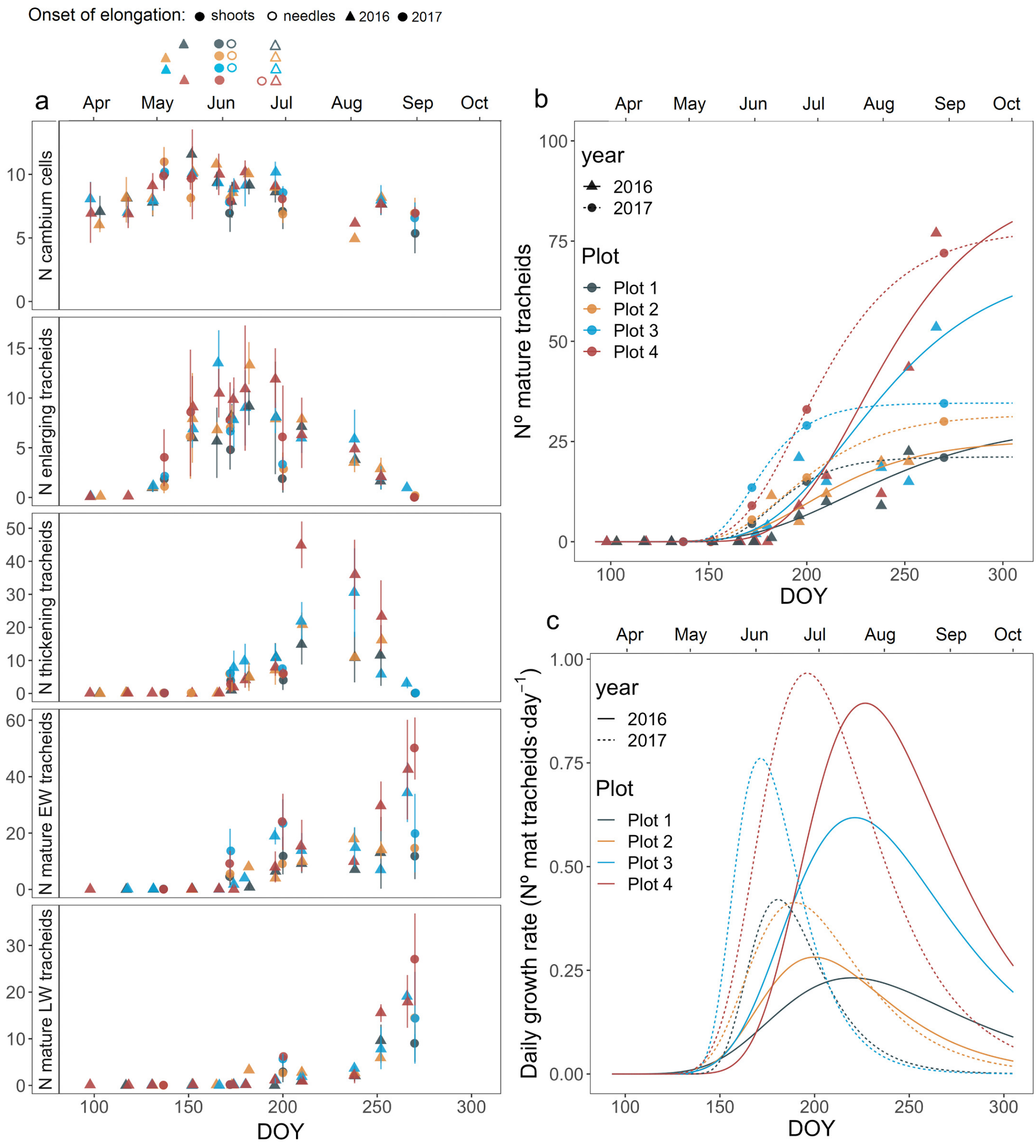

Figure 3. (a) Number of cambial cells and number of tracheids in the radial enlarging, wall-thickening and mature phases during 2016 and 2017. Median values by plot are shown. Bars represent inter-tree variability (standard deviation). Over the top of the plot the onset of shoot and needle elongation for each study plot and year are indicated. (b) Observed (dots) and Gompertz-modelled (lines) function of the number of mature tracheids during 2016 and 2017. (c) Estimated daily rates of production of mature tracheids by plot (daily number of produced mature tracheids) during 2016 and 2017. Timing is represented by the day of the natural year (DOY).

season limit growth of *P. uncinata* (Andreu et al., 2007; Camarero et al., 1998; Galván et al., 2014; Rolland and Schueller, 1994; Tardif et al., 2003). Nevertheless, due to the stronger coupling between mature tracheids and soil temperature observed in this study, we argue that 10°C soil temperature when first mature tracheids were developed should be also considered.

Tracheid maturation onset always occurred after complete melt-out. In most cases, it was observed that a later tracheid maturation leads to a shorter growing season and, therefore, limits growth and wood production (Lenz et al., 2013). The observed reduction in growth rates

Table 3
Average needle and sapwood concentrations (%) as soluble sugars (SS), starch and total non-structural carbohydrates (TNC) during 2016.

	Plot	Needles				Sapwood			
		April	June	August	October	April	June	August	October
SS	1	5.6	6.7	5.4	4.8	0.7	0.7	0.6	1.4
	2	4.6	7.6	10.5	7.2	3.9	4.0	3.9	5.6
	3	10.2	14.2	15.8	12.0	4.6	4.7	4.6	6.9
	4	5.4	4.6	3.9	4.2	0.5	0.7	0.7	1.0
Starch	1	14.1	20.4	6.7	7.9	3.4	3.9	3.7	4.8
	2	19.5	25.0	10.6	12.1	3.9	4.6	4.4	5.8
	3	5.5	4.6	5.2	4.8	0.6	0.6	0.8	1.1
	4	8.9	5.4	9.9	4.9	3.0	3.5	3.4	4.3
TNC	1	14.3	10.0	15.2	9.7	3.6	4.1	4.2	5.5
	2	5.9	4.7	7.0	4.2	1.5	0.8	1.1	1.2
	3	9.3	6.9	5.5	6.4	4.3	4.7	4.4	5.2
	4	15.2	11.6	12.5	10.6	5.8	5.5	5.4	6.4

induced by snow-related cold soil temperatures is more relevant to wood production than growing season duration (Cuny et al., 2015). Apart from that, low soil temperatures in September reduced xylem development; therefore, the soil cooling in early autumn seems also to affect the last phases of xylogenesis (Cuny et al., 2014). These results agree with the negative influences that Sanmiguel-Vallelado et al. (2019) found between winter snow accumulation and late spring snow presence on *P. uncinata* growth and provide an in-depth explanation at a finer temporal resolution.

Although the highest NSC concentration in sapwood was found in the coldest plot, no difference in NSC concentration was found among plots along the altitudinal gradient, and there was no link with growth dynamics. Similarly, Gruber et al. (2011) did not find evidence that an insufficient carbon balance limits growth at their upper elevational limit. This confirms that radial growth and the storage and mobilization of carbon pools are not necessarily coupled (Körner, 2012). The needle starch concentration was observed when needles started elongating during June in some plots (e.g. plot 2), and this was followed by a peak in SS concentration in August, suggesting the differential use of these NSCs to build the new foliage. Since highest NSC concentration in sapwood occurred in October, when xylogenesis finished, the observed dynamics of sapwood NSC did not follow xylogenesis, whereas in other studies they were more coupled to latewood formation (Oberhuber et al., 2011).

The onset of stem radial increment in *P. uncinata* (DOY 130 ± 15), occurred on average 15 days in advance of the onset of mature tracheid formation, probably reflected the date when stem re-hydration started (Zweifel et al., 2000). We observed a value of 6 °C in 7-day average soil temperature for the onset of stem radial increment, which agrees with the fact that soil temperatures lower than 6°C inhibit water uptake by roots in several conifers (Alvarez-Uria and Körner, 2007). As water from snow melting infiltrates into the soil during winter, it is available for trees even before the complete snow depletion, once the soil starts warming and triggers fine root activity. Warmer air temperatures in May – we observed a value of 8 °C in 7-day average air temperature for the onset of stem radial increment – promoted stem radial increment rates in the study area, may be because they facilitated water release from snow – we observed an important water contribution to soil moisture from snowmelt in that time – and stimulated cambium resumption (Camarero et al., 1998) Radial increment rates were mainly driven by soil moisture and air humidity, reflecting the strong linkage between stem radial fluctuations and changes in tree water status even in high-elevation forests (Zweifel et al., 2000). However, only a positive influence of early spring snowmelt on xylem development was observed in plot 1, where the lowest soil moisture values are found. Therefore, we cannot demonstrate that snowmelt water promoted *P. uncinata* growth in the study site. Similarly, Turcotte et al. (2009) reported that growth initiation in black spruce was not limited by the spring rehydration. This soil moisture limitation was reported in more arid mountain ranges (St. George, 2014). The cessation of the stem radial increment period and the start of latewood formation are triggered by warm-dry air and soil conditions in summer.

We found no clear microclimate influences on maximum rates of production of mature tracheids or radial increment, neither in terms of timing nor in magnitude. It has been reported that the maximum growth rates of conifers from cold sites synchronized with the longest day in the year (Rossi et al., 2006). Our observations agree with this idea since stem radial maximum rates occurred around 10 days earlier than the summer solstice.

We also observed a high variability in small spatial scale in microclimate conditions and also in tree growth and NSCs. All plots showed similar snow influences on seasonal growth dynamics, with some variation in strength; however, when considering annual snow-growth effects and the inter-plot variability, plot 4 stepped out of line. This plot (the coldest site situated at highest elevation and with a northern aspect) showed the longest growing season and largest growth rates despite the presence of the longest-lasting snowpacks, contrary to what was expected. This behavior in plot 4 could be explained by high solar radiation values in spring. In addition, more water availability, and for longer periods, may prevent *P. uncinata* from drought, in contrast to what can occur when water is scarce during summer in shallow and rocky soils (Galván et al., 2014). However, more research will be needed to determine which ultimate factors determine the differences between plots. Therefore, *P. uncinata* growth was determined, to a large extent, by snow dynamics in 3 out of the 4 studied plots. Excepting plot 4, a later snow melt-out date delayed and shortened the *P. uncinata* growing season, thus reducing growth. Rossi et al. (2011) previously confirmed that delayed snowmelt reduced growth in boreal forests of *Picea mariana* in Quebec, Canada. Previously, Vaganov et al. (1999) found that in the Russian taiga conifers showed a lower growth when snow melt was delayed in the early growing season. This study extends these observations to high-elevation mountain forests of mid-latitude ranges such as the Pyrenees, and highlights the need to consider the small-scale variability of microclimate effects on individual tree growth of mountain forests.

The abovementioned inter-plot variability in microclimate conditions and tree growth was much larger than inter-annual variability in most cases. Inter-annual variability in growth dynamics may be induced by microclimate conditions, at least in a part. For example, in 2016, the warmest air and soil temperatures observed during the TGS might promote the highest production of mature tracheids. All our four sites are mainly characterized by temperature limitation of growth, as we have discussed previously. Therefore, low temperatures during the growing season limit the tree growth (Rossi et al., 2008). In 2017, the earliest melt-out dates might lead to the earliest starting and peaking date of mature tracheids production. We previously mentioned that the energy-limited influence of snow on studied forest, due to long-lasting snowpacks, could be an appropriate explanation for the positive influence of soil temperature on tree growth found in this study (Helama et al., 2013; Kirdyanov et al., 2003). In 2018, the highest

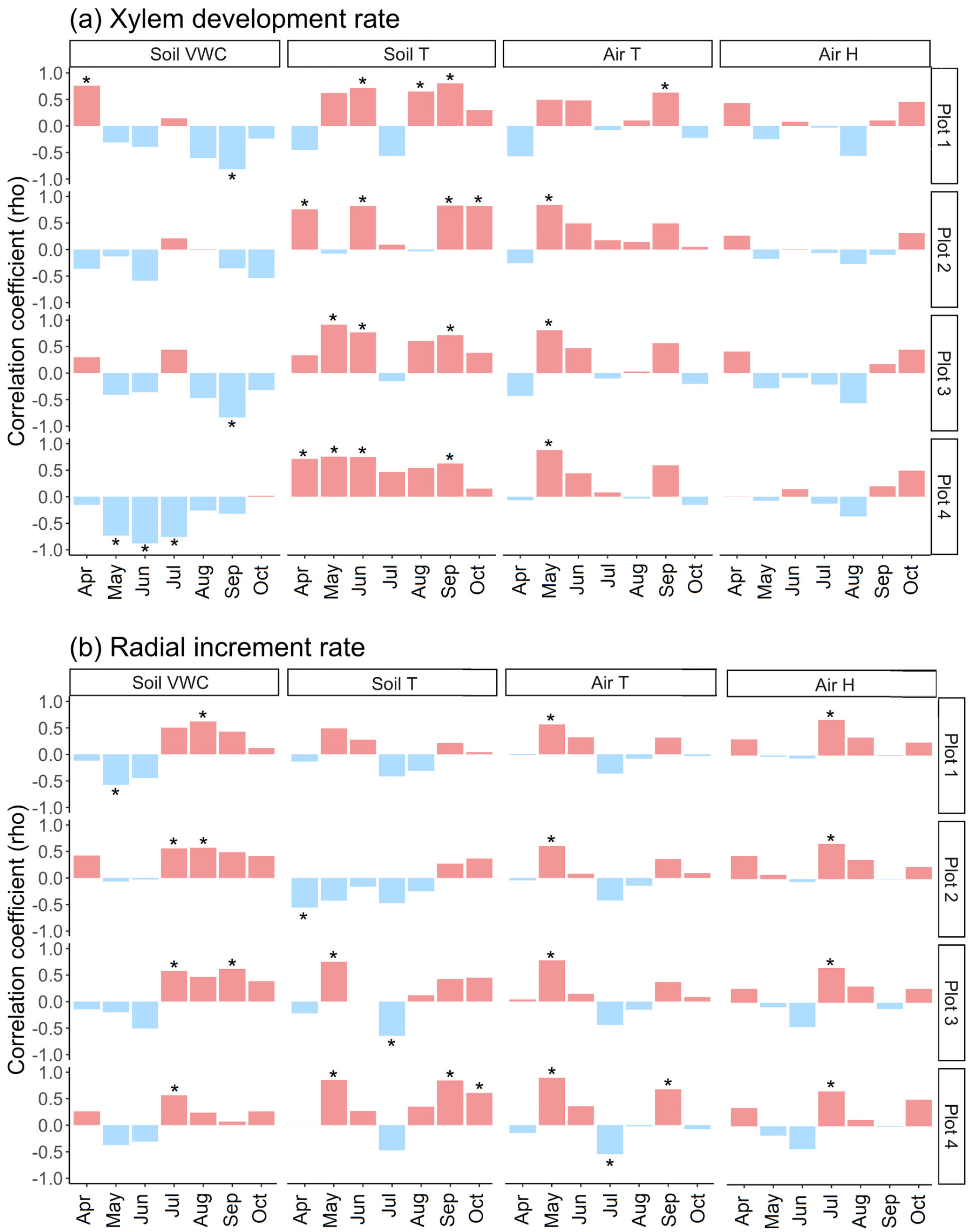

Figure 4. Spearman rho correlation coefficients calculated by month and plot between microclimate variables (weekly averages) and tree growth rates data series (weekly maximum values) of *P. uncinata* during the main growing period. (a) Xylem development rates corresponding to the production of mature tracheids comprised two years (2016, 2017) and (b) radial increment rates series comprised three years (2016, 2017, 2018). Therefore, the number of samples varied among correlations; as a consequence, critical values for Spearman coefficients varied too. Asterisks highlight significant correlations ($p < 0.05$).

radial growth observed might reflect the largest soil moisture conditions during the growing season. As previously stated, we found evidence that stem radial fluctuations were strongly related to tree hydrous state in the studied forests (Zweifel et al., 2000).Under the current climate warming context, increasing trends in air temperature had been already reported in the Spanish Pyrenees (El Kenawy et al., 2011). Future warmer air and soil temperatures are expected to prolong the *P. uncinata* growing season, and therefore, to enhance growth of

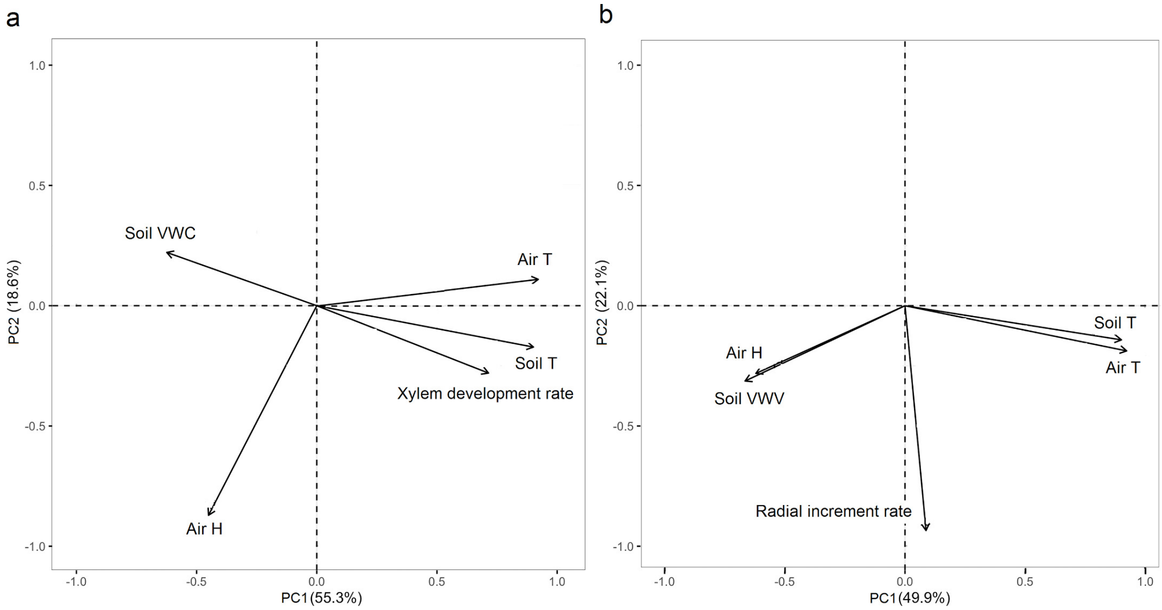

Figure 5. Principal component analysis of microclimate variables (weekly averages) and *P. uncinata* tree growth rates (weekly maximum values) during the main growing period. (a) Xylem development rates series corresponding to the production of mature tracheids comprised two years (2016, 2017) and (b) radial increment rates series comprised three years (2016, 2017 and 2018).

Pyrenean high-elevation forests and treelines during the late 21st century (Camarero et al., 2017; Sánchez-Salguero et al., 2012). An increase in precipitation variability has been also reported in this mountain range (López-Moreno et al., 2010). Therefore, these forecasts could be amplified if climate change also affects snow dynamics (accumulation, duration and melting) leading to shallower snowpacks and a longer snow-free period (Alonso-González et al., 2020; Morán-Tejeda et al., 2017; López-Moreno et al., 2017). Overall, growth of high-elevation *P. uncinata* novel forests could be benefited from the projected future snow and air temperature projections. This positive effect could be explained by a longer growing season, and a subsequently enhanced growth rate due to an earlier rise and a later cooling of soil temperatures. Faster growth rates are related to shorter tree longevity, and it is expected to lead to a reduced capacity of old forest ecosystems to store carbon under warmer future (Büntgen et al., 2019), but new young forests could also represent relevant carbon pools.

5. Conclusions

The seasonal growth dynamics of high-elevation *P. uncinata* forests were affected by snow dynamics. Soil temperature was the most relevant microclimate variable during the overall xylogenesis, mainly influencing the production of mature tracheids. Larger snow accumulation involved later snow depletion that produced a delay in soil warming onset. Low soil temperatures in spring, due to prolonged snow persistence, retarded the cambial onset and reduced growth rates. Wood production was affected by snow dynamics in three out of the four studied plots through a delayed and shorter growing season. This study highlights the large role of early and late growing season soil temperatures on radial growth, in addition to the widely reported effect of air temperature. A future shallower and more ephemeral snowpack in similar mountain, young forests, together with warmer air and soil temperatures, may enhance productivity and tree growth by prolonging the growing season through an earlier onset and a late cessation of xylogenesis.

Declaration of Competing Interest

The authors declare that they have no known competing financial interests or personal relationships that could have appeared to influence the work reported in this paper.

Acknowledgements

We sincerely thank colleagues, friends and relatives who helped during the field surveys. This study was supported by the projects: "*Bosque, nieve y recursos hídricos en el Pirineo ante el cambio global*" funded by Fundación Iberdrola, CGL2014-52599-P (IBERNIEVE) and CGL2017-82216-R (HIDROIBERNIEVE) funded by the Spanish Ministry of Economy and Competitiveness. ASV was supported by a pre-doctoral University Professor Training grant [FPU16/00902] funded by the Spanish Ministry of Education, Culture and Sports. EAG was supported by a pre-doctoral FPI grant [BES-2015-071466] funded by the Spanish Ministry of Economy and Competitiveness. JJC, AG and MC acknowledge funding by project RTI2018-096884-B-C31 (Spanish Ministry of Economy and Competitiveness).

Appendix

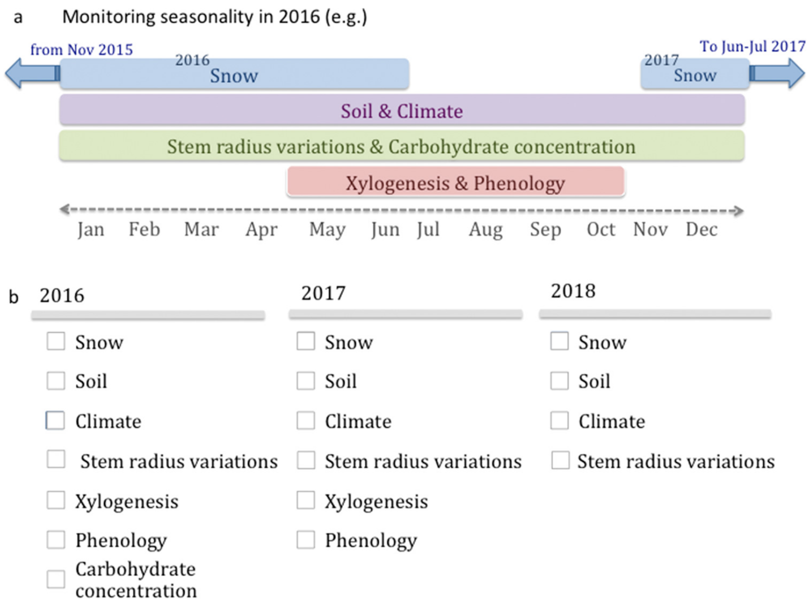

Figure A.1. (a) Monitoring seasonality throughout 2016 as an example of one year of data collection, and (b) differences in variables acquired among years.

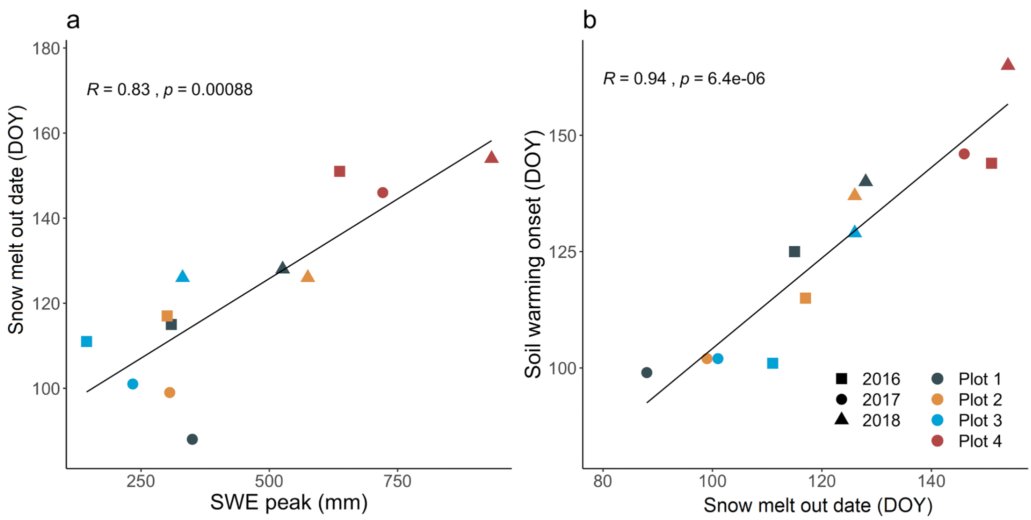

Figure A.2. Scatterplot of the relationships between (a) SWE peak and snowmelt out date and (b) between snow melt out date and soil warming onset. Pearson correlation coefficients between indices and *p* values are shown.

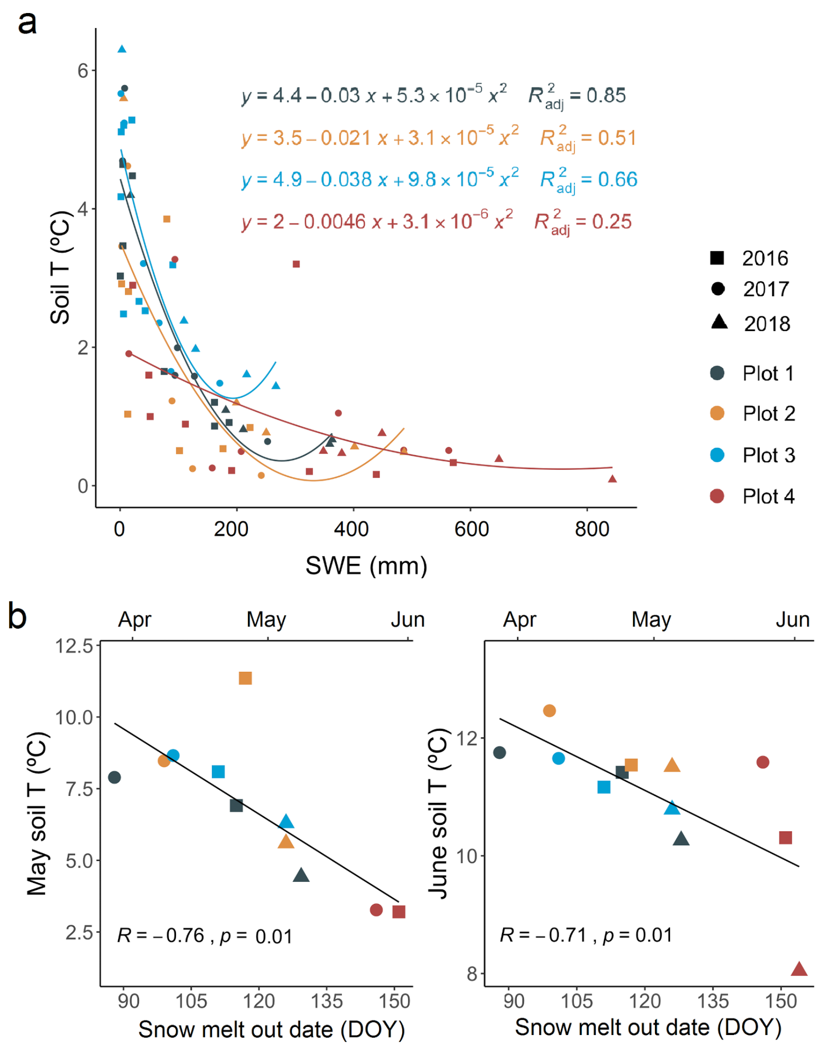

Figure A.3. (a) Polynomial regressions between monthly averages of SWE and soil temperature by plot for the four study plots considering data collected during 2016, 2017 and 2018. (b) Scatterplots of timing of melt-out date and May and June soil temperatures considering data collected during 2016, 2017 and 2018. Pearson correlation coefficients and p values are shown.

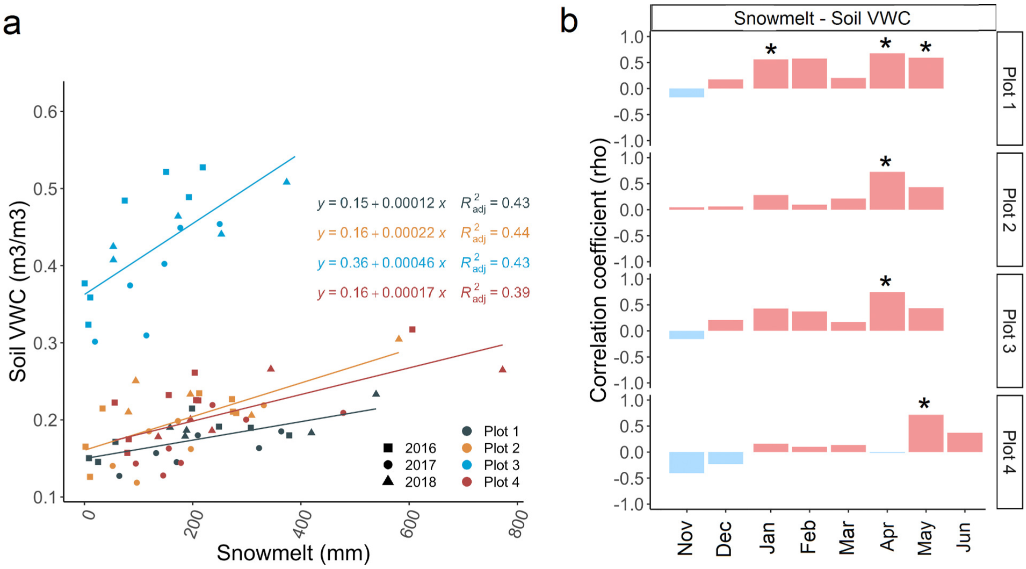

Figure A.4. (a) Linear regressions between monthly sums of snowmelt and monthly averages of soil VWC by plot considering data collected during 2016, 2017 and 2018 (b) Spearman correlation coefficients calculated by month and plot between snowmelt weekly sums and soil VWC weekly averages considering data collected during 2016, 2017 and 2018. Asterisks highlight significant correlations ($p < 0.05$). Note that the number of samples and significance levels varied among months and plots.

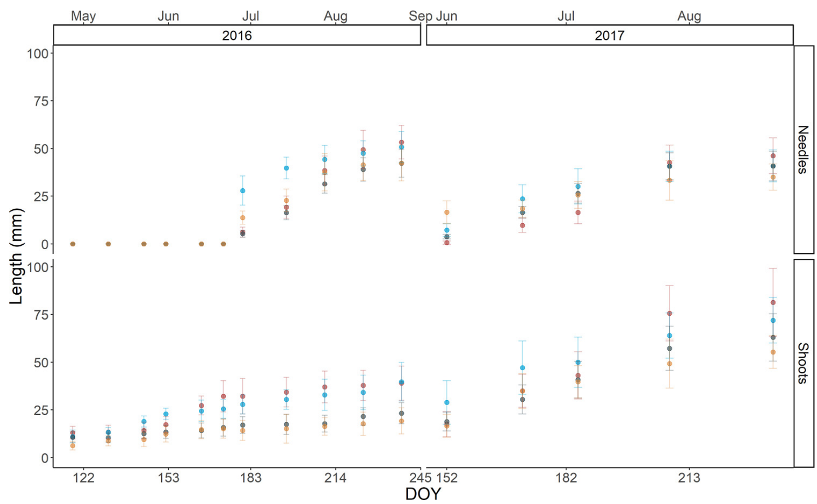

Figure A.5. Time series of needle (top panel) and shoot (bottom panel) length during the 2016 and 2017 growing seasons (dots: mean values; error bars: standard deviation). Timing is represented by the day of the natural year (DOY).

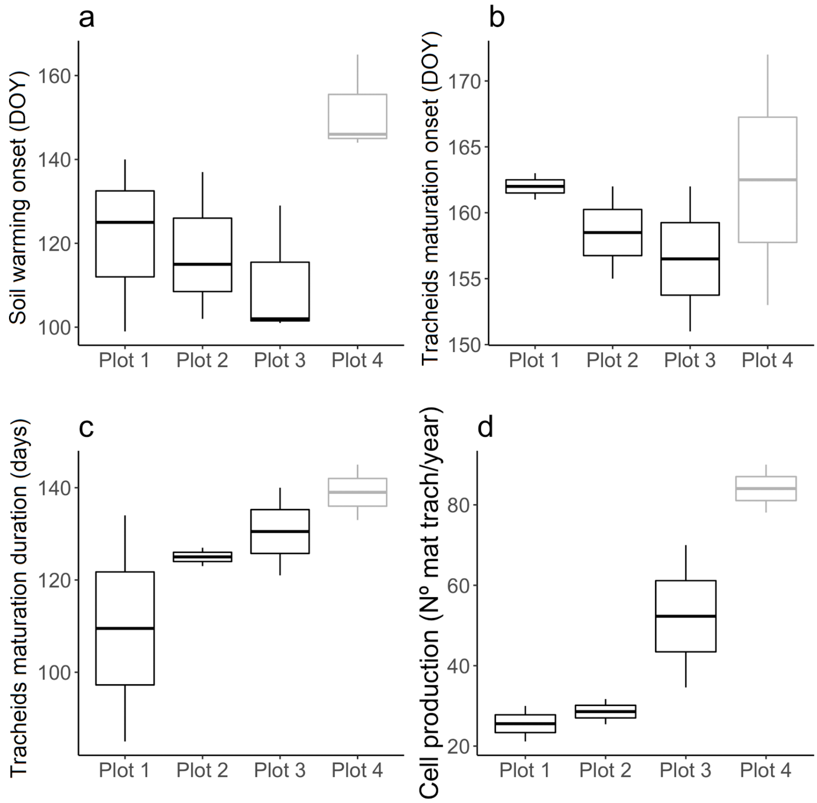

Figure A.6. Boxplots of related soil temperature and xylogenesis variables: (a) soil warming onset, (b) tracheid maturation onset, (c) tracheid maturation duration and (d) rate of production of mature tracheids. In grey, plot 4 was highlighted since it presented "outlier" microclimate conditions and growth characteristics.

Table A.1
Descriptive indices calculated from tree growth data.

	Index	Description
Stem radial increment	Total stem radial increment	Parameter A of Gompertz function adjusted to daily maximum radius series (upper asymptote).
	Stem radial increment onset	Date when daily rates of radial increment exceeded 3 μm•day − 1.
	Stem radial increment cessation	Date when daily rates of radial increment fell below 3 μm•day − 1.
	Stem radial increment duration	Time between the onset and cessation dates of stem radial increment.
	Maximum rate of radial increment	Maximum value obtained from estimated daily rates of radial increment series.
	Timing of maximum rate of radial increment	Date when maximum rate of radial increment was reached.
Mature tracheids	Production of mature tracheids	Parameter A of Gompertz function adjusted to mature cell number increase series (upper asymptote); i.e. number of mature tracheids developed per year.
	Maturation onset	Date when first mature tracheid was completely developed, obtained from Gompertz function adjusted to mature cell number increase series.
	Maturation cessation	Date when last mature tracheid was completely developed, obtained from Gompertz function adjusted to mature cell number increase series.
	Maturation duration	Time between the onset and cessation dates of tracheid maturation.
	Maximum rate of mature tracheid development	Maximum value obtained from estimated daily rates of mature tracheid development series.
	Timing of maximum rate of mature tracheid development	Date when maximum rate of mature tracheid development was reached.
Shoot and needle phenology	Onset of shoot elongation	First day when an increment in shoot length was recorded after dormancy.
	Shoots final lenght	Maximum shoot length recorded.
	Onset of needle elongation	First day when an increment in needle length was recorded after dormancy.
	Needle final length	Maximum needle length value recorded.

Table A.2
Average microclimate conditions during each year at each plot.

		Snowpack ‡					Soil									Air				
Year	Plot	Accum. Onset (DOY)	Melt out date (DOY)	Duration (days)	SWE peak (mm)	Day of SWE peak (DOY)	Infilt. onset (DOY)	VWC peak (m3•m−3) †	Day of VWC peak †	VWC during TGS (m3•m−3)	Min VWC (m3•m−3)	Day of min VWC (DOY)	Warming (DOY)	T during TGS (°C)	Cooling (DOY)	Warming (DOY)	Duration of TGS (days)	T during TGS (°C)	Cooling (DOY)	H during TGS (%)
2016	1	2	115	114	309	47	7	0.24	130	0.10	0.01	252	125	11.7	311	125	184	11.6	309	63.6
	2	347	117	137	301	80	350	0.29	130	0.14	0.04	252	115	12.2	311	108	201	11.5	309	62.7
	3	2	111	110	144	75	3	0.58	91	0.24	0.06	252	107	10.9	326	107	202	12.5	309	62.4
	4	347	151	171	637	104	350	0.41	130	0.15	0.03	252	144	11.2	286	138	147	11.7	285	60.3
2017	1	2	88	86	350	45	11	0.21	132	0.12	0.05	235	98	9.3	312	68	240	10.4	308	62.4
	2	328	99	137	306	37	339	0.27	132	0.15	0.08	235	101	9.6	310	68	240	11.0	308	61.6
	3	11	101	90	234	38	14	0.50	133	0.29	0.08	291	101	9.5	330	67	241	11.7	308	61.2
	4	319	146	193	721	85	322	0.28	132	0.15	0.05	235	145	7.7	293	70	238	9.2	308	60.8
2018	1	336	128	158	526	101	348	0.28	99	0.14	0.05	248	139	9.9	308	109	191	11.1	300	72.1
	2	336	126	156	575	80	342	0.37	98	0.18	0.08	218	136	10.9	308	107	193	11.8	300	71.2
	3	336	126	156	331	91	342	0.56	99	0.34	0.11	248	128	10.6	324	107	193	12.4	300	71.4
	4	310	154	210	933	102	329	0.34	129	0.17	0.06	219	164	9.0	300	110	189	10.0	299	70.6

Abbreviations: Accum.: Accumulation; SWE: Snow Water Equivalent, Infilt.: Infiltration, VWC: Volumetric water content, Min: minimum, T: temperature; TGS: Thermal growing season; H: humidity

(‡) To calculate snow indices, snow seasons temporality was taken into account, not natural years (see Figure A.1).

(†) The first peaks of soil moisture at plot 1, plot 2 and plot 3 during 2017 snow season were not considered because they preceded snow accumulation (explained by an extraordinary precipitation event in November 2017, see Figure A.3), thus the second peak was shown here and used in analysis.

Table A.3
Variance accounted for (%) the two first principal components (PC1 and PC2) and correlations between them and original variables (weekly average microclimate conditions and weekly maximum growth rates). Values in bold indicate the two variables which contributed the most to each PC.

Variable	PCA 1: mature tracheid production		PCA 2: stem radial increment	
	PC1 (55.3%)	PC2 (18.6%)	PC1 (49.9%)	PC2 (22.1%)
Soil T	0.54	-0.18	0.57	-0.14
Soil VWC	-0.38	0.23	-0.42	-0.29
Air T	0.55	0.11	0.58	-0.18
Air H	-0.27	-0.90	-0.39	-0.27
Daily growth rate	0.43	-0.29	0.06	-0.89

References

Albrich, K., Rammer, W., Seidl, R., 2020. Climate change causes critical transitions and irreversible alterations of mountain forests. Glob. Change Biol. https://doi.org/10.1111/gcb.15118.

Alonso-González, E., López-Moreno, J.I., Navarro-Serrano, F., Sanmiguel-Vallelado, A., Aznárez-Balta, M., Revuelto, J., Ceballos, A., 2020. Snowpack Sensitivity to Temperature, Precipitation, and Solar Radiation Variability over an Elevational Gradient in the Iberian Mountains. Atmos. Res. 243, 104973. https://doi.org/10.1016/j.atmosres.2020.104973.

Alvarez-Uria, P., Körner, C., 2007. Low temperature limits of root growth in deciduous and evergreen temperate tree species. Funct. Ecol. 21, 211–218. https://doi.org/10.1111/j.1365-2435.2007.01231.x.

Andreu, L., Gutiérrez, E., Macias, M., Ribas, M., Bosch, O., Camarero, J.J., 2007. Climate increases regional tree-growth variability in Iberian pine forests. Glob. Change Biol. 13, 804–815.

Antonova, G.F., Stasova, V.V., 1993. Effects of environmental factors on wood formation in Scots pine stems. Trees 7 (4), 214–219. https://doi.org/10.1007/BF00202076.

Babst, F., Bouriaud, O., Poulter, B., Trouet, V., Girardin, M.P., Frank, D.C., 2019. Twentieth century redistribution in climatic drivers of global tree growth. Sci. Adv. 5 eaat4313.

Barnett, T.P., Adam, J.C., Lettenmaier, D.P., 2005. Potential impacts of a warming climate on water availability in snow-dominated regions. Nature 438 (7066), 303–309. https://doi.org/10.1038/nature04141.

Beniston, M., 2012. Is snow in the Alps receding or disappearing? Wiley Interdiscip. Rev. Clim. Change 3, 349–358.

Breiman, L., 2001. Random forests. Mach. Learn 45, 5–32.

Büntgen, U., Krusic, P.J., Piermattei, A., Coomes, D.A., Esper, J., Myglan, V.S., Kirdyanov, A.V., Camarero, J.J., Crivellaro, A., Körner, C., 2019. Limited capacity of tree growth to mitigate the global greenhouse effect under predicted warming. Nat. Commun. 10, 2171. https://doi.org/10.1038/s41467-019-10174-4.

Camarero, J.J., Guerrero-Campo, J., Gutierrez, E., 1998. Tree-Ring Growth and Structure of Pinus uncinata and Pinus sylvestris in the Central Spanish Pyrenees. Arct. Alp. Res. 30, 1. https://doi.org/10.2307/1551739.

Camarero, J.J., Linares, J.C., García-Cervigón, A.I., Batllori, E., Martínez, I., Gutiérrez, E., 2017. Back to the future: the responses of alpine treelines to climate warming are constrained by the current ecotone structure. Ecosystems 20, 683–700.

Camarero, J.J., Olano, J.M., Parras, A., 2010. Plastic bimodal xylogenesis in conifers from continental Mediterranean climates. New Phytol 185, 471–480. https://doi.org/10.1111/j.1469-8137.2009.03073.x.

Cantegrel, R., 1983. Le Pin à crochets pyrénéen: biologie, biochimie, sylviculture. Acta Biol. Mont 2, 87–330.

Carlson, K.M., Coulthard, B., Starzomski, B.M., 2017. Autumn snowfall controls the annual radial growth of centenarian whitebark pine (*Pinus albicaulis*) in the southern Coast Mountains, British Columbia. Canada. Arct. Antarct. Alp. Res. 49, 101–113.

Cuny, H.E., Rathgeber, C.B.K., Frank, D., Fonti, P., Fournier, M., 2014. Kinetics of tracheid development explain conifer tree-ring structure. New Phytol 203, 1231–1241. https://doi.org/10.1111/nph.12871.

Cuny, H.E., Rathgeber, C.B.K., Frank, D., Fonti, P., Mäkinen, H., Prislan, P., Rossi, S., del Castillo, E.M., Campelo, F., Vavrčík, H., Camarero, J.J., Bryukhanova, M.V., Jyske, T., Gričar, J., Gryc, V., De Luis, M., Vieira, J., Čufar, K., Kirdyanov, A.V., Oberhuber, W., Treml, V., Huang, J.-G., Li, X., Swidrak, I., Deslauriers, A., Liang, E., Nöjd, P., Gruber, A., Nabais, C., Morin, H., Krause, C., King, G., Fournier, M., 2015. Woody biomass production lags stem-girth increase by over one month in coniferous forests. Nature Plants 1, 15160. https://doi.org/10.1038/nplants.2015.160.

D'Orangeville, L., Côté, B., Houle, D., Morin, H., Duchesne, L., 2013. A three-year increase in soil temperature and atmospheric N deposition has minor effects on the xylogenesis of mature balsam fir. Trees 27, 1525–1536. https://doi.org/10.1007/s00468-013-0899-4.

Dan Moore,, R., Spittlehouse, D., Story, A., 2005. Riparian microclimate and stream temperature response to forest harvesting: a review. Am. Water Resour. Assoc. 41, 813–834.

Del Barrio, G., Creus, J., Puigdefábregas, J., 1990. Thermal seasonality of the high mountain belts of the Pyrenees. Mt. Res. Dev. 227–233.

Denne, M.P., 1989. Definition of Latewood According to Mork (1928). Am. Water Resour. Assoc. 10, 59–62. https://doi.org/10.1163/22941932-90001112.

Deslauriers, A., Rossi, S., Anfodillo, T., 2007. Dendrometer and intra-annual tree growth: What kind of information can be inferred? Dendrochronologia 25, 113–124. https://doi.org/10.1016/j.dendro.2007.05.003.

Deslauriers, A., Rossi, S., Liang, E., 2015. Collecting and Processing Wood Microcores for Monitoring Xylogenesis, in: Yeung, E.C.T., Stasolla, C., Sumner, M.J., Huang, B.Q. (Eds.), Plant Microtechniques and Protocols. Springer International Publishing, Cham, pp. 417–429. https://doi.org/10.1007/978-3-319-19944-3_23.

El Kenawy, A., López-Moreno, J.I., Vicente-Serrano, S.M., 2011. Recent trends in daily temperature extremes over northeastern Spain (1960–2006). Nat. Hazards Earth Syst. Sci. 11, 2583–2603. https://doi.org/10.5194/nhess-11-2583-2011.

Galván, J.D., Camarero, J.J., Gutiérrez, E., 2014. Seeing the trees for the forest: drivers of individual growth responses to climate in *Pinus uncinata* mountain forests. J. Ecol 102, 1244–1257.

Gruber, A., Pirkebner, D., Oberhuber, W., Wieser, G., 2011. Spatial and seasonal variations in mobile carbohydrates in *Pinus cembra* in the timberline ecotone of the Central Austrian Alps. Eur. J. For. Res 130, 173–179. https://doi.org/10.1007/s10342-010-0419-7.

Harpold, A.A., Molotch, N.P., Musselman, K.N., Bales, R.C., Kirchner, P.B., Litvak, M., Brooks, P.D., 2015. Soil moisture response to snowmelt timing in mixed-conifer subalpine forests: Hydrol. Process 29, 2782–2798. https://doi.org/10.1002/hyp.10400.

Helama, S., Mielikainen, K., Timonen, M., Herva, H., Tuomenvirta, H., Venalainen, A., 2013. Regional climatic signals in Scots pine growth with insights into snow and soil associations. Dendrobiology 70.

Iivonen, S., Rikala, R., Ryyppö, A., Vapaavuori, E., 1999. Responses of Scots pine (Pinus sylvestris) seedlings grown in different nutrient regimes to changing root zone temperature in spring. Tree Physiology 19, 951–958.

Jolliffe, I.T., 2002. Choosing a Subset of principal Components or Variables. Principal Coponent Analysis. Springer Series in Statistics. Springer, New York, NY https://doi.org/10.1007/0-387-22440-8_6.

Kaiser, H.F., 1974. An index of factorial simplicity. Psychometrika 39, 31–36.

Kirdyanov, A., Hughes, M., Vaganov, E., Schweingruber, F., Silkin, P., 2003. The importance of early summer temperature and date of snow melt for tree growth in the Siberian Subarctic. Trees 17, 61–69.

Körner, C., 2012. Alpine treelines: functional ecology of the global high elevation tree limits. Springer Science & Business Media.

Kozlowski, T.T., 1964. Water Metabolism in Plants. Soil Science 98, 143.

Lenz, A., Hoch, G., Körner, C., 2013. Early season temperature controls cambial activity and total tree ring width at the alpine treeline. Plant Ecol. Divers. 6, 365–375. https://doi.org/10.1080/17550874.2012.711864.

López-Moreno, J.I., Gascoin, S., Herrero, J., Sproles, E.A., Pons, M., Alonso-González, E., Hanich, L., Boudhar, A., Musselman, K.N., Molotch, N.P., Sickman, J., Pomeroy, J., 2017. Different sensitivities of snowpacks to warming in Mediterranean climate mountain areas. Environ. Res. Lett. 12 (7), 074006.

López-Moreno, J.I., Vicente-Serrano, S.M., Angulo-Martínez, M., Beguería, S., Kenawy, A., 2010. Trends in daily precipitation on the northeastern Iberian Peninsula, 1955–2006. Int. J. Climatol. 30, 1026–1041.

Lupi, C., Morin, H., Deslauriers, A., Rossi, S., 2012. Xylogenesis in black spruce: does soil temperature matter? Tree Physiol 32, 74–82. https://doi.org/10.1093/treephys/tpr132.

McCabe, G.J., Wolock, D.M., 2009. Recent declines in western US snowpack in the context of twentieth-century climate variability. Earth Interact 13, 1–15.

Morán-Tejeda, E., López-Moreno, J.I., Sanmiguel-Vallelado, A., 2017. Changes in climate, snow and water resources in the Spanish Pyrenees: observations and projections in a warming climate, in: High Mountain Conservation in a Changing World. Springer, pp. 305–323.

Oberhuber, W., Swidrak, I., Pirkebner, D., Gruber, A., 2011. Temporal dynamics of non-structural carbohydrates and xylem growth in Pinus sylvestris exposed to drought. Can. J. For. Res. 41, 1590–1597. https://doi.org/10.1139/x11-085.

Palacio, S., Maestro, M., Montserratmarti, G., 2007. Seasonal dynamics of non-structural carbohydrates in two species of mediterranean sub-shrubs with different leaf phenology. Env. Exp. Bot. 59, 34–42. https://doi.org/10.1016/j.envexpbot.2005.10.003.

Pederson, G.T., Gray, S.T., Woodhouse, C.A., Betancourt, J.L., Fagre, D.B., Littell, J.S., Watson, E., Luckman, B.H., Graumlich, L.J., 2011. The unusual nature of recent snowpack declines in the North American Cordillera. Science 333, 332–335. https://doi.org/10.1126/science.1201570.

Peterson, D.W., Peterson, D.L., 2001. Mountain Hemlock Growth Responds to Climatic Variability at Annual and Decadal Time Scales. Ecology 82, 3330–3345 https://doi.org/10.1890/0012-9658(2001)082[3330:MHGRTC]2.0.CO;2.

Core Team, R, 2018. R Foundation for Statistical Computing; Vienna, Austria: 2015. R Lang. Environ. Stat. Comput. 2013.

Rasband, W.S., 1997. ImageJ. US National Institutes of Health, Bethesda, MD, USA. http://rsb.info.nih.gov/ij/.

Rodriguez Perez, D., 2013. Growthmodels: Nonlinear Growth Models. R package version 1.2.0. https://CRAN.R-project.org/package=growthmodels.
Rolland, C., Schueller, J.F., 1994. Relationships between mountain pine and climate in the French Pyrenees (Font-Romeu) studied using the radiodensitometrical method. Pirineos 143, 55–70.
Rossi, S., Deslauriers, A., Anfodillo, T., Carraro, V., 2007. Evidence of threshold temperatures for xylogenesis in conifers at high altitudes. Oecologia 152, 1–12. https://doi.org/10.1007/s00442-006-0625-7.
Rossi, S., Deslauriers, A., Anfodillo, T., Morin, H., Saracino, A., Motta, R., Borghetti, M., 2006. Conifers in cold environments synchronize maximum growth rate of tree-ring formation with day length. New Phytol 170, 301–310. https://doi.org/10.1111/j.1469-8137.2006.01660.x.
Rossi, S., Deslauriers, A., Griçar, J., Seo, J.W., Rathgeber, C.B., Anfodillo, T., Morin, H., Levanic, T., Oven, P., Jalkanen, R., 2008. Critical temperatures for xylogenesis in conifers of cold climates. Glob. Ecol. Biogeogr. 17, 696–707. https://doi.org/10.1111/j.1466-8238.2008.00417.x.
Rossi, S., Deslauriers, A., Morin, H., 2003. Application of the Gompertz equation for the study of xylem cell development. Dendrochronologia 21, 33–39. https://doi.org/10.1078/1125-7865-00034.
Rossi, S., Morin, H., Deslauriers, A., 2011. Multi-scale Influence of snowmelt on xylogenesis of Black Spruce. Arct. Antarct. Alp. Res. 43, 457–464. https://doi.org/10.1657/1938-4246-43.3.457.
Rossi, S., Rathgeber, C.B.K., Deslauriers, A., 2009. Comparing needle and shoot phenology with xylem development on three conifer species in Italy. Ann. For. Sci. 66, 206. https://doi.org/10.1051/forest/2008088.
Ruiz de la Torre, J., Ceballos, L., 1979. Arboles y Arbustos de la España Peninsular. ETSI de Montes, Madrid, pp. 512 ISBN 84–600–84–600.
Sánchez-Salguero, R., Navarro-Cerrillo, R.M., Swetnam, T.W., Zavala, M.A., 2012. Is drought the main decline factor at the rear edge of Europe? The case of southern Iberian pine plantations. For. Ecol. Manag 271, 158–169.
Sangüesa-Barreda, G., Linares, J.C., Camarero, J.J., 2012. Mistletoe effects on Scots pine decline following drought events: insights from within-tree spatial patterns, growth and carbohydrates. Tree Physiol 32, 585–598. https://doi.org/10.1093/treephys/tps031.
Sanmiguel-Vallelado, A., Camarero, J.J., Gazol, A., Morán-Tejeda, E., Sangüesa-Barreda, G., Alonso-González, E., Gutiérrez, E., Alla, A.Q., Galván, J.D., López-Moreno, J.I., 2019. Detecting snow-related signals in radial growth of Pinus uncinata mountain forests. Dendrochronologia 57, 125622. https://doi.org/10.1016/j.dendro.2019.125622.
Sanmiguel-Vallelado, A., López-Moreno, J.I., Morán-Tejeda, E., Alonso-González, E., Navarro-Serrano, F.M., Rico, I., Camarero, J.J., 2020. Variable effects of forest canopies on snow processes in a valley of the central Spanish Pyrenees. Hydrol. Process. Hyp 13721. https://doi.org/10.1002/hyp.13721.
St. George, S., 2014. An overview of tree-ring width records across the Northern Hemisphere. Quat. Sci. Rev. 95, 132–150. https://doi.org/10.1016/j.quascirev.2014.04.029.
Stekhoven, D.J., Buhlmann, P., 2012. MissForest–non-parametric missing value imputation for mixed-type data. Bioinformatics 28, 112–118. https://doi.org/10.1093/bioinformatics/btr597.
Tardif, J., Camarero, J.J., Ribas, M., Gutiérrez, E., 2003. Spatiotemporal variability in tree growth in the Central Pyrenees: climatic and site influences. Ecol. Monogr. 73, 241–257.
Truettner, C., Anderegg, W.R.L., Biondi, F., Koch, G.W., Ogle, K., Schwalm, C., Litvak, M.E., Shaw, J.D., Ziaco, E., 2018. Conifer radial growth response to recent seasonal warming and drought from the southwestern USA. For. Ecol. Manag. 418, 55–62. https://doi.org/10.1016/j.foreco.2018.01.044.
Turcotte, A., Morin, H., Krause, C., Deslauriers, A., Thibeault-Martel, M., 2009. The timing of spring rehydration and its relation with the onset of wood formation in black spruce. Agricultural and Forest Meteorology 149, 1403–1409. https://doi.org/10.1016/j.agrformet.2009.03.010.
Vaganov, E.A., Hughes, M.K., Kirdyanov, A.V., Schweingruber, F.H., Silkin, P.P., 1999. Influence of snowfall and melt timing on tree growth in subarctic Eurasia. Nature 400, 149–151. https://doi.org/10.1038/22087.
van der Maaten, E., van der Maaten-Theunissen, M., Smiljanić, M., Rossi, S., Simard, S., Wilmking, M., Deslauriers, A., Fonti, P., von Arx, G., Bouriaud, O., 2016. dendrometeR: Analyzing the pulse of trees in R. Dendrochronologia 40, 12–16. https://doi.org/10.1016/j.dendro.2016.06.001.
Vapaavuori, E.M., Rikala, R., Ryyppö, A., 1992. Effects of root temperature on growth and photosynthesis in conifer seedlings during shoot elongation. Tree Physiology 10, 217–230.
Watson, E., Luckman, B.H., 2016. An investigation of the snowpack signal in moisture-sensitive trees from the Southern Canadian Cordillera. Dendrochronologia 38, 118–130. https://doi.org/10.1016/j.dendro.2016.03.008.
Woelber, B., Maneta, M.P., Harper, J., Jencso, K.G., Gardner, W.P., Wilcox, A.C., López-Moreno, I., 2018. The influence of diurnal snowmelt and transpiration on hillslope throughflow and stream response. Hydrol. Earth Syst. Sc. 22 (8). https://doi.org/10.5194/hess-22-4295-2018.
Zeide, B., 1993. Analysis of growth equations. For. Sci. 39, 594–616.
Zhang, L., Axmacher, J.C., Sang, W., 2017. Different radial growth responses to climate warming by two dominant tree species at their upper altitudinal limit on Changbai Mountain. J. For. Res. 28, 795–804. https://doi.org/10.1007/s11676-016-0364-5.
Zhang, T., 2005. Influence of the seasonal snow cover on the ground thermal regime: An overview. Rev. Geophys. 43. https://doi.org/10.1029/2004RG000157.
Zhang, X., Manzanedo, R.D., D'Orangeville, L., Rademacher, T.T., Li, J., Bai, X., Hou, M., Chen, Z., Zou, F., Song, F., Pederson, N., 2019. Snowmelt and early to mid-growing season water availability augment tree growth during rapid warming in southern Asian boreal forests. Glob. Change Biol. 25, 3462–3471. https://doi.org/10.1111/gcb.14749.
Zweifel, R., Item, H., Häsler, R., 2000. Stem radius changes and their relation to stored water in stems of young Norway spruce trees. Trees 15, 50–57. https://doi.org/10.1007/s004680000072.

Chapter 6

Sensitivity of forest-snow interactions to climate forcing: local variability in a Pyrenean valley

This article was published in:

Sanmiguel-Vallelado, A., McPhee, J., Esmeralda Ojeda Carreño, P., Morán-Tejeda, E., Julio Camarero, J. & López-Moreno, J. I. (2022). Sensitivity of forest–snow interactions to climate forcing: Local variability in a Pyrenean valley. *Journal of Hydrology*, *605*, 127311. https://doi.org/10.1016/j.jhydrol.2021.127311

Authors thank ELSEVIER for the permission to present here the article in its entirely.

Journal of Hydrology 605 (2022) 127311

Contents lists available at ScienceDirect

Journal of Hydrology

journal homepage: www.elsevier.com/locate/jhydrol

Research papers

Sensitivity of forest–snow interactions to climate forcing: Local variability in a Pyrenean valley

Alba Sanmiguel-Vallelado [a,*], James McPhee [b], Paula Esmeralda Ojeda Carreño [b], Enrique Morán-Tejeda [c], J. Julio Camarero [a], Juan Ignacio López-Moreno [a]

[a] Pyrenean Institute of Ecology, CSIC (Spanish Research Council), Zaragoza 50059, Spain
[b] Department of Civil Engineering, University of Chile, Santiago 8370448, Chile
[c] Department of Geography, University of the Balearic Islands, Palma de Mallorca 07122, Spain

ARTICLE INFO

Keywords:
Cold regions hydrological model (CRHM)
Snow processes
Snowpack
Mountain forest
Warming
Snow water equivalent (SWE)

ABSTRACT

Mountain forests affect spatial and temporal variability of snow processes through snow interception and by modifying the energy balance of snowpack. The high sensitivity of snow cover to seasonal temperatures in mid–latitude mountains is well known and is of particular interest with regard to a future warmer climate. The snowpack in the Pyrenees is expected to be the most impacted by climate change in the Mediterranean mountains, where future climate trends project rising temperatures and decreasing precipitation. This study analyzes how changes in temperature and precipitation can affect current forest–snow interactions in four forests, located near each other but under contrasting topographic settings, in the Spanish Pyrenees. This understanding will allow us to anticipate the future hydrological responses of Pyrenean forested mountain basins. The research was accomplished by performing a sensitivity analysis using simulations from the Cold Regions Hydrological Model (CRHM) and by comparing forest canopy sites (F) vs. openings (O). The CRHM platform focuses on the incorporation of physically based descriptions of snow–dominated regions hydrological processes. It was found that forest cover induced different snowpack sensibility to climatic change conditions in the studied forests. Delayed onset of snow accumulation (F: 13 days·$^{\circ}C^{-1}$; O: 5 days·$^{\circ}C^{-1}$) and reduced snowpack duration (F: 28 %·$^{\circ}C^{-1}$; O: 23 %·$^{\circ}C^{-1}$) under warmer temperatures were more intense in areas beneath the forest canopy compared to openings. A lower annual peak of snow water equivalent (SWE) (F: 81 mm·$^{\circ}C^{-1}$; O: 129 mm·$^{\circ}C^{-1}$), earlier melt-out date (F: 8 days·$^{\circ}C^{-1}$; O: 10 days·$^{\circ}C^{-1}$) and slower melting rates (F: 0.4 mm·day^{-1}·$^{\circ}C^{-1}$; O: 0.5 mm·day^{-1}·$^{\circ}C^{-1}$) with increasing temperatures were more intense in forest openings. The forest–driven reduction in snowpack duration (40%) was significantly enhanced with warming (10% per °C). Lower precipitation (20% precipitation reduction) could increase the response of this forest effect to warming (32%), while higher precipitation (20% precipitation increment) could reduce it (−26%). There was relevant topographic variability in the forest−snow interactions in response to climate change among the study stands, despite their proximity.

1. Introduction

The importance of snow in mountains ranges from its role as an essential eco–hydrological resource to the economic activities associated with it. Mid–latitude mountain snowpacks represent a natural freshwater reservoir by storing solid water in winter and releasing it as snowmelt runoff in spring–summer, when human activity demands are usually highest (Barnett et al., 2005). Additionally, snowpack variability affects ecological processes such as forest growth (Vaganov et al., 1999), plant phenology (Asam et al., 2018), soil water stress (Harpold, 2016) and wildfire activity (Westerling, 2016).

Seasonal snowpack is affected by complex interactions between meteorological conditions, topography and vegetation (Bednorz, 2004; Ellis et al., 2013; Huerta et al., 2019; Lundquist and Cayan, 2007). Snow processes are heavily influenced by forest cover, since mid– and high–elevation forests co–exist across a large range of altitudes with mountain snow (Broxton et al., 2020). Tree leaves and branches intercept snow during winter, which affects under–canopy snow accumulation

* Corresponding author.
E-mail address: albasv@ipe.csic.es (A. Sanmiguel-Vallelado).

https://doi.org/10.1016/j.jhydrol.2021.127311
Received 5 May 2021; Received in revised form 26 October 2021; Accepted 2 December 2021
Available online 17 December 2021

(Varhola et al., 2010). Canopy interception generally leads to shallower snowpacks in forested areas relative to open areas, because a significant proportion of the snow stored in the canopy sublimates or melts (Molotch et al., 2007; Storck et al., 2002). Trees shelter the surface from wind, which modifies snow transport by wind and, thus, snow accumulation patterns compared to open areas (Hiemstra et al., 2002). Additionally, mountain forests alter the energy balance of the snowpack and, thus, condition snowmelt in different and complex ways (Sicart et al., 2004). For example, forest litter deposited over the under–canopy snowpack reduces snow albedo and increases shortwave absorption by the snowpack (Hardy et al., 2000). Forest cover can diminish melting rates by reducing shortwave radiation reaching the snowpack surface (i.e. "shading" effect) (Ellis et al., 2011; Musselman et al., 2015). On the other hand, longwave radiation can be enhanced in forested areas as a result of shortwave absorption by trees and consequent heating during the day; the forest canopy generally has a higher thermal emissivity than the clear sky during the night (i.e. "heating" effect) which can compensate for shortwave reduction by the shade effect, with consequent increase of melt rate (Essery et al., 2008; Lundquist et al., 2013; Sicart et al., 2006). The balance between reduced accumulation and diminished (or enhanced) melting determines snowpack duration in forests, which can be shortened or extended relative to open areas (Dickerson-Lange et al., 2017). The nature and extent of forest influences on snowpack rely on forest structure, topography, orientation, elevation, seasonality, and regional climate, among others (Currier and Lundquist, 2018; Jost et al., 2007; López-Moreno and Stähli, 2008; Moeser et al., 2016; Pomeroy et al., 2002; Roth and Nolin, 2017).

Many studies have investigated the impacts of current climate change on snow processes and related effects on stream flows in the main mid–latitude mountain ranges, such as reductions in snow accumulation and accelerated rain–on–snow processes which are expected to induce a shift to earlier snowmelt onset and melt out (e.g. Adam et al., 2009; Beniston, 2012; Fang and Pomeroy, 2020; Marshall et al., 2019; Morán-Tejeda et al., 2017; Pomeroy et al., 2015; Rasouli et al., 2015; Sun et al., 2016). However, the sensitivity of snow processes to climate change may differ depending on regional climates and the physiographic characteristics of different mountain ranges (Evan and Eisenman, 2021; López-Moreno et al., 2017; Marshall et al., 2019; Shrestha et al., 2021). This issue is especially relevant in Mediterranean climate mountains, as they are considered hot spots for climate change impacts, and the consequences may seriously affect the ecosystems, hydrological resources and the economy of these regions (Giorgi and Lionello, 2008; Vicente-Serrano et al., 2011). The future climate trends projected for Mediterranean mountains indicate rising temperatures (between + 1.6 °C and + 8.3 °C for 2085) as well as a reduction of precipitation (between −4.8% and −17% for 2085) (Nogués Bravo et al., 2008). Previous research determined that Mediterranean snowpacks are very sensitive to temperature increases (López-Moreno et al., 2017), although the extent of the change varied among mountain ranges. The Spanish Pyrenees is expected to be the European mountain range most impacted by climate change in terms of mean SWE and snowpack duration (López-Moreno et al., 2017). Understanding how forest cover can affect the sensitivity of snowpack to changes in climate will allow us to anticipate future hydrological responses of Pyrenean forested mountain basins under climate change conditions (Ellis et al., 2013; Fang and Pomeroy, 2020; López-Moreno et al., 2020; Rasouli et al., 2019; Tennant et al., 2017).

Research regarding the interactions between forest and snow in the Spanish Pyrenees (e.g. López-Moreno and Latron, 2008; Revuelto et al., 2015; Sanmiguel-Vallelado et al., 2020) observed that snow accumulation was 40–50% lower in areas beneath the forest canopy compared to forest openings, while the overall melting rate was reduced by 25% in forested areas. The forest cover reduced the annual peaks of snow accumulation by >50% and the snowpack duration by more than two weeks. The relative earlier snow disappearance in forested areas was mainly explained by greater forest–driven reduction of accumulation rate, in combination with occasional forest–driven enhancement of melting rate. However, the magnitude and timing of these forest–snow interactions had significant spatial and temporal variations. Based on these observations and on related previous research, a series of hypotheses [H1 to H4] were raised on how forest effects on snow may respond to climate change conditions in the Pyrenees. Since climate mediates forest–snow interactions involving snow accumulation (Currier and Lundquist, 2018) and melting processes (Dickerson-Lange et al., 2017), [H1] it was expected that snowpacks in areas beneath forest canopy and in forest openings might respond differently to a changing climate. Previous work has attributed higher canopy interception efficiency to warmer temperatures (Friesen et al., 2015) and to a lower amount of snowfall (Revuelto et al., 2015). Thus, [H2] it was expected that forest effects on snow accumulation processes might be enhanced under warming climate conditions, especially in a scenario that has less precipitation. In a warmer climate, the main melt season is projected to occur earlier and, thus, to shorten to a period of lower available energy to melt (Musselman et al., 2017). As the melt period shifts earlier in the year away from the summer solstice, the forest shading effect might be weaker because of the lower solar zenith angle (Lundquist et al., 2013). In a snowmelt scenario of lower energy, the forest heating effect might be smaller due to lower penetration of solar radiation into the forest (i.e., lower shortwave absorption by trees) and the subsequent lower thermal emissivity (Lundquist et al., 2013). In addition, the shift in melt timing with warming also decreased net longwave radiation as melt–period air temperatures decreased, because the shift of snowmelt timing can have a greater effect on air temperatures than the induced warming (Jennings and Molotch, 2020). This might contribute to diminishing the forest heating effect on melting. Thus, [H3] it was expected that both forest effects (shading and heating) on snow melting processes might be diminished with warming. It has been previously observed that the magnitude and timing of the forest effects on snow processes varied significantly among forest stands, despite their proximity (Sanmiguel-Vallelado et al., 2020). Topography, elevation and forest structure are relevant factors, among others, that explained why the forest–snow interactions vary spatially (Jenicek et al., 2018a; Musselman et al., 2012; Roth and Nolin, 2017). Thus, [H4] it was expected that the sensitivity of forest effects on snow processes to climate change might show significant spatial variability in nearby areas.

This study investigates how forest cover can affect the snowpack response to changes in climate in four nearby sub–alpine conifer forests in the Pyrenees. For this purpose, a sensitive analysis was done by simulating the shifts in snow water equivalent (SWE) and snowpack energy balance (SEB) at each forest stand under various degrees of climate forcing, comparing areas beneath forest canopy (F) and forest openings (O), during four snow seasons (2016/17–2019/20). Simulations were done using the forest–snow process modules in the Cold Regions Hydrological Model (CRHM), which were evaluated against field observations. CRHM is particularly well suited to the aim of this study and the study area, since this model has focused on the incorporation of physically based descriptions of cold regions hydrological processes, such as forest canopy snow interception, drip and unloading, blowing snow, canopy influence on radiation, energy balance snowmelt or long–wave radiation in complex terrain (Pomeroy et al., 2007). The specific objectives of this study were as follows: (1) to estimate how forest cover affects the sensitivity of snowpack to changes in climate; (2) to evaluate whether forest–driven effects on snow processes were enhanced or reduced under changing climate conditions; and (3) to explore spatial variability in the sensitivity of forest effects on snowpack to changing climate conditions.

2. Data and methods

2.1. Study sites

The study was performed in the central Spanish Pyrenees, in the northeastern Iberian Peninsula (Fig. 1). This mountain range is located in the transition area of the temperate–continental Atlantic–Eurosiberian and mild–dry Mediterranean climates (Del Barrio et al., 1990). The experimental setting comprised four forest stands located in the Balneario de Panticosa valley, which constitutes the headwater of the Caldarés River, a Pyrenean tributary of the Ebro river basin. In each forest an experimental plot of approximately 450 m^2 was designed. The plots were labeled (plot 1, plot 2, plot 3 and plot 4) based on their locations in the valley (from NE to SW and from 1674 to 2104 m a.s.l.). *Pinus uncinata* Ram. dominated the studied stands, which is a pioneer, long–lived and shade intolerant conifer; although plot 3 contained a few *Pinus sylvestris* L. individuals. Different microclimate conditions, topography and forest structure were observed across plots (Table 1). Plot 1 had the greatest tree density and canopy cover, and its forest openings were rather small. Plot 1 was also the steepest plot and mostly faced southward; it also had the lowest wind speed values. Plot 2 had a relatively dense forest. Its exposure was mostly eastward, and its winter temperatures and snow accumulation were similar to those of plot 1. Plot 3 had the lowest elevation, was the flattest plot, and faced westward. This plot had a relatively high canopy–cover and received a relatively high irradiance. Plot 3 also had the warmest winter temperatures, the largest irradiance and lower snow accumulation. Plot 4 had the highest elevation and faced northeastward. This plot had the lowest tree density and canopy–cover, the greatest wind speeds, the coldest winter temperatures and the deepest snowpacks.

2.2. Data sources

From October 2016 to May 2020 (2016/17, 2017/18, 2018/19 and 2019/20 snow seasons) information on climate was recorded at each experimental plot. This included air temperature (T), air relative humidity (RH), wind speed (Wind) and incoming shortwave radiation (QSI). Air temperature and relative humidity series were obtained using dataloggers (Tinytag-Plus-2; model TGP-4017, Gemini DataLoggers UK Ltd.) that were equipped with naturally ventilated radiation shields (Datamate ACS-5050 Weather Shield; Gemini DataLoggers UK Ltd.). One datalogger was installed at each plot, hanging from a tree branch, and measurements were recorded every 15 min. Wind speed and incoming shortwave radiation series were obtained every 15 min from automatic weather stations (HOBO U30 NRC, Onset Co.) located at forest openings within each plot. Average hourly T, RH, Wind and QSI series at each experimental plot were calculated. The Spanish State Meteorology Agency (AEMET) provided information on precipitation during the study period (2016/17, 2017/18, 2018/19 and 2019/20 snow seasons). The daily sum of total precipitation (ppt) was recorded by the 9451A AEMET's meteorological station located at the bottom of the Baños de Panticosa valley (1630 m a.s.l.). Missing data in the climate series were estimated using the missForest method (Stekhoven and Buhlmann, 2012), which is a nonparametric iterative imputation method based on Random Forests (Breiman, 2001) available in the missForest R package (Stekhoven, 2013). Climate data registered by another meteorological station operated by us and located beside the AEMET station was included in the T, RH, Wind and QSI data imputation process. The ppt data imputation process included information on precipitation provided by the meteorological station (E235) operated by the Automated Hydrological Information System for the Basin of the Ebro River (SAIH) of the River Ebro Hydrographic Confederation (CHE) and located at the Baños de Panticosa valley bottom mountain lake.

Snowpack data were collected during the two first snow seasons (2016/17 and 2017/18) from the onset of snow accumulation to the end of melting. The snow depth series were obtained from automatic time–lapse cameras (Bushnell, Trophy Cam, Kansas, USA) shooting every day at eight fixed snow poles at each plot: three poles were placed in a forest opening (O) and five were placed beneath the forest canopy (F) at each plot. Photographs were processed using ImageJ software (Rasband, 1997) to manually obtain a daily snow depth series for the set of poles at each experimental plot. Snow Water Equivalent was manually surveyed every 10 to 15 days using a snow cylinder and scale (ETH core sampler, Swiss Federal Institute of Technology, Zurich) at snow pits dug at two single locations in each plot, one in a forest opening and one below the forest canopy. Two replicates per location were collected. Snow density data was calculated from SWE collected data during each survey. Daily snow density series were estimated by linear interpolation between each pair of density measurements from consecutive surveys. Daily SWE series for the set of poles at each experimental plot were inferred from data on daily snow depth and estimated daily snow density. The methodology to obtain the snow dataset and its validation is described in Sanmiguel-Vallelado et al. (2020).

Soil temperature data (T_g) was obtained using miniature temperature loggers (Thermochron iButton; DS-1922l model, Dallas Semiconductors). Four to six dataloggers were installed at each studied forest stand in a distributed manner, covering both forest openings and beneath forest canopy areas. The dataloggers were wrapped with laboratory film and duct tape to prevent corrosion, tied to metallic picks to facilitate their retrieval, and were buried in the ground at a depth of 10 –

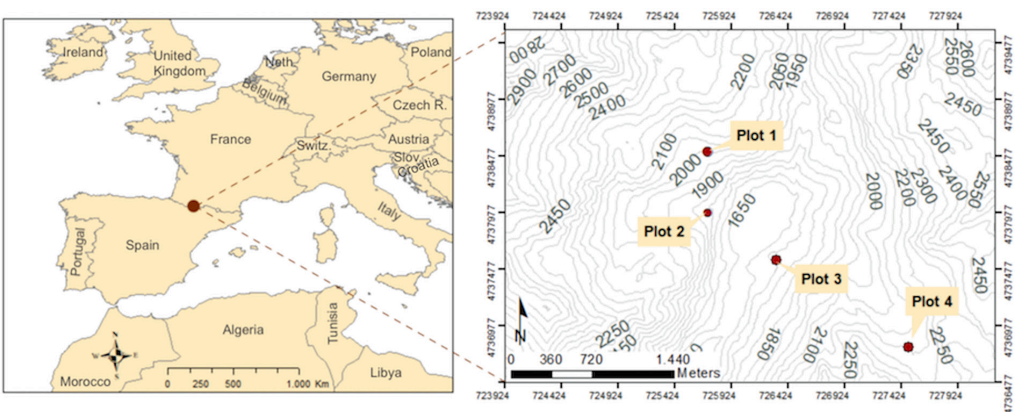

Fig. 1. Study location (Balneario de Panticosa valley) in the Spanish Pyrenees (at left) and location of the experimental plots in the study area (at right).

Table 1
Average values of topography, microclimate conditions and forest structure in the four forest stands.

Plot	Elevation (m a.s.l.)	Aspect	Slope (°)	DJF T (°C)	Peak SWE (mm)	MAM GSI ($W \cdot m^{-2}$)	RH (%)	Wind ($m \cdot s^{-1}$)	Canopy cover (%)	Density (ind.·ha^{-1})	LAI
1	2008	S	29.4	0.61	645	154	70	0.05	156	1689	1.92
2	1814	E	20.4	0.84	739	164	69	0.37	85	844	2.11
3	1674	W	9.3	1.91	578	207	65	0.47	119	533	1.83
4	2104	NE	22.7	−0.68	1245	202	68	0.83	29	356	2.55

Abbreviations: DJF T, winter mean air temperature from December to February; Peak SWE, maximum snow water equivalent value annually recorded in forest openings; MAM GSI, average global solar irradiance from March to May.
Notes: Climate data belongs to 2016/17–2019/20 snow seasons (November to May). Snow data belongs to 2016/17 and 2017/18 snow seasons. The methods used to obtain forest structure data were described in Sanmiguel-Vallelado et al. (2020). Canopy cover values higher than 100% indicate overlapping tree crowns projections on the ground.

20 cm. Soil temperature data were collected every hour during three snow seasons (2016/17, 2017/18 and 2018/19). Missing values in the T_g series were filled by linear or spline interpolation using the function *interpolate* included in the CRHMr R package (Shook, 2016), which is a CRHM implementation in the R statistical software (R Core Team, 2020) for pre– and post–processing.

Forest stand density, canopy cover, Leaf Area Index (LAI) and average height of *P. uncinata* individuals at each plot were obtained. The methods used to obtain stand structure data were described in Sanmiguel-Vallelado et al. (2020).

2.3. Hydrological modelling

2.3.1. CRHM implementation

The CRHM platform is a flexible and physically based modeling system created to simulate a range of hydrological processes in mountainous and cold regions. The full description of CRHM is provided by Pomeroy et al. (2007) and the software is available for downloading at https://research-groups.usask.ca/hydrology/modelling/crhm.php#Download. CRHM has been applied to diverse environments including artic, alpine and subalpine areas (DeBeer and Pomeroy, 2010; Ellis et al., 2010; Fang and Pomeroy, 2020; Krogh et al., 2015; López-Moreno et al., 2020; Rasouli et al., 2015). The CRHM platform has a modular structure that can address the wide range of processes typical of regions where snow has a key role in the cycle, e.g. snow redistribution by wind, snow interception by forest canopies, snow sublimation or snow melting. Users can construct their own model by selecting modules from the platform library, based on input data availability, the predictive variable of interest and research scale. It can be used to forecast, diagnose and understand hydrological processes, due to its heavy reliance on physically based process parameterizations.

CRHM was applied at each study plot, which were divided in two hydrological response units (HRUs) on the basis of forest cover, i.e. forest openings (O) and areas beneath forest canopy (F). Selection of the CRHM modules was based on the characteristics of the study plots and the available climate data, as presented in Table A1. Parameters have been adapted to each study plot, based on field measurements or by estimation based on other similar snow–dominated areas (Table A2). Climate data for the period 2016/17–2019/20 were used as the input to the CRHM platform. The climate database was converted into CRHM observations using the CRHMr R package (Shook, 2016).

Outputs of interest include hourly values of SWE and SEB components (net all wave radiation, net longwave radiation, net shortwave radiation, net latent heat turbulent flux, net sensible heat turbulent flux, energy from rainfall advection, net ground heat flux, and the change in internal energy of snow) for each HRU during the period 2016/17–2019/20 (4 snow seasons). CRHM resolves the snow energy balance as the sum of irradiative, turbulent, advective and conductive energy fluxes (Ellis et al., 2010). SWE series and energy fluxes were outputs from the SnobalCRHM module. The exception was the net long and shortwave radiation fluxes, which were outputs from the CanopyClearingGap module. CRHM output databases were post–processed using the CRHMr R package (Shook, 2016). Hourly series were converted into daily data by taking the maximum value reached each day, in the case of SWE series, and the mean value of each day, in the case of energy fluxes.

The studied snow seasons were representative of a wider range of local snow conditions. Daily maximum SWE series from 2008 to 2019 were obtained from a near tele–snow gauge operated by SAIH-CHE (N0004 Bachimaña). Values of peak SWE, seasonal average SWE and snowpack duration of analyzed snow seasons were within the range of percentiles 20–35 of the whole series.

2.3.2. Evaluation of model performance

Observed SWE daily series at each plot and HRU during the 2016/17 and 2017/18 snow seasons were compared to the model outputs to evaluate model performance in terms of the ability to represent:

a) The variation in peak SWE and snowpack duration between HRUs. The peak SWE is the maximum annual amount of SWE recorded at each HRU, while the duration of the snowpack was calculated as the number of days per year having a SWE > 5 mm (López-Moreno et al., 2020).
b) The magnitude of daily SWE at individual sites.

For a) and b) above, model performance was assessed by the following three measures described in Ellis et al. (2010): the model bias index (MB), the model efficiency index (ME), and the root mean square error (RMSE). The MB index compares the total simulation output to the total of observations, the ME index gives an indication of model performance compared to the mean of the observations, and the RMSE index quantifies the absolute unit error between simulations and observations.

Correlations using the Spearman coefficient (rho) were calculated between modeled and observed SWE variables. This non–parametric method was used since analyzed variables had not normal distributions (Shapiro–Wilk test, p–value < 0.05).

SWE estimates showed general good agreement with observed SWE during both analyzed snow seasons (Fig. 2) (MB = 1.01). A slight overestimation of daily SWE in areas beneath forest canopy in plots 1 and 4 during 2016/17 snow season was observed (Table A3). This could point to an underestimation of the interception effect by forest. On the other hand, certain snow accumulation events were underestimated, e.g. April-2017 in plot 4. Estimates represented pretty well the inter–plot variability in general (ME = 0.94), although the model's efficiency is reduced in areas beneath forest canopy. The RMSE value for all sites was 49 mm of daily SWE; greater absolute errors were found in forest openings. A high positive correlation was found between modeled and observed daily SWE data (Fig. A1), when all areas beneath forest canopy (rho = 0.91; p–value < 0.001) were considered and all forest openings (rho = 0.95; p–value < 0.001). Certain inter–plot variability was observed in the correlation between modeled and observed daily SWE data but, in all cases, it was statistically significant (rho > 0.87). In all cases, the percentage of total variance of the modeled SWE explained by

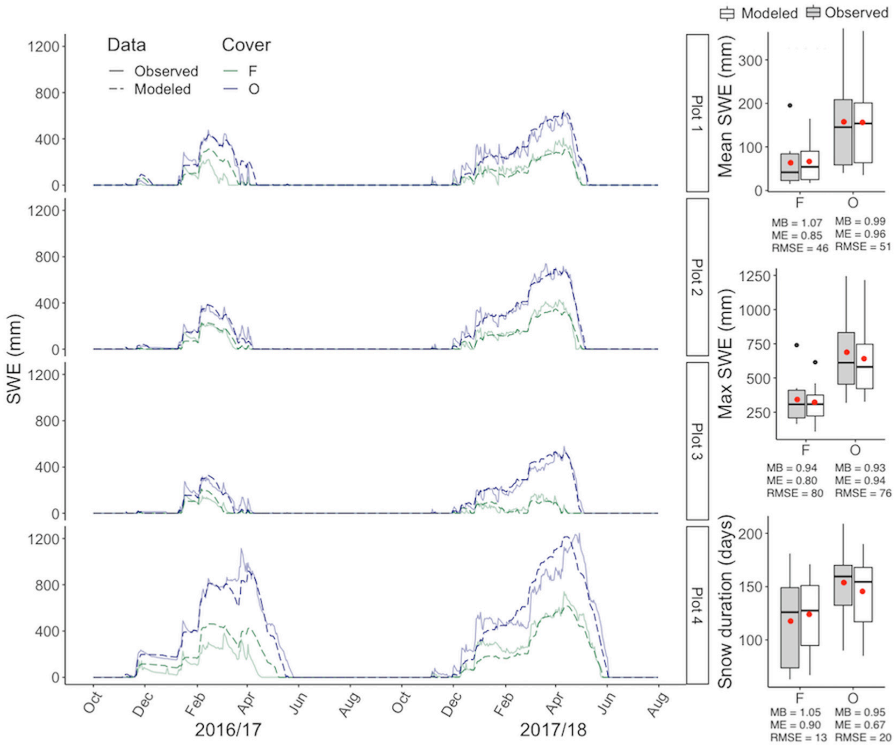

Fig. 2. At left: Time series of observed (solid lines) and modeled (dashed lines) daily SWE in areas beneath forest canopies (F, green lines) and in forest openings (O, blue lines) at plot level during 2016/17 and 2017/18 snow seasons. At right: Comparison of observed (boxplots shaded in grey) and modeled (boxplots without shading) mean SWE, peak SWE and snow duration in areas beneath forest canopies (F) and in forest openings (O) of all plots. Box indicates the interquartile range (IQR, Q1: 25% to Q3: 75 %); central line represents the median; inner red point represents the mean; whiskers indicate 1.5 × IQR; and points indicate outliers (>1.5 × IQR and < 3 × IQR). Model bias index (MB), model efficiency index (ME), and root mean square error (RMSE) of simulated daily SWE, peak SWE and snow duration at opening areas (O) and forest areas (F) during 2016/17 and 2017/18 snow seasons are shown. See Table A3 to check these index values at individual sites.

the regression was higher than 78% (Fig. A1). Apparently, overestimation errors happened more frequently when low daily SWE values occurred in forested areas, especially in plots 1 and 4 (Fig. A2). Similarly, underestimation errors in forested areas were more frequent when greater daily SWE occurred, especially above 400 mm. No evident relationship between model errors and the observed magnitude of SWE in forest openings was found.

Simulations showed minor underestimation of peak SWE (MB = 0.94) (Fig. 2). This strong correspondence occurred in both forest openings and areas beneath forest canopy. Estimates also represented well the peak SWE variability among plots, based on the ME index value (ME = 0.94), although the model efficiency was reduced in areas beneath forest canopy. The RMSE of peak SWE (78 mm) in areas beneath the forest canopy was slightly greater than that found in forest openings.

In general terms, the simulation of snow duration was accurate (MB = 0.99), despite SWE being slightly overestimated in areas beneath the forest canopy and slightly underestimated in forest openings (Fig. 2). Model efficiency in snow duration (ME = 0.80) was higher in areas beneath the forest canopy than in forest openings. The RMSE of snow duration was 17 days for all sites and areas; in forest openings it was 7 days higher than in areas beneath forest canopy.

Summarizing, the CRHM model performed sufficiently well in capturing the snow accumulation and ablation magnitude and timing to be used for sensitivity analysis to climate in the four study sites and F–O areas. Estimates did not show systematic errors that might interfere with conclusions drawn from subsequent climate analysis.

2.4. Sensitivity analysis

A sensitivity analysis was performed to assess the response of forest effect on snow processes to changing climate conditions. For this purpose, SWE and energy fluxes were simulated under scenarios of combined temperature and precipitation departs from the control period (2016/17–2019/20). Air temperature and precipitation were modified in the observation module of the CRHM platform. Temperature was forced to increase from +1 °C to +4 °C and precipitation was considered to change from −20% to + 20% yielding a total of 14 scenarios of perturbed climate. The ± 20% value approximates the uncertainty of precipitation simulated in climate models for the Mediterranean region (Knutti and Sedláček, 2013). Relative humidity was assumed to be constant under temperature forcing.

Climate–forced CRHM outputs were again postprocessed using the CRHMr R package (Shook, 2016). Hourly series were converted into daily data by taking the maximum value reached each day in the case of the SWE series and the mean value of each day in the case of energy fluxes. From the modeled daily SWE series, several snow indices were derived for each HRU at each plot for further analysis: (i) the snow accumulation onset (date of first day having SWE > 5 mm); (ii) the melt–out date (last date having SWE > 5 mm); (iii) the snow duration (number of days annually having SWE > 5 mm (López-Moreno et al., 2020)); (iv) the peak SWE (the maximum annual amount of SWE) and (v) the date of peak SWE. Daily melting series were calculated by performing a first–order differencing, day–by–day, from the modeled daily

SWE series. Only those days when melting (mm·day^{-1} < 0) occurred at both HRUs were considered, and when the melting rate value was higher than −1 mm·day^{-1}. From daily melting series, another snow index was derived: (vi) the melting rate (median value for each HRU at each plot). Sensitivity of snow indices magnitude to combined temperature and precipitation changes was calculated for each HRU at each plot. The relative change of snow indices under combined temperature and precipitation perturbed scenarios, with respect to observed conditions, was calculated for each HRU at each plot. Forest effects on snow processes were calculated as a percentage (increase or decrease) in snow indices magnitude for each HRU at each plot.

The Wilcoxon test was used to detect the significance of differences between HRUs in the snow indices magnitude and in percentage of change under the different climate variations. This non–parametric method was used since none of the calculated indices had normal distributions (Shapiro – Wilk normality test: $p < 0.05$).

3. Results

3.1. Sensitivity of snow processes to climate perturbation in F and O areas

Under increasing temperatures, the modeled seasonal snowpack experienced a decrease in magnitude and duration (Fig. 3). In scenarios that combined increased temperatures and diminished precipitation, these effects were exacerbated (Fig. A3). To better discriminate the effects of climate perturbation on forest–snow interactions, hereafter this study focuses on snow–index responses in F and O areas.

Increasing temperatures induced a shorter snow accumulation period, more noticeable in F areas, due to the delayed timing of snow accumulation onset and to an earlier timing of peak SWE (Table 2). Increasing temperature also induced a shorter melting period, slightly more pronounced in O areas, due to an earlier timing of melt out. Overall, increasing temperatures induced 30 days shorter snowpack duration per °C of warming in both O and F areas, which was driven by later snow accumulation onset in F areas and by earlier snow depletion in O areas. Snowpack duration in F areas was significantly more sensitive to increasing temperatures than in O areas (Table A4). Sensitivity of snow duration to warming showed low spatial variability (F CV = 0.1; O CV = 0.2). Nevertheless, plot 4 showed the largest sensitivity values in both F and O areas, followed by plot 2, while plot 3 showed the smallest sensitivity (Table A5). Plots 4 and 2 presented the longest lasting snowpacks, while plots 3 and 1 presented the most ephemeral snowpacks. A−20% precipitation reduction aggravated snow duration sensitivity to warming in a similar way in both F and O areas (22% on average); while a + 20% precipitation increment reduced it (19% on average) (Fig. 4).

Increasing temperatures reduced peak SWE values in absolute terms, especially in O areas (Table 2). In relative terms, the percentage of change of peak SWE with warming did not significantly differ between O and F areas (Table A4). All plots showed similar peak SWE sensitivity to warming (F CV = 0.1; O CV = 0.1). Nevertheless, plot 4 showed the largest sensitivity values in both F and O areas, while plot 3 showed the lowest sensitivity (Table A5). Plot 4 presented the largest peak SWE, and plot 3 presented the smallest peak SWE values. The sensitivity of peak SWE to warming was intensified with 20% precipitation reduction, especially in O areas (F: 23%; O: 29%); while 20% precipitation increment reduced it (F: 27%; O: 35%) (Fig. 4).

Melting rates experienced an overall slowdown with increasing temperature, more pronounced in O areas in absolute terms (Table 2). In relative terms, the percentage of change of melting rates with warming did not significantly differ between O and F areas (Table A4). The response of melting rates to warming was not linear since, at lower degrees of warming, a slight increase in melting rates occurred in most cases. Large spatial variability was found in the sensitivity of melting rates to warmer temperatures (F CV = 0.9; O CV = 3.6). Melting rates were reduced with warming in plots 2 and 4. Conversely, melting rates were increased under warmer conditions in plot 1 (only in O areas) and plot 3. Plot 4 showed the highest sensitivity to warming in snow melting, in absolute and relative terms, followed by plot 2; while plots 3 and 1 showed the lowest sensitivity (Table A5). Plots 4 and 2 experienced the

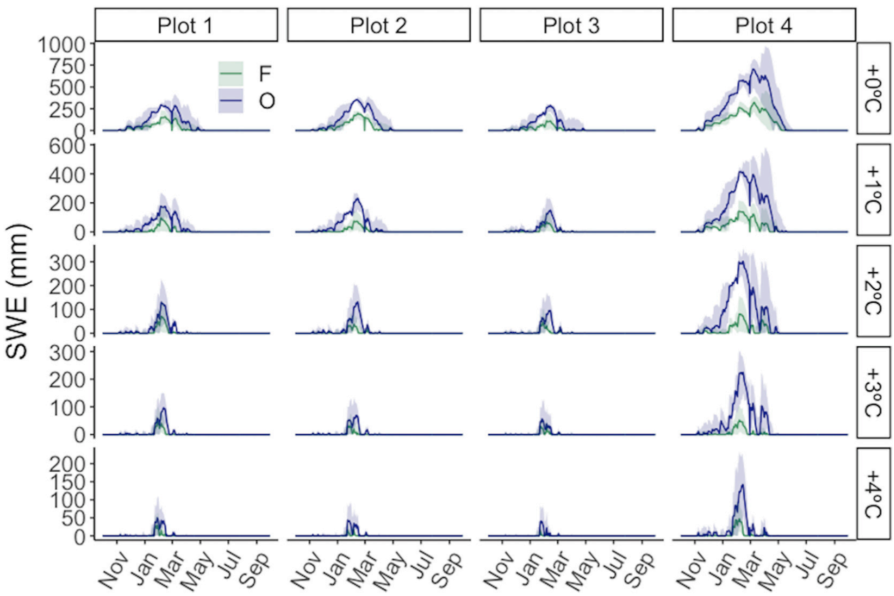

Fig. 3. Sensitivity of daily SWE to temperature change in areas beneath forest canopy (F, green lines) and in forest openings (O, blue lines). Lines represent the median value and ribbons represent the interquartile range (Q1: 25% to Q3: 75%) of the four–modeled snow seasons (2016/17 – 2019/20). See Fig. A3 to check sensitivity of daily SWE to combined temperature and precipitation changes.

Table 2
Snow indices change per °C of temperature increment with regard to the non–perturbed conditions. Both types of changes in magnitude and percentage of change are presented. The different areas analyzed at each study site (F: beneath forest canopy; O: forest openings) are distinguished. Sites average value of the four modeled snow seasons (2016/17–2019/20) medians are shown. See Table A5 to check snow indices change per °C at each site.

Area	Accum. onset		Melt out date		Peak SWE date		Snow duration		Peak SWE		Melting rate	
	(days)	(%)	(days)	(%)	(days)	(%)	(days)	(%)	(mm)	(%)	($mm{\cdot}d^{-1}$)	(%)
F	13	32	−8	−4	−7	−5	−31	−28	−81	−30	−0.4	−5
O	5	13	−10	−5	−7	−5	−30	−23	−129	−27	−0.5	−3

Table 3
Snow energy content and individual snow energy fluxes change per °C of temperature increment with regard to the non–perturbed conditions. Both types of changes in magnitude and percentage of change are presented. The different areas analyzed at each study site (F: beneath forest canopy; O: forest openings) are distinguished. Sites average value of the four–modeled snow seasons (2016/17–2019/20) means are shown. See Table A6 to check snow indices change per °C at each site.

Area	Change in stored energy of snow		Net radiation		Latent heat[1]		Sensible heat		Precipitation heat		Ground heat	
	($W{\cdot}m^{-2}$)	(%)	($W{\cdot}m^{-2}$)	(%)	($W{\cdot}m^{-2}$)	(%)	($W{\cdot}m^{-2}$)	(%)	($W{\cdot}m^{-2}$)	(%)	($W{\cdot}m^{-2}$)	(%)
F	−2.7	−34	−1.2	−44	1.6	34	−0.8	−47	−0.1	−24	−2.3	−29
O	−3.8	−29	−3.2	−36	0.4	29	−0.2	−25	−0.1	−19	−0.8	−15

[1] Latent heat flux is a negative component, so positive changes values lead to reductions in the component's magnitude.

largest melting rates, while plots 1 and 3 experienced the lowest. The overall reduction in melting rates with warming was intensified in a similar way in both F and O areas when a 20% precipitation reduction was considered (188% on average); while with a 20% precipitation increment it was reduced (114%) (Fig. 4).

3.2. *Sensitivity of forest effects on snow processes under different climate perturbations*

Under observed climate conditions, statistically significant forest effects on snow were found (Table A4): a delayed snow accumulation onset (4 days, on average), an earlier date of snowmelt (12 days, on average) and a peak SWE reduction (40%, on average) in F areas with respect to O areas. Other effects under observed climate were reduction in snowpack duration (17%, on average) and an overall reduction in melting rates (14%, on average). However, two different forest effects over melting rates could be discerned, depending on the individual sites: (i) forest cover enhanced the melting rates compared to O areas in plots 1 and 3 (1% and 12%, on average), which present the most ephemeral snowpacks; (ii) melting rates were reduced in plots 2 and 4 (33% and 36%, on average), where the longer lasting snowpacks occurred.

Under warming scenarios, the forest effect driving delay in snow accumulation onset was enhanced (7 days per °C, on average) (Fig. 5). This forest effect on snow remained statistically significant under most warming climate scenarios (Table A4). Conversely, the effect of forest driving earlier snowpack melt out was reduced with warming (2 days per °C, on average). As a result, this forest effect ceased to be statistically significant under perturbed climate conditions (Table A4). All in all, the forest–driven reduction on snow duration was enhanced + 10% per °C warming, on average. Thus, this forest effect was statistically significant under all warming scenarios (Table A4). The sensitivity of the forest effect on snow duration to warming showed some spatial variability (CV = 0.4). Plot 2 showed the largest sensitivity values for this forest effect, while plot 3 showed the smallest. Under combined temperature increase and − 20% precipitation reduction, the forest–driven reduction on snow duration was aggravated (32%, on average); while 20% precipitation increment reduced it (26%, on average).

Under increasing temperatures, the forest–driven reduction of peak SWE did not show a substantial response (1% increased per °C, on average) (Fig. 5). Nevertheless, this forest effect remained statistically significant under most climate perturbation scenarios (Table A4). Large spatial variability was found in the sensitivity of the forest effect on peak SWE to warming (CV = 1.81). In plots 1 and 4 the forest–driven reduction of peak SWE showed small enhancement values per °C; in plots 2 and 3 it did not show a clear response. With 20% precipitation reduction and no warming, forest–driven reduction of peak SWE was enhanced (14%). But, under combined temperature increase and precipitation change, the forest effect on peak SWE did not show a clear response.

The overall forest–driven reduction of melting rates became lower under increasing temperatures (2% per °C, on average) (Fig. 5), but the response was not linear and varied highly among sites (CV = 4.3). In plots 1 and 3, it was observed an enhancement of melting rates by forest under non–disturbed climate conditions. However, under warmer conditions the forest effect shifted, and a reduction of melting was observed. On the contrary, the forest–driven reduction in melting observed under current climate in plots 2 and 4 became lower under warming conditions. Precipitation changes did not produce a clear response in the effects of forest on melting rates.

3.3. *Sensitivity of snow energy balance to increasing temperatures*

Under observed climate conditions, snowpacks beneath forest canopy had 42% lower seasonal stored energy than snowpacks in forest openings, on average. Net all–wave radiation was 70% lower in F areas than in O areas, on average. This is because the higher net longwave radiation in the forest did not compensate for the lower net shortwave radiation (Fig. A7). Net all–wave radiation contributed the most to the seasonal snow energy balance (SEB) (69%) in O areas, followed by ground heat (36%, on average) (Fig. A8). The ground heat was 67% higher in F areas than in O areas, on average. This energy flux was the most relevant component of seasonal SEB in F areas (101%); followed by net all–wave radiation (35%, on average). Latent heat was a negative component in both areas, but in F areas its magnitude was higher than in O areas, and it was much more relevant to the SEB (F: 61%; O: 10%, on average). Sensible heat was only a relevant component of seasonal SEB in F areas (F: 22%; O: 3%, on average). Advected heat from precipitation was not a relevant component of seasonal SEB in F or O areas (F: 3%; O: 2%, on average). Plot 4 showed the greatest values of net all–wave radiation, turbulent fluxes and advected heat from precipitation in both F and O areas, and the smallest values of ground heat. Plot 4 also presented the lowest compensation between the higher net longwave radiation in the forest and the lower net shortwave radiation. This plot, located at the highest elevation, presented longer lasting snowpacks that were exposed to a higher insolation time of the year (late spring/early summer) (Fig. A7). Conversely, plot 3 showed the greatest magnitude of ground heat flux in both F and O areas and presented the greatest compensation between the higher net longwave radiation in the forest

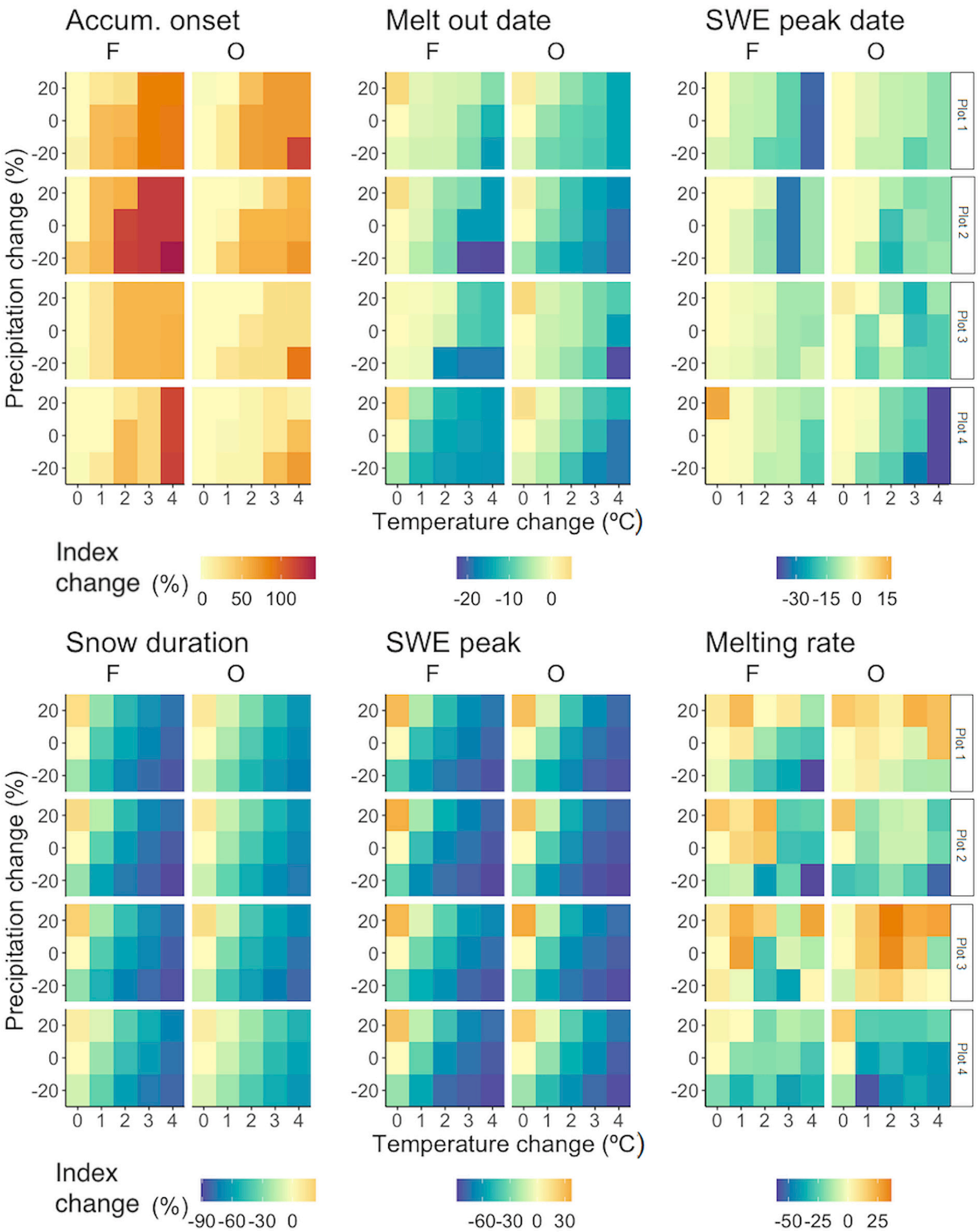

Fig. 4. Snow indices percentage of change, with regard to the non–perturbed conditions, to combined temperature and precipitation changes. The different areas analyzed at each study site (F: beneath forest canopy; O: forest openings) are distinguished. Median values of the four modeled snow seasons (2016/17–2019/20) are shown. See Figs. A4, A5 and A6 to check sensitivity of snow indices magnitude to climate perturbation.

and the lower net shortwave radiation. This plot, located at the lowest elevation, was the warmest, presented the densest forest, and experienced the most ephemeral snowpacks.

Under increasing temperature scenarios, the average seasonal energy stored in the snowpack experienced an overall decrease, more pronounced in O areas in absolute terms (Table 3). However, in relative terms, seasonal energy stored in the snowpack was relatively more sensitive to increasing temperatures in F areas. Net all–wave radiation experienced a reduction with warming, more pronounced in O areas (but F areas were relatively more sensitive), and its contribution to seasonal SEB was also reduced (F: 5% per °C; O: 9% per °C, on average) (Fig. 6). Differences in net shortwave and net longwave radiation

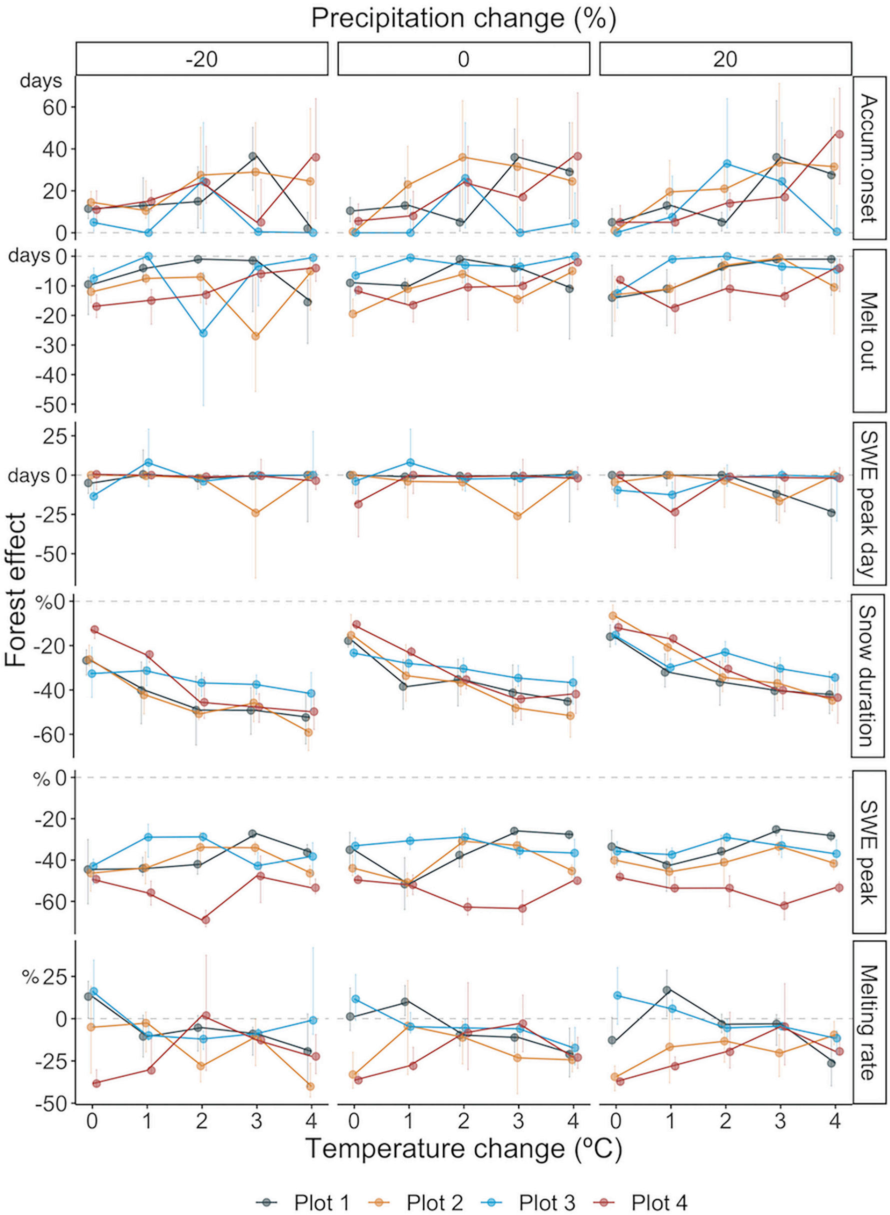

Fig. 5. Sensitivity of forest effects on snow processes (values in F areas with regard to the O areas, expressed as days apart or percentage) to combined temperature and precipitation change. Colors indicate the different studied plots. Data from the four modeled snow seasons (2016/17–2019/20) are shown as dots (median values) and whiskers (percentiles 25 and 75).

between F and O areas were reduced under warmer conditions (3 $W{\cdot}m^{-2}$ [24%] per °C and 2 $W{\cdot}m^{-2}$ [51%] per °C, respectively and on average) (Fig. A8). Thus, the higher longwave radiation in the forest tended to compensate for the lower shortwave radiation with increasing temperatures. Ground heat was reduced under warmer temperatures, much more pronounced in F areas in absolute and relative terms, but its contribution to seasonal SEB was enhanced (F: 41% per °C; O: 9% per °C, on average). The sensitivity of turbulent fluxes to warming was much more pronounced in F areas in absolute and relative terms, where latent heat was increased and sensible heat was reduced. The contribution of both turbulent fluxes to seasonal SEB experienced a reduction with warming (−29% and − 8% per °C respectively in F areas, on average, with almost no change in O areas). In absolute terms, plot 4 showed the largest reductions in net–all wave radiation and turbulent fluxes, while it presented the smallest reductions of ground heat (Table A6). However, in relative terms, plot 4 was the least sensitive to changes in the most relevant energy flux components to the SEB (net all wave radiation and ground flux), while plot 3 was the most sensitive.

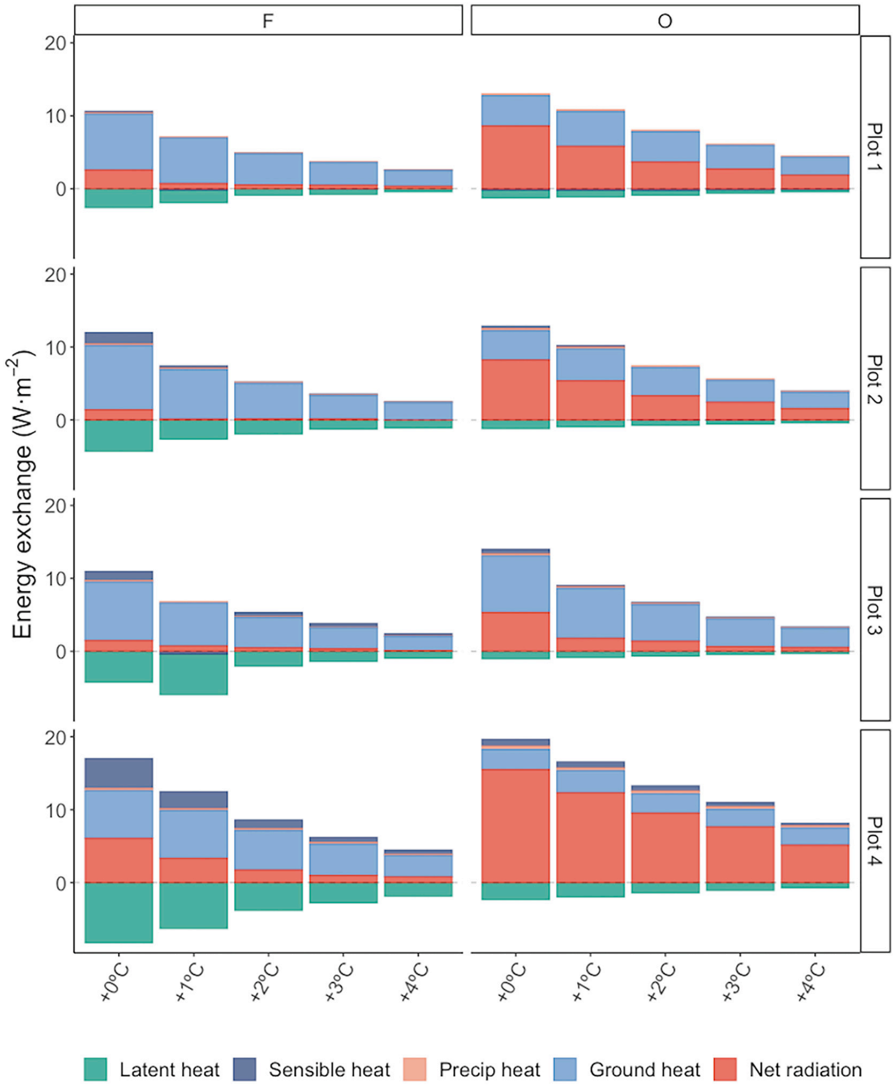

Fig. 6. Sensitivity of seasonal snowpack energy balance under warmer conditions. Represented energy fluxes are net latent heat turbulent flux, net sensible heat turbulent flux, energy from rainfall advection, net ground heat flux, and net all wave radiation. The different areas analyzed at each study site (F: beneath forest canopy; O: forest openings) are distinguished. Mean values of the four–modeled snow seasons (2016/17 – 2019/20) are shown. See Fig. A8 to check the monthly snowpack energy balance under non–perturbed climate conditions.

4. Discussion

This study confirms the sensitivity of forest effects on snow processes to perturbed climate conditions (increasing temperature and varying precipitation) in subalpine forest stands of the Spanish Pyrenees and highlights how it varies spatially even among close sites. Understanding the relationship between mountain forests and snow processes under changing climate conditions will benefit future water and forest management objectives in similar mid–latitude mountains and related lowland regions. Overall, our results show that the CRHM model sufficiently represented the quantity and timing of snow accumulation and ablation beneath forest cover and in forest openings (e.g., in all cases the percentage of total variance of the modeled SWE explained by the regression was higher than 78%, and the Spearman correlation coefficient between the modeled and observed SWE variables was higher than 0.87). The model was able to capture the differences in snow processes in forest stands with varying microclimate conditions, topography and forest structure. This supports the statement of Ellis et al. (2010) claiming that the CRHM model is a useful analytic and predictive tool for snow processes in coniferous forest environments. Since CRHM considers the full array of physical processes involved in snow redistribution, snowmelt dynamics, and runoff generation, as well as the main processes that mediates in the interaction between snow and canopy, we think that obtained findings should not be affected by model selection. The presence of forest cover affected the snowpack response to climate perturbations, as expected [H1], which is consistent with Tennant et al. (2017). Some other factors that have been reported to induce variability in the response of snowpacks to a changing climate are elevation, slope and aspect (López-Moreno et al., 2014; Pierce and Cayan, 2013). It was observed that forest effects on snow accumulation processes were highly sensitive to warming temperatures; as a consequence, the forest–driven reduction in snowpack duration was significantly enhanced with warming. In general, the forest effects on snow melting processes were diminished with warming.

4.1. Sensitivity of forest effects on snow accumulation processes to climate perturbations

We expected to find that forest effects on snow accumulation processes were enhanced with warming climate conditions, especially in a scenario with lower precipitation [H2]. However, our hypothesis can be only partially confirmed. Forest–driven reductions on snow accumulation were clearly enhanced with warmer climate conditions during the beginning of the snow season. Nevertheless, the forest–driven reduction in maximum accumulation was more sensitive to changes in precipitation. More detail about each of these arguments is provided in the paragraphs that follow.

Forest effects on snow accumulation were mostly enhanced with warming climate during the beginning of the snow season, when the first snowfalls begin to form the snowpack. First snowfalls occurred in late autumn in the study site, when temperatures are still relatively warm. Previous studies related these conditions, lower amount of snowfall and warm temperatures, to more effective snow interception by forest canopy (Friesen et al., 2015; Revuelto et al., 2015). Under increasing temperatures, it has been reported that the snowfall fraction of precipitation is reduced (Mote et al., 2005); consequently, snow interception by forest canopies was promoted. It has been previously reported that interception is inversely related to snowfall magnitude (Sanmiguel-Vallelado et al., 2020) since trees have a limited capacity of snow interception (Revuelto et al., 2015). Dickerson-Lange et al. (2017) described another reason why accumulation rates between O and F areas could differ in warmer climates. Under warmer temperatures, the dominant mechanism for loss of snow stored in the canopy is melting rather than sublimation, while wind unloading of snow and subsequent redistribution under the forest canopy are expected to be lower due to the higher cohesion of warm snow (Kobayashi, 1987; Shidei, 1952). This could explain the increasing differences in accumulated snow at the beginning of the season between F and O areas simulated under warming conditions, as well as the 7% per °C enhancement of the forest–driven delaying of snow accumulation.

The enhancement of the forest–driven reduction of snow accumulation processes under warmer conditions was not markedly reflected in the peak SWE values. The forest–driven reduction in peak SWE remained significant under warmer conditions, but it was not significantly enhanced by warming (1% per °C). This forest effect was more sensitive to precipitation changes than to temperature warming, as 20% reduction in precipitation and no warming induced 15% enhancement of the forest–driven reduction in peak SWE. Greater declines of peak SWE were found in forest openings compared to under forest canopies for every °C of warming, according to Fang and Pomeroy (2020) projections. In relative terms, peak SWE decreased 29% per °C across all sites, which corresponds to the $>$ 20% decrease per °C sensitivity values of mean SWE to warming that have been reported in previous studies developed in the Pyrenees (López-Moreno et al., 2013; 2017).

4.2. Sensitivity of forest effects on snow melting processes to climate perturbations

Warming can accelerate the initiation of snowmelt (Rasouli et al., 2015). Thus, it was observed that the date of peak SWE occurred earlier under warming conditions. Although the main period of snowmelt shifted forward into a lower solar irradiance period, the melt–out date occurred earlier as temperatures increased (Rasouli et al., 2015). In O areas this response was more pronounced, due to the greater decline of peak SWE with warming compared to forest areas. Roth and Nolin (2017) observed how the effects of reduced solar inputs in forests become secondary and the efficiency of the canopy interception is the main factor controlling the melt–out date. Therefore, differences between F and O areas in the timing of melt out significantly decreased with warming, and the effect of forest driving earlier snowpack melt out was reduced (2 days per °C, on average).

The overall forest shading effect on melting that takes place in our study area was diminished under warmer conditions (2% per °C). Conversely, no clear influence of precipitation changes was found in that response. As previously mentioned, the melt season occurred earlier with increasing temperatures, thus, it shortened to a period of lower available energy. This means that, in a warmer world, much less snow–cover will be exposed to high energy fluxes sufficient to drive moderate to high snowmelt rates (Musselman et al., 2017). For this reason, an overall reduction in melting rates with warming (-0.4 mm·day^{-1} per °C) was observed. This melting slow–down under warmer temperatures was more pronounced in O areas: they experienced a greater shortening of the period of higher energy because of a larger advancement to earlier melt–out dates. As a consequence, O areas showed larger reductions in the available energy to melt. Therefore, the overall differences between F and O areas in the available energy to melt (and thus, in melting rates) decreased with warming, and the overall forest–driven reduction of melting rates was reduced. In addition, this forest effect over melting rates may be undermined under an earlier snowmelt scenario because the solar angle will be lower and the amount of incoming radiation blocked by the forest canopy will therefore be smaller (Lundquist et al., 2013).

4.3. Different seasonal SEB responses to climate perturbation in forested and open areas

Some differences arose in seasonal SEB and its sensitivity to warming between F and O areas. Most studies that have focused on both measuring and modeling the snow cover energy balance reported that radiation and turbulent fluxes are the main energy sources for melting (e.g. Ellis et al., 2010; Gelfan et al., 2004; Hardy et al., 1998; Hedstrom and Pomeroy, 1998; Hotovy and Jenicek, 2020; López-Moreno et al., 2017; Sicart et al., 2004). Our results partially agree with their findings because net all–wave radiation and ground heat, followed by latent heat, dominated the seasonal SEB. Ground heat generally represents a relatively minor component in seasonal SEBs (Hotovy and Jenicek, 2020). Nevertheless, in this study, ground heat flux became especially important in F areas, maybe due to better radiance transmission to the soil in these partially snow–covered areas (Lund et al., 2017). Turbulent energy fluxes were found to be more relevant contributions to seasonal SEB in F areas relative to O areas, contrary to Marks et al. (1998) observations. Advected heat from precipitation adds rather negligible additional energy to the seasonal SEB in any of the studied sites, similar to that reported by other studies (Hotovy and Jenicek, 2020). In a warmer climate, the importance of rain heat input into the snowpack is expected to increase, as more precipitation will fall as rain than as snow (Jenicek et al., 2018b; Musselman et al., 2018), but a relevant increase of rain advected heat contribution to seasonal SEB was not observed.

It is known that forest cover attenuates the transmittance of shortwave radiation and enhances longwave irradiance to the snow surface (Ellis et al., 2011; Essery et al., 2008; Lundquist et al., 2013; Musselman et al., 2008). Shortwave energy reduction was the dominant effect in the study area; hence, net all–wave radiation and melting were reduced in F areas, as previously reported (Dickerson-Lange et al., 2017; Link and Marks, 1999; Musselman et al., 2012; Sicart et al., 2004). Under warmer conditions, net radiative fluxes decreased as a result of earlier snowmelt timing, especially in O areas. This decline is mainly caused by reduced shortwave radiation, leading the melt period to shift earlier in the year towards lower solar zenith angles and shorter daylight lengths (Jennings and Molotch, 2020; Lundquist et al., 2013). Additionally, overall longwave radiation decreased with warming because of the earlier melt period. Jennings and Molotch (2020) observed that the advance of snowmelt timing decreased melting–period air temperatures and resultant incoming longwave radiation, which has a greater effect than the applied melting.

4.4. Spatial variability of forest–snow interactions under a changing climate

In a previous study, it was observed that the magnitude and timing of the forest effects on snow processes varied significantly among closely located stands in the study area (Sanmiguel-Vallelado et al., 2020). In the current study, deeper and more persistent snowpacks were found in forest stands with more snow accumulation and lower rates of ablation promoted by a more efficient forest shading effect (plots 2 and 4), whereas shallower snow conditions were found in forest stands with lower snow accumulation and higher rates of ablation promoted by a more efficient forest heating effect (plots 1 and 3). Broxton et al. (2020) attributed the differences in accumulation and ablation under forest cover to the prevailing aspect (north or south) of the slopes. Our results indicate differential behavior of snow accumulation and ablation under forest canopy in the sites more exposed to sunlight (west and south faced slopes, i.e. plots 3 and 1) with respect to north and east faced slopes (plots 4 and 2); however the small number of experimental plots does not allow to statistically attribute the observed differences to the slope-dependent response of snowpack to forest cover observed by Broxton et al. (2020). It has been reported that a regional increase in temperature may have different effects on snow processes at the local scale, depending on elevation, topography, and exposure to wind and solar radiation (López-Moreno et al., 2013). In accordance with this, and confirming [H4], it also was found that sensitivity of forest–snow interactions to perturbed climate conditions largely varied among neighboring forest stands.

Higher and slightly colder sites have been reported to be less sensitive to the effects of climate warming on snow accumulation, snow energy balance, and snowmelt (Harpold et al., 2012; Kapnick and Hall, 2012; López-Moreno et al., 2017; Mote et al., 2018; Musselman et al., 2017; Rasouli et al., 2019). Our results cannot confirm these observations, probably because of the local scale of our study. The coldest and highest site analyzed in this study (plot 4) showed the largest reductions in snow accumulation and energy available for melting (and thus, the largest reductions in melting rates) with warming.

The reported increased efficiency in snow interception with warming temperatures (Friesen et al., 2015) and subsequent enhanced forest–driven reduction in snow accumulation (Revuelto et al., 2015) could be more pronounced in plots with higher LAI values (Hedstrom and Pomeroy, 1998; Varhola et al., 2010). This may explain the observed enhanced forest–driven reduction in snowpack duration with warming, especially in plot 2, while the warmest and lowest site with the lowest LAI values (plot 3) showed the least sensitivity.

It is known that conifer forests modify the snowpack energy balance by reducing the total amount of shortwave radiation and enhancing total longwave exchange with that emitted by trees, which results in both shading and heating effects, respectively (Sicart et al., 2004). In this study, one forest effect prevailed over the other during the snow season, depending on the analyzed forest stand. In plots 2 and 4, the forest–driven reduction in melting rates (shading effect) was more pronounced than in plots 1 and 3. Plots 2 and 4 presented longer lasting snowpacks than plots 1 and 3, mainly due to higher snow accumulation. More ephemeral snowpacks did not resist long enough into the late spring to benefit from the forest shading effect (Lundquist et al., 2013; Roth and Nolin, 2017; Sicart et al., 2004). Thus, in plots 1 and 3 there was more marked forest–driven increment in melting rates (heating effect). In these stands, the higher longwave radiation by trees compensated the lower shortwave radiation. Under warmer conditions, both heating and shading forest effects were reduced in the studied forest stands, as expected [H3]. It was found that under an earlier snowmelt (i.e. lower incoming energy) scenario, melting rates beneath the forest canopy became similar to those in open areas because differences in net shortwave and net longwave radiation between F and O areas were reduced under warmer conditions. Thus, the higher longwave radiation in the forest tended to compensate for the lower shortwave radiation with increasing temperatures. Therefore, in those sites where the forest shading effect was prevalent (plots 2 and 4), the high melt rate period experienced a greater constriction (i.e. high energy period) and, thus, a higher reduction of melting rates was observed. The undermined shading effect of forest over snowpack under an earlier snowmelt scenario was especially pronounced in plot 2. The forest heating effect was reduced in those sites where it was prevalent (plots 1 and 3), may be because of the lower tree absorption of solar radiation and subsequent lower thermal emissivity that occurs earlier in the year (Lundquist et al., 2013). In addition, the shift in melt timing with warming also decreased net longwave radiation as melt–period air temperatures decreased, because a shift of snowmelt timing can have a greater effect on air temperatures than induced warming (Jennings and Molotch, 2020) and might contribute to diminishing the forest heating effect on melting. The undermined warming effect of forest over snowpack under an earlier snowmelt scenario was especially pronounced in plot 3.

Our simulations of snow-forest interactions were restricted to four forest stands, each of them showing particular environmental characteristics. This represents certain limitation for identifying the different roles of climate, topography and forest structure on the observed variability in forest effects on snow processes and energy balance under climate change conditions. Our simulations were validated with manual and semi-automated measurements, making it difficult to increase the number of study sites due to the significant manual labor and time required for fieldwork in such environments.

5. Conclusions

Forest–snow interactions showed large sensitivity to perturbed climate conditions in the studied mountain forests.

Forest–driven reductions on snow accumulation were clearly enhanced with warmer climate conditions during the beginning of the snow season. Nevertheless, the forest–driven reduction in maximum accumulation was more sensitive to changes in precipitation. On the other hand, an increase in temperature reduced the heating and shading effects of the forest on snowmelt. It was found a significant enhancement of forest–driven reduction in snowpack duration under warming conditions (+10% per $^{\circ}$C).

In a drier and warmer climate scenario, the forest effects on snow accumulation processes could be enhanced, while greater precipitation could partially mask these effects. Under warmer conditions, both shading and heating forest effects could be reduced, but no clear responses were found under combined temperature and precipitation perturbations.

The sensitivity of forest effects on snow processes to perturbed climate conditions varied among nearby stands. Sites with higher canopy interception showed higher warming sensitivity in forest effects on snow accumulation processes, while the duration of the snowpack seemed to determine the prevailing effect of the forest on melting processes (shading or heating) and thus its response to warming. The ability to identify the different roles of climate, topography and forest structure is, however, limited by the low number of forest stands considered in the simulations.

Funding

This study was supported by the projects: "*Bosque, nieve y recursos hídricos en el Pirineo ante el cambio global*" funded by Fundación Iberdrola, CGL2014-52599-P (IBERNIEVE) and CGL2017-82216-R (HIDROIBERNIEVE) funded by the Spanish Ministry of Economy and

Competitiveness. ASV was supported by a pre–doctoral University Professor Training grant [FPU16/00902] funded by the Spanish Ministry of Education, Culture and Sports. JJC acknowledges funding by project RTI2018-096884-B-C31 (Spanish Ministry of Economy and Competitiveness).

CRediT authorship contribution statement

Alba Sanmiguel-Vallelado: Conceptualization, Formal analysis, Investigation, Validation, Visualization, Writing – original draft, Writing – review & editing. **James McPhee:** Conceptualization, Supervision, Validation, Writing – review & editing. **Paula Esmeralda Ojeda Carreño:** Validation, Writing – review & editing. **Enrique Morán-Tejeda:** Conceptualization, Funding acquisition, Resources, Supervision, Writing – review & editing. **J. Julio Camarero:** Funding acquisition, Resources, Supervision, Writing – review & editing. **Juan Ignacio López-Moreno:** Conceptualization, Funding acquisition, Project administration, Resources, Supervision, Writing – review & editing.

Declaration of Competing Interest

The authors declare that they have no known competing financial interests or personal relationships that could have appeared to influence the work reported in this paper.

Acknowledgements

We would like to thank the Spanish State Meteorology Agency (AEMET) and the Automated Hydrological Information System for the Basin of the Ebro River (SAIH) for providing the precipitation and telesnow gauge databases used in this study. We sincerely thank colleagues, friends and relatives who helped with the fieldwork.

Appendix A. Supplementary data

Supplementary data to this article can be found online at https://doi.org/10.1016/j.jhydrol.2021.127311.

References

Adam, J.C., Hamlet, A.F., Lettenmaier, D.P., 2009. Implications of global climate change for snowmelt hydrology in the twenty-first century. Hydrol. Process. Int. J. 23, 962–972.
Asam, S., Callegari, M., Matiu, M., Fiore, G., De Gregorio, L., Jacob, A., Menzel, A., Zebisch, M., Notarnicola, C., 2018. Relationship between spatiotemporal variations of climate, snow cover and plant phenology over the Alps—An earth observation-based analysis. Remote Sens. 10, 1757. https://doi.org/10.3390/rs10111757.
Barnett, T.P., Adam, J.C., Lettenmaier, D.P., 2005. Potential impacts of a warming climate on water availability in snow-dominated regions. Nature 438 (7066), 303–309. https://doi.org/10.1038/nature04141.
Bednorz, E., 2004. Snow cover in eastern Europe in relation to temperature, precipitation and circulation. Int. J. Climatol. 24 (5), 591–601. https://doi.org/10.1002/joc.1014.
Beniston, M., 2012. Is snow in the Alps receding or disappearing? Wiley Interdiscip. Rev. Clim. Change 3 (4), 349–358.
Breiman, L., 2001. Random forests. Mach. Learn. 45, 5–32.
Broxton, P.D., Leeuwen, W.J.D., Biederman, J.A., 2020. Forest cover and topography regulate the thin, ephemeral snowpacks of the semiarid Southwest United States. Ecohydrology 13. https://doi.org/10.1002/eco.2202.
Currier, W.R., Lundquist, J.D., 2018. Snow depth variability at the forest edge in multiple climates in the Western United States. Water Resour. Res. 54, 8756–8773. https://doi.org/10.1029/2018WR022553.
DeBeer, C.M., Pomeroy, J.W., 2010. Simulation of the snowmelt runoff contributing area in a small alpine basin. Hydrol. Earth Syst. Sci. 14, 1205–1219. https://doi.org/10.5194/hess-14-1205-2010.
Del Barrio, G., Creus, J., Puigdefábregas, J., 1990. Thermal seasonality of the high mountain belts of the Pyrenees. Mt. Res. Dev. 227–233.
Dickerson-Lange, S.E., Gersonde, R.F., Hubbart, J.A., Link, T.E., Nolin, A.W., Perry, G.H., Roth, T.R., Wayand, N.E., Lundquist, J.D., 2017. Snow disappearance timing is dominated by forest effects on snow accumulation in warm winter climates of the Pacific Northwest, United States. Hydrol. Process. 31, 1846–1862. https://doi.org/10.1002/hyp.11144.
Ellis, C., Pomeroy, J., T, B., J, M., 2010. Simulations of snow accumulation and melt in needleleaf forest environments. Hydrol. Earth Syst. Sci. Discuss. 14. 10.5194/hessd-7-1033-2010.
Ellis, C.R., Pomeroy, J.W., Essery, R.L.H., Link, T.E., 2011. Effects of needleleaf forest cover on radiation and snowmelt dynamics in the Canadian Rocky Mountains. Can. J. For. Res. 41, 608–620.
Ellis, C.R., Pomeroy, J.W., Link, T.E., 2013. Modeling increases in snowmelt yield and desynchronization resulting from forest gap-thinning treatments in a northern mountain headwater basin. Water Resour. Res. 49, 936–949. https://doi.org/10.1002/wrcr.20089.
Essery, R., Pomeroy, J., Ellis, C., Link, T., 2008. Modelling longwave radiation to snow beneath forest canopies using hemispherical photography or linear regression. Hydrol. Process. Int. J. 22, 2788–2800.
Evan, A., Eisenman, I., 2021. A mechanism for regional variations in snowpack melt under rising temperature. Nat. Clim. Change. 10.1038/s41558-021-00996-w.
Fang, X., Pomeroy, J.W., 2020. Diagnosis of future changes in hydrology for a Canadian Rockies headwater basin. Hydrol. Earth Syst. Sci. 24, 2731–2754. https://doi.org/10.5194/hess-24-2731-2020.
Friesen, J., Lundquist, J., Van Stan, J.T., 2015. Evolution of forest precipitation water storage measurement methods. Hydrol. Process. 29, 2504–2520. https://doi.org/10.1002/hyp.10376.
Gelfan, A.N., Pomeroy, J.W., Kuchment, L.S., 2004. Modeling forest cover influences on snow accumulation, sublimation, and melt. J. Hydrometeorol. 5, 785–803.
Giorgi, F., Lionello, P., 2008. Climate change projections for the Mediterranean region. Glob. Planet. Change, Mediterranean climate: trends, variability and change 63, 90–104. 10.1016/j.gloplacha.2007.09.005.
Hardy, J.P., Davis, R.E., Jordan, R., Ni, W., Woodcock, C.E., 1998. Snow ablation modelling in a mature aspen stand of the boreal forest. Hydrol. Process. 12, 1763–1778.
Hardy, J.P., Melloh, R., Robinson, P., Jordan, R., 2000. Incorporating effects of forest litter in a snow process model. Hydrol. Process. 14, 3227–3237. https://doi.org/10.1002/1099-1085(20001230)14:18<3227::AID-HYP198>3.0.CO;2-4.
Harpold, A., Brooks, P., Rajagopal, S., Heidbuchel, I., Jardine, A., Stielstra, C., 2012. Changes in snowpack accumulation and ablation in the intermountain west. Water Resour. Res. 48 https://doi.org/10.1029/2012WR011949.
Harpold, A.A., 2016. Diverging sensitivity of soil water stress to changing snowmelt timing in the Western U.S.
Hedstrom, N.R., Pomeroy, J.W., 1998. Measurements and modelling of snow interception in the boreal forest. Hydrol. Process. 12, 1611–1625.
Hiemstra, C.A., Liston, G.E., Reiners, W.A., 2002. Snow redistribution by wind and interactions with vegetation at upper treeline in the Medicine Bow Mountains, Wyoming. USA. Arct. Antarct. Alp. Res. 34, 262–273.
Hotovy, O., Jenicek, M., 2020. The impact of changing subcanopy radiation on snowmelt in a disturbed coniferous forest. Hydrol. Process. 34, 5298–5314. https://doi.org/10.1002/hyp.13936.
Huerta, M.L., Molotch, N.P., McPhee, J., 2019. Snowfall interception in a deciduous Nothofagus forest and implications for spatial snowpack distribution. Hydrol. Process. 33, 1818–1834. https://doi.org/10.1002/hyp.13439.
Jenicek, M., Pevna, H., Matejka, O., 2018a. Canopy structure and topography effects on snow distribution at a catchment scale: Application of multivariate approaches. J. Hydrol. Hydromech. 66, 43–54. https://doi.org/10.1515/johh-2017-0027.
Jenicek, M., Seibert, J., Staudinger, M., 2018b. Modeling of future changes in seasonal snowpack and impacts on summer low flows in alpine catchments. Water Resour. Res. 54, 538–556.
Jennings, K.S., Molotch, N.P., 2020. Snowfall fraction, cold content, and energy balance changes drive differential response to simulated warming in an alpine and subalpine snowpack. Front. Earth Sci. 8 https://doi.org/10.3389/feart.2020.00186.
Jost, G., Weiler, M., Gluns, D.R., Alila, Y., 2007. The influence of forest and topography on snow accumulation and melt at the watershed-scale. J. Hydrol. 347, 101–115. https://doi.org/10.1016/j.jhydrol.2007.09.006.
Kapnick, S., Hall, A., 2012. Causes of recent changes in western North American snowpack. Clim. Dyn. 38, 1885–1899. https://doi.org/10.1007/s00382-011-1089-y.
Knutti, R., Sedláček, J., 2013. Robustness and uncertainties in the new CMIP5 climate model projections. Nat. Clim. Change 3, 369–373.
Kobayashi, D., 1987. Snow accumulation on a narrow board. Cold Reg. Sci. Technol. 13, 239–245.
Krogh, S.A., Pomeroy, J.W., McPhee, J., 2015. Physically based mountain hydrological modeling using reanalysis data in Patagonia. J. Hydrometeorol. 16, 172–193. https://doi.org/10.1175/JHM-D-13-0178.1.
Link, T.E., Marks, D., 1999. Point simulation of seasonal snow cover dynamics beneath boreal forest canopies. J. Geophys. Res. Atmospheres 104, 27841–27857.
López-Moreno, J.I., Gascoin, S., Herrero, J., Sproles, E.A., Pons, M., Alonso-González, E., Hanich, L., Boudhar, A., Musselman, K.N., Molotch, N.P., Sickman, J., Pomeroy, J., 2017. Different sensitivities of snowpacks to warming in Mediterranean climate mountain areas. Environ. Res. Lett. 12, 074006 https://doi.org/10.1088/1748-9326/aa70cb.
López-Moreno, J.I., Latron, J., 2008. Influence of canopy density on snow distribution in a temperate mountain range. Hydrol. Process. 22, 117–126. https://doi.org/10.1002/hyp.6572.
López-Moreno, J.I., Pomeroy, J.W., Alonso-González, E., Morán-Tejeda, E., Revuelto, J., 2020. Decoupling of warming mountain snowpacks from hydrological regimes. Environ. Res. Lett. 15, 114006 https://doi.org/10.1088/1748-9326/abb55f.
López-Moreno, J.I., Pomeroy, J.W., Revuelto, J., Vicente-Serrano, S.M., 2013. Response of snow processes to climate change: spatial variability in a small basin in the Spanish Pyrenees. Hydrol. Process. 27, 2637–2650.
López-Moreno, J.I., Revuelto, J., Gilaberte, M., Morán-Tejeda, E., Pons, M., Jover, E., Esteban, P., García, C., Pomeroy, J.W., 2014. The effect of slope aspect on the response of snowpack to climate warming in the Pyrenees. Theor. Appl. Climatol. 117, 207–219. https://doi.org/10.1007/s00704-013-0991-0.

López-Moreno, J.I., Stähli, M., 2008. Statistical analysis of the snow cover variability in a subalpine watershed: assessing the role of topography and forest interactions. J. Hydrol. 348, 379–394.
Lund, M., Stiegler, C., Abermann, J., Citterio, M., Hansen, B.U., van As, D., 2017. Spatiotemporal variability in surface energy balance across tundra, snow and ice in Greenland. Ambio 46, 81–93.
Lundquist, J.D., Cayan, D.R., 2007. Surface temperature patterns in complex terrain: daily variations and long-term change in the central Sierra Nevada. California. J. Geophys. Res. 112, D11124. https://doi.org/10.1029/2006JD007561.
Lundquist, J.D., Dickerson-Lange, S.E., Lutz, J.A., Cristea, N.C., 2013. Lower forest density enhances snow retention in regions with warmer winters: a global framework developed from plot-scale observations and modeling. Water Resour. Res. 49, 6356–6370. https://doi.org/10.1002/wrcr.20504.
Marks, D., Kimball, J., Tingey, D., Link, T., 1998. The sensitivity of snowmelt processes to climate conditions and forest cover during rain-on-snow: a case study of the 1996 Pacific Northwest flood. Hydrol. Process. 12, 1569–1587.
Marshall, A.M., Abatzoglou, J.T., Link, T.E., Tennant, C.J., 2019. Projected changes in interannual variability of peak snowpack amount and timing in the Western United States. Geophys. Res. Lett. 46, 8882–8892. https://doi.org/10.1029/2019GL083770.
Moeser, D., Mazzotti, G., Helbig, N., Jonas, T., 2016. Representing spatial variability of forest snow: implementation of a new interception model. Water Resour. Res. 52, 1208–1226. https://doi.org/10.1002/2015WR017961.
Molotch, N.P., Blanken, P.D., Williams, M.W., Turnipseed, A.A., Monson, R.K., Margulis, S.A., 2007. Estimating sublimation of intercepted and sub-canopy snow using eddy covariance systems. Hydrol. Process. 21, 1567–1575. https://doi.org/10.1002/hyp.6719.
Morán-Tejeda, E., López-Moreno, J.I., Sanmiguel-Vallelado, A., 2017. Changes in climate, snow and water resources in the Spanish Pyrenees: observations and projections in a warming climate, in: High Mountain Conservation in a Changing World. Springer, pp. 305–323.
Mote, P.W., Hamlet, A.F., Clark, M.P., Lettenmaier, D.P., 2005. Declining mountain snowpack in western North America. Bull. Am. Meteorol. Soc. 86, 39–50. https://doi.org/10.1175/BAMS-86-1-39.
Mote, P.W., Li, S., Lettenmaier, D.P., Xiao, M., Engel, R., 2018. Dramatic declines in snowpack in the western US. NPJ Clim. Atmospheric Sci. 1, 2. https://doi.org/10.1038/s41612-018-0012-1.
Musselman, K.N., Clark, M.P., Liu, C., Ikeda, K., Rasmussen, R., 2017. Slower snowmelt in a warmer world. Nat. Clim. Change 7, 214–219. https://doi.org/10.1038/nclimate3225.
Musselman, K.N., Lehner, F., Ikeda, K., Clark, M.P., Prein, A.F., Liu, C., Barlage, M., Rasmussen, R., 2018. Projected increases and shifts in rain-on-snow flood risk over western North America. Nat. Clim. Change 8, 808–812.
Musselman, K.N., Molotch, N.P., Brooks, P.D., 2008. Effects of vegetation on snow accumulation and ablation in a mid-latitude sub-alpine forest. Hydrol. Process. 22, 2767–2776. https://doi.org/10.1002/hyp.7050.
Musselman, K.N., Molotch, N.P., Margulis, S.A., Kirchner, P.B., Bales, R.C., 2012. Influence of canopy structure and direct beam solar irradiance on snowmelt rates in a mixed conifer forest. Agric. For. Meteorol. 161, 46–56.
Musselman, K.N., Pomeroy, J.W., Link, T.E., 2015. Variability in shortwave irradiance caused by forest gaps: measurements, modelling, and implications for snow energetics. Agric. For. Meteorol. 207, 69–82. https://doi.org/10.1016/j.agrformet.2015.03.014.
Nogués Bravo, D., Araújo, M.B., Lasanta, T., López Moreno, J.I., 2008. Climate change in Mediterranean mountains during the 21st century. Ambio 37, 280–285. https://doi.org/10.1579/0044-7447(2008)37[280:ccimmd]2.0.co;2.
Pierce, D.W., Cayan, D.R., 2013. The uneven response of different snow measures to human-induced climate warming. J. Clim. 26, 4148–4167. https://doi.org/10.1175/JCLI-D-12-00534.1.
Pomeroy, J.W., Fang, X., Rasouli, K., 2015. Sensitivity of snow processes to warming in the Canadian Rockies. In: in: 72nd Eastern Snow Conference, pp. 9–11.
Pomeroy, J.W., Gray, D.M., Brown, T., Hedstrom, N.R., Quinton, W.L., Granger, R.J., Carey, S.K., 2007. The cold regions hydrological model: a platform for basing process representation and model structure on physical evidence. Hydrol. Process. 21, 2650–2667. https://doi.org/10.1002/hyp.6787.
Pomeroy, J.W., Gray, D.M., Hedstrom, N.R., Janowicz, J.R., 2002. Prediction of seasonal snow accumulation in cold climate forests. Hydrol. Process. 16, 3543–3558. https://doi.org/10.1002/hyp.1228.
R Core Team, 2020. R: A language and environment for statistical computing. R Foundation for Statistical Computing, Vienna, Austria.
Rasband, W., 1997. ImageJ. US National Institutes of Health, Bethesda, MD, USA.
Rasouli, K., Pomeroy, J.W., Marks, D.G., 2015. Snowpack sensitivity to perturbed climate in a cool mid-latitude mountain catchment. Hydrol. Process. 29, 3925–3940. https://doi.org/10.1002/hyp.10587.
Rasouli, K., Pomeroy, J.W., Whitfield, P.H., 2019. Hydrological responses of headwater basins to monthly perturbed climate in the North American Cordillera. J. Hydrometeorol. 20, 863–882. https://doi.org/10.1175/JHM-D-18-0166.1.
Revuelto, J., López-Moreno, J.I., Azorin-Molina, C., Vicente-Serrano, S.M., 2015. Canopy influence on snow depth distribution in a pine stand determined from terrestrial laser data. Water Resour. Res. 51, 3476–3489. https://doi.org/10.1002/2014WR016496.
Roth, T.R., Nolin, A.W., 2017. Forest impacts on snow accumulation and ablation across an elevation gradient in a temperate montane environment. Hydrol. Earth Syst. Sci. 21, 5427–5442. https://doi.org/10.5194/hess-21-5427-2017.
Sanmiguel-Vallelado, A., López-Moreno, J.I., Morán-Tejeda, E., Alonso-González, E., Navarro-Serrano, F.M., Rico, I., Camarero, J.J., 2020. Variable effects of forest canopies on snow processes in a valley of the central Spanish Pyrenees. Hydrol. Process. 34, 2247–2262. https://doi.org/10.1002/hyp.13721.
Shidei, T., 1952. Study of the fallen snow on the forest trees. I. Bull. Gov. Exp. Stn. 54, 115–164.
Shook, K., 2016. CRHMr: pre- and post- processing for the Cold Regions Hydrological Modelling (CRHM) platform.
Shrestha, R.R., Bonsal, B.R., Bonnyman, J.M., Cannon, A.J., Najafi, M.R., 2021. Heterogeneous snowpack response and snow drought occurrence across river basins of northwestern North America under 1.0°C to 4.0°C global warming. Clim. Change 164, 40. https://doi.org/10.1007/s10584-021-02968-7.
Sicart, J.E., Essery, R.L., Pomeroy, J.W., Hardy, J., Link, T., Marks, D., 2004. A sensitivity study of daytime net radiation during snowmelt to forest canopy and atmospheric conditions. J. Hydrometeorol. 5, 774–784.
Sicart, J.E., Pomeroy, J.W., Essery, R.L.H., Bewley, D., 2006. Incoming longwave radiation to melting snow: observations, sensitivity and estimation in Northern environments. Hydrol. Process. 20, 3697–3708. https://doi.org/10.1002/hyp.6383.
Stekhoven, D.J., 2013. missForest: Nonparametric missing value imputation using random forest.
Stekhoven, D.J., Buhlmann, P., 2012. MissForest–non-parametric missing value imputation for mixed-type data. Bioinformatics 28, 112–118. https://doi.org/10.1093/bioinformatics/btr597.
Storck, P., Lettenmaier, D.P., Bolton, S.M., 2002. Measurement of snow interception and canopy effects on snow accumulation and melt in a mountainous maritime climate, Oregon, United States. Water Resour. Res. 38, 1–5.
Sun, F., Hall, A., Schwartz, M., Walton, D.B., Berg, N., 2016. Twenty-First-Century Snowfall and Snowpack Changes over the Southern California Mountains. J. Clim. 29, 91–110. https://doi.org/10.1175/JCLI-D-15-0199.1.
Tennant, C.J., Harpold, A.A., Lohse, K.A., Godsey, S.E., Crosby, B.T., Larsen, L.G., Brooks, P.D., Kirk, R.W.V., Glenn, N.F., 2017. Regional sensitivities of seasonal snowpack to elevation, aspect, and vegetation cover in western North America. Water Resour. Res. 53, 6908–6926. https://doi.org/10.1002/2016WR019374.
Vaganov, E.A., Hughes, M.K., Kirdyanov, A.V., Schweingruber, F.H., Silkin, P.P., 1999. Influence of snowfall and melt timing on tree growth in subarctic Eurasia. Nature 400, 149–151. https://doi.org/10.1038/22087.
Varhola, A., Coops, N.C., Weiler, M., Moore, R.D., 2010. Forest canopy effects on snow accumulation and ablation: an integrative review of empirical results. J. Hydrol. 392, 219–233.
Vicente-Serrano, S.M., López-Moreno, J.I., Drumond, A., Gimeno, L., Nieto, R., Morán-Tejeda, E., Lorenzo-Lacruz, J., Beguería, S., Zabalza, J., 2011. Effects of warming processes on droughts and water resources in the NW Iberian Peninsula (1930–2006). Clim. Res. 48, 203–212.
Westerling, A.L., 2016. Increasing western US forest wildfire activity: sensitivity to changes in the timing of spring. Philos. Trans. R. Soc. B Biol. Sci. 371, 20150178. https://doi.org/10.1098/rstb.2015.0178.

Appendix A. Supplementary data

Table A1. Selected CRHM Modules and particular specifications included in our simulations.

Module	Variation	Characteristics and particular specifications
Basin		Holds commonly used physical and control parameters.
Global		Calculates theoretical shortwave radiation using the method proposed by Garnier and Ohmura (1970).
Obs		Converts measurement observations to HRU variables with corrections, original interval version.
calcsun	#1	Calculates sunshine hours to replace field data. Use observed incident shortwave variable to estimate sunshine hours.
longVt		Calculates incoming longwave radiation variable using terrain view factor (Sicart et al., 2006). Using observed incident shortwave variable to calculate daily average.
Netall		Models net all–wave radiation from sunshine hours, temperature and humidity using Brunt formulation.
Evap		Calculates interval evaporation using Granger, Priestley–Taylor or Penman–Monteith methods.
CanopyClearingGap	#1	Prototype all season canopy/clearing module. Calculates short–, long– and all–wave radiation components at the snow surface. Inputs are observed incident shortwave radiation and calculated incoming long–wave radiation. Areas beneath forest canopy at studied sites were classified as "canopy" areas in the module and forest openings as "gap" areas.
albedo_Richard		Calculates snow cover albedo from a method proposed by Essery (2013).
walmsey_wind		A parametric version of the wind flow model (Mason and Sykes, 1979).
pbsmSnobal	#1	Calculates snow transport and sublimation (Essery et al., 1999). Uses adjusted wind speed from Walmsley_wind module instead of observed wind speed.
SnobalCRHM	#1	A model using the energy balance to calculate snowmelt (Marks et al., 1998). Use variables incident shortwave and longwave at snow surface from module CanopyClearingGap. Hourly soil temperature could not be used as observed variable since there was a year of missing data (2019/20). Thus, median values at each plot and snow season, distinguishing gap and canopy areas, were calculated and included as parameters in this module.

Table A2. Parameters used in the CRHM modeling framework. Individual models were performed at each plot. Two hydrological response units (HRUs) were distinguished at each plot: O – forest openings or gaps–, and F – areas beneath forest canopy, forested.

Module	Parameter	Units	Plot 1		Plot 2		Plot 3		Plot 4	
			O	F	O	F	O	F	O	F
Shared	basin_area	[km^2]	$4.5\cdot e^{-4}$		$4.5\cdot e^{-4}$		$4.5\cdot e^{-4}$		$4.5\cdot e^{-4}$	
	hru_area	[km^2]	$2.25\cdot e^{-4}$	$2.25\cdot e^{-4}$	$2.25\cdot e^{-4}$	$2.25\cdot e^{-4}$	$2.25\cdot e^{-4}$	$2.25\cdot e^{-4}$	$2.25\cdot e^{-4}$	$2.25\cdot e^{-4}$
	hru_ASL	[°]	194	194	120	120	262	262	300	300
	hru_elev	[m]	2008	2008	1814	1814	1674	1674	2104	2104
	hru_GSL	[°]	29.4	29.4	20.4	20.4	9.3	9.3	22.7	22.7
	hru_lat	[°]	42.8	42.8	42.8	42.8	42.8	42.8	42.8	42.8
	Ht	[m]	0.08	9.20	0.08	8.60	0.08	9.00	0.08	9.10
	Inhibit_evap	[-]	0	0	0	0	0	0	0	0
	Zwind	[m]	3	3	3	3	3	3	3	3
Albedo_Richard	a1	[s]	$1.08\cdot e^{7}$	$1.08\cdot e^{7}$	$1.08\cdot e^{7}$	$1.08\cdot e^{7}$	$1.08\cdot e^{7}$	$1.08\cdot e^{7}$	$1.08\cdot e^{7}$	$1.08\cdot e^{7}$
	a2	[s]	$7.20\cdot e^{5}$	$7.20\cdot e^{5}$	$7.20\cdot e^{5}$	$7.20\cdot e^{5}$	$7.20\cdot e^{5}$	$7.20\cdot e^{5}$	$7.20\cdot e^{5}$	$7.20\cdot e^{5}$
	Albedo_Bare	[-]	0.17	0.17	0.17	0.17	0.17	0.17	0.17	0.17
	Albedo_Snow	[-]	0.85	0.85	0.85	0.85	0.85	0.85	0.85	0.85
	amax	[-]	0.84	0.84	0.84	0.84	0.84	0.84	0.84	0.84
	amin	[-]	0.4	0.2	0.4	0.2	0.4	0.2	0.4	0.2
	smin	[mm·int^{-1}]	10	15	10	15	10	15	10	15
Annandale	krs	[-]	0.16	0.16	0.16	0.16	0.16	0.16	0.16	0.16
CanopyClearingGap	Alpha_c	[-]	0.1	0.1	0.1	0.1	0.1	0.1	0.1	0.1
	B_canopy	[-]	0.038	0.038	0.038	0.038	0.038	0.038	0.038	0.038
	CanopyClearing	[-]	2	0	2	0	2	0	2	0
	Gap_diameter	[m]	12	12	20	20	32	32	47	47
	LAI	[-]	0.1	1.92	0.1	2.11	0.1	1.83	0.1	2.55
	Sbar	[kg·m^{-2}]	1	40	1	30	1	15	1	55
	Surrounding_Ht	[m]	9.2	9.2	8.6	8.6	9.0	9.0	9.1	9.1
	unload_t	[°C]	0	0	0	0	0	0	0	0
	unload_t_water	[°C]	1	1	1	1	1	1	1	1
	Z0snow	[m]	0.005	0.010	0.005	0.010	0.005	0.010	0.005	0.010
	Zref	[m]	2	2	2	2	2	2	2	2
	Zvent	[-]	0.75	0.75	0.75	0.75	0.75	0.75	0.75	0.75
Evap	evap_type	[-]	1	1	1	1	1	1	1	1
	F_Qg	[-]	0.1	0.1	0.1	0.1	0.1	0.1	0.1	0.1
	rs	[d·m^{-1}]	$8.100\cdot e^{-4}$	$2.315\cdot e^{-3}$	$8.100\cdot e^{-4}$	$2.315\cdot e^{-3}$	$8.100\cdot e^{-4}$	$2.315\cdot e^{-3}$	$8.100\cdot e^{-4}$	$2.315\cdot e^{-3}$
Global	Time_Offset	[H]	-2	-2	-2	-2	-2	-2	-2	-2
LongVt	epsilon_s	[-]	0.98	0.98	0.98	0.98	0.98	0.98	0.98	0.98
	Vt	[-]	0.6	0.6	0.5	0.5	0.3	0.3	0.6	0.6
pbsm_Snobal	A_S	[m]	0.003	0.003	0.003	0.003	0.003	0.003	0.003	0.003
	distrib	[-]	1	1	1	1	1	1	1	1
	fetch	[m]	1000	1000	1000	1000	1000	1000	1000	1000
	inhibit_bs	[-]	0	0	0	0	0	0	0	0
	inhibit_subl	[-]	0	0	0	0	0	0	0	0
	N_S	[m^{-2}]	1	350	1	200	1	126	1	100
SnobalCRHM	HRU_F_g	[W·m^{-2}]	0	0	0	0	0	0	0	0
	Hru_rho_snow	[kg·m^{-3}]	100	100	100	100	100	100	100	100
	Hru_t_g	[°C]	1	1.7	1.00	1.87	2	2	0.39	0.7
	KT_sand	[-]	0.08	0.08	0.08	0.08	0.08	0.08	0.08	0.08
	maxh2o_vol	[-]	0.0001	0.0001	0.0001	0.0001	0.0001	0.0001	0.0001	0.0001
	max_z_s_0	[m]	0.35	0.35	0.35	0.35	0.35	0.35	0.35	0.35
	rain_soil_snow	[-]	1	1	1	1	1	1	1	1
	relative_hts	[-]	1	1	1	1	1	1	1	1
	T_g_or_G_flux	[-]	0	0	0	0	0	0	0	0
	z_0	[m]	0.001	0.1	0.001	0.1	0.001	0.1	0.001	0.1
	z_g	[m]	0.1	0.1	0.1	0.1	0.1	0.1	0.1	0.1
	z_T	[m]	2	2	2	2	2	2	2	2
	z_u	[m]	3	3	3	3	3	3	3	3
obs	catchadjust	[-]	3	3	3	3	3	3	3	3

	ClimChng_flag	[-]	0	0	0	0	0	0	0	0
	ClimChng_precip	[-]	1	1	1	1	1	1	1	1
	ClimChng_t	[°C]	0	0	0	0	0	0	0	0
	ElevChng_t	[-]	0	0	0	0	0	0	0	0
	HRU_OBS[1]	[-]	5	5	5	5	5	5	5	5
	HRU_OBS[2]	[-]	5	5	5	5	5	5	5	5
	HRU_OBS[3]	[-]	5	5	5	5	5	5	5	5
	HRU_OBS[4]	[-]	5	5	5	5	5	5	5	5
	HRU_OBS[5]	[-]	5	5	5	5	5	5	5	5
	Lapse_rate	[°C·100m^{-1}]	0.52	0.52	0.52	0.52	0.52	0.52	0.52	0.52
	Obs_elev[1]	[m]	2008	2008	1814	1814	1674	1674	2104	2104
	Obs_elev[2]	[m]	1630	1630	1630	1630	1630	1630	1630	1630
	Ppt_daily_distrib	[-]	0	0	0	0	0	0	0	0
	Precip_elev_adj	[100m^{-1}]	0.06	0.06	0.18	0.18	0.6	0.6	0.07	0.07
	Snow_rain_determination	[-]	2	2	2	2	2	2	2	2
	Tmax_allrain	[ºC]	4	4	4	4	4	4	4	4
	Tmax_allsnow	[ºC]	0	0	0	0	0	0	0	0
Walmsley_wind	A		3	3	3	3	3	3	3	3
	B		2	2	2	2	2	2	2	2
	L		1000	1000	1000	1000	1000	1000	1000	1000
	Walmsley_Ht	[m]	100	100	100	100	100	100	100	100

Table A3. Determined model bias index (MB), model efficiency index (ME), and root mean square error (RMSE) for simulations of daily snow water equivalent (SWE) at the four study plots considering areas beneath forest canopy (F) and forest openings (O). Data of 2016/17 and 2017/18 snow seasons is shown.

Plot	Area	MB	ME	RSME (mm)
Plot 1	F	1.11	0.76	43
	O	1.06	0.94	42
Plot 2	F	0.96	0.95	24
	O	0.98	0.98	26
Plot 3	F	1.04	0.78	18
	O	1.03	0.95	29
Plot 4	F	1.11	0.81	77
	O	0.96	0.95	83

Table A4. Statistically significant differences ($p < 0.05$) between areas beneath forest canopy (F) and forest openings (O) in the magnitude and percentage of change of snow indices. Wilcoxon tests were performed using data from all plots and snow seasons.

		Index magnitude						Index % of change					
Δpp (%)	ΔT (ºC)	Accum. onset	Melt out date	Peak SWE date	Snow duration	Peak SWE	Melting rate	Accum. onset	Melt out date	Peak SWE date	Snow duration	Peak SWE	Melting rate
	0	< 0.05				< 0.001					< 0.01		
+20	1	< 0.01			< 0.05	< 0.001					< 0.01		
	2	< 0.01			< 0.05	< 0.01					< 0.01		

	3	< 0.01			< 0.01	< 0.05					< 0.01		
	4	< 0.01			< 0.01						< 0.01		
	0	< 0.05	< 0.05			< 0.001		-	-	-	-	-	-
	1	< 0.05			< 0.05	< 0.001					< 0.01		
0	2	< 0.01			< 0.01	< 0.05					< 0.05		
	3	< 0.05			< 0.01	< 0.05					< 0.05		
	4	< 0.05			< 0.01						< 0.05		
	0	< 0.05				< 0.001		< 0.01			< 0.01		
	1	< 0.05			< 0.01	< 0.01	< 0.05				< 0.01		
-20	2	< 0.05			< 0.01	< 0.05	< 0.01				< 0.01		
	3	< 0.05			< 0.01		< 0.05				< 0.01		
	4				< 0.01						< 0.01		

Table A5. Snow indices change per ºC of temperature increment with regard to the non–perturbed conditions at each site. Both types of changes in magnitude and relative change are presented. The different areas analyzed at each study site (F: beneath forest canopy; O: forest openings) are distinguished. Median values of the fourmodeled snow seasons (2016/17 – 2019/20) are shown.

Type of change per ºC	Site	Accum. Onset		Melt out date		SWE peak date		Snow duration		SWE peak		Melting rate	
		F	O	F	O	F	O	F	O	F	O	F	O
In magnitude (days; days; days; days; mm; mm·day^{-1})·C^{-1}	Plot 1	13	6	-7	-12	-8	-6	-30	-30	-79	-110	-0.4	0.3
	Plot 2	18	3	-10	-15	-12	-12	-33	-32	-75	-105	-0.5	-0.7
	Plot 3	14	7	-6	-9	-4	-7	-22	-27	-59	-99	0.1	0.5
	Plot 4	9	2	-10	-5	-4	-14	-40	-30	-112	-201	-0.7	-1.9
Relative (%·C^{-1})	Plot 1	28	18	-4	-6	-6	-4	-30	-23	-30	-28	-6.2	4.3
	Plot 2	18	48	-6	-5	-4	-9	-23	-31	-28	-32	4.3	-7.3
	Plot 3	48	9	-5	-7	-9	-2	-31	-24	-32	-26	-7.3	-8.1
	Plot 4	9	31	-7	-3	-2	-3	-24	-29	-26	-30	-8.1	1.9

Table A6. Individual snow energy fluxes per ºC of temperature increment with regard to the non–perturbed conditions at each site. Both types of changes in magnitude and relative change are presented. The different areas analyzed at each study site (F: beneath forest canopy; O: forest openings) are distinguished. Median values of the four modeled snow seasons (2016/17 – 2019/20) are shown.

Type of change per ºC	Site	Net radiation		Latent heat[1]		Sensible heat		Precipitation heat		Ground heat	
		F	O	F	O	F	O	F	O	F	O
In magnitude (W·m^{-2}·C^{-1})	Plot 1	-1.1	-3.0	1.0	0.3	-0.1	0.0	-0.05	-0.04	-2.3	-0.5
	Plot 2	-0.7	-3.0	1.5	0.3	-0.8	-0.2	-0.07	-0.06	-2.8	-0.6
	Plot 3	-0.6	-2.3	1.3	0.3	-0.5	-0.3	-0.07	-0.09	-2.6	-2.1
	Plot 4	-2.5	-4.3	2.8	0.7	-1.7	-0.2	-0.06	-0.05	-1.3	-0.1
Relative (%·C^{-1})	Plot 1	-43.0	-35.1	37.6	29.0	-58.2	10.2	-23.9	-14.9	-30.4	-12.2
	Plot 2	-49.6	-36.3	34.9	28.2	-49.2	-45.8	-27.5	-20.2	-31.6	-14.2
	Plot 3	-41.3	-43.6	30.5	29.1	-39.1	-42.4	-29.3	-28.5	-32.9	-27.0
	Plot 4	-41.2	-27.7	33.8	28.5	-40.6	-23.5	-16.5	-11.3	-19.7	-4.9

[1]Latent heat flux is a negative component, so positive changes values lead to reductions in the component's magnitude.

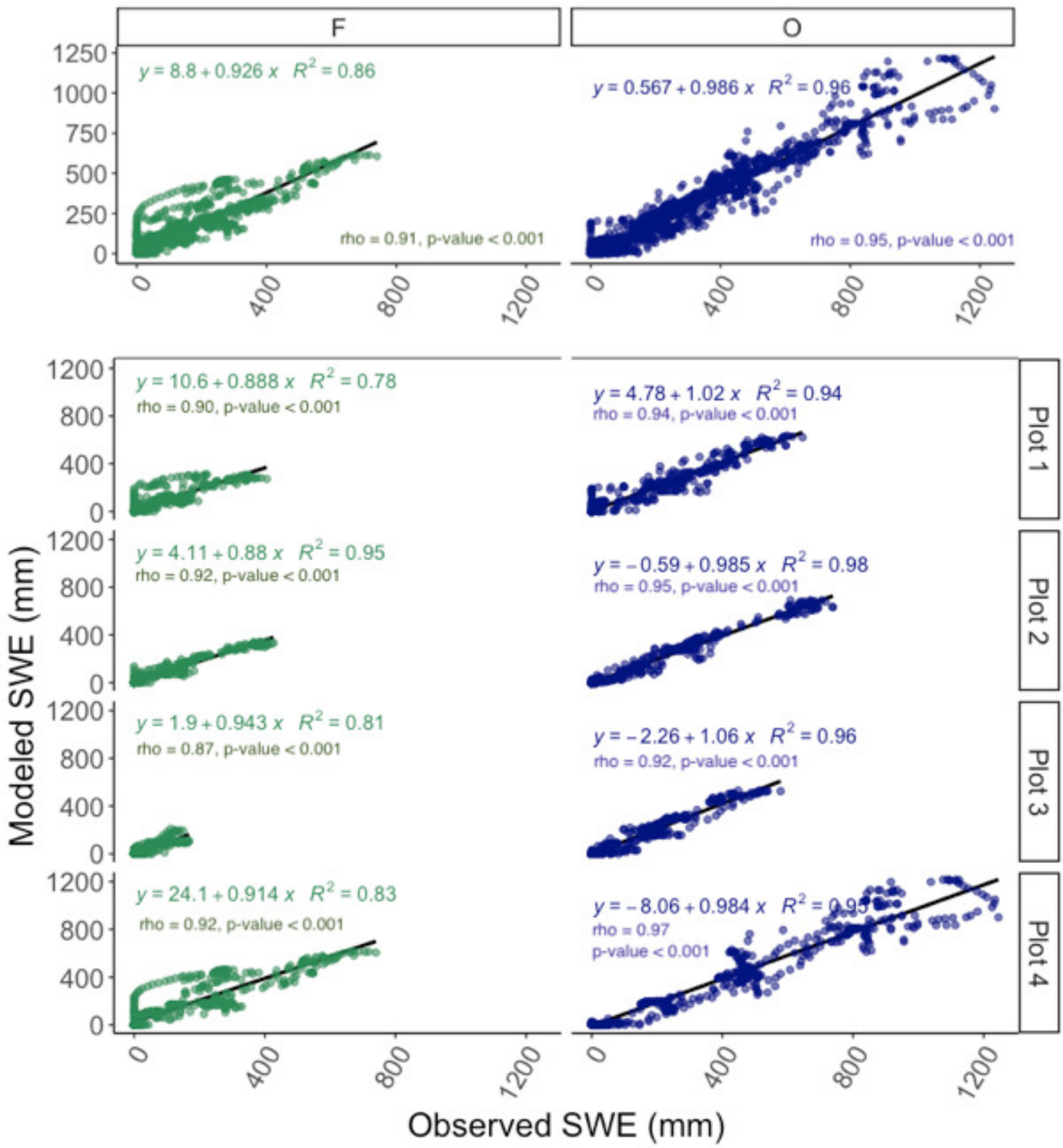

Figure A1. Scatter plots of modeled daily SWE vs. observed daily SWE in areas beneath forest canopy (F, green lines) and in forest openings (O, blue lines). Data of 2016/17 and 2017/18 snow seasons is shown. Spearman coefficient of correlation (rho) and *p*–values are labeled.

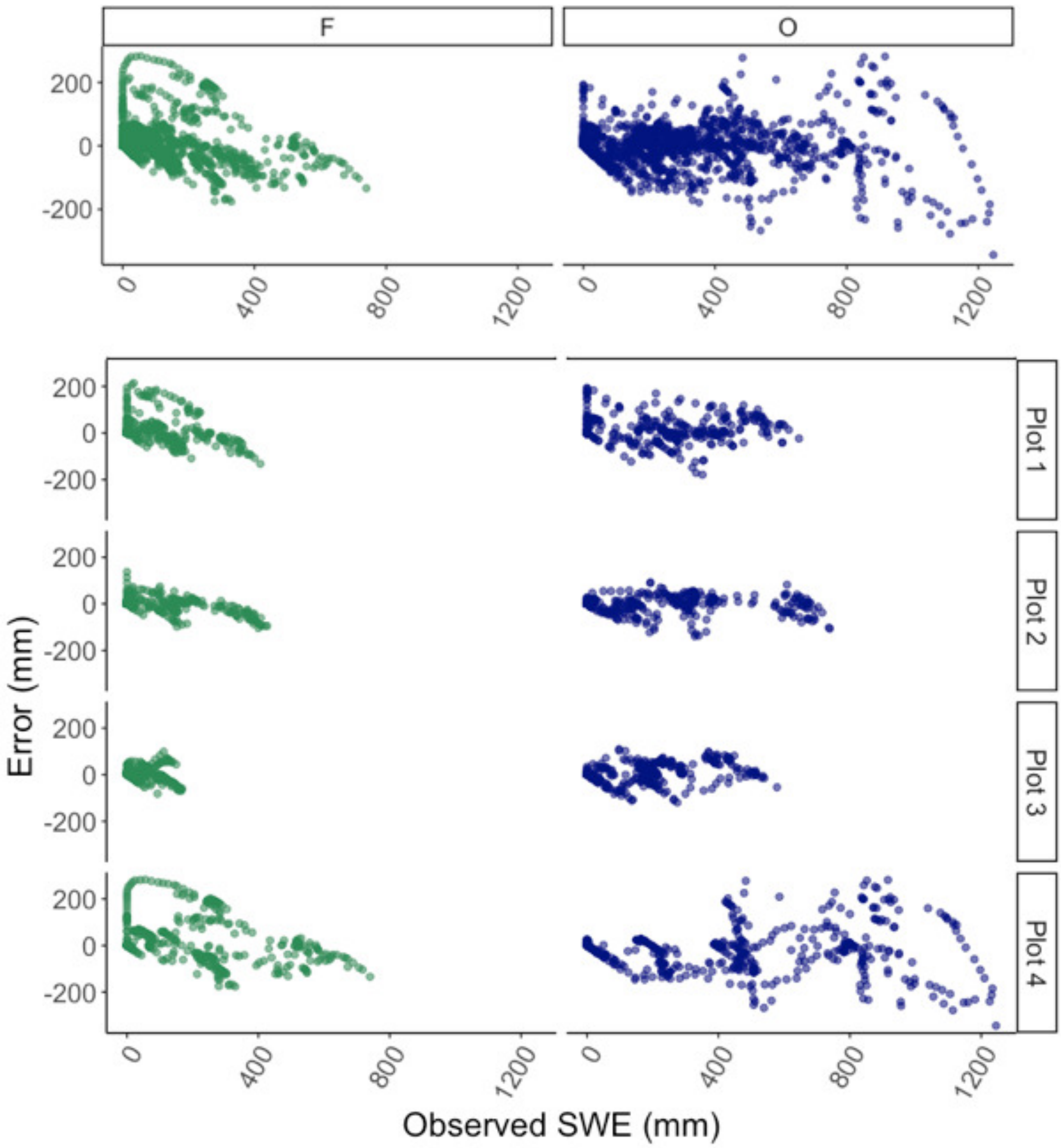

Figure A2. Error plots (error = modeled daily SWE – observed daily SWE) about daily SWE simulations in areas beneath forest canopy (F, green lines) and in forest openings (O, blue lines). Data of 2016/17 and 2017/18 snow seasons is shown.

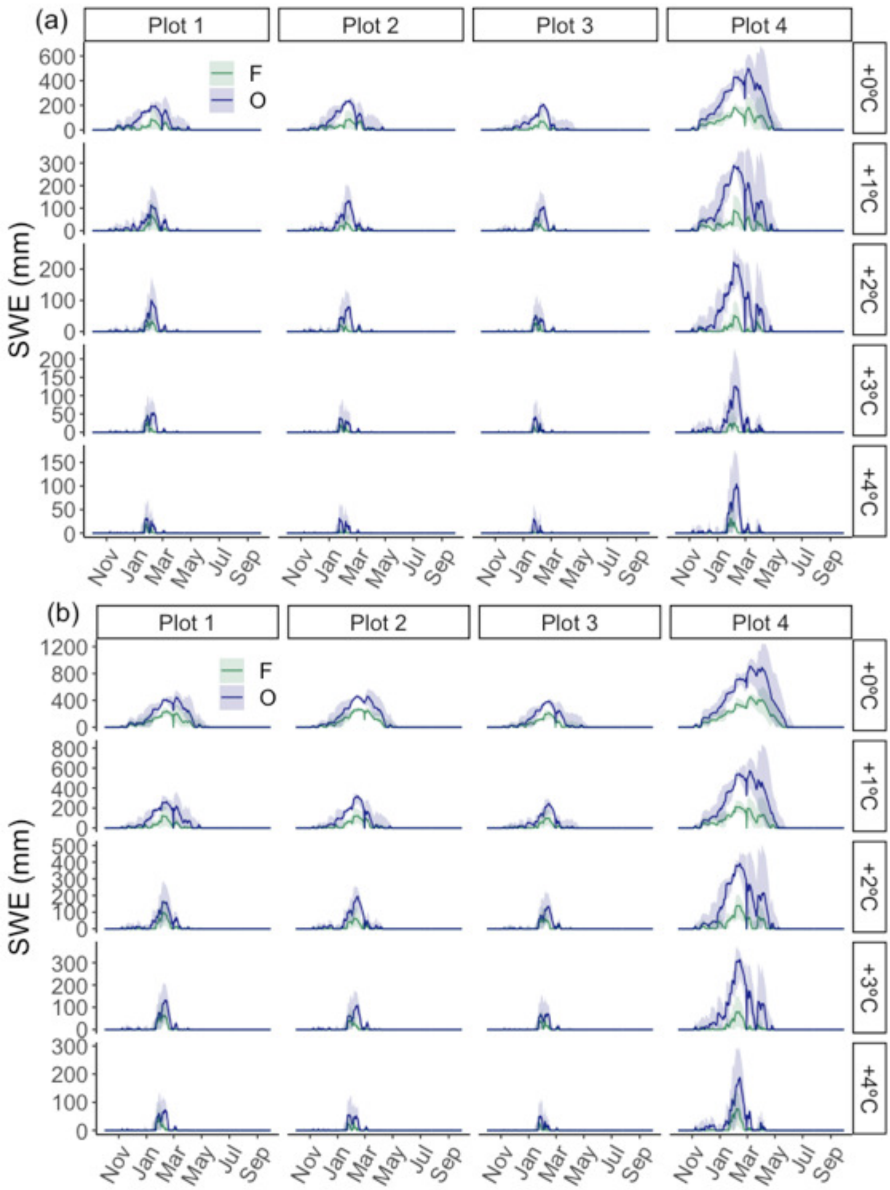

Figure A3. Sensitivity of daily SWE to combined temperature and precipitation change (a: -20%; b: +20%) in areas beneath forest canopy (F, green lines) and in forest openings (O, blue lines). Lines represent the median value and ribbons represent the interquartile range (Q1: 25% to Q3: 75%) of the four modeled snow seasons (2016/17 – 2019/20).

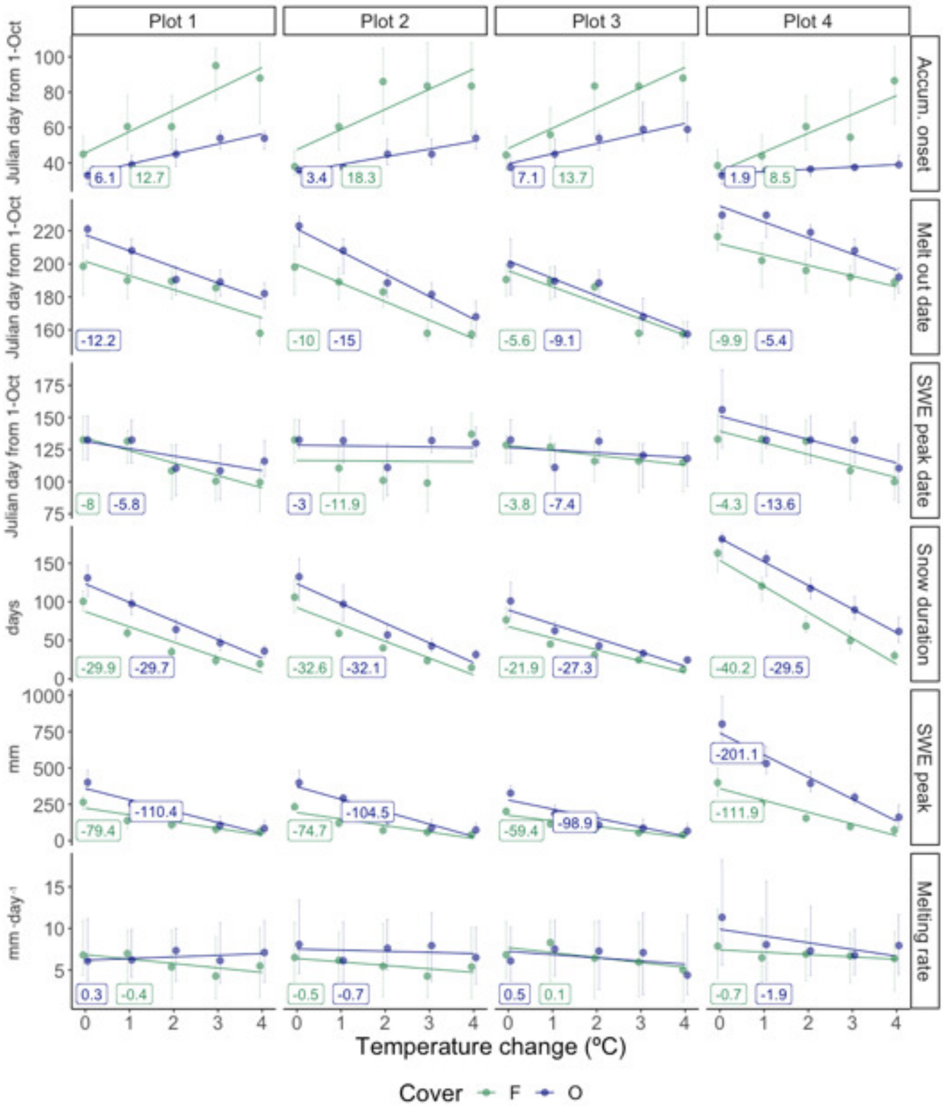

Figure A4. Sensitivity of snow indices magnitude to temperature changes. Colors indicate the different areas analyzed at each study site (F: beneath forest canopy; O: forest openings). The average magnitude change per ºC with regard to the non–perturbed conditions is labeled. Dots: median values; whiskers: interquartile range (Q1: 25% to Q3: 75%); lines: linear adjustments. Data from the four modeled snow seasons (2016/17 – 2019/20) is shown.

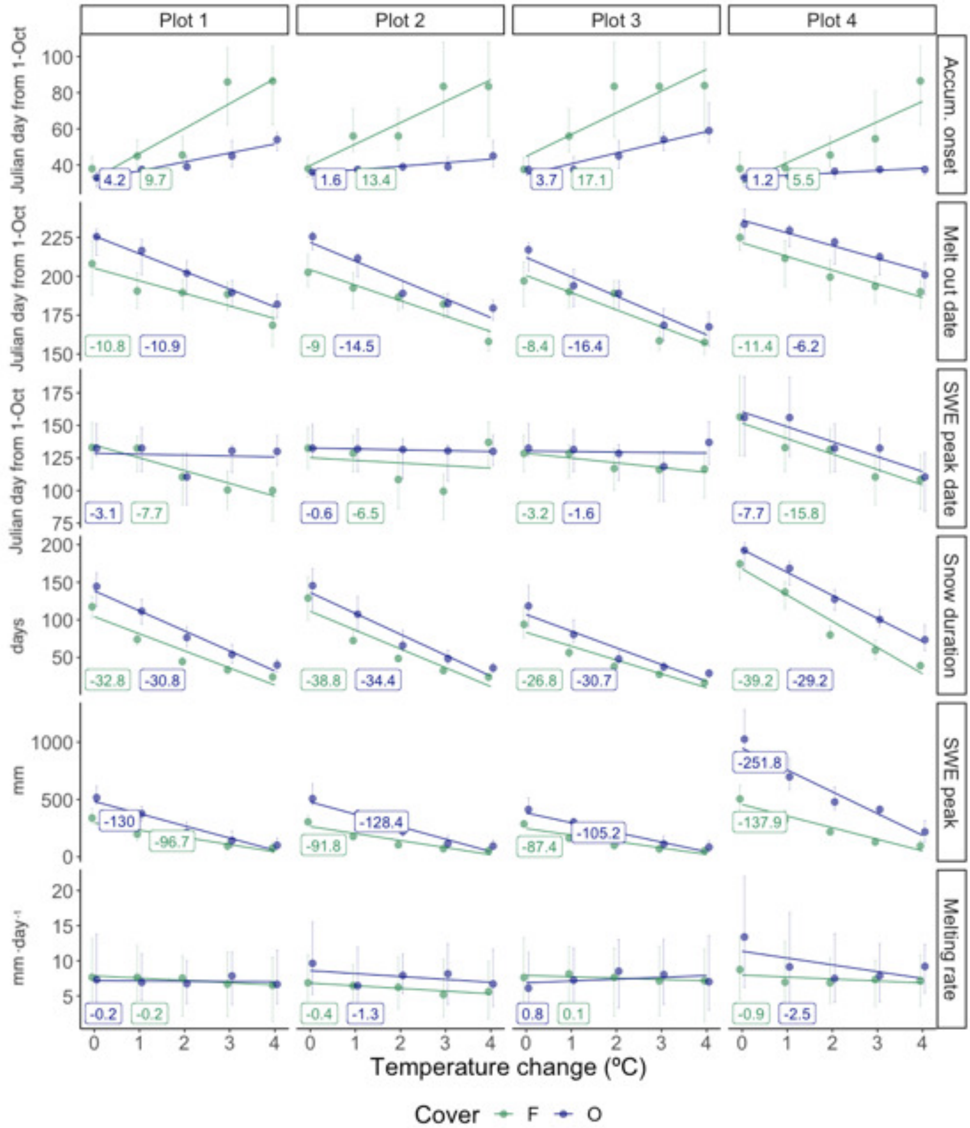

Figure A5. Sensitivity of snow indices to combined temperature and +20% precipitation change. The colors indicate the different areas analyzed at each study site (F: beneath forest canopy; O: forest openings). The average magnitude change per ºC with regard to the non–perturbed conditions is labeled. Dots: median values; whiskers: interquartile range (Q1: 25% to Q3: 75%); lines: linear adjustments. Data from the four modeled snow seasons (2016/17 – 2019/20) is shown.

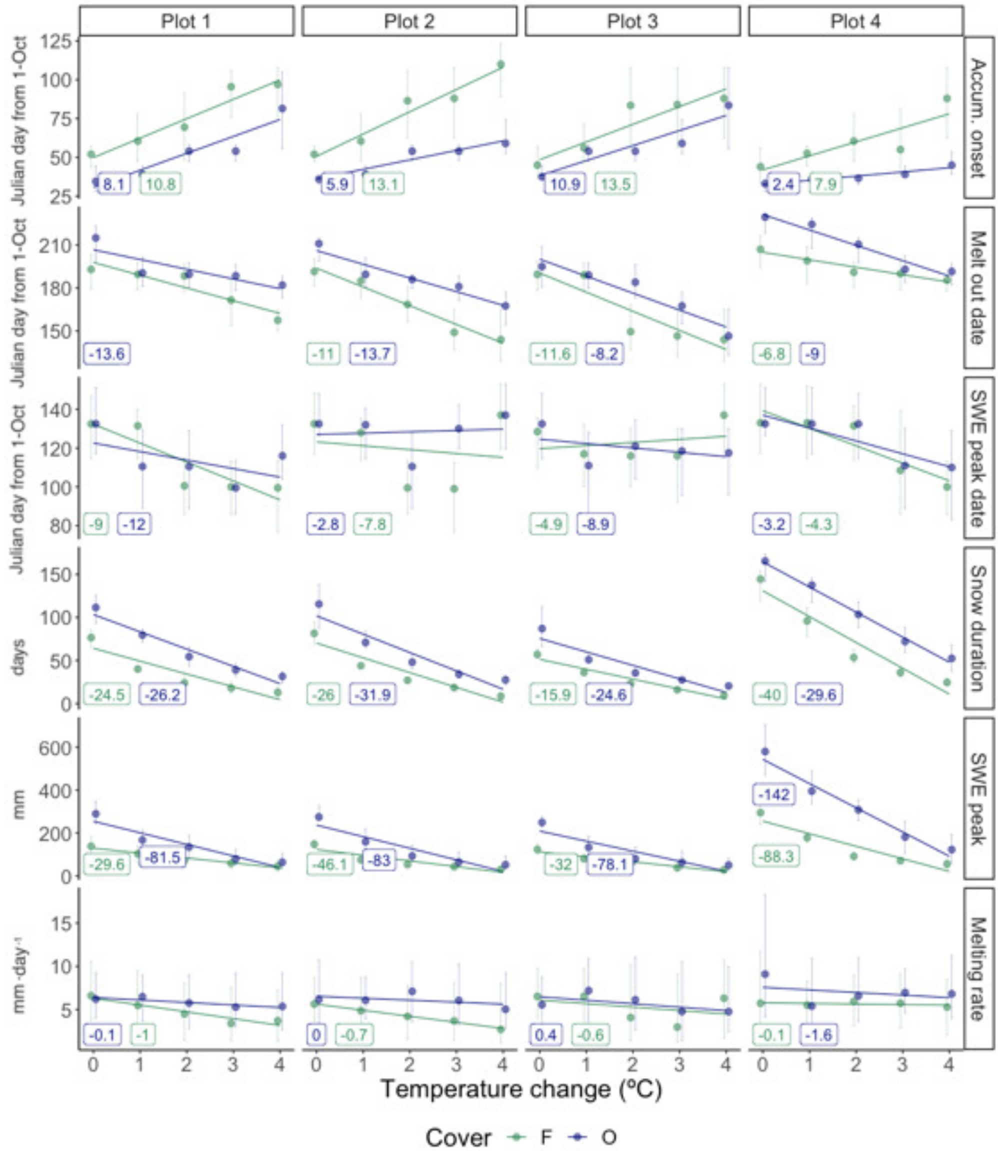

Figure A6. Sensitivity of snow indices to combined temperature and -20% precipitation change. The colors indicate the different areas analyzed at each study site (F: beneath forest canopy; O: forest openings). The average magnitude change per ºC with regard to the non–perturbed conditions is labeled. Dots: median values; whiskers: interquartile range (Q1: 25% to Q3: 75%); lines: linear adjustments. Data from the four modeled snow seasons (2016/17 – 2019/20) is shown.

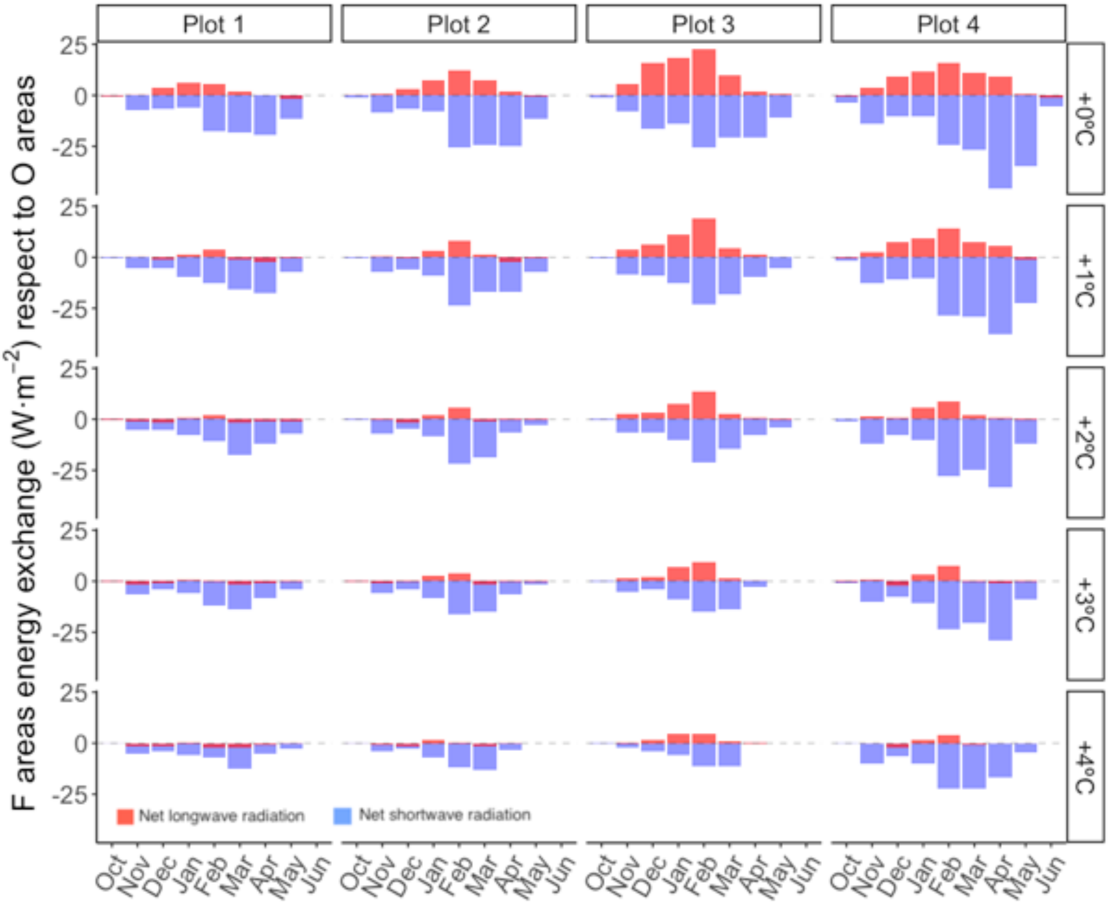

Figure A7. Monthly average differences in net shortwave radiation and net longwave radiation between areas beneath the forest canopy (F) and forest openings (O). Represented values correspond to the subtraction of F energy flux values from O values under non–perturbed climate conditions and under warmer conditions. Mean values of the four modeled snow seasons (2016/17 – 2019/20) are shown.

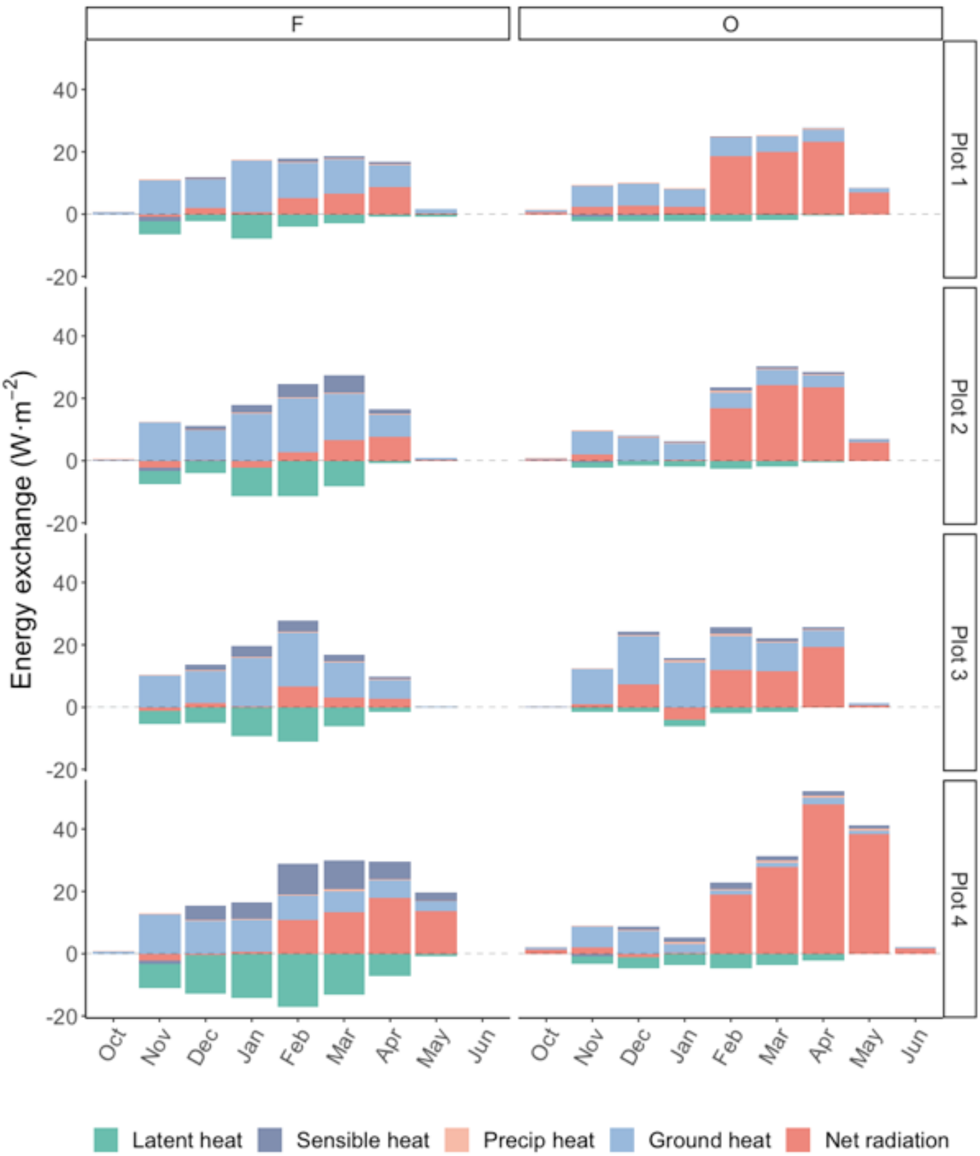

Figure A8. Monthly snowpack energy balance under non–perturbed climate conditions. Represented energy fluxes are net latent heat turbulent flux, net sensible heat turbulent flux, energy from rainfall advection, net ground heat flux, and net all–wave radiation. The different areas analysed at each study site (F: beneath forest canopy; O: forest openings) are distinguished. Mean values of the four modeled snow seasons (2016/2017 – 2019/20) are shown.

Chapter 7
Discussion

This section is the common thread of this Thesis' findings on forest-snow interactions, since the importance, meaning and relevance of the results obtained from each research have been already stated in the previous sections (Chapter 3, Chapter 4,Chapter 5,Chapter 6). Moreover, it is described the applicability of the outcomes in forest and water resources management in the Pyrenees. Ultimately, future work lines are proposed in order to advance the understanding of the two-way interactions between snowpack and forest cover in mountainous terrain.

The terrain in which this Thesis has been carried out is the high mountain. The Earth's mountains comprise some of the most breathtaking landscapes, a quarter of all terrestrial biodiversity, virtually all the major rivers sources, a wide variety of habitats, refugia and migration corridors, and play a major role in determining the climate at regional and continental scale (Hoorn et al., 2018). The global importance of mountains lies in the fact that they cover almost 40 million km^2, i.e. ~27% of the Earth's land surface, and directly support 22% of the people who live within them (Blyth, 2002). Lowland people also depend on mountain environments for their livelihood or culture because of the wide range of goods and services provided, including water, energy, timber, biodiversity maintenance and opportunities for recreation and spiritual renewal. In view of these circumstances, mountain regions are priority candidates for global conservation action (Kollmair et al., 2005).

Among all the diverse elements that make up the entity and environmental role of mountains, this Thesis focused on snow and high-altitude forests. In this Thesis' introduction, snow was presented as the main component of the cryosphere in terms of extension with a critical role in the hydrological cycle (Armstrong & Brun, 2008) and climate system (Cohen, 1994). Furthermore, snow is one of the most important factors governing the ecology of mountain ecosystems (Jones et al., 2001) and a fundamental pillar in those socio-economic systems based on the snow tourism industry (Gilaberte-Búrdalo et al., 2017). On the other hand, mountain forests were presented as hotspots of biodiversity and sources of essential ecosystem services to human communities (Millennium Ecosystem Assessment, 2005), with a strong influence on the quality and quantity of water resources (Hewlett, 1982). Single-discipline studies have resulted in a deeper understanding of the processes related to current and future snow conditions and forest development in the mountains around the world. The emergence of ecology as an integrative discipline has led to integrate this knowledge across disciplines, for a better understanding of mountain environments. This is the framework in which this multidisciplinary Thesis has been conducted, allowing for the research of the relationships established between these both elements, snow cover and mountain forests, using methods taken from hydrology, climatology, forest ecology and botany.

Forest effects on snow processes have been previously assessed in mid-latitude mountain ranges at different altitudinal ranges (Huerta et al., 2019; Lundquist et al., 2013; Musselman et al., 2008), while studies on snow influences on tree growth have been more extensively developed at high latitudes across boreal forests (Kirdyanov et al., 2003; Reinmann et al., 2019; Vaganov et al., 1999). In any case, forest-snow interactions had not been researched in depth in the Mediterranean mountains and, more specifically, in the Pyrenees, where many significant differences in their biotic, ecological, physical and environmental characteristics are exhibited (Vogiatzakis, 2012). This is the main goal that this Thesis has sought to address. For that purpose, we have intensively monitored four *Pinus uncinata* forests in a mountain valley (*Baños de Panticosa*) located in the central Spanish Pyrenees over a time span from 2015 to 2020, while part of the Thesis has been contextualized into a wider spatio-temporal framework in the NE Iberian Peninsula mountains. To detect and analyze the forest-snow interactions in such forest stands, a great field work effort had to be done to perform weekly and/or biweekly manual monitoring of snow conditions, tree growth, and metabolism dynamics. In addition, manual measurements were complemented with automatic and semi-automatic measurements on tree growth as well as snow, soil and climate conditions using snow stakes, time-lapse cameras, dendrometers and a wide variety of environmental sensors placed within the studied forests stands.

Mountain forests and snow cover interact in diverse and complex ways

The results obtained show that snow cover and *P. uncinata* forests interacted both ways in the studied Pyrenean sites. On the one hand, forest cover, mostly through snowfall interception and snow energy balance alteration, determined snowpack distribution, magnitude and timing (Chapter 3). Canopy interception of snowfall explains the relevant forest effect in reducing the snow accumulation observed in the studied sites (Varhola et al., 2010). As a consequence, shallower and more variable snowpacks were observed in areas beneath the forest cover relative to openings. Additionally, the capacity of trees to modify the energy balance of snow was expressed in different ways (Sicart et al., 2004). The forest effect in reducing the snow melting (i.e. shading effect; Ellis et al. (2011)) was more common than the forest-driven enhancement of melting (i.e. warming effect; Essery et al. (2008)) in the sampled forests. It is known that the balance between reduced accumulation and diminished (or enhanced) melting determines snowpack duration in forests (Dickerson-Lange et al., 2017). Thus, in the studied sites, snowpacks were shortened under the forest cover relative to openings due to a more intense forest-mediated reduction on accumulation than on melting, in combination with the occasional enhancement of melting. Since few studies have previously examined the effect of forest cover on snow dynamics in the Pyrenees (López-Moreno &

Latron, 2008; Revuelto et al., 2015), this Thesis provide additional information on it (Chapter 3). Furthermore, although previous studies have already documented the different ways that snowpacks and forests interact in other mid-latitude mountains, this Thesis evaluated the magnitude of these interactions among nearby areas and during different years thanks to a reliable dataset derived from the intensive monitoring of contrasting environments. This is of great relevance to the representativeness of the experimental designs, which I will address below.

On the other hand, snow cover, mostly through affecting soil temperature, influenced *P. uncinata* inter-annual (Chapter 4) and intra-annual growth (Chapter 5), regardeless of the widely reported effect of growing season air temperature on their tree-ring development (Andreu et al., 2007; Camarero et al., 1998; Galván et al., 2014; Rolland & Schueller, 1994; Tardif et al., 2003). There are two major ways that existing literature has demonstrated that snow influences tree radial growth. Both are based on the strong influence that snow dynamics exert on soil temperature and moisture availability (Wilson et al., 2020), particularly before and during the early growing season as shown here (Chapter 5). The first relationship is based on moisture-limitation. It has been reported that spring snowmelt affects positively on soil moisture and therefore on tree growth during the next growing season in drought-prone mountain areas (Watson & Luckman, 2016; Zhang et al., 2019). This relationship is more typical of semiarid or seasonal dry forests from mid to low latitudes (St. George, 2014). This moisture-limitation was not even detected in the potential drought-prone sampled sites in this Thesis (Pre-Pyrenees and southern Iberian System), suggesting no drought stress, while the rest of sites (Pyrenees and northern Iberian System) are considered to be under cool and wet conditions (Chapter 4). One explanation might be that since snowmelt water infiltrated into the soil during winter, it was available for trees even before the complete snow depletion, once the soil starts warming and triggers fine root activity (Chapter 5). The 6ºC soil temperature was considered the threshold for the water up-taking by roots in conifers (Alvarez-Uria & Körner, 2007). According to this, the onset of stem radial increment began when that soil temperature threshold was reached in the *Baños de Panticosa* site, reflecting stem re-hydration (but not yet wood formation). Another explanation might be that the role of snowmelt on tree growth can be overshadowed by spring rainfalls which would introduce an extra source of water to the snowmelt. Although radial increment rates were mainly driven by soil moisture (and air humidity) in those forests, which reflected the strong linkage between stem size and water dynamics (King et al., 2013; Zweifel & Häsler, 2000), no clear positive influence of moisture from snowmelt on intra- or inter-annual growth of *P. uncinata* was detected (Chapter 4, Chapter 5). Therefore, this Thesis cannot demonstrate that moisture from spring snowmelt promoted *P. uncinata* growth in the studied sites. The second relationship is based on energy-limitation, in which delayed soil warming in spring induced by long-lasting snowpacks negatively influences tree growth since it delays root activity and cambial onset, thus truncating the next growing season length (Kirdyanov et al., 2003; Rossi et al., 2011; Vaganov et al., 1999). This energy-limitation can explain the negative influence of winter and, more especially, spring snow depth on inter-annual *P. uncinata* growth found in the studied sites (Chapter 4). In addition, it has been presented evidence that snow dynamics influenced intra-annual *P. uncinata* growth dynamics by influencing soil temperature (Chapter 5). What is more, cold soil temperature was proved to be the most constraining microclimate variable to the production of mature tracheids (a key phase in wood formation), highly influencing timing (onset and cessation) and resulting growth rates in *P. uncinata*. This Thesis proposed a 10ºC minimal soil temperature threshold to tracheid maturation onset in high-elevation forests of *P. uncinata*, which always occurred after complete snow depletion. This temperature threshold should be considered critical for *P. uncinata* wood formation, together with the 6ºC minimum air temperature observed for cambial activity onset which substantially agrees with the 5ºC threshold proposed by Rossi et al. (2008) for conifers from cold sites. Therefore, this Thesis findings confirm for the first time the influence of snow cover on *P. uncinata* growth and provide additional information about the effects of climate and soil conditions on it.

Spatio-temporal variability of forest-snow interactions

Forest-snow interactions, in both ways, were subjected to spatial and temporal sources of variability. Snow cover influences on tree growth and functioning showed higher spatial variability than temporal variability (Chapter 5), while the opposite happened in the case of forest cover influences on snow conditions (Chapter 3). In the vast majority of cases, the spatial (regional and local) and temporal (inter- and intra-annual) variability showed by the forest-snow interactions involved differences in their strength and timing. That was to a large extent due to (1) the topographic complexity (e.g. elevation, aspect and slope) results in the creation of large microclimatic variability from the regional climate and, consequently, involves different snow regimes (Albrich et al., 2020; Hungerford et al., 1989); (2) the forest structure (Jenicek et al., 2018; Musselman et al., 2012); (3) the typically high temporal variability of climate in mountainous areas which induces inter- and intra-annual variability in snow conditions (Fayad et al., 2017); and (4) the time of the year which determines the quantity of incoming solar radiation and air temperature (Lundquist et al., 2013). Whereas, only in certain cases, the nature of the forest-snow interactions showed spatio-temporal variability. That was the case of the observed geographical distribution of *P. uncinata* growth response to snow along the NE Iberian Peninsula mountains (Chapter 4): while the central and western Pyrenean *P. uncinata* forests were particularly sensitive to snow cover conditions, any snow influence on *P. uncinata* growth was found in the Pre-Pyrenees, eastern Pyrenees, and in most Iberian System sampled sites. This geographical variability reflect in a broad sense the different snow climatologies presented by these mountain areas, since a snowpack depth was the most negatively influence on *P. uncinata* growth in those forests where deeper and longer lasting seasonal snowpacks occurred (Alonso-González et al., 2020a). Another example is the case of the dynamic nature of the forest cover effect on snowmelt, since two different types of effect have been observed in the *Baños de Panticosa* sites: shading and heating (Chapter 3). Which one was more prevalent seemed to depend on the time of the year and site characteristics (e.g. average winter temperature, snowpack duration, irradiation and forest structure), as previous studies had been reported (Lundquist et al., 2013). The variable mountain climatology, together with the complex topography of the studied mountainous area, allowed this Thesis to obtained reliable data on the spatial and temporal variability of forest-snow interactions under contrasting environmental conditions. Therefore, the obtained results allowed to assess for the uncertainty on the magnitude of these interactions, and thus to highlight the importance to take into account this uncertainty when evaluating the representativeness of a study site and study period.

Future responses of forest-snow interactions to forecasted hydroclimatic change

The issue, also addressed in this Thesis, takes on even greater importance since the Mediterranean region is expected to be one of the most sensitive to climate change (Giorgi, 2006). Therefore, the potential impacts of the future changes in this transitional climate zone, which will affect water resources, ecosystems and human livelihood, requires particular attention. During the 21st century this climate zone is expected to be expanded northward and eastward over both the Euro-Mediterranean and western North America, as well as its equatorward margins are expected to be replaced by more arid climate types (Alessandri et al., 2014). More particularly, the future climate trends projected for Mediterranean mountains indicate rising temperatures and a reduction of precipitation (Nogués Bravo et al., 2008), as mentioned above (Chapter 1). Among the most likely impacted elements are snowpacks and high-elevation forests, since both are highly sensitive to climate factors (Camarero et al., 2017; Galván et al., 2014; López-Moreno et al., 2017; Martínez et al., 2012; Morán-Tejeda et al., 2017). In fact, the Spanish Pyrenees are expected to be the Mediterranean mountain range most impacted by climate change in terms of mean SWE and snowpack duration (López-Moreno et al., 2017). However, although there has been some discussion of the future responses of forest-snow interactions to forecasted hydroclimatic change, no specific research on the subject had been undertaken in this region until this research was accomplished. The importance of this topic lies in the fact that the knowledge derived from its research will benefit future water and forest management objectives in these mountains and related lowland areas.

This Thesis seeks to make a small contribution to this issue by exploring how changing climate conditions can affect current forest-driven effects on snow processes in the *Baños de Panticosa* experimental site (Chapter 6). To this end, we performed a sensitivity analysis of snow conditions at each forest stand under various degrees of climate forcing. We used the physically based the Cold Region Hydrological Model platform (CRHM) as the modelling tool. Obtained results confirmed the sensitivity of forest-driven effects on snow processes under changing climate conditions, which was expected as climate mediates forest–snow interactions involving both snow accumulation (Currier & Lundquist, 2018) and melting processes (Dickerson-Lange et al., 2017). In addition, it is worth mentioning how that sensitivity varied spatially even among close sites. It was highlighted the sensitivity of forest-driven reduction on snowpack duration to perturbed climate conditions, which was enhanced in the studied forest stands under increasing temperature and lower precipitation conditions. This was mainly due to a delay in the onset of snowpack development under the forest canopy, as a result of an increased forest-driven reduction on snow accumulation at the beginning of the snow season, which in turn was attributed to higher canopy interception efficiency (Friesen et al., 2015) and to a lower amount of snowfall (Revuelto et al., 2015) under that perturbed climate conditions. Thus, according to this Thesis findings and those found by Tennant et al. (2017), the presence of forest cover must be added to the list of factors that can induce variability in the response of snowpacks to a changing climate, such as elevation, slope, aspect and atmospheric humidity (Harpold & Brooks, 2018; López-Moreno et al., 2020; López-Moreno et al., 2014; Pierce & Cayan, 2013). Accurate modelling of the climate change effects on snow dynamics and related hydrology should include changes in vegetation in future climates. As a matter of fact, effects of vegetation changes can be as large as those of climate change alone (Rasouli et al., 2019).

The other half of the issue, that is, what will be the future response of forests to snow dynamics under changing climate conditions, is more complicated to address, so it may be a potential field of work for future research. In this Thesis, only some assumptions have been made in this regard (Chapter 4, Chapter 5). The starting point is that *P. uncinata* growing season length and growth rates are expected to be enlarged and enhanced, respectively, by future warmer air and soil temperatures during the late 21st century, and therefore, high-elevation forests and treelines growth will likely be promoted in the Pyrenees (Camarero et al., 2017). This Thesis suggests that these projections could be amplified if we take into account that climate change also affects snow dynamics, leading to the expected shallower and less lasting snowpacks over the next decades (López-Moreno et al., 2017; Morán-Tejeda et al., 2017). This is based on the generalized positive response of *P. uncinata* radial growth to the negative trend showed by the snowpack depth that we found in the studied sites during the last decades, suggesting that these novel high-elevation forests could be benefited from predicted snow conditions where soil conditions allow it (Chapter 4). This positive effect could be explained by a longer growing season, and a subsequently enhanced growth rate, consequence of an earlier rise and a later cooling of soil temperatures (Chapter 5). However, in moisture-limited sites which depend on snowmelt, a shallower snowpack due to warmer temperatures could lead to limited soil water content in spring and reduce tree growth (Pederson et al., 2011; Truettner et al., 2018). In addition, future soil moisture declines related to an earlier snowmelt may involve compositional changes in mountain forests because the role of spring snowpack on high-elevation conifers varies among species (Hankin & Bisbing, 2021). Therefore, this Thesis highlights the importance of considering snow conditions to accurately interpret the drivers of forest encroachment and densification in further studies about past, recent and future forest expansion in this region. The reasoning behind this is that the way in which soil microclimate will respond to climate change, and thus plant-soil interactions, largely depends on future snow cover dynamics. Since soil is the key interface that allows snow influences on forest growth, future research needs to advance the understanding of those soil characteristics that may play a role in forest-snow interactions and their future changes.

Applicability of the outcomes in forest and water resources management

The snow phenomena plays a key role in the Pyrenees hydrology, as it was highlighted previously (Chapter 1). The overall findings of this Thesis showed that forest cover induced shallower and shortened snowpacks in the studied sites, and although there was a forest-driven reduction in snow melting rates, the date of snow disappearance was most affected by the forest-driven reduction in snow accumulation through canopy interception (Chapter 3). These results suggest that certain forest cover changes at the montane and subalpine belts, as forest harvesting or forest encroachment, could have an important impact on the water storage capacity provided by the seasonal snowpack and it may ultimately be reflected in streamflow changes. However, it should be considered that the effects of forest cover changes on hydrology are watershed specific and complex (Zhang & Wei, 2014). Snow-feeding basins, that are also forest covered in the range comprised between 1600 and 2300–2500 m a.s.l., should be the most sensitive to natural or anthropic forest cover disturbances in the Pyrenees in terms of snow hydrology. In case of forest cover reduction (due to harvesting, pest defoliation or forest burning), snow accumulation can be increased due to the lack of snow interception by canopies (Schelker et al., 2013). In the opposite case, if high-elevation forest cover increases (Camarero et al. (2017) reported that subalpine forests are densifying and encroaching into alpine grasslands and shrublands induced by combined non-management, land-use abandonment and climate warming), snow interception can be enhanced. Nevertheless, this does not necessarily result in deeper and more lasting snowpacks in the first case, or in shallower and more ephemeral snowpacks in the second case. Although reduced forest cover implies an increase in incoming solar radiation to snowpack, and therefore faster snow melting rates might be expected (Boon, 2012), it is wise not to oversimplify and remember that snowmelt rates do not only depends on this energy flux. For example, the direction and magnitude of a forest cover reduction on net radiation for snowmelt can depend on slope and aspect (Ellis et al., 2011), the expected enhanced snowmelt rates may be boosted by increased needle litter after a pest defoliation reducing snow albedo (Pugh & Small, 2012), and snowmelt rates can even be reduced contrary to what one might initially think (Jeníček et al., 2017). Therefore, a deep understanding of the consequences for the snow energy balance in case of forest cover change would be also necessary in order to foresee the dates of snow disappearance, which highly determines the snow signal in mountain river regimes (Morán-Tejeda et al., 2014). This highlights the complex interrelationships between mountain forests and watershed response in snow dominated hydrologic regimes, as the Pyrenean. Snow hydrology response to forest management practices or natural disturbances is highly variable, but certainly forest cover changes are able to modify both mean and peak flows over the snowmelt period (Pomeroy et al., 2012). In this regard, Dickerson-Lange et al. (2020) presented a decision tree model that synthesises the forest-snow relationships and guide decisions that consider how and where forest can be management to optimise water storage. During the following decades, the following snow and hydrological scenario is expected as a consequence of climate change in the Pyrenees: 30 days shorter duration of the snow bulk reserves, 28% decrease in the average snow accumulation and 2.4% reduction in the average flow (Lastrada et al., 2021). However, it is necessary to assess the impact of combined climate–vegetation–soil changes on future snow dynamics and related hydrology in a global change context (Rasouli et al., 2019). As a starting point in this region, this Thesis findings about how current forest cover determines the sensitivity of snowpack to warming and lower precipitation (Chapter 6), provides crucial information for estimating future shifts in the timing and contribution of snowmelt to runoff. So, if at some point managers consider intervening in those mountain forests, the information derived from this Thesis can be very useful in order to realize the importance of certain forest treatments (such as forest gap-thinning, harvesting and pruning) that can be favourable for snow accumulation, since this ultimately affects runoff production and it may also be beneficial in reducing the risk of fire or maintaining forest health and productivity in some cases (Ellis et al., 2013; Revuelto et al., 2016; Zhang & Wei, 2014).

Future work lines

Accurate quantification of seasonal snowpack is critical for hydrological management in snow-fed basins and to validate model predictions (DeWalle & Rango, 2008; Hedrick et al., 2018). The spatial distribution of SWE is a key variable for these purposes. Snow surveying is a proven approach to quantify snowpack SWE from snow depth and density measurements (Haberkorn, 2019), and our experimental design confirmed that accurate local SWE data in forested landscapes could be representative of a larger area at the plot scale (Chapter 3). To resolve the spatial variability of snowpack beneath the forest canopy at larger scales (local, regional and global), remote sensing techniques are being used. However, the advance in the measurement of snowpack density across space has not been concurrent to the revolution in snow depth measurement (Kinar & Pomeroy, 2015a). Satellite remote sensing applicability across forested mountain basins is difficult mainly because forest canopy obscure the underlying snowpack, it is not always available, and it does not provide direct measurements of SWE in all settings (Nolin, 2010). However, major improvements are being made in optical satellite-based snow cover monitoring over forested landscapes by evaluating the algorithms performance based on reliable in-situ data, such as those collected in this Thesis, which have already been used for this purpose (Muhuri et al., 2021). The emerging techniques of remote sensing based on Unmanned Aerial Vehicles (UAVs) represent a promising opportunity to overcome some of the satellite remote sensing limitations. UAVs will be applied in the Pyrenees to obtain reliable high-resolution and large-scale sub-canopy snow depth information in the future, particularly those equipped with LIDAR technology (Laser Imaging Detection and Ranging) (Harder et al., 2020). However, since the ultimate variable of interest is SWE, the obtained snow depth must be combined with density values that be measured manually with available technologies (Kinar & Pomeroy, 2015b), or simulated from physically based snow models (McCreight & Small, 2014).

The findings of this Thesis may have significant implications for interpreting annual and sub-annual tree-ring width and wood anatomical properties as paleo-environmental proxies for past snow conditions. Tree-ring chronologies offer an opportunity for reconstructing, quantifying, and understanding long-term mountain snowpack dynamics (Woodhouse, 2003). In our case, the found snow-related energy limitation of tree-ring development could represent a snow-sensitive proxy variable to paleo-snow reconstruction, such as past snow droughts (Coulthard et al., 2021). This represents a great opportunity for future work on tree-ring-based reconstruction that will provide unique information on past Pyrenean snow conditions.

Although there has not been detected a clear moisture-limitation of radial growth in the analyzed mountain forests, snow and climate conditions are expected to change, and thus this tree growth limitation could become more relevant in certain drier forest stands. Future work could make use of C, H, and O stable isotopes in wood to track the exact use of snowmelt water by high-elevation trees (Hu et al., 2018). This issue may give rise to predict future tree dependency on different sources of soil moisture, focusing on snowmelt, thus contributing to the understanding of future responses of Pyrenean mountain forests to hydroclimatic change.

Further research is needed to analyze the specific mechanisms by which snow affects Pyrenean mountain forest growth and functioning focusing on soil structure, properties and processes. For example, snow cover impacts on soil microbial activities and hence on element biochemical cycling in mountain forests, which in turn can condition tree growth (Tan et al., 2014). This will serve as a basis for assessing the combined impact of climate–vegetation–soil–snow changes on future Pyrenean ecosystems and hydrology in a global change context.

Last but not least, the existence of feedback processes among snow dynamics and tree growth is definitely not something that we should just write off. However, this is a difficult subject to verify. Long-term studies could take up the challenge of answering questions such as the following:

- Will a more or less dense forest cover result in a more or less durable snow cover, which in the long term may affect the forest growth?
- Will a more or less durable snow cover result in a more or less dense forest, which in the long term may affect the snow accumulation?

References

Albrich, K., Rammer, W. & Seidl, R. (2020). Climate change causes critical transitions and irreversible alterations of mountain forests. *Global Change Biology*, *26*(7). https://doi.org/10.1111/gcb.15118

Alessandri, A., De Felice, M., Zeng, N., Mariotti, A., Pan, Y., Cherchi, A., Lee, J.-Y., Wang, B., Ha, K.-J., Ruti, P. & Artale, V. (2014). Robust assessment of the expansion and retreat of Mediterranean climate in the 21 st century. *Scientific Reports*, *4*(1), 7211. https://doi.org/10.1038/srep07211

Alonso-González, E., López-Moreno, J. I., Navarro-Serrano, F., Sanmiguel-Vallelado, A., Revuelto, J., Domínguez-Castro, F. & Ceballos, A. (2020a). Snow climatology for the mountains in the Iberian Peninsula using satellite imagery and simulations with dynamically downscaled reanalysis data. *International Journal of Climatology*, *40*(1), 477–491. https://doi.org/10.1002/joc.6223

Alvarez-Uria, P. & Körner, C. (2007). Low temperature limits of root growth in deciduous and evergreen temperate tree species. *Functional ecology*, *21*(2), 211–218.

Andreu, L., Gutiérrez, E., Macias, M., Ribas, M., Bosch, O. & Camarero, J. J. (2007). Climate increases regional tree-growth variability in Iberian pine forests. *Global Change Biology*, *13*(4), 804–815. https://doi.org/10.1111/j.1365-2486.2007.01322.x

Armstrong, R. L. & Brun, E. (2008). *Snow and climate: Physical processes, surface energy exchange and modeling*. Cambridge University Press.

Blyth, S. (2002). *Mountain watch: Environmental change & sustainable developmental in mountains*. UNEP/Earthprint.

Boon, S. (2012). Snow accumulation following forest disturbance. *Ecohydrology*, *5*(3), 279–285.

Camarero, J. J., Guerrero-Campo, J. & Gutiérrez, E. (1998). Tree-Ring Growth and Structure of Pinus uncinata and Pinus sylvestris in the Central Spanish Pyrenees. *Arctic and Alpine Research*, *30*(1), 1–10. https://doi.org/10.2307/1551739

Camarero, J. J., Linares, J. C., García-Cervigón, A. I., Batllori, E., Martínez, I. & Gutiérrez, E. (2017). Back to the Future: The Responses of Alpine Treelines to Climate Warming are Constrained by the Current Ecotone Structure. *Ecosystems*, *20*(4), 683–700. https://doi.org/10.1007/s10021-016-0046-3

Cohen, J. (1994). Snow cover and climate. *Weather*, *49*(5), 150–156. https://doi.org/10.1002/j.1477-8696.1994.tb05997.x

Coulthard, B. L., Anchukaitis, K. J., Pederson, G. T., Cook, E., Littell, J. & Smith, D. J. (2021). Snowpack signals in North American tree rings. *Environmental Research Letters*, *16*(3), 034037. https://doi.org/10.1088/1748-9326/abd5de

Currier, W. R. & Lundquist, J. D. (2018). Snow Depth Variability at the Forest Edge in Multiple Climates in the Western United States. *Water Resources Research*, *54*(11), 8756–8773. https://doi.org/10.1029/2018WR022553

DeWalle, D. R. & Rango, A. (2008). *Principles of snow hydrology*. Cambridge University Press.

Dickerson-Lange, S. E., Jessica, L., Vano, J. A. & Gersonde, R. (2020). Ranking Forest Effects on Snow Storage: A Hierarchical Framework To Support Forest Management. *2020*, C006–08.

Dickerson-Lange, S. E., Gersonde, R. F., Hubbart, J. A., Link, T. E., Nolin, A. W., Perry, G. H., Roth, T. R., Wayand, N. E. & Lundquist, J. D. (2017). Snow disappearance timing is dominated by forest effects on snow accumulation in warm winter climates of the Pacific Northwest, United States. *Hydrological Processes*, *31*(10), 1846–1862. https://doi.org/10.1002/hyp.11144

Ellis, C. R., Pomeroy, J. W., Essery, R. L. H. & Link, T. E. (2011). Effects of needleleaf forest cover on radiation and snowmelt dynamics in the Canadian Rocky Mountains. *Canadian Journal of Forest Research*, *41*(3), 608–620.

Ellis, C. R., Pomeroy, J. W. & Link, T. E. (2013). Modeling increases in snowmelt yield and desynchronization resulting from forest gap-thinning treatments in a northern mountain headwater basin. *Water Resources Research*, *49*(2), 936–949. https://doi.org/10.1002/wrcr.20089

Essery, R., Pomeroy, J., Ellis, C. & Link, T. (2008). Modelling longwave radiation to snow beneath forest canopies using hemispherical photography or linear regression. *Hydrological Processes: An International Journal*, *22*(15), 2788–2800.

Fayad, A., Gascoin, S., Faour, G., López-Moreno, J. I., Drapeau, L., Page, M. L. & Escadafal, R. (2017). Snow hydrology in Mediterranean mountain regions: A review. *Journal of Hydrology*, *551*, 374–396. https://doi.org/10.1016/j.jhydrol.2017.05.063

Friesen, J., Lundquist, J. & Van Stan, J. T. (2015). Evolution of forest precipitation water storage measurement methods. *Hydrological Processes*, *29*(11), 2504–2520. https://doi.org/10.1002/hyp.10376

Galván, J. D., Camarero, J. J., Ginzler, C. & Büntgen, U. (2014). Spatial diversity of recent trends in Mediterranean tree growth. *Environmental Research Letters*, *9*(8), 084001. https://doi.org/10.1088/1748-9326/9/8/084001

Galván, J. D., Camarero, J. J. & Gutiérrez, E. (2014). Seeing the trees for the forest: Drivers of individual growth responses to climate in Pinus uncinata mountain forests. *Journal of Ecology*, *102*(5), 1244–1257. https://doi.org/10.1111/1365-2745.12268

Gilaberte-Búrdalo, M., López-Moreno, J. I., Morán-Tejeda, E., Jerez, S., Alonso-González, E., López-Martín, F. & Pino-Otín, M. R. (2017). Assessment of ski condition reliability in the Spanish and Andorran Pyrenees for the second half of the 20th century. *Applied Geography*, *79*, 127–142.

Giorgi, F. (2006). Climate change hot-spots. *Geophysical Research Letters*, *33*(8). https://doi.org/10.1029/2006GL025734

Haberkorn, A. (2019). European Snow Booklet – an Inventory of Snow Measurements in Europe. https://doi.org/10.16904/ENVIDAT.59

Hankin, L. & Bisbing, S. (2021). Let it snow? Spring snowpack and microsite characterize the regeneration niche of high-elevation pines. *Journal of Biogeography*. https://doi.org/10.1111/jbi.14136

Harder, P., Pomeroy, J. W. & Helgason, W. D. (2020). Improving sub-canopy snow depth mapping with unmanned aerial vehicles: Lidar versus structure-from-motion techniques. *The Cryosphere*, *14*(6), 1919–1935. https://doi.org/10.5194/tc-14-1919-2020

Harpold, A. A. & Brooks, P. D. (2018). Humidity determines snowpack ablation under a warming climate. *Proceedings of the National Academy of Sciences*, *115*(6), 1215–1220.

Hedrick, A. R., Marks, D., Havens, S., Robertson, M., Johnson, M., Sandusky, M., Marshall, H.-P., Kormos, P. R., Bormann, K. J. & Painter, T. H. (2018). Direct Insertion of NASA Airborne Snow Observatory-Derived Snow Depth Time Series Into the *iSnobal* Energy Balance Snow Model. *Water Resources Research*, *54*(10), 8045–8063. https://doi.org/10.1029/2018WR023190

Hewlett, J. D. (1982). *Principles of forest hydrology.* University of Georgia press.

Hoorn, C., Perrigo, A. & Antonelli, A. (2018). *Mountains, Climate and Biodiversity*. John Wiley & Sons.

Hu, J., Martin, J. T., Clute, T., Hoylman, Z. H. & Jencso, K. (2018). Differential Use of Winter Precipitation by Upper and Lower Elevation Douglas FIR in the Northern Rockies. *2018*, H11W–1777.

Huerta, M. L., Molotch, N. P. & McPhee, J. (2019). Snowfall interception in a deciduous Nothofagus forest and implications for spatial snowpack distribution. *Hydrological Processes*, *33*(13), 1818–1834. https://doi.org/10.1002/hyp.13439
_eprint: https://onlinelibrary.wiley.com/doi/pdf/10.1002/hyp.13439

Hungerford, R. D., Nemani, R. R., Running, S. W. & Coughlan, J. C. (1989). *MTCLIM: A mountain microclimate simulation model* (tech. rep. INT-RP-414). U.S. Department of Agriculture, Forest Service, Intermountain Forest and Range Experiment Station. Ogden, UT.

Jenicek, M., Pevna, H. & Matejka, O. (2018). Canopy structure and topography effects on snow distribution at a catchment scale: Application of multivariate approaches. *Journal of Hydrology and Hydromechanics*, *66*(1), 43–54. https://doi.org/10.1515/johh-2017-0027

Jeníček, M., Hotový, O. & Matějka, O. (2017). Snow accumulation and ablation in different canopy structures at a plot scale: Using degree-day approach and measured shortwave radiation. *AUC GEOGRAPHICA*, *52*(1), 61–72.

Jones, H. G., Pomeroy, J. W., Walker, D. A. & Hoham, R. W. (2001). *Snow ecology: An interdisciplinary examination of snow-covered ecosystems*. Cambridge University Press.

Kinar, N. J. & Pomeroy, J. W. (2015a). Measurement of the physical properties of the snowpack. *Reviews of Geophysics*, *53*(2), 481–544. https://doi.org/10.1002/2015RG000481

Kinar, N. J. & Pomeroy, J. W. (2015b). SAS2: The system for acoustic sensing of snow. *Hydrological Processes*, *29*(18), 4032–4050.

King, G., Fonti, P., Nievergelt, D., Büntgen, U. & Frank, D. (2013). Climatic drivers of hourly to yearly tree radius variations along a 6 C natural warming gradient. *Agricultural and Forest Meteorology*, *168*, 36–46.

Kirdyanov, A., Hughes, M., Vaganov, E., Schweingruber, F. & Silkin, P. (2003). The importance of early summer temperature and date of snow melt for tree growth in the Siberian Subarctic. *Trees*, *17*(1), 61–69. https://doi.org/10.1007/s00468-002-0209-z

Kollmair, M., Gurung, G. S., Hurni, K. & Maselli, D. (2005). Mountains: Special places to be protected? An analysis of worldwide nature conservation efforts in mountains. *International Journal of Biodiversity*

Science & Management, *1*(4), 181–189. https://doi.org/10.1080/17451590509618091

Lastrada, E., Garzón-Roca, J., Cobos, G. & Torrijo, F. J. (2021). A Decrease in the Regulatory Effect of Snow-Related Phenomena in Spanish Mountain Areas Due to Climate Change. *Water*, *13*(11), 1550. https://doi.org/10.3390/w13111550

López-Moreno, J. I., Gascoin, S., Herrero, J., Sproles, E. A., Pons, M., Alonso-González, E., Hanich, L., Boudhar, A., Musselman, K. N., Molotch, N. P., Sickman, J. & Pomeroy, J. (2017). Different sensitivities of snowpacks to warming in Mediterranean climate mountain areas. *Environmental Research Letters*, *12*(7), 074006. https://doi.org/10.1088/1748-9326/aa70cb

López-Moreno, J. I. & Latron, J. (2008). Influence of canopy density on snow distribution in a temperate mountain range. *Hydrological Processes*, *22*(1), 117–126. https://doi.org/10.1002/hyp.6572

López-Moreno, J. I., Pomeroy, J. W., Alonso-González, E., Morán-Tejeda, E. & Revuelto, J. (2020). Decoupling of warming mountain snowpacks from hydrological regimes. *Environmental Research Letters*, *15*(11), 114006. https://doi.org/10.1088/1748-9326/abb55f

López-Moreno, J. I., Revuelto, J., Gilaberte, M., Morán-Tejeda, E., Pons, M., Jover, E., Esteban, P., García, C. & Pomeroy, J. W. (2014). The effect of slope aspect on the response of snowpack to climate warming in the Pyrenees. *Theoretical and Applied Climatology*, *117*(1-2), 207–219. https://doi.org/10.1007/s00704-013-0991-0

Lundquist, J. D., Dickerson-Lange, S. E., Lutz, J. A. & Cristea, N. C. (2013). Lower forest density enhances snow retention in regions with warmer winters: A global framework developed from plot-scale observations and modeling. *Water Resources Research*, *49*(10), 6356–6370. https://doi.org/10.1002/wrcr.20504

Martínez, I., González-Taboada, F., Wiegand, T., Camarero, J. J. & Gutiérrez, E. (2012). Dispersal limitation and spatial scale affect model based projections of Pinus uncinata response to climate change in the Pyrenees. *Global Change Biology*, *18*(5), 1714–1724. https://doi.org/10.1111/j.1365-2486.2012.02660.x

McCreight, J. L. & Small, E. E. (2014). Modeling bulk density and snow water equivalent using daily snow depth observations. *The Cryosphere*, *8*(2), 521–536. https://doi.org/10.5194/tc-8-521-2014

Millennium Ecosystem Assessment, ((2005). *Ecosystems and Human Well-being: Synthesis* (Vol. 1). Island Press. Muller & Burkhard.

Morán-Tejeda, E., López-Moreno, J. I. & Sanmiguel-Vallelado, A. (2017). Changes in climate, snow and water resources in the Spanish Pyrenees: Observations and projections in a warming climate. *High Mountain Conservation in a Changing World* (pp. 305–323). Springer.

Morán-Tejeda, E., Lorenzo-Lacruz, J., López-Moreno, J. I., Rahman, K. & Beniston, M. (2014). Streamflow timing of mountain rivers in Spain: Recent changes and future projections. *Journal of hydrology*, *517*, 1114–1127.

Muhuri, A., Gascoin, S., Menzel, L., Kostadinov, T., Harpold, A., Sanmiguel-Vallelado, A. & Moreno, J. I. L. (2021). Performance Assessment of Optical Satellite Based Operational Snow Cover Monitoring Algorithms in Forested Landscapes. *IEEE Journal of Selected Topics in Applied Earth Observations and Remote Sensing*.

Musselman, K. N., Molotch, N. P. & Brooks, P. D. (2008). Effects of vegetation on snow accumulation and ablation in a mid-latitude sub-alpine forest. *Hydrological Processes*, *22*(15), 2767–2776. https://doi.org/10.1002/hyp.7050
_eprint: https://onlinelibrary.wiley.com/doi/pdf/10.1002/hyp.7050

Musselman, K. N., Molotch, N. P., Margulis, S. A., Kirchner, P. B. & Bales, R. C. (2012). Influence of canopy structure and direct beam solar irradiance on snowmelt rates in a mixed conifer forest. *Agricultural and Forest Meteorology*, *161*, 46–56.

Nogués Bravo, D., Araújo, M. B., Lasanta, T. & López Moreno, J. I. (2008). Climate change in Mediterranean mountains during the 21st century. *Ambio*, *37*(4), 280–285. https://doi.org/10.1579/0044-7447(2008)37[280:ccimmd]2.0.co;2

Nolin, A. W. (2010). Recent advances in remote sensing of seasonal snow. *Journal of Glaciology*, *56*(200), 1141–1150.

Pederson, G. T., Gray, S. T., Woodhouse, C. A., Betancourt, J. L., Fagre, D. B., Littell, J. S., Watson, E., Luckman, B. H. & Graumlich, L. J. (2011). The Unusual Nature of Recent Snowpack Declines in the North American Cordillera. *Science*, *333*(6040), 332–335. https://doi.org/10.1126/science.1201570

Pierce, D. W. & Cayan, D. R. (2013). The Uneven Response of Different Snow Measures to Human-Induced Climate Warming. *Journal of Climate*, *26*(12), 4148–4167. https://doi.org/10.1175/JCLI-D-12-00534.1

Pomeroy, J., Fang, X. & Ellis, C. (2012). Sensitivity of snowmelt hydrology in Marmot Creek, Alberta, to forest cover disturbance. *Hydrological Processes*, *26*(12), 1891–1904. https://doi.org/10.1002/hyp.9248

Pugh, E. & Small, E. (2012). The impact of pine beetle infestation on snow accumulation and melt in the headwaters of the Colorado River. *Ecohydrology*, *5*(4), 467–477. https://doi.org/10.1002/eco.239

Rasouli, K., Pomeroy, J. W. & Whitfield, P. H. (2019). Are the effects of vegetation and soil changes as important as climate change impacts on hydrological processes? *Hydrology and Earth System Sciences*, *23*(12), 4933–4954. https://doi.org/10.5194/hess-23-4933-2019

Reinmann, A. B., Susser, J. R., Demaria, E. M. C. & Templer, P. H. (2019). Declines in northern forest tree growth following snowpack decline and soil freezing. *Global Change Biology*, *25*(2), 420–430. https://doi.org/10.1111/gcb.14420

Revuelto, J., López-Moreno, J. I., Azorin-Molina, C. & Vicente-Serrano, S. M. (2015). Canopy influence on snow depth distribution in a pine stand determined from terrestrial laser data. *Water Resources Research*, *51*(5), 3476–3489. https://doi.org/10.1002/2014WR016496

Revuelto, J., López-Moreno, J.-I., Azorin-Molina, C., Alonso-González, E. & Sanmiguel-Vallelado, A. (2016). Small-Scale Effect of Pine Stand Pruning on Snowpack Distribution in the Pyrenees Observed with a Terrestrial Laser Scanner. *Forests*, *7*(8), 166. https://doi.org/10.3390/f7080166

Rolland, C. & Schueller, J. F. (1994). Relationships between mountain pine and climate in the French Pyrenees (Font-Romeu) studied using the radiodensitometrical method. *Pirineos*, *143–144*(0), 55–70. https://doi.org/10.3989/pirineos.1994.v143-144.156

Rossi, S., Deslauriers, A., Griçar, J., Seo, J.-W., Rathgeber, C. B., Anfodillo, T., Morin, H., Levanic, T., Oven, P. & Jalkanen, R. (2008). Critical temperatures for xylogenesis in conifers of cold climates. *Global Ecology and Biogeography*, *17*(6), 696–707. https://doi.org/10.1111/j.1466-8238.2008.00417.x

Rossi, S., Morin, H. & Deslauriers, A. (2011). Multi-scale Influence of Snowmelt on Xylogenesis of Black Spruce. *Arctic, Antarctic, and Alpine Research*, *43*(3), 457–464. https://doi.org/10.1657/1938-4246-43.3.457

Schelker, J., Kuglerová, L., Eklöf, K., Bishop, K. & Laudon, H. (2013). Hydrological effects of clear-cutting in a boreal forest – Snowpack dynamics, snowmelt and streamflow responses. *Journal of Hydrology*, *484*, 105–114. https://doi.org/10.1016/j.jhydrol.2013.01.015

Sicart, J. E., Essery, R. L., Pomeroy, J. W., Hardy, J., Link, T. & Marks, D. (2004). A sensitivity study of daytime net radiation during snowmelt to forest canopy and atmospheric conditions. *Journal of Hydrometeorology*, *5*(5), 774–784.

St. George, S. (2014). An overview of tree-ring width records across the Northern Hemisphere. *Quaternary Science Reviews*, *95*, 132–150. https://doi.org/10.1016/j.quascirev.2014.04.029

Tan, B., Wu, F.-z., Yang, W.-q. & He, X.-h. (2014). Snow removal alters soil microbial biomass and enzyme activity in a Tibetan alpine forest. *Applied Soil Ecology*, *76*, 34–41. https://doi.org/10.1016/j.apsoil.2013.11.015

Tardif, J., Camarero, J. J., Ribas, M. & Gutiérrez, E. (2003). Spatiotemporal variability in tree growth in the Central Pyrenees: Climatic and site influences. *Ecological Monographs*, *73*(2), 241–257.

Tennant, C. J., Harpold, A. A., Lohse, K. A., Godsey, S. E., Crosby, B. T., Larsen, L. G., Brooks, P. D., Kirk, R. W. V. & Glenn, N. F. (2017). Regional sensitivities of seasonal snowpack to elevation, aspect, and vegetation cover in western North America. *Water Resources Research*, *53*(8), 6908–6926. https://doi.org/10.1002/2016WR019374

Truettner, C., Anderegg, W. R., Biondi, F., Koch, G. W., Ogle, K., Schwalm, C., Litvak, M. E., Shaw, J. D. & Ziaco, E. (2018). Conifer radial growth response to recent seasonal warming and drought from the southwestern USA. *Forest ecology and management*, *418*, 55–62.

Vaganov, E. A., Hughes, M. K., Kirdyanov, A. V., Schweingruber, F. H. & Silkin, P. P. (1999). Influence of snowfall and melt timing on tree growth in subarctic Eurasia. *Nature*, *400*(6740), 149–151. https://doi.org/10.1038/22087

Varhola, A., Coops, N. C., Weiler, M. & Moore, R. D. (2010). Forest canopy effects on snow accumulation and ablation: An integrative review of empirical results. *Journal of Hydrology*, *392*(3-4), 219–233.

Vogiatzakis, I. (2012). *Mediterranean Mountain Environments*. John Wiley & Sons.

Watson, E. & Luckman, B. H. (2016). An investigation of the snowpack signal in moisture-sensitive trees from the Southern Canadian Cordillera. *Dendrochronologia*, *38*, 118–130. https://doi.org/10.1016/j.dendro.2016.03.008

Wilson, G., Green, M., Brown, J., Campbell, J., Groffman, P., Durán, J. & Morse, J. (2020). Snowpack affects soil microclimate throughout the year. *Climatic Change*, *163*(2), 705–722. https://doi.org/10.1007/s10584-020-02943-8

Woodhouse, C. A. (2003). A 431-yr reconstruction of western Colorado snowpack from tree rings. *Journal of Climate*, *16*(10), 1551–1561.

Zhang, M. & Wei, X. (2014). Contrasted hydrological responses to forest harvesting in two large neighbouring watersheds in snow hydrology dominant environment: Implications for forest management and future forest hydrology studies. *Hydrological Processes*, *28*(26), 6183–6195. https://doi.org/10.1002/hyp.10107

Zhang, X., Manzanedo, R. D., D'Orangeville, L., Rademacher, T. T., Li, J., Bai, X., Hou, M., Chen, Z., Zou, F., Song, F. & Pederson, N. (2019). Snowmelt and early to mid-growing season water availability augment tree growth during rapid warming in southern Asian boreal forests. *Global Change Biology*, *25*(10), 3462–3471. https://doi.org/10.1111/gcb.14749

Zweifel, R. & Häsler, R. (2000). Frost-induced reversible shrinkage of bark of mature subalpine conifers. *Agricultural and forest meteorology*, *102*(4), 213–222.

Chapter 8

Conclusions

This Thesis investigated the forest-snow interactions in the Aragonese Pyrenees, from an eco-hydrological perspective, through intensively monitoring of *Pinus uncinata* forests. In the following paragraphs, the conclusions raised from the specific objectives stated in this Thesis (see Section 1.4) are presented:

- First objective: *To deepen understanding of forest-snow interactions in the Pyrenees, as well as to account for the uncertainty on the magnitude of forest effects on snowpack among nearby areas and during different years.* This objective was developed in Chapter 3. It can be concluded that forest cover, relative to forest openings, on average reduced the duration of snowpack in more than two weeks, reduced the snow accumulation by about 60% (in terms of SWE) and increased the small-scale spatial variability of snowpack by 190%. The most common effect of forest that was observed in the studied forest stands was reduced melting rate, thus suggesting that the effect of shadowing by the forest canopy exceeded the heating of trees. The contrary case can be considered to have taken place only occasionally, since it was observed a forest-mediated increase in the melting rate on 26% of days with snow melting. Therefore, the observed earlier snow depletion beneath forest cover can be mostly explained by the overall more intense forest-mediated reduction in accumulation (40% on average) than on melting (25% on average), and it can be facilitated by the occasional forest-mediated enhancement of melting rate. The same general forest effects on snowpack were found in all studied forest stands and during all snow seasons. However, the magnitude and timing of these effects experienced significant differences at local scale and temporal (inter- and intra-annual) variability. This research highlights the need to consider the effects of forests as a source of uncertainty when selecting the location of the experimental site and a time period for study when undertaking snow science research in mountain areas.

- Second objective: *To discern how and where snow dynamics affects* P. uncinata *growth and functioning.* This objective was developed in Chapter 4 and Chapter 5. It can be concluded that inter- and intra-annual growth dynamics of *P. uncinata* forests were affected by snow cover conditions. Snow dynamics influenced *P. uncinata* growth dynamics by influencing soil temperature in mountain forests, whereas it could not be demonstrated that snowmelt water exerted a relevant influence on *P. uncinata* growth in the study sites. It was observed that larger snow accumulation involved a prolonged snow persistence in spring that produced a delay in soil warming onset, and those resulting low soil temperatures in spring retarded and reduced the production of mature tracheids, which is an essential step during xylogenesis. However, the magnitude and timing of the snow influence on forest growth showed relevant spatial differences at both regional and local scales, and inter-annual variability. In addition, some tree characteristics (as height) also explained differences in the mentioned forest-snow interactions. This research highlights the large role of early and late growing season soil temperatures on *P. uncinata* radial growth, in addition to the widely reported effect of air temperature. Furthermore, this research suggests that a future shallower and more ephemeral snowpack in similar mountains forests, together with warmer temperatures, may benefit the growth and productivity of *P. uncinata* over the next decades by prolonging the growing season through an earlier onset and a late cessation of xylogenesis, although certain forests might experience warming-induced drought stress.

- Third objective: *To explore how forest cover can affect the snowpack sensitivity to changes in climate in the Pyrenees, as well as how these changes in climate can affect current forest effects on snowpack.* This objective was developed in Chapter 6. It can be concluded that under warmer conditions, areas beneath the forest cover (compared to openings) experienced a more intense delay in the onset of snow accumulation (F: 13 days · ºC^{-1}; O: 5 days · ºC^{-1}) and a larger reduction in snowpack duration (F: 28% · ºC^{-1}; O: 23% · ºC^{-1}). Whereas, the forest covered areas experienced a weaker reduction in SWE peak (F: 81 mm · ºC^{-1}; O: 129 mm · ºC^{-1}), a less intense earlier melt-out date (F: 8 days · C$^{º-1}$; O: 10 days · ºC^{-1}) and a less pronounced slower melting rates (F: 0.4 mm · day^{-1} · ºC^{-1}; O: 0.5 mm · day^{-1} · ºC^{-1}) with increasing temperatures. It was observed that forest effects on snow accumulation processes were highly sensitive to warming temperatures during the beginning of the snow season. As a consequence, the forest-driven delaying onset of snow accumulation was enhanced with warming, which mostly explained the significant enhancement of the forest-driven reduction in snowpack duration obtained (10% per ºC). Drier conditions increased the response of this latter mentioned forest effect to warming. Whereas, the forest-driven reduction in maximum snow accumulation was more sensitive to changes in precipitation. In general, the forest effects on snow melting processes (heating and shading effects) were both diminished with warming. However, the sensitivity of forest effects on snow processes to perturbed climate conditions showed relevant variability at local scale. This research highlights the influence of forest cover in the snowpack response to climate perturbations, which will allow us to anticipate the future hydrological responses of Pyrenean forested mountain basins, and thus, to benefit future water and forest management objectives in similar mid-latitude mountains and surrounding regions.

Conclusiones

Esta Tesis ha investigado las interacciones que tienen lugar entre los bosques de montaña y el manto de nieve en el Pirineo Aragonés, desde una perspectiva eco-hidrológica, y mediante el monitoreo intensivo de bosques de *Pinus uncinata*. En los siguientes párrafos, se presentan las conclusiones extraídas de acuerdo con los objetivos específicos establecidos en esta Tesis (ver Sección 1.4):

- Primer objetivo: *Profundizar en el conocimiento de las interacciones bosque-nieve en los Pirineos, así como evaluar la variabilidad de los efectos del bosque sobre el manto de nieve entre zonas cercanas y durante diferentes años.* Este objetivo ha sido desarrollado en el Capítulo 3. A este respecto, puede concluirse que la cubierta forestal redujo la acumulación de nieve en un $\sim$60% (en términos de SWE acumulado), redujo de media la duración del manto de nieve en más de dos semanas, y aumentó en un $\sim$190% la variabilidad espacial a pequeña escala del manto de nieve en comparación con los claros de bosque estudiados. En cuanto al efecto del bosque sobre el proceso de fusión de la nieve, se produjo principalmente una ralentización de la fusión, lo que sugiere que el efecto sombra de la cubierta forestal dominó sobre el papel de los árboles como emisores térmicos. La situación contraria tuvo lugar de manera ocasional, dado que sólo se observó un aumento de la tasa de fusión bajo la cubierta forestal el 26% de los días que se produjo fusión de nieve. La temprana desaparición del manto de nieve bajo la cubierta forestal puede explicarse en buena medida debido al mayor efecto que ejerce el bosque reduciendo la tasa de acumulación de nieve (un 40% de media) que ralentizando su tasa de fusión (un 25% de media), y que además es promovido por el ocasional incremento de la fusión. Considerando los diferentes bosques y temporadas analizadas, se observó que el tipo de efectos que ejerció el bosque sobre el manto de nieve fue el mismo. Si bien, la magnitud y la temporalidad de dichos efectos experimentaron diferencias significativas local y temporalmente (a escala inter- e intra- anual). Por tanto, esta tesis señala la necesidad de considerar los efectos del bosque como fuente de incertidumbre a la hora de seleccionar el emplazamiento del lugar y el periodo de estudio en el desarrollo de estudios nivológicos en zonas de montaña.

- Segundo objectivo: *Determinar cómo y dónde los procesos que experimenta el manto del nieve afectan al crecimiento y funcionamiento de* P. uncinata. Este objetivo ha sido desarrollado en el Capítulo 4 y en el Capítulo 5. A este respecto, puede concluirse que la dinámica de crecimiento inter- e intra-anual de los bosques de *P. uncinata* estuvo influenciada por las condiciones nivales. El manto de nieve condicionó el crecimiento de *P. uncinata* al determinar la temperatura del suelo de estos bosques de montaña, mientras que no se pudo demostrar que el agua procedente de la fusión de la nieve afectara de manera relevante a dicho crecimiento en los sitios estudiados. Se observó que una mayor acumulación de nieve conllevó a una prolongada persistencia de la nieve en primavera que a su vez produjo un retraso del calentamiento del suelo. En consecuencia, la resultante baja temperatura del suelo en primavera, retrasó y redujo la producción de traqueidas maduras, siendo este un proceso esencial durante la xylogénesis. Sin embargo, la magnitud y la temporalidad del efecto de la nieve sobre el crecimiento forestal mostró importantes diferencial espaciales (a escala regional y local), así como una gran variabilidad inter-anual. Así mismo, determinadas características de los árboles (como su altura) también pudieron explicar parte de la recién mencionada variabilidad espacio-temporal en el efecto de la nieve sobre el bosque. Esta Tesis destaca el importante papel de la temperatura del suelo al comienzo y final de la temporada de crecimiento en el crecimiento radial de *P. uncinata*, que se suma al ampliamente reportado efecto de la temperatura del aire sobre dicho crecimiento. Además, esta Tesis sugiere que un futuro manto de nieve previsiblemente menos profundo y más efímero, junto con el aumento de las temperaturas, podría beneficiar el crecimiento y la productividad de *P. uncinata* en las siguientes décadas en bosques de montaña de características similares a los aquí estudiados, como resultado del prolongamiento de su temporada de crecimiento al dar comienzo antes la xylogénesis y finalizar más tarde. Si bien, determinados bosques podrían experimentar estrés hídrico inducido por el calentamiento del clima.

- Tercer objetivo: *Explorar cómo la cubierta forestal puede condicionar la sensibilidad del manto de nieve ante posibles cambios que experimente el clima de los Pirineos, y evaluar cómo un cambio climático puede alterar los actuales efectos del bosque sobre la nieve.* Este objetivo se ha desarrollado en el Capítulo 6. A este respecto, puede concluirse que al considerar un clima más cálido, las áreas situadas bajo una cubierta forestal (en comparación con los claros de bosque) experimentaron un mayor retraso en el comienzo de la acumulación de nieve (F: 13 días $\cdot$ ºC^{-1}; O: 5 días $\cdot$ ºC^{-1}) y una mayor reducción de la duración del manto (F: 28% $\cdot$ ºC^{-1}; O: 23% $\cdot$ ºC^{-1}). Estas mismas áreas, situadas bajo la cubierta forestal, ante un incremento de las temperaturas, experimentaron una menor reducción del pico de SWE (F: 81 mm $\cdot$ ºC^{-1}; O: 129 mm $\cdot$ ºC^{-1}), una menos temprana fecha de final de la fusión de la nieve (F: 8 días $\cdot$ C$^{\text{º}-1}$; O: 10 días $\cdot$ ºC^{-1}), y una menor ralentización de las tasas de fusión (F: 0.4 mm $\cdot$ day^{-1} $\cdot$ ºC^{-1}; O: 0.5 mm $\cdot$ day^{-1} $\cdot$ ºC^{-1}). Se observó que los efectos del bosque sobre el proceso de acumulación de la nieve fueron muy sensibles al incremento de las temperaturas al comienzo de la temporada de nieve. Como consecuencia, el retraso en el comienzo de la formación del manto de nieve que produce el bosque fue potenciado por el calentamiento, lo que a su vez explica en su mayor parte el significativo incremento del efecto del bosque sobre la reducción de la duración del manto (10% per ºC). La sensibilidad de este último efecto del bosque sobre la nieve ante el calentamiento se potenció al considerar un clima más seco (menor precipitación). Mientras que, la reducción que produce el bosque del pico de SWE fue más sensible a los cambios en la precipitación que a los cambios en la temperatura. Por otra parte, los efectos del bosque sobre el proceso de fusión de la nieve (sombreo de las copas y emisión térmica de los árboles) se redujeron al considerar un aumento de las temperaturas, en general. Sin embargo, la sensibilidad de los efectos del bosque sobre los procesos nivales ante condiciones climáticas alteradas mostró una importante variabilidad espacial a escala local. Esta Tesis pone de manifiesto la influencia que tiene la cubierta forestal en la respuesta del manto de nieve ante los cambios del clima, lo que puede permitirnos anticipar la futura respuesta hidrológica de las cuencas forestadas de los Pirineos, para el beneficio de los futuros objetivos en la gestión del agua y forestal en cordilleras montañosas de caracterísiticas similares a las estudiadas y regiones circundantes.

Appendix I

Journal statistics and subject areas of the publications that constitute the main body of this Thesis, and contribution of the doctoral student to them

The published research paper featured in **Chapter 3** is "Sanmiguel-Vallelado, A., López-Moreno, J. I., Morán-Tejeda, E., Alonso-González, E., Navarro-Serrano, F. M., Rico, I. & Camarero, J. J. (2020). Variable effects of forest canopies on snow processes in a valley of the central Spanish Pyrenees. *Hydrological Processes*, *34*, 2247–2262. https://doi.org/10.1002/hyp.13721". The contribution of the doctoral student, as well as the contribution of the other authors of this manuscript, is specified below. Alba Sanmiguel-Vallelado contributed to study design and implement the research, carried out the data collection, processed the time-lapse photographs, performed the analytic calculations, interpreted the results and wrote the manuscript. Juan I. López-Moreno and Enrique Morán-Tejeda designed and implemented the research, contributed to the data collection and to the interpretation of the results. Esteban Alonso-González, Francisco M. Navarro-Serrano and Ibai Rico contributed to the data collection. Juan Ignacio López-Moreno, J. Julio Camarero and Enrique Morán-Tejeda supervised the findings of this work. All authors provided critical feedback and helped shape the research and manuscript.

ISSN	Research Area	Impact factor (2020)	Quartile
08856087, 10991085	Water Resources	3.565	Q1

The published research paper featured in **Chapter 4** is "Sanmiguel-Vallelado, A., Camarero, J. J., Gazol, A., Morán-Tejeda, E., Sangüesa-Barreda, G., Alonso-González, E., Gutiérrez, E., Alla, A. Q., Galván, J. D. & López-Moreno, J. I. (2019). Detecting snow-related signals in radial growth of Pinus uncinata mountain forests. *Dendrochronologia*, *57*, 125622. https://doi.org/10.1016/j.dendro.2019.125622". The contribution of the doctoral student, as well as the contribution of the other authors of this manuscript, is specified below. Alba Sanmiguel-Vallelado contributed to study design, performed the analytic calculations, interpreted the results and wrote the manuscript. J. Diego Galván, Gabriel Sanguesa-Barreda, Antonio Gazol, J. Julio Camarero, Emilia Gutiérrez and Arben Q. Alla collected and processed the wood samples and provided the derived tree-ring width data series. Esteban Alonso-González provided the snow and temperature data series. Antonio Gazol and Enrique Morán-Tejeda helped with the calculations. Juan Ignacio López-Moreno, J. Julio Camarero, Antonio Gazol and Enrique Morán-Tejeda conceived of the study, contribute to the interpretation of the results and supervised the findings of this work. All authors provided critical feedback and helped shape the research and manuscript.

ISSN	Research Area	Impact factor (2020)	Quartile
11257865, 16120051	Forestry; Physical Geography	2.691	Q1

The published research paper featured in **Chapter 5** is "Sanmiguel-Vallelado, A., Camarero, J. J., Morán-Tejeda, E., Gazol, A., Colangelo, M., Alonso-González, E. & López-Moreno, J. I. (2021). Snow dynamics influence tree growth by controlling soil temperature in mountain pine forests. *Agricultural and Forest Meteorology*, *296*, 108205. https://doi.org/10.1016/j.agrformet.2020.108205". The contribution of the doctoral student, as well as the contribution of the other authors of this manuscript, is specified below. Alba Sanmiguel-Vallelado contributed to study design and to implement the research, carried out the data collection, processed the time-lapse photographs and the wood samples, performed the analytic calculations, interpreted the results and wrote the manuscript. Juan Ignacio López-Moreno, J. Julio Camarero, Enrique Morán-Tejeda and Antonio Gazol conceived of the study, implemented the research, contributed to the data collection, contributed to the interpretation of the results and supervised the findings of this work. Michele Colangelo contribute to process the wood samples. Esteban Alonso-González contributed to the data collection. All authors provided critical feedback and helped shape the research and manuscript.

ISSN	Research Area	Impact factor (2020)	Quartile
01681923	Agronomy; Forestry; Meteorology and Atmospheric Sciences	5.734	Q1

The published research paper featured in **Chapter 6** is "Sanmiguel-Vallelado, A., McPhee, J., Esmeralda Ojeda Carreño, P., Morán-Tejeda, E., Julio Camarero, J. & López-Moreno, J. I. (2022). Sensitivity of forest–snow interactions to climate forcing: Local variability in a Pyrenean valley. *Journal of Hydrology*, *605*, 127311. https://doi.org/10.1016/j.jhydrol.2021.127311". The contribution of the doctoral student, as well as the contribution of the other authors of this manuscript, is specified below. Alba Sanmiguel-Vallelado: contributed to study design and to implement the research, carried out the data collection, processed the time-lapse photographs, requested the supplementary data series to authorities, made the simulations, performed the analytic calculations, interpreted the results and wrote the manuscript. Juan Ignacio López-Moreno, James McPhee and Enrique Morán-Tejeda conceived of the study, contributed to the interpretation of the results and supervised the findings of this work. Juan I. López-Moreno and Enrique Morán-Tejeda implemented the research and contributed to the data collection. Paula Esmeralda Ojeda Carreño helped with the simulations. J. Julio Camarero supervised the findings of this work. All authors provided critical feedback and helped shape the research and manuscript.

ISSN	Research Area	Impact factor (2020)	Quartile
00221694	Civil Engineering; Multidisciplinary Geosciences; Water Resources	5.772	Q1


IPE
CSIC
Universidad Zaragoza